

**WestminsterResearch**

<http://www.westminster.ac.uk/westminsterresearch>

**Development of a biocathode system in microbial fuel cells for improved treatment of azo dyes**

**Mani, P.**

This is an electronic version of a PhD thesis awarded by the University of Westminster.  
© Miss Priyadharshini Mani, 2019.

---

The WestminsterResearch online digital archive at the University of Westminster aims to make the research output of the University available to a wider audience. Copyright and Moral Rights remain with the authors and/or copyright owners.

---

Whilst further distribution of specific materials from within this archive is forbidden, you may freely distribute the URL of WestminsterResearch: (<http://westminsterresearch.wmin.ac.uk/>).

In case of abuse or copyright appearing without permission e-mail [repository@westminster.ac.uk](mailto:repository@westminster.ac.uk)

**Development of a biocathode system in  
microbial fuel cells for treatment of azo dyes**

By

**Priyadharshini Mani**

University of Westminster  
Faculty of Science and Technology

A thesis submitted in partial fulfilment of the requirements of  
the University of Westminster for the degree of

Doctor of Philosophy

June 2019

## Abstract

Microbial fuel cells (MFCs) hold great promise for simultaneous wastewater treatment and electricity production. However, their performance is currently hampered by several challenges including high cathodic potential losses and cost of platinum (and other materials) used as a catalyst for the oxygen reduction reaction. These challenges could be overcome by using biological catalysts (oxidoreductase enzymes e.g. laccase & microbes). This work investigated the treatment of azo dye (Acid orange 7, AO7) in MFC utilising biological catalysts as replacements for platinum.

Various ways of mitigating pH changes in the cathode of MFCs and its effect on laccase activity were studied initially. Use of Nafion 117 membrane limited salinity and pH changes in the cathode (0.1 M acetate buffer) leading to prolonged laccase activity and faster anodic dye decolourization compared to using CMI7000 membrane; similarly, automatic pH control was better than using a higher acetate buffer strength (0.2 M). To improve robustness and shelf life, laccase was immobilized by different approaches using polyaniline (PANI), copper alginate beads and Nafion polymer. PANI-laccase showed the highest activity, producing a power density of  $38.2 \pm 1.7 \text{ mW m}^{-2}$  compared to  $28 \pm 1 \text{ mW m}^{-2}$  freely suspended enzyme. There was 81% activity retained after 1 cycle (5 days) for PANI laccase compared to 23.8% for freely suspended laccase. The cathodic dye decolourization was over 85% for freely suspended laccase, 81% for Cu-alginate systems, 76% for PANI, and 73% for Nafion-immobilized laccase.

The efficiency and mechanism of dye degradation were compared between feeding the dye in the anode (*S. oneidensis*) and the cathode chamber (laccase). Power density and decolourization rate were better when dye was fed in the cathode (> 80% decolourization in 24 h,  $P_{\max} 50 \pm 4 \text{ mW m}^{-2}$ ) compared to anode (20% decolourization in 24 h,  $P_{\max} 42.5 \pm 2.6 \text{ mW m}^{-2}$ ). GC-MS analysis revealed benzoic acid and hexanoic acid for laccase degradation products, whereas *S. oneidensis* produced colourless unstable aromatic amines that underwent auto-oxidation to produce colour. Further, to improve the efficiency of laccase, two natural redox mediators (syringaldehyde (Syr), acetosyringone (As)) and artificial mediator ABTS were used in the cathode. The presence of ABTS and As increased power density from  $54.7 \pm 3.5 \text{ mW m}^{-2}$  to  $77.2 \pm 4.2 \text{ mW m}^{-2}$  and  $62.5 \pm 3.7 \text{ mW m}^{-2}$  respectively. The power decreased to  $23.2 \pm 2.1 \text{ mW m}^{-2}$  for laccase with syr. There was increase in decolourization by 20% with addition of mediators. Thus, the natural mediator As improved dye decolourization and power.

To develop an efficient microbial biocathode, activated sludge from textile treatment plant was enriched by potentiostatic method. The biofilm produced a power density of  $64.6 \pm 3.5 \text{ mW m}^{-2}$  compared to platinum (Pt)  $72.7 \pm 1.2 \text{ mW m}^{-2}$  in a MFC. The rate of dye decolourization at the anode was similar in both Pt and biocathode MFCs. The microbial community analysis revealed a selection of chemolithoautotrophic organisms that fix  $\text{CO}_2$  for their metabolism. Altogether, these results suggest that laccase and microbial biocathode have the potential to be an excellent catalyst for ORR in MFC with efficiency equivalent to Pt.

# TABLE OF CONTENTS

<b>Abstract .....</b>	<b>i</b>
<b>Abbreviations .....</b>	<b>xviii</b>
<b>Chapter 1 .....</b>	<b>1</b>
<b>General Introduction.....</b>	<b>1</b>
1.1 Overview .....	1
1.1.1 Microbial Fuel cells in dye treatment .....	1
1.1.2 Statement of the problem.....	2
1.1.3 Biocathodes in MFCs.....	3
1.2 Aims and Objectives .....	3
1.2.1 Specific Objectives .....	4
1.3 Literature Review .....	6
1.3.1 History of Dyes .....	6
1.3.2 Classification of Dyes .....	6
1.3.2.1 Cellulose Textile Dyes.....	7
1.3.2.2 Protein Textile Dyes .....	8
1.3.2.3 Synthetic Textile Dyes.....	8
1.3.3 Colour Chemistry.....	9
1.3.4 Azo Dyes.....	10
1.3.5 Azo dye usage and it's environmental impacts .....	12
1.3.6 Current methods in treatment of textile wastewater.....	14
1.3.6.1 Chemical Methods.....	14
1.3.6.2 Physical Methods.....	16
1.3.6.3 Biological Methods.....	17
1.3.7 Bio electrochemical systems and wastewater treatment.....	20
1.3.7.1 Internal losses in MFC.....	22
1.3.7.2 Electron transfer mechanisms in MFCs.....	24
1.3.7.3 Microbial fuel cells in dye treatment.....	27
1.3.8 Biological catalysts .....	31
1.3.8.1 Laccase Enzyme .....	32
1.3.8.2 Laccase application in treatment of dyes.....	35

1.3.8.3	Laccase catalysed fuel cells .....	39
1.3.8.4	Laccase as cathode catalyst in Microbial Fuel cells .....	41
1.3.8.5	Laccase application in MFC dye decolourization .....	42
1.3.8.6	Challenges in using laccase biocathodes in MFCs .....	42
1.3.8.7	Microorganisms as cathode catalysts in MFC .....	43
1.4	Summary .....	45
1.5	Highlights .....	45
<b>Chapter 2.....</b>		<b>46</b>
<b>Materials and Methods.....</b>		<b>46</b>
2.1	Chemicals .....	47
2.2	Bacterial strains .....	47
2.3	MFC Anode media components .....	48
2.4	MFC Cathode components.....	49
2.5	Design of bioelectrochemical systems used in this study .....	51
2.6	Analytical Procedures .....	52
2.6.1	Acid Orange 7 Decolourization .....	52
2.6.2	Electrochemical Analysis .....	52
2.6.3	Coulombic efficiency (CE).....	53
2.6.4	Chemical Oxygen Demand (COD).....	53
2.6.5	Laccase Enzyme Activity .....	54
2.6.6	Detection of metabolites by chromatographic methods .....	54
2.6.7	Morphological characterisation using Scanning Electron Microscopy (SEM) .....	56
2.6.8	Functional group identification by Fourier-transform infrared spectroscopy (FTIR).....	56
2.6.9	Identification of metabolites from laccase dye degradation by Gas Chromatography/Mass Spectrometry (GC-MS) .....	57
2.6.10	Microtox toxicity analysis .....	59
2.6.11	Cyclic Voltammetry.....	60
2.6.12	Chronoamperometry (CA).....	62
2.6.13	Microbial community analysis by PCR-DGGE .....	63

2.6.14	Metagenomic analysis by Illumina Next Generation Sequencing (NGS) method.....	66
2.6.15	Statistical analysis.....	68
<b>Chapter 3.....</b>	<b>69</b>	
	<b>Decolourization of Acid orange 7 in MFC with a laccase-based biocathode: Influence of mitigating pH changes in the cathode chamber.....</b>	<b>69</b>
3.1	Background .....	70
3.2	Materials and Methods.....	70
3.2.1.	Experimental design.....	70
3.2.2	Operating conditions.....	71
3.2.3	Analytical Procedures .....	72
3.3	Results and Discussion.....	72
3.3.1	AO7 decolourization.....	72
3.3.2	pH and salinity changes in the cathode chamber.....	73
3.3.3	Current and Power generation .....	75
3.3.4	Laccase Enzyme Activity at the cathode .....	77
3.3.5	Detection of degradation products through HPLC .....	78
3.3.6	Toxicity Testing.....	78
3.4	Conclusion.....	79
<b>Chapter 4.....</b>	<b>81</b>	
	<b>Laccase immobilization strategies for application as a cathode catalyst in microbial fuel cells for azo dye decolourization.....</b>	<b>81</b>
4.1	Background .....	82
4.1.1	Immobilization for stability and better direct electron transfer (DET).....	82
4.1.2	Types of enzyme immobilization .....	82
4.1.2.1	Adsorption .....	82
4.1.2.2	Covalent bonding.....	83
4.1.2.3	Entrapment.....	84

4.1.2.4	Encapsulation.....	85
4.1.3	Types of laccase immobilization used in this study .....	87
4.2	Materials and Methods .....	88
4.2.1	Chemicals.....	88
4.2.2	Laccase Immobilization .....	88
4.2.3	Platinum and Fe–N/C Electrode Preparation.....	89
4.2.4	Experimental design.....	89
4.2.5	Operation of the Microbial fuel cell .....	90
4.3	Results and Discussion.....	91
4.3.1	Characterization of immobilized laccase biocathode system	91
4.3.1.1	Functional group analysis of Laccase biocathodes by FTIR .....	91
4.3.1.2	Morphological analysis of the immobilized laccase biocathode using SEM.....	93
4.3.1.3	Electrochemical analysis of PANI and Nafion Laccase electrodes	95
4.3.2	Power generation of Laccase biocathodes .....	97
4.3.3	Dye decolourization in laccase biocathodes .....	98
4.3.4	Enzyme activity of the laccase biocathodes in MFC.....	100
4.3.5	Comparison of laccase system with the conventional Pt and Fe impregnated catalyst (Fe-N/C) .....	102
4.4	Conclusion.....	105
<b>Chapter 5.....</b>		<b>107</b>
<b>Degradation of Acid orange 7 in a microbial fuel cell: comparison between feeding the dye in the anode vs the cathode .....</b>		<b>107</b>
5.1	Background .....	108
5.2	Materials and Methods .....	109
5.2.1	Experimental Design.....	109
5.2.2	Operating conditions.....	110
5.2.3	Analytical procedures .....	110
5.3	Results and Discussion.....	110
5.3.1	Power Generation and COD reduction .....	110

5.3.2	AO7 dye decolourization .....	113
5.3.3	Pyruvate consumption and growth curve of <i>S. oneidensis</i> MR1	114
5.3.4	Electrochemical analysis of dye degradation products.....	116
5.3.5	Auto-oxidation of <i>S. oneidensis</i> (anode) decolourized products .....	118
5.3.6	GC-MS analysis of dye degradation products .....	120
5.3.6.1	S.O MR1 (anode) dye degradation products .....	120
5.3.6.2	Auto-oxidation products and mechanism .....	120
5.3.6.3	Laccase dye degradation products and mechanism .....	122
5.3.7	Toxicity Analysis .....	124
5.4	Conclusion.....	126
<b>Chapter 6.....</b>		<b>127</b>
<b>Role of laccase redox mediators in dye decolourization and power production in a MFC..</b>		<b>127</b>
6.1	Background .....	128
6.1.1	Phenolic Mediators .....	129
6.2	Materials and methods .....	131
6.2.1	Experimental Design.....	131
6.2.2	Operating conditions.....	131
6.2.3	Analytical procedures .....	132
6.3	Results and Discussion.....	132
6.3.1	Power Generation.....	132
6.3.2	Acid Orange 7 decolourization .....	135
6.3.3	Electrochemical activity of the laccase-mediator systems ..	136
6.4	Conclusion.....	141
<b>Chapter 7.....</b>		<b>142</b>
<b>Enrichment of microbial biocathodes to replace platinum catalyst in microbial fuel cells .....</b>		<b>142</b>
7.1	Background .....	143
7.2	Materials and Methods .....	147

7.2.1	Preparation of half-cell for enrichment.....	147
7.2.2	Operation of the half-cell.....	148
7.2.3	Platinum Electrode Preparation.....	149
7.2.4	Experimental design.....	149
7.2.5	Operation of the Microbial fuel cell.....	149
7.2.5.1	Anode of the Microbial fuel cell.....	149
7.2.5.2	Cathode of the microbial fuel cell.....	150
7.2.6	Analytical Procedures.....	150
7.3	Results and Discussion.....	150
7.3.1	Enrichment of electron-accepting microbes using chronoamperometry.....	150
7.3.2	Power Density.....	152
7.3.3	Dye Decolourization.....	153
7.3.4	Microbial community analysis.....	154
7.4	Conclusion.....	165
	<b>Chapter 8.....</b>	<b>166</b>
	<b>Concluding Remarks.....</b>	<b>166</b>
	<b>Chapter 9.....</b>	<b>171</b>
	<b>Future Work.....</b>	<b>171</b>
9.1	Enhancement of power production in microbial biocathode.....	172
9.2	Use of crude laccase extracts in MFC.....	173
9.3	Photosynthetic biocathodes as cathode catalysts.....	174
	<b>References.....</b>	<b>176</b>
	<b>Research Outputs.....</b>	<b>213</b>
	<b>Conference Publications.....</b>	<b>215</b>
	<b>Appendix 1.....</b>	<b>216</b>
	<b>Appendix 2.....</b>	<b>217</b>
	<b>Appendix 3.....</b>	<b>218</b>
	<b>Appendix 4.....</b>	<b>219</b>

<b>Appendix 5</b> .....	<b>221</b>
<b>Appendix 6</b> .....	<b>223</b>
<b>Appendix 7</b> .....	<b>224</b>
<b>Appendix 8</b> .....	<b>226</b>

# LIST OF FIGURES

## Chapter 1

- Figure 1.1:** Examples of chromophoric groups present in organic dyes...9
- Figure 1.2:** (a) Structure of haemoglobin with Fe metal complex and (b) Acid Violet 78 dye indicating Cr metal complex chromophores .....10
- Figure 1.3:** General chemical formula for azo dyes. R and R' may be alkyl but they are usually aromatic..... 11
- Figure 1.4(a):** The first step in azo dye formation: Conversion of aromatic amines to diazonium salts ..... 11
- Figure 1.4(b):** The second step in azo dye formation: Diazonium salt coupling with 2-naphthol gives orange/red dye colour..... 11
- Figure 1.5:** Examples of azo dyes: (a) Acid orange 7, a monoazo dye (b) Congo Red, a diazo dye. ....12
- Figure 1.6:** Discharge of textile dyeing effluents in natural water bodies..... 13
- Figure 1.7:** Mechanisms of dye degradation by bacteria under anaerobic conditions.....18
- Figure 1.8:** Schematic representation of a microbial fuel cell depicting bacteria at the anode and the ORR at the cathode .....22
- Figure 1.9:** The voltage vs current plot depicting the potential losses occurring in a MFC compared to the theoretical potential.....22
- Figure 1.10:** Possible mechanisms for bacterium/anode electron transfer and oxygen reduction at cathode. (A) Direct transfer through cytochromes; (B) Electron transfer through “nanowires” or pili; (C) Through redox mediators; (D) Direct oxidation of excreted catabolites (e.g. formate, H<sub>2</sub>, etc.) (E) Direct reduction of oxygen to water, commonly platinum electrode; (F) Through catalysis at an electrode modified by e.g. transition metal complex catalysts; (G) Bacterial catalysis; (H) Through an enzymatic catalyst with mediator (e.g. laccase + ABTS) .....24
- Figure 1.11:** An example illustrating the anaerobic reductive cleavage of azo bond in Acid orange 7 dye .....28
- Figure 1.12:** Structure of Laccase indicating the Cu<sup>2+</sup> active sites.....33

<b>Figure 1.13:</b> Mechanism of laccase oxidation of lignin by producing phenoxy radicals and quinones.....	34
<b>Figure 1.14:</b> Possible mechanism of degradation of azo dyes by laccase.....	38
<b>Figure 1.15:</b> Direct Electron transfer and Mediated Electron transfer between laccase and electrode in a fuel cell .....	40

## Chapter 2

<b>Figure 2.1:</b> (a) Structure of Acid Orange 7; (b) Congo Red dye used in the study.....	47
<b>Figure 2.2 :</b> A H-type microbial fuel cell used in this study .....	51
<b>Figure 2.3:</b> A CV of Flavin adenine dinucleotide (0.1 mM) at scan rate of 50 mV s <sup>-1</sup> from -0.7 V to -0.1 V. ....	61
<b>Figure 2.4:</b> The hypervariable regions of 16s rRNA with V3 and V4 highly targeted region for PCR amplification.....	63

## Chapter 3

<b>Figure 3.1:</b> Comparison of Acid orange 7 decolourization rates in the various MFC systems over a period of 100 hours .....	73
<b>Figure 3.2:</b> Initial (time 0) and final (10 days) pH and ionic strength in each setup over a period of 7 days.....	74
<b>Figure 3.3:</b> (a) Polarisation curves for each system (b)Power density curve with P <sub>max</sub> for each system obtained by varying the external resistance from 10Ω-1MΩ.....	76
<b>Figure 3.4:</b> Laccase Activity indicating the change in absorbance over time for a period of 10 days .....	77
<b>Figure 3.5:</b> HPLC analysis of degradation products with peaks representing the dye decolourization products with their retention time.....	78
<b>Figure 3.6:</b> Relative luminescence inhibition in relationship to COD. There was no statistically significant difference in the levels of toxicity in the systems tested after a run time of 10 days. ....	79

## Chapter 4

- Figure 4.1:** Laccase formation of covalent bonds on carbon nano tubes .....83
- Figure 4.2:** FTIR spectra indicating the presence of functional groups of the polymer and immobilized laccase (a) PANI/Laccase (b) TBAB/Nafion/laccase .....92
- Figure 4.3:** SEM image of (a) Laccase-PANI Arrows indicate laccase, Inset-PANI (b) Cu-Alg-Laccase, Inset: EDS spectra (c) Nafion-Laccase, Inset-Nafion-TBAB .....94
- Figure 4.4:** Cyclic voltammetry of immobilized electrodes at  $20 \text{ mV s}^{-1}$  of (a) PANI and PANI cross-linked with laccase (b) Nafion-TBAB and Nafion-TBAB laccase system. Insets: Immobilized laccase at different scan rates.....96
- Figure 4.5:** Comparison of  $P_{\text{max}}$  (Maximum power density) for the different laccase based biocathode systems obtained by varying the external resistance from  $10\Omega$ - $1\text{M}\Omega$ .....98
- Figure 4.6(a):** Comparison of decolourization rates of AO7 in the different laccase based MFC systems over a period of 5 days.....99
- Figure 4.6(b):** Dye adsorption in copper alginate beads. Blue - Initial bead colour, Green- On adsorption of dye. ....99
- Figure 4.7:** Laccase electrochemical activity with time (a) PANI-Laccase (b) Nafion-Laccase. Inset: Cathodic peak current vs time at  $20 \text{ mV s}^{-1}$ .101
- Figure 4.8:** Comparison of relative enzyme activity for each immobilized and free laccase system for a period of 5 days. ....102
- Figure 4.9:** Comparison of maximum power density for Pt catalyst, Fe-N/C and PANI-Laccase. ....103

## Chapter 5

- Figure 5.1:** (a) Comparison of MFC performance for all MFC systems obtained by varying the external circuit resistance ( $10\Omega$  – $1\text{M}\Omega$ ) (b) Polarisation curves for all the systems used in the study .....112
- Figure 5.2:** Decolourization of AO7 in the anode (*S.oneidensis*) and cathode (Laccase) of MFC over a period of 4 days.....114

<b>Figure 5.3:</b> (a)HPLC analysis of Pyruvate consumption by MR1 for each time interval (b) Comparison of MR1 growth rate with pyruvate concentration.....	115
<b>Figure 5.4:</b> Cyclic Voltammetry of (a) parent dye (AO7), standards SA and 1-A-2-N (b) anode and cathode decolourized products, at 50 mV s <sup>-1</sup> vs Ag/AgCl.....	117
<b>Figure 5.5:</b> The depiction of initial coloured dye together with the decolourized products and the coloured auto-oxidation products.....	118
<b>Figure 5.6:</b> UV-Scan of AO7 and CR initial dye, decolourized products and Auto-oxidation products indicating the colour in the auto-oxidation products was not a result of diazotization.....	119
<b>Figure 5.7:</b> Putative dye degradation pathway by <i>S. oneidensis</i> MR 1 at the anode and the auto-oxidation mechanism based on the intermediate products obtained from GC-MS analysis .....	121
<b>Figure 5.8:</b> Putative laccase dye degradation pathway deduced from the intermediates form GC-MS analysis .....	123
<b>Figure 5.9(a):</b> <i>V. fischeri</i> toxicity profile indicating the % inhibition for each dilution for all the products (b) Percentage inhibition per concentration of the products.....	124

## Chapter 6

<b>Figure 6.1:</b> Laccase substrate oxidation through mediators and subsequent reduction of mediators .....	128
<b>Figure 6.2:</b> (a) Maximum Power density for mediator based and control MFCs obtained by varying the external resistance from 10Ω-1MΩ (b)Voltage vs Current plot (Slope=internal resistance).....	134
<b>Figure 6.3:</b> Decolourization of AO7 dye by laccase in the presence and absence of mediators over a period of 4 days.....	135
<b>Figure 6.4:</b> Cyclic voltammetry of syringaldehyde in the presence and absence of laccase at a scan rate of 50 mV s <sup>-1</sup> .....	136
<b>Figure 6.5:</b> Laccase oxidation of syringaldehyde to syringic acid and subsequent oxidation to benzoquinones. ....	137
<b>Figure 6.6:</b> CV of acetosyringone indicating the oxidation/reduction peak in the presence and absence of laccase at a scan rate of 50 mV s <sup>-1</sup> .....	138

<b>Figure 6.7:</b> Electron transfer (ET) and Hydrogen atom transfer (HAT) oxidation mechanisms of acetosyringone mediated by laccase. ....	138
<b>Figure 6.8:</b> (a) Two step oxidation of ABTS (b): CV of ABTS with and without laccase at 50 mV s <sup>-1</sup> . ....	139
<b>Figure 6.9:</b> Chronoamperometry depicting the reduction current for each mediator at a concentration of 50 μM. ....	140

## Chapter 7

<b>Figure 7.1:</b> Electrochemical set-up used in this study .....	148
<b>Figure 7.2:</b> Chronoamperometry of biofilm showing the peak current for each cycle.....	150
<b>Figure 7.3 :</b> Enriched biofilm after 70 days of chronoamperometry with arrows indicating the two types of biofilm formed i.e. near the wired connection and at centre of the electrode. ....	151
<b>Figure 7.4:</b> Maximum power density for each cathode catalysts. Inset: Voltage/current graph for the cathodes indicating the losses. ....	153
<b>Figure 7.5:</b> Anodic dye decolourization in <i>Shewanella oneidensis</i> based MFC for different cathode catalysts. ....	154
<b>Figure 7.6:</b> Observed number of species in each sample. Inset: OTUs obtained from each of the samples. ....	155
<b>Figure 7.7:</b> Shannon index for diversity variance among the species population in each sample.....	156
<b>Figure 7.8:</b> PCoA analysis of all the samples based on Unweighted Unifrac similarity .....	157
<b>Figure 7.9:</b> The relative abundance for the dominant class in each phylum for all samples. ....	158
<b>Figure 7.10:</b> Ternary plot for the Orders between Sludge, EB and Plank samples.....	159
<b>Figure 7.11:</b> Representation of microbial orders present in all the samples.....	160
<b>Figure 7.12:</b> Representation of microbial families present in all the samples.....	161
<b>Figure 7.13:</b> Ternary plot indicating the dominant species in the enriched samples.....	163

**Figure 7.14:** Schematic representation of metabolic activity between the microbes enriched in the biofilm .....164

## **Chapter 9**

**Figure 9.1 :** Suggested mechanism of of azo dyes degradation by algae.....175

# LIST OF TABLES

## Chapter 1

<b>Table 1.1:</b> The types of dyes treated with laccase from different fungal sources .....	36
--	----

## Chapter 2

<b>Table 2.1</b> The composition of vitamin mix stock solution (100x) used in this study .....	48
--	----

<b>Table 2.2:</b> The composition of the trace elements stock solution (100x) used in this study.....	49
---	----

<b>Table 2.3:</b> Structure and molecular weights of redox mediators used in chapter 6.....	50
---	----

<b>Table 2.4:</b> Composition of Oceanibulbus medium for <i>Vibrio fischeri</i> ....	59
--	----

<b>Table 2.5:</b> The components of the denaturing gradient gel used in this study.....	66
---	----

## Chapter 3

<b>Table 3.1:</b> Summary of variables employed in this study along with the rationale for employing them.....	71
--	----

## Chapter 4

<b>Table 4.1:</b> Types of enzyme immobilization with their advantages and disadvantages .....	86
--	----

<b>Table 4.2:</b> Summary of the measured parameters for each system and the normalized power output .....	105
--	-----

## Chapter 5

<b>Table 5.1:</b> Features of dye degradation in the anode vs cathode of MFCs.....	109
--	-----

## Chapter 7

<b>Table 7.1:</b> BES employed in development of microbial biocathode and the dominant microbial communities identified.....	145
--	-----

## **Acknowledgements**

I would like to express my sincere gratitude to my Director of Studies Dr. Godfrey Kyazze for his endless support, mentorship and encouragement throughout my PhD program. His unwavering guidance and patience was of immense help during tough times. I am grateful to Professor Tajalli Keshavarz for his support in initiating my PhD program, his guidance and constant belief in me throughout my research program. I would also like to thank Professor T.S. Chandra for giving me the opportunity to work at her laboratory at the Indian Institute of Technology (IIT), Madras and for her expert advice and feedbacks on my research. I extend my thanks to IIT, Madras for availing me the facilities and financial support during my stay there.

I would like to thank all the technical staff at Cavendish campus especially Dr. Thakor Tandel and Dr. Zhi Song for enabling me to access all research materials and for their technical support.

I extend my appreciation to my colleague Segun Fapetu for his help and support during my study. Special thanks to Kyle Bowman for his skill in making the odd things I needed during my research and his help with the enrichment setup and DGGE analysis. I extend my thanks to Mark Breheny for his help with HPLC analysis and for his review and feedback on my research paper. Thanks goes to Quratulain Khalid and Ola Gomaa for their friendship, support and encouragement throughout this program.

My sincere gratitude to my dear friend Fidal Kumar who assisted me in various research works and provided valuable inputs and help in editing my thesis. His patience towards my antics and his unfailing emotional and moral support during tough times were immensely helpful.

I am truly grateful to my parents Mr. K.S.Mani, Mrs. Parameswari and my brother Madhu Mohan for their unconditional love, enormous support and belief in me. They have taught me the value of education and I am thankful for their constant encouragement throughout my studies.

Finally, my heartfelt gratitude to my partner Suresh Paul Jones for persuading me to pursue a PhD program. I am indebted to him for his unconditional support, love, encouragement and confidence in me without which this research would not have been possible.

## **Author's Declaration**

I declare that the present work was carried out in accordance with the Guidelines and Regulations of the University of Westminster.

This thesis is entirely my own work and that where any material could be construed as the work of others, it is fully cited and referenced, and/or with appropriate acknowledgement given.

Until the outcome of the current application to the University of Westminster, the work will not be submitted for any such qualification at another university or similar institution.

Signed:

Date: 10<sup>th</sup> June 2019



Priyadharshini Mani

## Abbreviations

AA	Aromatic Amines
AAPy	Amino AntiPyrine
ABTS	2,2'-azino-bis (3-ethylbenzothiazoline-6-sulphonic acid)
AC	Activated Carbon
Ag/AgCl	Silver-Silver chloride
AL	Activation Losses
AO7	Acid Orange 7
AOP	Advanced Oxidation Process
AQDS	Anthraquinone-2,6-disulfonate
AQS	Anthraquinone-2-sulfonate
ATR	Attenuated Total Reflection
BES	Bioelectrochemical Systems
BOD	Biological Oxygen Demand
C.I.	Colour Index
CE	Coulombic Efficiency
CEM	Cation Exchange Membrane
CNT	Carbon NanoTube
COD	Chemical Oxygen Demand
Co <sub>x</sub> O <sub>y</sub> /NC	Cobalt Oxide incorporated with Nitrogen doped Carbon
CP	Chlorophenols
CPCB	Central Pollution Control Board
CR	Congo Red
CA	ChronoAmperometry
Cu-Alg	Copper alginate beads
CV	Cyclic Voltammetry
DCM	Dichloromethane
DCP	Dichlorophenol
DDT	Dichlorodiphenyltrichloroethane
DE	Decolourization Efficiency

DET	Direct Electron Transfer
DGGE	Denaturing Gradient Gel Electrophoresis
dNTPs	deoxyribonucleotide Triphosphates
DO	Dissolved Oxygen
EDS	Energy-Dispersive X-ray spectroscopy
EET	Extracellular Electron Transfer
EIS	Electrochemical Impedance Spectroscopy
EPA	Environmental Protection Agency
ET	Electron Transfer
FAD	Flavin Adenine Dinucleotide
Fe-EDTA	Ferric- Ethylenediaminetetraacetic Acid
FeVO <sub>4</sub>	Iron Vanadate
FMN	Flavin Mononucleotide
FTIR	Fourier Transform InfraRed spectroscopy
GC-MS	Gas Chromatography-Mass Spectrometry
GMO	Genetically Modified Organisms
HAT	Hydrogen Atom Transfer
HBT	1-Hydroxybenzotriazole
HPLC	High Performance Liquid Chromatography
HRP	Horse Radish Peroxidase
IC	Ion Chromatography
IC50	Inhibitory Concentration for 50% decrease in viability
IrO <sub>2</sub>	Iridium(IV) Oxide
IUPAC	International Union of Pure and Applied Chemistry
LiP	Lignin Peroxidase
LMS	Laccase Mediator System
MEC	Microbial Electrolysis Cell
MET	Mediated Electron Transfer
MFC	Microbial Fuel Cell
ML	Mass transfer Losses
MnP	Manganese Peroxide

Mn <sub>x</sub> O <sub>y</sub> /NC	Manganese Oxide incorporated Nitrogen doped Carbon
MO	Methyl Orange
MSM	Minimal Salts Media
N=N	Azo bond
NADPH	Nicotinamide Adenine Dinucleotide Phosphate
NaOCl	Sodium Hypochlorite
NC	Nitrogen doped Carbon
NF	Nano Filtration
NGS	Next Generation Sequencing
SHE	Normal Hydrogen Electrode
OCP	Open Circuit Potential
OCV	Open Circuit Voltage
OER	Oxygen Evolution Reaction
OL	Ohmic Losses
ORR	Oxygen Reduction Reaction
OUT	Operational Taxonomic Units
PAH	Polyaromatic Hydrocarbon
PANI	Poly Aniline
PCA	Principal Component Analysis
PCB	Polychlorinated Biphenyls
PCoA	Principal Coordinates Analysis
PCP	Pentachlorophenol (PCP)
PCR	Polymerase Chain Reaction
PEI	Polyethylenimine
PGM	Platinum Group Metals
PHA	Polyhydroxyalkanoates
Ppy	Polypyrrole
Pt	Platinum
Pt-Co	Platinum-Cobalt scale
PTFE	Polytetrafluoroethylene
RE	Reference Electrode
RO	Reverse Osmosis

RP-HPLC	Reverse Phase High Performance Liquid Chromatography
rRNA	Ribosomal RNA
RuO <sub>2</sub>	Ruthenium(IV) Oxide
SCE	Standard Calomel Electrode
SEM	Scanning Electron Microscopy
SRB	Sulphate Reducing Bacteria
TBAB	Tetra-n-butylammonium Bromide
TCP	Trichlorophenol
TDS	Total Dissolved Solids
TEMPO	2,2,6,6-tetramethylpiperidin-N-oxyl
TiO <sub>2</sub>	Titanium dioxide
UF	Ultra-Filtration
V <sub>2</sub> O <sub>5</sub>	Vanadium Oxide
VA	Violuric Acid
WE	Working Electrode

# **Chapter 1**

## **General Introduction**

## **1.1 Overview**

### **1.1.1 Microbial Fuel cells in dye treatment**

Azo dyes constitute 60%-70% of dyes worldwide and are widely used in textile, food, cosmetics, paper and leather industries (Rawat et al., 2016). Due to their low substrate fixation rate they are washed out into the water discharged from these industries. Azo dyes are aromatic compounds with one or more -N=N- present in their molecular structure. The breakdown products of azo dyes are aromatic amines which are known to be carcinogenic and genotoxic. European Union (Annex XVII of the REACH regulation; No, 1907/2006) regulation has banned 22 aromatic amines (AA) that are carcinogenic in humans and animals (Brüschweiler and Merlot, 2017). This constitutes about 48% of parent azo dyes with the banned AA but the remaining 52% of azo dyes used still contain non-regulated amines that are toxic. These discharged AAs affect the ecology of the natural water streams and the surrounding soil. The azo dyes go through conventional activated sludge systems unchanged; this affects light penetration in the receiving water bodies and is not aesthetically pleasing.

The various physicochemical methods currently used for textile effluent treatment include membrane filtration, coagulation/flocculation, adsorption and advanced oxidation processes such as chlorination, bleaching, ozonation and Fenton oxidation (Slokar and Majcen Le Marechal, 1998; Robinson et al., 2001; Pizzolato et al., 2002; Kusvuran et al., 2004; Gogate and Pandit, 2004). These methods have shown to be effective but there are several limitations in terms of environmental impact, energy consumption, secondary sludge production and cost. Biological methods include using bacteria and fungi to treat the dye containing wastewater (Ooi et al., 2007; Pandey et al., 2007). The microorganisms in anaerobic sludge systems may be affected by high salinity and toxicity of the dyes. Moreover, under anaerobic conditions the dyes are not completely degraded (Singh and Arora, 2011). Wild type strains are incapable of assimilating large dye molecules under aerobic conditions and therefore the dye remains unaffected.

In recent years, microbial fuel cells (MFCs) have shown promise in treating dyeing effluents with simultaneous power production. The major advantage of using MFCs are low sludge production, a robust process that can withstand high salinity (5% TDS) and wide pH ranges (pH 6-9) and is suitable for small installations with low organic

load (1-10 Kg BOD per day). MFC is a bioelectrochemical system that utilizes microorganisms to oxidize organic substrates at the anode to produce electrons and protons that are transferred via the electrode and proton exchange membrane to the cathode for oxygen reduction. Exoelectrogens such as *Shewanella*, *Geobacter* species shuttle the electrons extracellularly to the electrode in the absence of oxygen and these electrons are captured as electric current. Many studies have focussed on decolourization of azo dyes at the anode of MFCs (Fernando et al., 2012; Hsueh et al., 2014; Jayaprakash et al., 2016). At the anode under anaerobic conditions the -N=N- bond is cleaved in the presence of microorganisms to form aromatic amines (Hou et al., 2011a; Fernando et al., 2012). The aromatic amines as discussed above are toxic and they need to be degraded further under aerobic conditions.

To commercialize MFCs for effluent treatment, there should be high power production and complete dye degradation with low cost. Many studies to improve power, focus on electron transfer mechanisms, microorganisms present, use of various substrates and redox mediators etc. at the anode of MFCs (Gorby et al., 2006; Aeschbacher et al., 2010; Cao et al., 2010). At the cathode, the catalyst used plays an important role in carrying out efficient oxygen reduction reaction (ORR). In this thesis, the focus was on improving the ORR at the cathode of MFCs with simultaneous dye degradation.

### **1.1.2 Statement of the problem**

A major limiting factor in a MFC is the oxygen reduction reaction (ORR) at the cathode. This is partly due to the high overpotentials and partly due to oxygen mass transfer limitation in the cathode. The most effective and commonly used cathode catalyst thus far is platinum. The high cost of Pt (1gm = £192: Sigma Aldrich) and low sustainability of platinum hinders the scaling up of MFCs for wastewater treatment. Many transition metal-based catalysts such Mn, Co, V and their oxide forms have been used as cathode catalysts in MFCs as a replacement for platinum (Gong et al., 2014; Noori et al., 2016). These catalysts have produced power comparable to Pt but the stability of these metals have been a challenging issue. The possible leaching of the metals into the environment and their toxic effects should be taken into consideration (Yuan et al., 2016). Furthermore, the aromatic amines formed by the cleaving of azo bond could have potential toxic effects. The complete degradation of the azo dye-containing wastewater in a more efficient, sustainable and eco-friendly manner is required for its safe disposal into water streams.

### **1.1.3 Biocathodes in MFCs**

A possible alternative for platinum and other noble metal catalysts is the use of biological catalysts (e.g. enzymes, microorganisms) because they are cheap, environmentally friendly and sustainable. Oxidoreductase enzyme e.g. laccase could be used as cathode catalysts in MFCs as possible alternative to platinum (Luo et al., 2010; Bakhshian et al., 2011). Laccase is a multi-copper containing oxidoreductase enzyme that is capable of one electron oxidation of other substrates and four electron reduction of O<sub>2</sub> to H<sub>2</sub>O (Galhaup and Haltrich, 2001). Laccase from the fungi *Trametes versicolor* is thermodynamically favourable for oxygen reduction at the cathode due to its high redox potential (780 mV vs SHE). Laccase is also capable of azo dye degradation through a free radical mechanism forming phenolic compounds, therefore avoiding the formation of toxic aromatic amines (Tauber et al., 2008).

There is also potential to use microorganisms with the ability to accept electrons from the electrode to catalyse the oxygen reduction reaction at the cathode. Such microbes are enriched from various environmental sources to produce electroactive bacteria (Wang et al., 2013; Milner et al., 2016) Biocathodes could contribute to advancements needed to implement MFCs for practical applications with potential cost savings and operational sustainability.

## **1.2 Aims and Objectives**

Very few studies have utilized laccase and laccase producing fungi at the cathode of MFCs for ORR and dye decolourization (Bakhshian et al., 2011; Savizi et al., 2012; Lai et al., 2017; Lai et al., 2017). The use of enzymatic cathodes maybe expected to be limited by the poor stability of the enzymes in the system and environmental factors such as pH, salinity, metal ions etc. To develop an enzyme based biocathode it is important to extend enzyme lifetime and protect them from deactivation.

To my knowledge, there are no studies that observed the effect of pH changes on laccase activity or various immobilization methods to improve the activity in a MFC with simultaneous dye decolourization. In addition to improving the robustness it was also necessary to understand the degradation mechanism of laccase in comparison to the microbial metabolic route. This will provide the insight not only to understand the

toxicity of the by-products but motive to prefer the cathode-based degradation instead of anode-based. Although many studies have individually been reported on anode and cathode-based degradation of dye, no study have determined the exact difference in the efficiency and mechanism of degradation. Further on laying the groundwork on stability of the system and mechanism, there are several approaches to accelerate the dye degradation rate which mainly involves use of natural mediators. Biocathode alternative to laccase can be pursued in a microbial system for ORR as it would be of interest to determine if laccase-like reaction can be performed in a stable manner by microbial biofilm under similar conditions. This will greatly reduce the cost further as these systems once developed are robust and easy to maintain.

The overall aim and objective of this work was to develop a laccase and microbial based biocathode for oxygen reduction reaction (ORR) and investigate their effect on dye decolourization in a double chambered microbial fuel cell.

To achieve the above aim the research was directed through the following specific objectives.

### **1.2.1 Specific Objectives**

#### **a. To investigate the methods for mitigating pH changes in the cathode of MFC for maintaining laccase activity**

In this study various strategies to mitigate pH changes in the cathode chamber and their impact on laccase activity and power production in a MFC were investigated. The investigation was carried out in the context of azo dye decolourization at the anode.

#### **b. To compare different laccase immobilization methods with regards to their application of biocathodes for azo dye treatment**

In this study, laccase in the three immobilized states (Cross-linking, entrapment in beads and micellar encapsulation) was compared with freely suspended enzyme with respect to dye decolourization, enzyme activity retention, power production and reusability in the cathode of a microbial fuel cell. This study aimed to emphasize the effect of immobilization on laccase ability to perform as efficient cathode catalyst. The performance of the laccase electrode was evaluated against platinum and Fe-N/C catalysts at the cathode of MFCs.

**c. To understand and compare the dye degradation mechanism in the anode and cathode chamber of MFC.**

In this study, the rate of decolourization and degradation of dye under anaerobic condition in the presence of bacteria at the anode of MFC and in aerobic condition in the presence of laccase enzyme at the cathode of MFC was compared independently to understand the difference in the mechanism and the nature of the products formed in both types of degradation.

**d. To utilize natural mediators to enhance laccase activity and rate of dye decolourization**

Redox mediators are needed if substrates cannot directly interact with the active site of the enzyme. The effect of natural phenolic mediators such as syringaldehyde and acetosyringone on dye decolourization and power density in a laccase biocathode MFC was investigated. The synergistic effect of dye and mediator as oxidising substrates for laccase were also inferred in this study.

**e. To develop a microbial catalyst for efficient oxygen reduction reaction at the cathode of MFC.**

Electron accepting microorganisms could be a feasible alternative to platinum or enzymes as cathode catalysts. This study therefore, enriched and identified new electron accepting microorganisms from an inoculum of activated sludge from a textile treatment plant. The biocathode developed was compared with platinum to evaluate the performance at the cathode of MFC.

## **1.3 Literature Review**

### **1.3.1 History of Dyes**

The art of dyeing is as old as the human civilization. Natural dyes have been used since ancient times for colouring and printing purposes. The earliest written record of dyestuff dates to 2600 BC in China. There are mentions of dyed fabrics in Persia and India in 331 BC and 327 BC respectively. These natural dyes were made from plants (indigo), animal sources (cochineal) and minerals (ocher). The blue colour in indigo dye was derived from plants in India and South-East Asia and purple colour was made from molluscs found in the Mediterranean Sea. The madder dye made from the root of the madder plant was most popular natural dye in the 19<sup>th</sup> Century due to the brilliant and exotic red colour. Indigo was widely used until the early 1900s as it achieved a bright blue colour that was fast to washing and light. The natural dyes were expensive due to the demand for the sources of its production.

In 1856, an English chemist William Henry Perkin accidentally discovered a purple dye while trying to synthesize quinine an antimalarial drug from aniline. This dye readily dyed silk and had good colour fastness compared to any other dye. This was the first synthetic dye produced and it was named mauveine after the French word for purple mallow flower. The first synthetic azo was Bismarck Brown synthesized by the German chemist Johann Peter Griess in the year 1858.

### **1.3.2 Classification of Dyes**

The synthetic dyes can be classified in several ways depending on the nature of their chromophore, method of application to the substrate, the substrate type etc. Some dyes are directly applied to the fabrics while others require mordants. Mordants are chemicals that help bind the dye to the fabric by forming co-ordination complex with the dye, which then binds to the fabric (IUPAC, 1997). Commonly used mordants are alum, sodium chloride and some salts of aluminium, copper, tin, iron, potassium etc. The textile industry-based classification of dyes and their substrates are:

- a. Cellulose Textile Dyes
- b. Protein Textile Dyes
- c. Synthetic Textile Dyes

### 1.3.2.1 Cellulose Textile Dyes

These textile dyes are used for cellulosic fibres such as cotton, jute and their blends.

#### a. Direct Dyes

Direct dyes are used for cotton and other cellulosic fibres without the use of mordants. They are bound to the substrate by Van der Waals, hydrogen and dipole bonds. These dyes are highly soluble in water and are applied in baths containing electrolyte and salts to control the adsorption rate of the dyes. However, they have poor fastness during the wash and tend to fade out quickly. This is due to the weak bonding between the dye and the fibre (Waring and Hallas, 1990). The commonly used direct dyes are Brilliant Blue (C.I. Direct Blue 106), copper blue 2R (C.I. Direct Blue 151).

#### b. VAT Dyes

VAT dyes are insoluble in water; therefore, they are solubilised with a reducing agent such as sodium dithionate in the presence of sodium hydroxide (alkali) and affixed to the fibre. Oxidation of the dyed fabric returns the native insoluble form of the dye (Kiernan, 2001). These dyes are the fastest for cotton, linen and rayon. Indigo, a natural dye derived from Indigo plant, is the original dye characteristic to this class. The dyes are used with mordants to dye other type of fibres such as wool, polyester, nylon. Examples of VAT dyes are VAT Blue 1 (C.I. 73000), VAT Orange 2 (C.I. 59300).

#### c. Fibre Reactive Dyes

Reactive dyes are highly coloured organic substances that form covalent bonds with fibre molecules. Due to the strong bonding with the fibre they are light and wash fastness. These dyes can be used for all types of fibre such as cotton, rayon, silk, wool, nylon and even for printing purposes. They become integral part of the textile fibre and are used by weavers for blending them into the fabric. The dyes are divided into 'hot' and 'cold' dyes depending on the temperature of application. These are the most permanent of all dyes and the colour cannot be removed once fixed to the fabric (Waring and Hallas, 1990). Some examples of reactive dyes are CI Reactive Black 5, C.I. Reactive Red 3 etc.

### 1.3.2.2 Protein Textile Dyes

These dyes are best suited for protein fibres i.e. those obtained from animals. They include silk, wool, mohair (goats).

#### d. Acid Dyes

Acid Dyes (Anionic) are highly soluble in water and are effective for protein fibres such as silk, wool, nylon and modified acrylics. They contain sulphonic acid groups that are usually present as sodium sulphonate salts which increase the solubility in water by imparting a negative charge. In an acidic solution, the  $-NH_2$  functionalities of the fibres are protonated to give a positive charge that interacts with the negative dye to form ionic interactions. Apart from this, Van-der-Waals bonds, dipolar bonds and hydrogen bonds are also formed between the dye and fibre. Most acid dyes possess azo, anthraquinone and triarylmethane structures (Sekar, 2011). Most commercially used acid dyes are Acid Red 88, Acid Orange 7, Acid Blue 45 etc.

### 1.3.2.3 Synthetic Textile Dyes

These dyes are used for fibres such as nylon, acrylic, rayon, polyester etc.

#### e. Basic Dyes

They are a class of dyes containing the cationic functional groups such as  $-NR_3^+$  or  $=NR_2^+$ . Since they have the cationic functional group they are well suited for fabrics that are anionic or negatively charged to form a strong bond. The dyes are very bright in colour but their poor colourfastness and have limited use in natural fibres. Basic dyes are best suited for acrylic fibres. The first synthetic dye mauveine discovered accidentally by Perkin was a basic dye. Methylene blue and crystal violet are some of the prominent basic dyes used today (Clark, 2011). These dyes are prominently used for staining in microbiology studies. The bacterial cells (nucleic acids) are negatively charged so they bind easily to the positively charged dye.

#### f. Disperse Dyes

These dyes have low water solubility, non-ionic and usually appear as colloidal or fine aqueous suspensions. They are used for dyeing nylon, cellulose triacetate, polyester and acrylic fibres. Disperse dyes are applied at high temperature ( $130^\circ C$ ) and pressure in dye baths as dispersions by direct colloidal adsorption by the hydrophobic fibres. The high temperatures sublime the dye which makes it easier to enter the fibre and

once cooled down the dye condenses to the colloidal state and is adsorbed by the fibre. The dyeing rate can be influenced by the choice of dispersing agent used and they have fair to good light fastness (Gulrajani, 2011). Disperse Yellow 18, Disperse Blue 14 are some examples of disperse dyes.

### 1.3.3 Colour Chemistry

The dyes possess colour due to the presence of a chromophore in their molecular structure. In a chromophore moiety the energy difference between the two molecular orbitals falls within the range of the visible spectrum. As the visible light falls on the molecule it is absorbed when the electron is excited from the ground state to an excited state (Allen, 1971). In addition to chromophores, dyes also contain auxochromes that are functional groups which modifies the ability of chromophore to absorb light by altering the wavelength. Some of the functional groups are carboxylic acid, sulfonic acid, amino and hydroxyl groups.

The two different types of chromophores are:

a. Conjugated pi systems

In conjugated pi systems chromophore, the electrons jump between eight extended pi orbitals creating a series of alternating single and double bonds. Extending the conjugated systems with multiple bonds will tend to shift it to longer wavelengths and vice versa. The shift between short and long wavelengths will influence the absorption and reflection of different colours. Some examples of this chromophores are retina, food colourings, fabric dyes (Figure 1.1),  $\beta$ -carotene, lycopene, pH indicators (Abrahart, 1977).

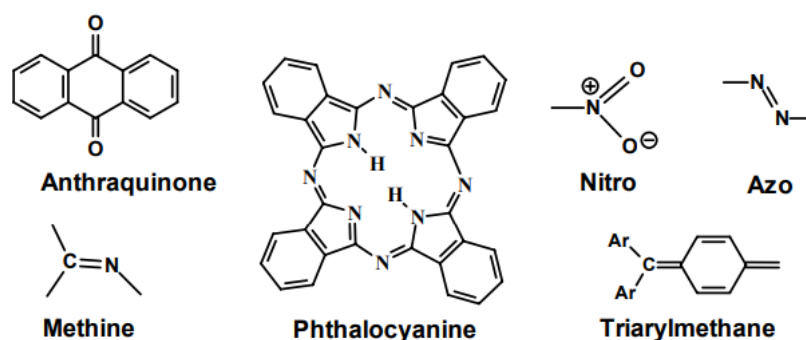


**Figure 1.1:** Examples of chromophoric groups present in organic dyes (Abrahart, 1977).

## b. Metal complex chromophores

These chromophores contain transition metal complexes bound to a ligand. Common examples are chlorophylls in plants, haemoglobin in the red blood cells and metal complex dyes. In the two examples the metal being iron in porphyrin ring for haemoglobin (Figure 1.2(a)) and magnesium in chlorin-type ring for chlorophyll. The highly conjugated pi-bonding system of the macrocycle ring absorbs visible light. The excited state lifetime and the nature of the central metal can influence the absorption spectrum of the metal-macrocycle complex (Gouterman, 1978).

In dyes they are typically monoazo dyes that form co-ordination complex with transition metals such as nickel, chromium, cobalt and copper. They are used for wool, silk and nylon to achieve excellent colour and light fastness. Some examples are Acid Violet 78 (Figure 1.2(b)), Acid Blue 159 (Chakraborty, 2011).

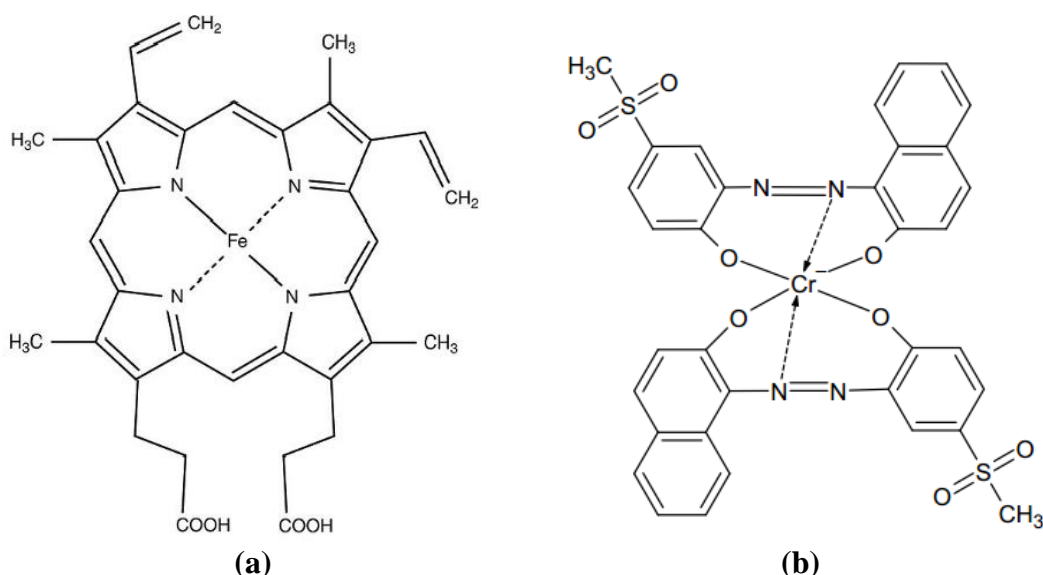


**Figure 1.2:** (a) Structure of haemoglobin with Fe metal complex (Wu et al., 2010) and (b) Acid Violet 78 dye indicating Cr metal complex chromophores

### 1.3.4 Azo Dyes

Azo dyes have excellent colouring properties and are the largest group of synthetic dyes and pigments used in the industry (Pandey et al., 2007). Over 60%-70% of all dyes used in the textile industry are azo-based (Rawat et al., 2016); other dye classes

being anthraquinone dyes, xanthene dyes, triphenylmethane dyes etc. They are characterised by the functional group -N=N- usually linked to an aromatic ring (Figure 1.3). Azo dyes come in various classes (disperse, acid, direct) based on their mode of attachment to fibre surfaces. The most common classes used in industry include acidic dyes (e.g. Acid orange-7 (AO7) (Fig. 1.5a), Acid black 107), reactive dyes (e.g. Reactive red 3, Reactive black 5) and disperse dyes (e.g. Disperse blue-79) (www.sophied.net).

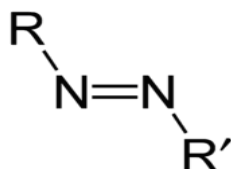
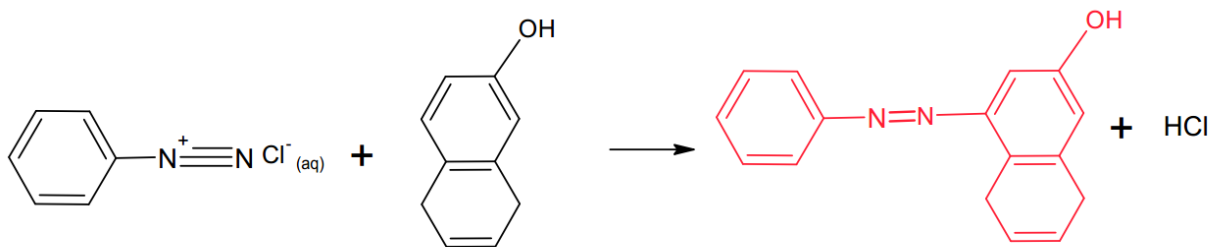


**Figure 1.3:** General chemical formula for azo dyes. (Source: IUPAC, 1997). R and R' may be alkyl but they are usually aromatic.

Azo dyes are synthesized in two stages i.e. in Step 1 is the conversion of an aromatic compound to diazonium salt (Figure 1.4(a)). These diazonium salts are prepared at temperatures below 5° C therefore they relatively unstable at room temperature (Aljamali, 2015).



**Figure 1.4(a):** The first step in azo dye formation: Conversion of aromatic amines to diazonium salts (Aljamali, 2015).



Step 2: The diazonium salts are then coupled with phenol, naphthol, aromatic amine to produce azo dyes (Figure 1.4(b)). The resulting azo group is the chromophore and the hydroxyl, amino groups are the auxochromes **Figure 1.4(b):** The second step in azo dye formation: Diazonium salt coupling with 2-naphthol gives orange/red dye colour (Aljamali, 2015).

The addition of electron donating groups ( $-\text{NH}_2^+$ ) to the azobenzene structure results in bathochromic shift (shift of emission spectrum to longer wavelength) and the presence of electron withdrawing group ( $-\text{OH}$ ) produces a hypsochromic shift (shorter wavelength). This attributes to the different maximum absorbance ( $\lambda_{\text{max}}$ ) for structurally similar dyes with different substituent groups.

Azo dyes are classified based on their number of azo bonds ( $\text{N}=\text{N}$ ) present in their structure. Most commonly used in the textile industry are the monoazo (Figure 1.5(a)) and diazo dyes (Figure 1.5(b)).

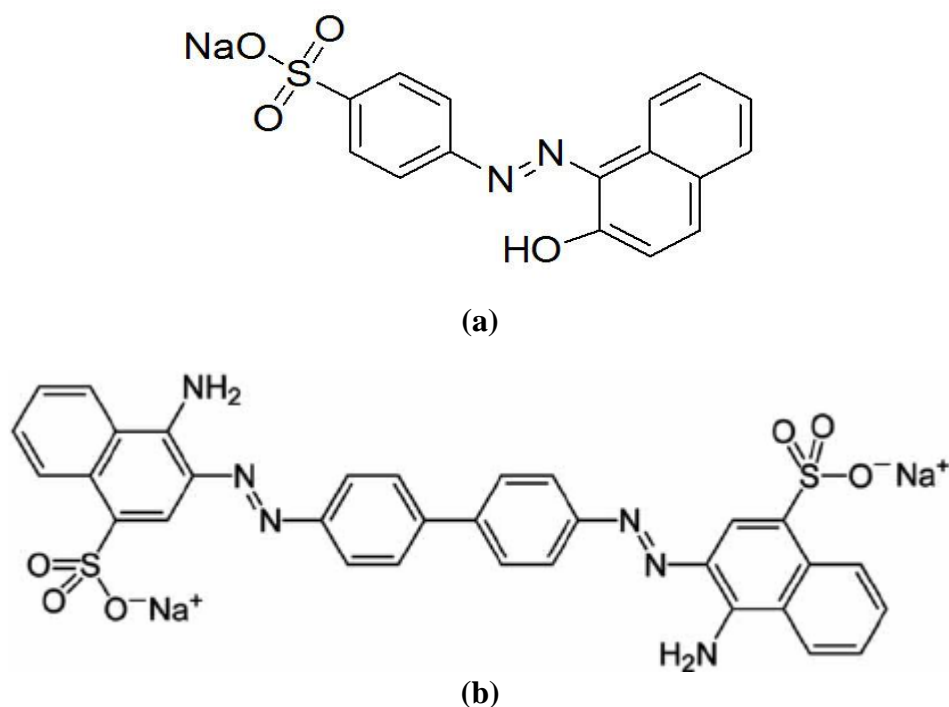


**Figure 1.5:** Examples of azo dyes: (a) Acid orange 7, a monoazo dye (b) Congo Red, a diazo dye.

### 1.3.5 Azo dye usage and it's environmental impacts

At present there are over 2000 azo dyes used in industries for fabrics, printing inks, paints, varnish, lacquer and wood stains. The highest usage is in textile industry for dyeing the fabrics. The azo dyes are produced within the cellulosic fibres, by first impregnating the fibre with one dye component followed by treatment with the other component thus forming the dye. Since the dye is formed within the fibre it is very fast to washing and is widely preferred in the textile industry.

To dye 1 Kg of cotton fabric 150-200 litres of water is utilised by the dyeing factories. The fixation rate of azo dyes is as low as 50%, so the remaining dyes are disposed through the wastewater. There is an estimated  $2.8 \times 10^5$  tons of textile dyes discharged into the effluent water from textile industries worldwide (Jin et al., 2007). The coloured effluents affect transparency and aesthetic appearance of the water (Figure 1.6). The decrease in light penetration impacts the aquatic eco system and results in loss of biodiversity (de Aragao Umbuzeiro et al., 2005). Azo dyes have potential toxic effects on human health with certain azo dyes having nitro groups are known to be mutagenic (Chung and Cerniglia, 1992). The toxic, mutagenic effects of the dye may result from direct action of dye or from the aromatic/alkyl amines derived from their biotransformation.



**Figure 1.6:** Discharge of textile dyeing effluents in natural water bodies (<https://civildigital.com/pollution-control-in-dye-industry/>)

Typical effluent from textile industries have a COD ranging from 150-12,000 mg L<sup>-1</sup>, pH (7-12), salinity (1000-1600 mg L<sup>-1</sup> as chloride), colour (50-2500 on a Pt-Co scale), total nitrogen (70-80 mg L<sup>-1</sup>) and total suspended solids (15-8000 mg L<sup>-1</sup>) (Fernando, 2014). At present there are tough regulations in place to monitor the discharge of azo compounds into the environment. Consent discharge limits vary from country to country depending also on whether the discharge is to a sewer line or to a natural water body. In England, according to the Water Framework Directive the permissible limits for discharged water are: BOD (18.7 mg L<sup>-1</sup>), COD (24.6 mg L<sup>-1</sup>), ammonia (17.3 mg

L<sup>-1</sup>), phosphorous (63.3 mg L<sup>-1</sup>) (www.wfduk.org). In India the water quality standard for discharge set by the Central Pollution Control Board (CPCB) is 35 mg L<sup>-1</sup> for BOD, 250 mg L<sup>-1</sup> for COD, and 100 mg L<sup>-1</sup> for suspended solids (Murty and Kumar, 2011). Therefore, there are strict regulations in all the countries to treat the textile wastewater before discharging it into natural water bodies.

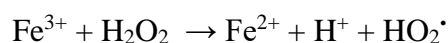
### **1.3.6 Current methods in treatment of textile wastewater**

Azo dyes are known to be xenobiotic compounds that possess electron withdrawing groups that generates electron deficiency thereby making them resistant to degradation (Singh et al., 2014). There are several physio-chemical and biological methods developed to treat azo dye containing wastewater. The methods used in the treatment of dyes are as follows:

#### **1.3.6.1 Chemical Methods**

##### **a. Advanced Oxidation Process (AOP)**

AOP produces a highly reactive, non-specific hydroxyl radical (OH<sup>•</sup>) capable of degrading organic substances in the wastewater. In photocatalytic oxidation process UV light is irradiated on a photocatalyst to induce oxidation of organic molecules. On photoexcitation the electrons jump from the valence to the conduction band leaving a hole (h<sup>+</sup>) in the valence band. The highly oxidative h<sup>+</sup> may directly react with the organics in wastewater or indirectly oxidise them through the formation of OH<sup>•</sup> radicals (Giménez et al., 1997). TiO<sub>2</sub> is commonly used for dyeing effluents due to its non-toxic, photochemical stability and highly reactive nature in the presence of UV irradiation. The other AOP is the Fenton's reaction, in which OH<sup>•</sup> radicals are produced by addition of H<sub>2</sub>O<sub>2</sub> to Fe<sup>2+</sup> salts. Hydrogen peroxide is added to an acidic solution (pH 2-3) of Fe<sup>2+</sup> to form the hydroxyl radicals.



The OH<sup>•</sup> radicals are powerful oxidisers and are capable of non-specific oxidation of the organic and inorganic substances in wastewater to reduce the COD, BOD. Fe<sup>3+</sup> reacts with H<sub>2</sub>O<sub>2</sub> to regenerate the Fe<sup>2+</sup> ions (Gogate and Pandit, 2004). It is used as a pre-treatment for decolourizing the dyeing effluents. Fenton's process involves four stages namely pH adjustment, oxidation, neutralization and coagulation for

precipitation of the organic substances. The major limitation of this method is the high requirement of acid and alkali to maintain the required pH, high sludge yield etc (Wang et al., 2011).

b. Sodium Hypochlorite (NaOCl)

NaOCl has been widely used in bleaching, disinfection and cleaning operation in food industry. In a solution at pH 5-10 NaOCl exists in equilibrium between two forms i.e. undissociated hypochlorous acid (HOCl) and the dissociated hypochlorite ion (OCl<sup>-</sup>) (Urano and Fukuzaki, 2005). HOCl confers the antimicrobial property whereas the OCl<sup>-</sup> is responsible for the cleaning efficiency. Urano and Fukuzaki, 2011 have observed the mode of action of NaOCl on decolourising azo dye Acid Orange 7. They have determined that the dissociated form of OCl<sup>-</sup> has high polarity which chlorinates the electron density azo linkage in the dye acid orange 7 leading to the decolourization of the dye. The undissociated form HOCl showed low reactivity with the dye due to its neutral charge (Urano and Fukuzaki, 2011).

c. UV light/H<sub>2</sub>O<sub>2</sub>

The photochemical degradation of dyes is favoured due to its complete mineralization while operating at mild temperature and pressure. UV light acts on H<sub>2</sub>O<sub>2</sub> to produce OH<sup>•</sup> free radicals which in turn attacks the azo bond in dyes (Yiqi Yang et al., 1998). It is highly efficient for contaminants that require high level of oxidation such as chlorinated hydrocarbons and inorganic substances (e.g. cyanides). When UV light hits H<sub>2</sub>O<sub>2</sub> it is cleaved to produce two hydroxyl radical per unit of radiation absorbed (Glaze et al., 1987).

The hydroxyl radical reacts with organic compounds to form organic radicals which then reacts with oxygen to produce peroxy radicals that initiates the thermal oxidation of the organic contaminants to less harmful products (Legrini et al., 1993). The major drawback in this reaction is the presence of Cl<sup>-</sup>, CO<sub>3</sub><sup>-</sup> in the water as they react with OH<sup>•</sup> and decrease the number of free radicals available for oxidation (Liao et al., 2001). Another limitation is that the molar extinction co-efficient of H<sub>2</sub>O<sub>2</sub> (19.6 M<sup>-1</sup>cm<sup>-1</sup>) is relatively small, therefore the UV light absorbed is less and the number of hydroxyl radicals produced is reduced (Glaze et al., 1987). Due to this high volume of H<sub>2</sub>O<sub>2</sub> are used which increases the cost of the treatment method.

#### d. Coagulation/flocculation

Coagulation is the addition of chemicals to the wastewater to alter the physical state of the particles in the water to form aggregated suspended solids. In flocculation, these aggregates are bridged together to form larger agglomerates that are then removed by sedimentation. In effluent treatment plants, coagulation is the most efficient pre-treatment method and is suitable for large molecular weight dyes and surfactants. The commonly used coagulants/flocculants are  $\text{FeCl}_3$ ,  $\text{Al}_2(\text{SO}_4)_3$ , cationic and anionic polyacrylamide etc. Golob et al, 2005 have observed that combination of a cationic flocculant and  $\text{Al}_2(\text{SO}_4)_3 \cdot 18\text{H}_2\text{O}$  produced best results (98% decolourization, 45% COD reduction) for dye baths that contain acid and reactive dyes (Golob et al., 2005). The drawback in this method is the production of sludge which poses disposal problems and it is less effective for dyes that are highly soluble in water (Anjaneyulu et al., 2005).

#### 1.3.6.2 Physical Methods

##### a. Adsorption

This method of decolourization does not involve any chemical reactions, is simple and economically feasible. This phenomenon is based on the intra-molecular forces (usually Van der Waals forces) of attraction between the solution and the highly porous solid adsorbent (Nageeb, 2013). Various factors influence the dye adsorption efficiency such as dye/sorbent interaction, pH, adsorbent surface area, adsorbent pore size, temperature etc (Crini, 2006). The different types of adsorbents used are activated carbon, peat, wood chips, fly ash and coal, silica gel. Activated carbon (AC) is the most commonly used adsorbent and is highly effective for acid, mordant, cationic dyes and less effective for VAT, disperse and reactive dyes. The major disadvantage of AC is that it is suitable only for particular type of pollutant and 10-15% of the sorbent is lost during its regeneration. In recent years natural substrates such as clay, corn cobs and rice hulls are used to replace activated carbon. They are available readily and their decolourization efficiency is equivalent to that of AC (Robinson et al., 2001).

## b. Membrane Filtration

One of the most commonly used and important method in wastewater treatment is the ultrafiltration (UF), nanofiltration (NF) and reverse osmosis (RO) process. These involve passing water at high pressure through microporous membranes for filtration and purification. UF is the first stage of filtration to remove the suspended solid particles and insoluble dyes from the water. The pore size of UF membranes are 0.01 microns. NF membranes have pore size ranging from 0.5-2.0 nm and are capable of filtering out organic substances, viruses and salts in the wastewater (Liang et al., 2014). UF and NF require significantly low pressure compared to RO membranes. RO is highly effective for removing the total dissolved solids (TDS) to reduce the hardness of the water and is the last process employed in effluent treatment plants. The pore size of RO membrane is 0.1 nm and it removes all microorganisms in the water. RO is used widely in water filters for purifying drinking water. The disadvantage of these methods is the high cost of membranes, fouling and the water requires extensive pre-treatment (Robinson et al., 2001). There is 40% water wastage during the RO process.

### 1.3.6.3 Biological Methods

Biological methods are widely used in treating textile effluents to reduce the amount of chemicals and to develop eco-friendly water treatment systems.

#### a. Bacteria

Activated sludge is the widely used process in textile treatment plants to reduce the COD and BOD but it is less efficient in removing the colour from dyeing effluents. Dye degradation takes place in aerobic and anaerobic conditions and the mechanism varies under each condition. Due to the recalcitrant nature of the dyes they are resistant to bacterial degradation under aerobic conditions. The azo dye degradation by bacteria in anaerobic conditions takes place by the reductive cleavage of the N=N bond and involve different mechanisms using enzymes, redox mediators and reduction by sulphides etc (Pandey et al., 2007) (Figure 1.7).

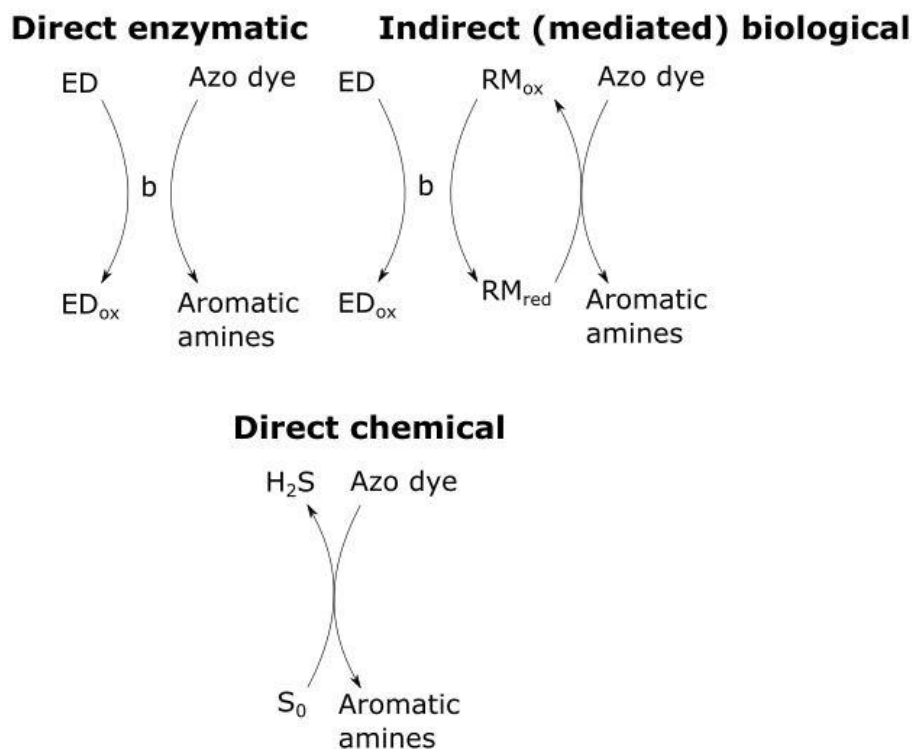


**Figure 1.7:** Mechanisms of dye degradation by bacteria under anaerobic conditions (Pandey et al., 2007).

The bacteria degrade the azo dyes in two stages and there is two electron transfer mechanism at each stage to the azo dye that acts a final electron acceptor (Saratale et al., 2011) . The mechanism involves flavin dependent reductase that act as electron shuttle between nicotinamide adenine dinucleotide phosphate (NADPH)-dependent flavoproteins and the azo dyes that results in dye reduction. These were classified as flavin dependent azo reductase enzymes (dos Santos et al., 2007). It is suggested that the azo dye decolourization may be a fortuitous one in which the dye acts as electron acceptor during the electron transport chain (Russ et al., 2000). Since azo dyes are large and usually charged, they are likely to be reduced extracellularly or with membrane bound enzymes. Bacteria that are capable of decolourizing the dyes under anaerobic and microaerophilic environments are *Klebsiella* sp., *Bacillus* sp., *Pseudomonas aeruginosa*, *Enterobacter* sp., *Pseudomonas* sp., *Morganella* sp. (Barragán et al., 2007; Sarayu and Sandhya, 2012). These bacteria are incapable of utilizing dye as the sole carbon source and require additional carbon source as electron donor for dye decolourization.

Redox mediators are known to increase the rate of electron transfer from the bacteria to the azo dye. Flavin derivatives such as riboflavin, FAD, FMN and quinone

compounds such as anthraquinone-2,6-disulfonate (AQDS), anthraquinone-2-sulfonate (AQS) have been studied as redox mediators for azo dye decolourization. The redox potential for the redox mediators determines the efficiency and rate at which it transfers electrons. Most redox mediators have a redox potential ranging from -200 mV to -350 mV and the more negative it is the greater the potential for dye decolourization (Saratale et al., 2011). The rate of azo dye Reactive Red decolourization was enhanced 3.7-fold with addition of 25  $\mu$ M AQDS as redox mediator in a one stage anaerobic sludge reactor (Rodrigues da Silva et al., 2012).

Another mechanism is the non-specific extracellular reactions occurring between reduced compounds of anaerobic metabolism e.g. sulphides. Inorganic compounds such as sulphide, ferrous ion formed as end metabolites can decolourize the dye extracellularly. It was observed that sulphate reducing bacteria (SRB) decolourized Congo red azo dye extracellularly while producing H<sub>2</sub>S (Diniz et al., 2002).

Few organisms when acclimated with the dye for a period of time, grow aerobically on dye as sole carbon source and utilise the degradation products for their energy and growth. *Pseudomonas* sp. KF46 and *Pseudomonas* sp. K24 can grow aerobically on azo dye Orange I and Orange II (Blumel et al., 2001). The limitation is that these species cannot utilize other dyes (sulfonated) and is limited to the specific dye used for their acclimatization.

The degradation of aromatic amines under aerobic environment is favoured as the bacteria possess enzymes that can degrade them. A standalone aerobic or anaerobic system cannot completely mineralize the dyes. A sequential anaerobic/anaerobic coupled system is required for complete breakdown of the aromatic amines. Eustace et al, 2014 have observed that the anaerobic/aerobic sequential reactor can completely degrade acid orange 7 dye (AO7) into less toxic products compared to a single anaerobic system (Fernando et al., 2014).

#### b. Fungi

There are wide varieties of fungal species used for bioremediation and they are more efficient than bacteria in degrading dyes. White rot fungi such as *Trametes versicolor*, *P. chrysosporium*, have been studied extensively for their dye degrading properties (Gomaa et al., 2008; Casas et al., 2009; Yang et al., 2017). Fungal bioreactors have been developed by immobilizing the fungal mycelia in continuous packed-bed

bioreactor, fed batch and continuous fluidized-bed bioreactor to test for decolourization of Orange II dye. All three reactors were efficient in decolourizing the dye and were suitable for long term operation (2 months). However the use of fungi for continuous reactors is limited due to poor mass transfer a result of mycelia clogging the reactor bed (Zhang et al., 1999). The maintenance of aseptic condition is required as bacterial contamination, which tends to grow faster than fungi, will inhibit the fungal action (Sen et al., 2016). Their extracellular enzymes namely laccase, manganese peroxide and lignin peroxidase are capable of non-specific degradation of a wide range of dyestuff. The use of the enzymes reduces the need for nutritional supplements and decreases the substrate diffusion limitation caused by the bacterial cells (Jin et al., 2007). Laccase in particular is known for its complete degradation of dyes and their aromatic amines (Chivukula and Renganathan, 1995; Tauber et al., 2005).

The above methods have shown to be effective but there are several limitations in terms of environmental impact, energy consumption and cost. The chemical methods utilise large quantities of chemicals, produce high volumes of sludge and the end products from these reactions are unpredictable (dos Santos et al., 2007). Adsorption on activated carbon is the most popular and highly effective treatment for wastewater containing dyes. The major disadvantage is the high cost of regeneration of the adsorbent and the method is less effective against disperse, reactive and direct dyes (Robinson et al., 2001). Membrane separations remove all types of dyes and produce high quality effluent but the membranes suffer from limited lifetime, the process of fouling and the periodic replacement is not cost effective (Wu et al., 1998). Biological treatment methods have environmental benefits and offer economic advantage over the physicochemical methods. Wild type strains are incapable of assimilating large dye molecules under aerobic conditions and therefore dye remains unaffected. Although genetically modified (GMO) bacteria act on the dye under microaerophilic conditions (Pandey et al., 2007), these GMOs are not regulated for use outside laboratory settings.

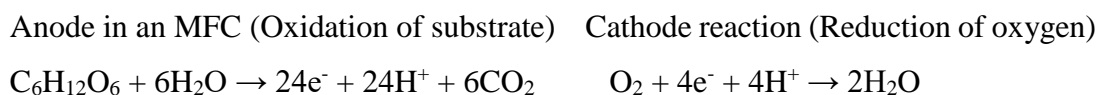
### **1.3.7 Bio electrochemical systems and wastewater treatment**

From the above discussion it is apparent alternative wastewater treatment methods that are cost effective and eco-friendly must be explored. In recent years, bioelectrochemical systems such as microbial fuel cell (MFC) and microbial

electrolysis cell (MEC) have shown great promise in not only wastewater treatment but also in power production (Logan et al., 2006).

The concept of bioelectrochemical system dates to 1911 when M.C. Potter discovered that microbes utilise organic substances and produce energy in the form of electricity (Potter, 1911). Further development was carried out in 1931 by Cohen who observed the potential difference between various microorganisms and built a battery that produced 2 mA of current from 35 volts (Cohen, 1931). In a period of 50-60 years there were few discoveries based on renewable energy from organic waste, the use of mediators to shuttle electrons from inside the cell to the electrodes. In the late 1990's, with the discovery of extracellular electron transfer (EET) there was significant interest in this field and work on BES had started to increase. The demonstration of the mechanism of EET by microorganisms in the absence of mediators to produce electric current spurred the onset of microbial fuel cell studies (Kim et al., 1999).

An MFC consists of an anode and cathode connected by an external circuit and separated by a cation exchange membrane (Figure 1.8). The microorganisms present at the anode metabolise the organic matter to produce protons and electrons. These electrons and protons are transferred to the cathode via electrode and cation exchange membrane where they combine with oxygen to form water in the presence of a catalyst. Microorganisms such as *Shewanella*, *Geobacter*, *Rhodospirillum rubrum* are exoelectrogens that can form biofilms on the electrode without any mediators (Logan et al., 2006) (Figure 1.8). At the cathode there are metal based catalyst such as platinum, gold, titanium; chemical catalysts - potassium ferricyanide, potassium bromate; biological catalysts - bacteria, fungi, enzymes that carry out oxygen reduction reaction (ORR). An example of reactions at anode and cathode of MFC is given below.



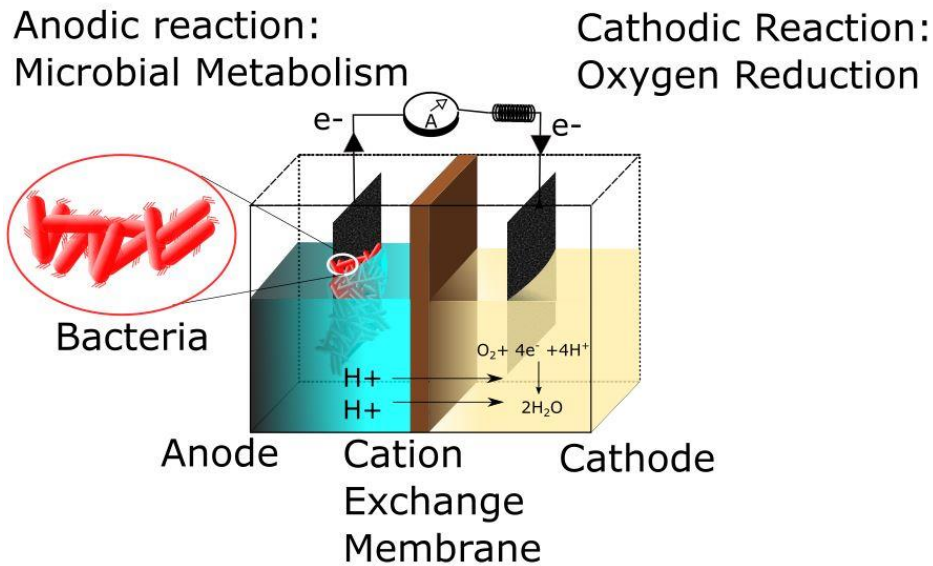


**Figure 1.8:** Schematic representation of a microbial fuel cell depicting bacteria at the anode and the ORR at the cathode

Microbial electrolysis cell (MEC) is similar technology to MFC but instead of an external load, power is supplied to the system to drive the reaction. MECs are studied for producing hydrogen and methane which can serve as an alternative to fossil fuels. They may also be used to treat pollutants such as azo dyes, chlorinated hydrocarbons, metal ions etc. (Logan et al., 2006).

### 1.3.7.1 Internal losses in MFC

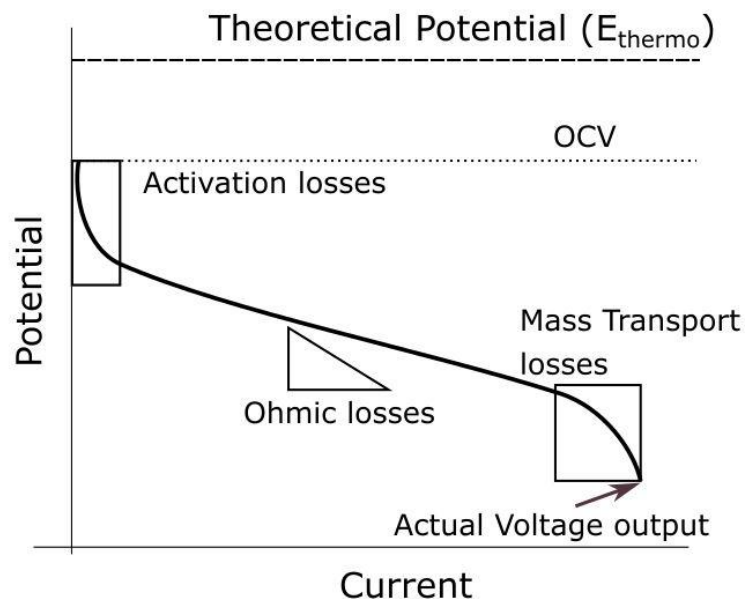


**Figure 1.9:** The voltage vs current plot depicting the potential losses occurring in a MFC compared to the theoretical potential (Modified from (Rismani-Yazdi et al., 2008)).

In a fuel cell the theoretical efficiency is calculated to be 100% at standard temperature and pressure. In practice it cannot reach the calculated theoretical values due to the number of potential losses encountered while running a MFC. The polarisation curve depicts the three typical losses occurring in a MFC (Figure 1.9).

#### **a. Activation Losses**

In any reaction there is an initial activation energy barrier that needs to be overcome for the reaction to proceed. To overcome this energy barrier, current is drawn from the fuel cell by the reactants present at the anode and cathode. The potential loss due to activation of the reactions is called activation losses or activation overpotentials (Rismani-Yazdi et al., 2008). At the anode during oxidation reaction these losses occur at electrode surface when electrons are transferred to and from the bacterial cell via mediators or electron shuttles. These losses are dominated at low current densities and increase exponentially as current increases (Figure 1.9). The activation loss can be reduced by increasing the temperature or the electrode surface area and employing enriched biofilms (Logan et al., 2006).

In the cathode the losses are a result of catalyst present that accepts electrons from the electrode for oxygen reduction reaction. A number of metal cathode catalysts have high activation overpotentials thus causing major limitation in a MFC (Kodali et al., 2017). To improve cathode reactions catalyst with low overpotentials should be developed.

#### **b. Ohmic Losses**

The ohmic loss is the resistance to flow of electrons through the electrodes and electrode interconnections and ions through the ion exchange membrane or electrolyte. This loss can be minimized by decreasing the electrode spacing, increasing the electrolyte conductivity and good electrical interconnections (Logan et al., 2006). An efficient reactor design can drastically reduce the ohmic loss.

#### **c. Concentration/mass transport losses**

These losses occur due to the mass transfer limitation of the reactants to and from the electrode and due to the development of concentration gradients near the surface of the electrodes (Fernando, 2014). This results in reactant depletion or product accumulation that prevent diffusion of electrons and ions (Rismani-Yazdi et al., 2008).

Concentration losses occur at high current density and they can be minimized by proper mixing of the bulk electrolyte. This is a major loss at the cathode due to the low oxygen solubility in aqueous solutions. The mass transfer of oxygen to the electrode surface is slow and contributes to the loss in voltage (Erable et al., 2012).

### 1.3.7.2 Electron transfer mechanisms in MFCs

Electron transfer plays a vital role in electricity production in an MFC. The transfer mechanisms at the anode and cathode depends on the substrate, catalyst, mediator etc. (Figure 1.10). The figure below illustrates the type of electron transfer mechanisms at the anode and cathode of MFC.

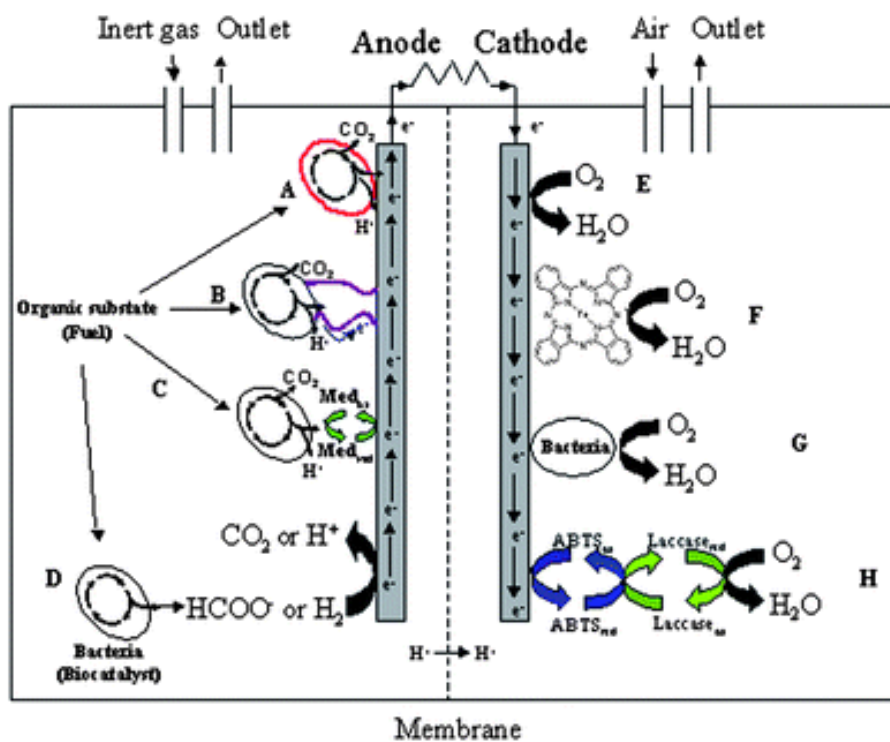


**Figure 1.10:** Possible mechanisms for bacterium/anode electron transfer and oxygen reduction at cathode. (A) Direct transfer through cytochromes; (B) Electron transfer through “nanowires” or pili; (C) Through redox mediators; (D) Direct oxidation of excreted catabolites (e.g. formate, H<sub>2</sub>, etc.) (E) Direct reduction of oxygen to water, commonly platinum electrode; (F) Through catalysis at an electrode modified by e.g. transition metal complex catalysts; (G) Bacterial catalysis; (H) Through an enzymatic catalyst with mediator (e.g. laccase + ABTS) (Schuetzle et al., 2009).

## a. Anode

The two types of electron transfer mechanism from the bacteria to the electrodes are direct electron transfer and mediated electron transfer.

### i) Direct Electron Transfer

The direct electron transfer is carried out by bacteria such as *Shewanella sp.*, *Geobacter sp.* and *Rhodospirillum rubrum* through extracellular cytochromes or nanowires known as 'pili'. These bacteria conduct electrons transfer to the electrode via extracellular membrane bound cytochromes (Bond et al., 2012). *Shewanella oneidensis* MR1 is the most widely studied organism for its EET pathway. It has been observed that the Mtr pathway comprising of five protein complexes namely CymA, MtrA, MtrB, MtrC, and OmcA is responsible for the electron transfer to the surface of the anode in a MFC (Kouzuma et al., 2015). The other type of DET observed in both *G. sulfurreducens* and *S. oneidensis* is through conductive appendages that are called nanowires or 'pili' (Reguera et al., 2005; Gorby et al., 2006). These bacteria form biofilm on the electrode surface and the composition and thickness of biofilm is directly dependent on the power output.

### ii) Mediated Electron Transfer

Before the discovery of DET, mediators were added externally to aid the shuttling of electrons from the bacterial cell to the electrode surface. These exogenous electron shuttles were neutral red, methylene blue, anthraquinone-2,6-disulfonic acid (AQDS) and anthraquinone-2-sulfonic acid (AQS) (Park et al., 2000; Aeschbacher et al., 2010). The production of natural endogenous electron mediators by the bacteria was discovered by (Rabaey et al., 2005). *Shewanella* was observed to produce flavins and *P. aeruginosa* to produce pyocyanin as mediators that facilitate the electron transfer (Rabaey et al., 2005; Marsili et al., 2008). Another method of redox mediator production is the oxidation of the catabolites (eg. H<sub>2</sub>, formate). Schroder et al, produced hydrogen gas from *E. coli*, the H<sub>2</sub> was then re-oxidized at a polyaniline modified platinum catalyst electrode and produced a current density of 1.5 mA cm<sup>-2</sup> (Schröder et al., 2003).

The exact mechanism of electron transfer is a controversy as it is not clear whether it is through nanowires, cytochromes or endogenous mediators.

## b. Cathode

The electrons and protons from the anode are transferred to the cathode where they are reduced to water by oxygen. The oxygen reduction reaction (ORR) at the cathode is a limiting factor in a MFC due to high overpotentials on the electrode and partly due to oxygen mass transfer limitation in the cathode.



There are various metal-based catalysts that carry out the ORR at the cathode in a microbial fuel cell.

### i) Direct oxygen reduction by noble metal-based catalysts

Platinum was the most commonly used cathode catalysts in fuel cells due to its low over potential and to improve the ORR. For decades, considering its superior performance platinum is the benchmark for all cathode catalyst comparisons. The standard redox potential of platinum is 1.2 V vs SHE which is close to that of oxygen, thus making Pt the favourable catalyst for ORR. Logan et al, 2005 demonstrated that Pt-MFC produced a power density of 33 mW m<sup>-2</sup> compared to 3.4 mW m<sup>-2</sup> for MFC with plain carbon electrode (Logan et al., 2005a). The power was further increased to 480 mW m<sup>-2</sup> in a single chamber MFC consisting of Pt catalyst prepared by Nafion binder (Cheng et al., 2006). Although platinum produces good power output the high cost and low sustainability hinders the scaling up of MFCs. Gold coated copper (Cu-Au) wires have been utilized as cathode catalyst in a MFC to treat wastewater and obtained a power density of 2.9 mW m<sup>-2</sup> (Kargi and Eker, 2007). The use of gold, silver electrodes is not economically feasible for large scale water treatment MFCs.

### ii) ORR by Metal Oxide catalysts

In recent years there has been a transition to PGM (Platinum Group Metals) free catalysts for oxygen reduction reactions with transition metal compounds impregnated with Nitrogen doped Carbon (N-C) serving as a good replacement for Pt. Transition metals such as Fe, Mn, Co and Ni in their salt forms have been infused with precursor aminoantipyrine (AAPyr) and used as cathode catalysts in MFC. AAPyr is an organic precursor rich in carbon and nitrogen. The maximum power density obtained was highest for Fe-AAPyr with 251 mW cm<sup>-2</sup> followed by 196 mW cm<sup>-2</sup> (Co-AAPyr), 171 mW cm<sup>-2</sup> (Ni-AAPyr) and 161 mW cm<sup>-2</sup> (Mn-AAPyr) (Santoro et al., 2015; Kodali et

al., 2017). Trace (1.05%) levels of Fe was impregnated with nitrogen doped carbon (NC) and observed electrochemically that the ORR activity of Fe-N/C matched that of Pt/C (Rincón et al., 2014). The same group have used macrocyclic complex ( $MnN_4$ ,  $CoN_4$ ) infused with nitrogen doped carbon (NC) to study the oxygen reduction reaction (ORR) and oxygen evolution reaction (OER). Metal macrocyclic compounds contain a central metal ion surrounded by four nitrogen ( $N_4$ ) atoms. They observed that  $Mn_xO_y/NC$ ,  $Co_xO_y/NC$  catalysts produced very low over potential and were efficient ORR and OER catalyst compared to Pt,  $RuO_2$  and  $IrO_2$  (Masa et al., 2014). The possible leaching of the metal into wastewater, their toxicity and the environmental impacts should be taken into consideration when using metal based catalysts (Yuan et al., 2016).

### iii) Chemical catalysts as terminal electron acceptors

Apart from oxygen chemicals such as potassium ferricyanide, permanganate, bromate have been used as electron acceptors at the cathode of double chambered MFCs. Ferricyanide used as catholyte increased the power by a factor of 1.5 -1.8 compared to oxygen alone with a Pt-carbon electrode in an MFC. This was due to the increase in efficiency of mass transfer and large cathode potential (Oh and Logan, 2006) . The redox potential of ferricyanide ( $E^\circ \sim 436$  mV vs SHE) is not as high as platinum but it has low over potentials, thereby increasing the speed of the reaction and producing high power output. However for practical applications ferricyanide is not economical, is toxic and difficult to recycle (Ucar et al., 2017).

Potassium permanganate is another chemical catholyte used in MFCs owing to its high redox potential of  $E^\circ \sim 1.52$  V vs SHE. You et al, 2006 have observed a power density of  $115.60$  mW  $m^{-2}$  for permanganate catholyte compared to  $25.62$  mW  $m^{-2}$  for hexaferrocyanate and  $10.2$  mW  $m^{-2}$  for oxygen alone. Similar to all soluble catholytes it requires constant replenishment and is therefore not suitable for large scale applications (You et al., 2006).

### 1.3.7.3 Microbial fuel cells in dye treatment

MFC are extensively explored for treatment of dye containing wastewater and simultaneous electricity production. The major advantages of MFC compared to the conventional wastewater treatment methods are 1) Potential for power production rather than power consumption 2) Low sludge yield 3) Operates at mild temperatures



with air cathode (Hou et al., 2011a). The synergy between the different microorganisms present in wastewater and sludge also increase the power output.

Various substrates used in the anode include glucose, acetate, lactate, cysteine, ethanol (Logan et al., 2005b; Kim et al., 2007; Manohar and Mansfeld, 2009). Cao et al, 2010 investigated the effects of using glucose, ethanol and acetate as substrates for degradation of Congo Red in a single chamber MFC with air cathode. They had observed that glucose produced the maximum power density of  $103 \text{ mW m}^{-2}$  with 98% decolourization of the dye (Cao et al., 2010). The effect of co-metabolism to degrade azo dyes have been studied by Fernando et al, 2012. Cheap co-substrates such as rapeseed cake, molasses, corn steep liquor were used with sodium pyruvate as the primary carbon source to observe the decolourization kinetics of Acid Orange 7 dye by *Shewanella oneidensis*. The rate of decolourization (>90% in 30 hours) was high in the presence of the co-substrates (Fernando et al., 2012). The process of decolourization is a fortuitous one, carried out during the biotransformation of the co-substrates.

Wastewater from breweries, textile plants, meat processing plant, food processing, swine waste etc were also used for their organic content (Min et al., 2005; Oh and Logan, 2005; Heilmann and Logan, 2006; Feng et al., 2008).

There are certain redox mediators used to accelerate the electron transfer for reduction of the azo dyes and other pollutants in the wastewater. Redox mediators such as riboflavin and humic acids were electrodeposited on polypyrrole graphite electrodes in MFC containing anaerobic: aerobic sludge to study the effect of Congo red decolourization. The redox mediators modified electrode decreased the internal resistance by 31% to 49% and increased the power output by 20% to 66%, depending on the concentration of the mediators, compared to bare graphite electrode (Huang et al., 2017). Although the redox mediators are effective in enhancing the wastewater treatment, they are quite expensive to use in real time applications.

#### **b. Cathode dye treatment**

Since the anode dye treatment could only decolourize the dye others have utilized it at the cathode to determine if complete degradation could be obtained with dye being the terminal electron acceptor.

Dye decolourization at the cathode was studied with graphite electrodes in a microbial electrolysis cell. A 0.012 KWh power was applied to the cathode to cleave the azo bond of Acid Orange 7 dye and decolourize it to form aromatic amines. The azo dye is reduced by accepting electrons and protons from the anode (Mu et al., 2009). The possibility of using azo dyes as the electron acceptor in the cathodes was experimented by (Liu et al., 2009). The dye received electrons from the respiration of *K. pneumoniae* strain L17 in the anode in the absence of oxygen in the cathode. As a result, the -N=N- double bond was broken down and the dye decolourized. There was complete reduction of Methyl Orange, Orange I, Orange II dye to aromatic amines in three days with peak power density of 34.77 mW m<sup>-2</sup> (Liu et al., 2009). To decrease the internal resistance and increase dye decolourization modified tubular type MFC was designed. Various concentrations (0.14 mM to 2 mM) of AO7 dye was fed to the cathode to observe the rate of decolourization. The dye acted as terminal electron acceptor and there was rapid decolourization with >90% in 12 h and the overall decolourization was >98% (Kong et al., 2013). The electron transfer between the electrode and dye was enhanced by modifying the electrode with redox mediators with thionine and AQDS to observe the decolourization of methyl orange dye. Thionine modified system increased the rate of decolourization by 20% and power density by three times compared to unmodified system (Liu et al., 2011).

In a MFC the dye can be decolourized under anaerobic conditions at anode in the presence of microorganisms or at the cathode by accepting electrons and protons from the fuel cell. In both the mechanisms there is only dye decolourization and not complete degradation. Therefore, an aerobic treatment is required for complete degradation of the dye. The advantage of anode dye decolourization is the presence of aerobic cathode can improve the power production in MFC compared to anaerobic cathode conditions (Liu et al., 2009; Li et al., 2010). This is due to the high reduction potential of oxygen (1.23 V).

To achieve the complete degradation of azo dye and produce electricity an MFC was combined with Fenton like advanced oxidation process. There was 89% AO7 degradation with a power density of 16 mW m<sup>-3</sup> and GC-MS analysis of AO7 degradation indicated the presence of benzaldehyde and phenol- based intermediates which can be further mineralized to CO<sub>2</sub> and H<sub>2</sub>O by Fenton's oxidation. Although the

performance of  $\text{FeVO}_4$  is excellent, the reusability after each cycle is a major hindrance in practical applications (Luo et al., 2011).

Chemicals such as Fe-EDTA, persulphate, potassium ferricyanide have been used as catholytes in aiding azo dye decolourization. Orange G dye achieved a decolourization efficiency of 97% and maximum power density of  $91.1 \text{ mW m}^{-2}$  with Fe-EDTA and potassium persulphate as the cathode solution and glucose as substrate at the anode (Niu et al., 2012). In large scale industrial applications chemicals are expensive and their reaction are not sustainable.

### **1.3.8 Biological catalysts**

The methods discussed above for azo dye treatment were effective in only decolourizing the dye and not complete degradation. The complete degradation of the azo dye-containing wastewater in a more efficient, sustainable and eco-friendly manner is required for its safe disposal into water streams. To efficiently degrade azo dyes and develop cheap alternatives to platinum, biological catalysts (e.g. enzymes, microorganisms) are investigated for their use in the cathode of MFCs to carry out oxygen reduction reaction and dye degradation.

In recent times, enzymes and microorganisms are being explored for their catalytic efficiency due to the eco-friendly nature and sustainability. Enzymes such as peroxidases (Manganese peroxidase (MnP), lignin peroxidase (LiP), horse radish peroxidase) and oxidases (laccase, bilirubin oxidase, ascorbate oxidase) have been used for fuel cell and bioremediation applications (Fernández, 2011; Durand et al., 2012; Falade et al., 2017). MnP and LiP are widely used for lignin degradation in paper and pulp industry and for degradation of synthetic dyes. HRP is efficient in removal of phenols and aromatic amines from industrial effluents (Regalado et al., 2004). However, these peroxidases cannot be used as cathode catalyst in a fuel cell as they require  $\text{H}_2\text{O}_2$  that is expensive for water treatment and fuel cell applications.

Bilirubin oxidase (BOD) and laccase are blue copper proteins that have been used in fuel cell and bioremediation applications (Liu et al., 2009; Madhavi and Lele, 2009; Szczupak et al., 2012). Laccase is widely preferred for industrial application due to the high redox potential ( $780 \text{ mV}/690 \text{ mV}$  vs SHE for BOD), high catalytic activity, wide substrate specificity and easy protein engineering. It is easily produced by large number of fungal sources and can be upscaled for large scale applications.

### 1.3.8.1 Laccase Enzyme

Laccases (EC 1.10.3.2, oxidoreductases) are extracellular enzymes that belong to a family of multicopper oxidase that also include ascorbate oxidase, ceruloplasmin and bilirubin oxidase. They are found in higher plants, fungi, insects and few bacteria. The first laccase was discovered in 1883 in the sap of Japanese lacquer tree, *Rhus vernicifera* by Yoshida. The presence of laccase in fungi was revealed in 1889 by Bertrand and Laborde and since then they have been found in various fungal sources (Ascomycetes, Basidiomycetes and Deuteromycetes) especially in white rot fungi that degrade lignin (Upadhyay et al., 2016). The most common wood rot fungi that produce laccase are *Trametes versicolor*, *Pycnoporus cinnabarinus*, *Trametes hirsuta*, *Trametes villosa*, *Pleurotus ostreatus* etc. There are few bacteria such as *Bacillus subtilis*, *Azospirillum lipoferum* etc that produce the enzyme (Madhavi and Lele, 2009).

Laccase enzymes have a molecular weight ranging from 60-100 KDa and exist as monomers or homodimers with an isoelectric point ranging from 3 to 7 (Figure 1.12). Most fungal laccases have a pH optimum ranging from 3.6 to 5.

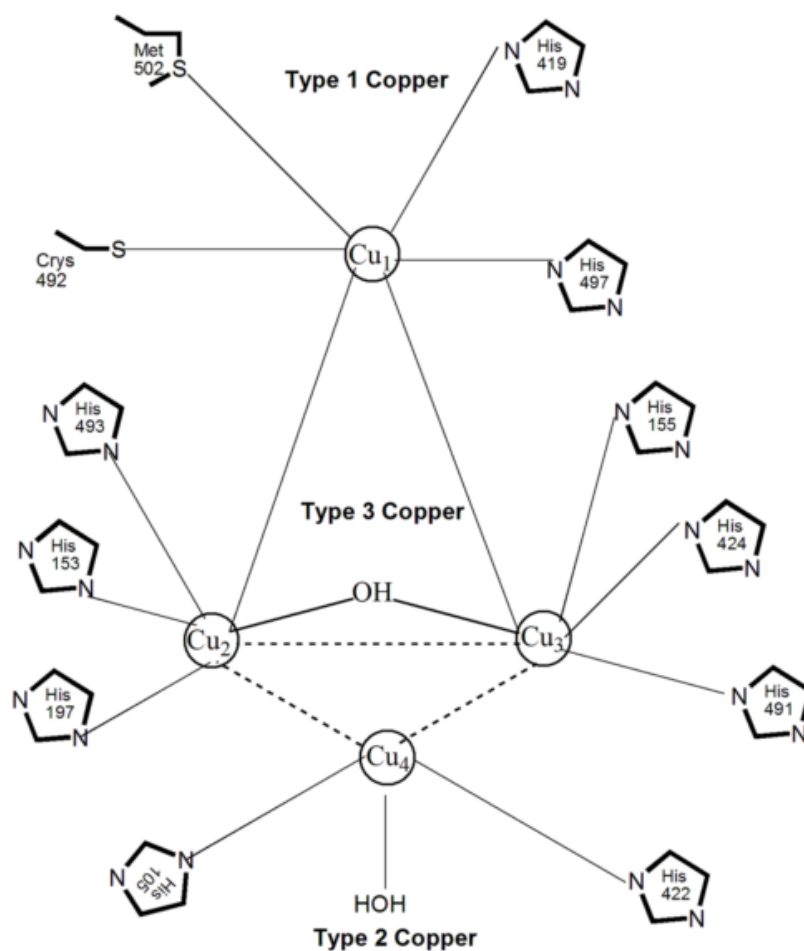


**Figure 1.12:** Structure of Laccase indicating the  $\text{Cu}^{2+}$  active sites (Christopher et al., 2014)

Laccase catalytic centre contains four copper atoms distributed in three redox sites (Figure 1.12). The Type 1  $\text{Cu}^{2+}$  confers the blue colour of the protein in its reducing state, where the oxidation of substrate takes place. The electrons from oxidation is transferred from T1  $\text{Cu}^{2+}$  to the Type 2/Type 3  $\text{Cu}^{2+}$  cluster where oxygen is reduced to water. Laccase is capable of one electron oxidation of other substrates and four electron reduction of  $\text{O}_2$  to  $\text{H}_2\text{O}$  (Fernández, 2011).

In native form of enzyme all four copper atoms exist in fully oxidized state ( $\text{Cu}^{2+}$ ) (Christopher et al., 2014). The redox potential of T1 Cu site is higher for fungal laccase (780 mV vs SHE) compared to plant (430 mV vs SHE) and bacterial laccases (455 mV vs SHE) (Kunamneni et al., 2007). Due to the high redox potential there are wide range of substrates that include phenols, aromatic amines and other environmental pollutants. The enzyme acts directly to oxidise phenolic substrates whereas it requires

mediators for non-phenolic substrates. In nature, laccase is used by white rot fungi in the breakdown and complete degradation of lignin. Laccase mechanism of oxidation of its natural substrates such as phenolic compounds is given below (Figure 1.13).

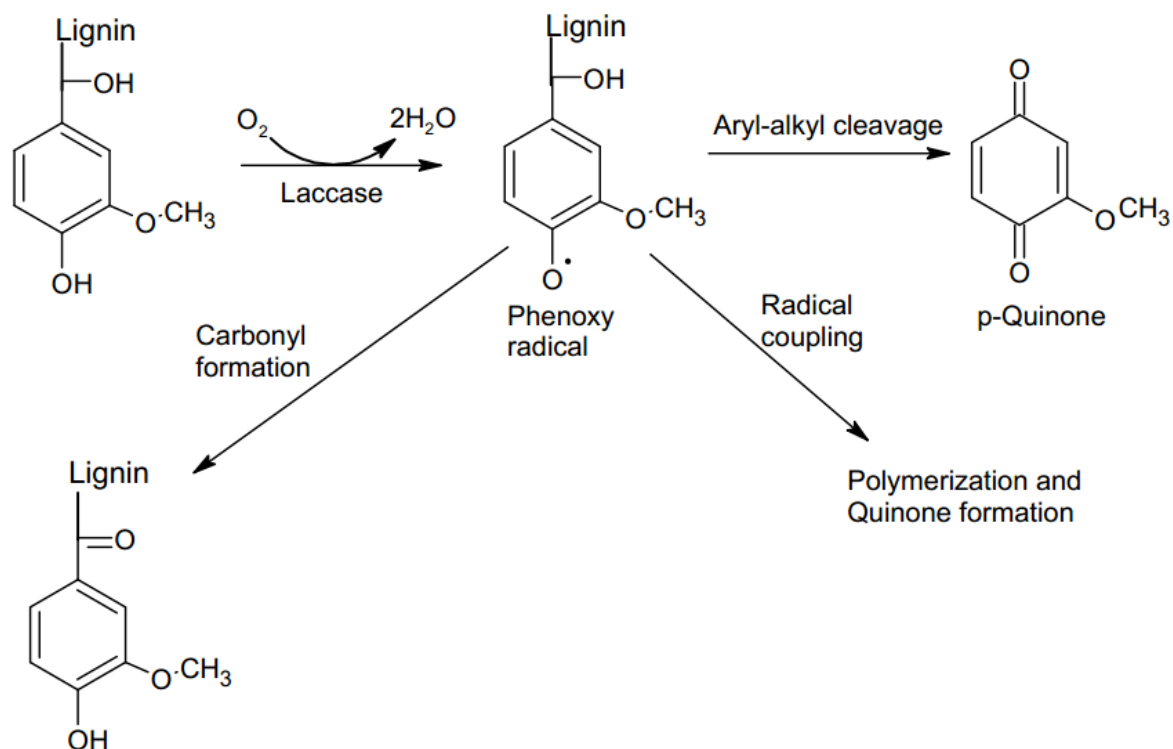


**Figure 1.13:** Mechanism of laccase oxidation of lignin by producing phenoxy radicals and quinones (Modified from (Madhavi and Lele, 2009))

Laccase attacks the phenolic subunits leading to  $C\alpha$  oxidation,  $C\alpha-C\beta$  cleavage and aryl-alkyl cleavage. The oxidation of substrates involves loss of a single electron and production of phenoxy radicals (Figure 1.13). These radicals are unstable and further bring about a variety of reactions such as non-specific bond cleavage, radical polymerization, modification of functional groups etc. leading to complete oxidation of substrate and subsequent reduction of water to complete the catalytic cycle (Madhavi and Lele, 2009). Redox potential between T1 copper site in laccase and the substrate is plays a vital role in efficient oxidation and laccases with higher redox potential than the substrates have higher rate of oxidation.

Laccase has been widely studied in the past decades for application in food industry, textile industry, paper and pulp industry, bioremediation and as biosensors (Upadhyay et al., 2016).

### **1.3.8.2 Laccase application in treatment of dyes**

Laccase enzyme has been employed in textile industry for bio-bleaching of cotton fabrics, roving treatment to improve the yarn regularity, anti-shrink treatment of wool, improving the dye fixation on wool etc (Couto and Toca-herrera, 2006). Laccase was also used in denim garments to obtain a stone wash finish where the excess indigo is removed from the fabrics. Phenol induced laccase from *T. versicolor* was very effective to obtain stone washing finish for denim garments in the absence of mediators (Pazarloğlu et al., 2005).

The major application of the enzyme is its ability to decolourize and degrade dyes present in the textile wastewater. Most commonly used laccase is of fungal origin but there are also few bacterial laccases reported. Laccase can oxidise both phenolic and non-phenolic dyes directly, therefore it acts on a variety of dye chromophore groups such as azo, anthraquinone, triarylmethane, indigoid etc. Purified laccase from fungus *T. hirsuta* was used to treat textile effluents containing azo, anthraquinone, triarylmethane, indigoid dyes etc. The effluents were decolourized, and their toxicity reduced by 80% making it suitable for reuse the water for dyeing purposes (Abadulla et al., 2000). Isolated laccase enzymes and their various fungal sources have been used for textile water treatment (Table 1.1). White rot fungi *Coriolus versicolor* was able to decolourize 14 different structured dyes with decolourization >80% for 10 dyes (Knapp et al., 1995). There is a combination of enzymes such as manganese peroxidase, lignin peroxidase and laccase acting on the dye while using the fungal source. The major disadvantage of using fungi is the need for maintaining aseptic conditions and it requires constant replenishment of media.

**Table 1.1:** The types of dyes treated with laccase from different fungal sources

<b>Laccase Source</b>	<b>Dye Treated</b>	<b>References</b>
<i>T. hirsute</i>	Triarylmethane, indigoid, azo, and anthraquinonic dyes	(Abadulla et al., 2000)
<i>T. versicolor</i>	Acid orange 7 (AO7), acid blue 74 (AB74), reactive red 2 (RR2) and reactive black 5 (RB5)	(Ramírez-Montoya et al., 2015)
<i>T. villosa</i>	Azo dye: 3-(4-dimethylamino-1-phenylazo) benzenesulfonic acid (dye I) and 3-(2-hydroxy-1-naphthylazo) benzenesulfonic acid (dye II)	(Zille et al., 2005)
<i>Pycnoporus cinnabarinus</i>	Azo dye -direct blue	(Schliephake et al., 2000)
<i>Pleurotus ostreatus</i>	Triphenylmethane Dyes, anthraquinone dye	(Hou et al., 2004; Yan et al., 2009)
<i>Trametes pubescens</i>	Anthraquinonic AB62, RB19, Azoic AB194, Acid Red 266, and Acid Yellow 49, reactive dyes	(Spina et al., 2016; Casieri et al., 2008)
<i>Coriolopsis gallica</i>	Remazol Brilliant Blue R (RBBR), Reactive Black 5 (RB5) and Bismark Brown R (BBR)	(Daâssi et al., 2014)
<i>Pycnoporus sanguineus</i>	Reactive blue 4 and Orange G	(Atteke et al., 2013)
<i>Paraconiothyrium variable</i>	Bromophenol blue, commassie brilliant blue, pansou-S, Rimazol brilliant blue R, Congo red, and methylene blue	(Forootanfar et al., 2012)

<b>Laccase Source</b>	<b>Dye Treated</b>	<b>References</b>
<i>T. modesta</i>	Acid blue, Acid violet, Basic red, Direct blue, reactive black, Triphenylmethane Dyes, heterocyclic azo dye, indigo carmine	(Kandelbauer et al., 2004; Nyanhongo et al., 2002)
<i>T.trogii</i>	Azo dye, Remazol Brilliant Blue R, 69.6% Reactive Blue 4, and Acid Blue	(Zeng et al., 2011a; Daâssi et al., 2013)
<i>Aspergillus tamaris</i>	Coomassie brilliant blue (CBB), bromophenol blue (BPB), and malachite green (MG)	(Ramalingam et al., 2010)
<i>Aspergillus bombycis</i>	Reactive Red 31	(Khan and Fulekar, 2017)
<i>Aspergillus ochraceus</i>	Vinyl sulfone, sulfonated monoazo	(Telke et al., 2010)
<i>Streptomyces ipomoeae</i>	Reactive blue, cresol red, indigo carmine azo dye	(Blánquez et al., 2018)
<i>Funalia trogii</i>	Acid red, acid black, reactive blue, reactive red, Lanazol Black R	(Tilli et al., 2011)

The use of enzymes such as peroxidases and phenol oxidases for azo dye degradation is well documented by various researches (Chivukula and Renganathan, 1995; Kwang-Soo and Chang-Jin, 1998). There are various mechanisms reported by which laccase degrades the dyes. Some studies reported the non-cleavage of azo bond followed by a non-specific free radical mechanism by the enzyme which results in phenolic end products, while other observed azo bond cleavage (Tauber et al., 2008; Pereira et al., 2009; Telke et al., 2010). Chivukula and Renganathan, 1995 studied the degradation of azo dyes by laccase from *P. oryzae*. This mechanism of laccase is initiated by two sequential abstraction of electrons from the phenol ring of the dye (Figure 1.14). The first electron removal is from the -OH moiety of the phenol resulting in phenoxy ion (phenol-O $\cdot$ ) and the second electron removal results in the formation of carbonium ion (C $^+$ ) which is stabilized in the ring through resonance. These electrons reduce the Cu $^{2+}$  of the laccase to Cu $^+$ . The carbonium ion is attacked by nucleophilic water resulting in the cleavage between nitrogen and phenolic ring. This causes the formation of benzoquinone and 4-sulfophenyldiazene. 4-sulfophenyldiazene reacts rapidly with oxygen and the nitrogen moiety is cleaved resulting in phenyl diazene radical.

Phenyl diazene radical rapidly loses nitrogen as gas molecule and reacts with another oxygen molecule to form 4-sulphophenyl hydroperoxide (Chivukula and Renganathan, 1995).

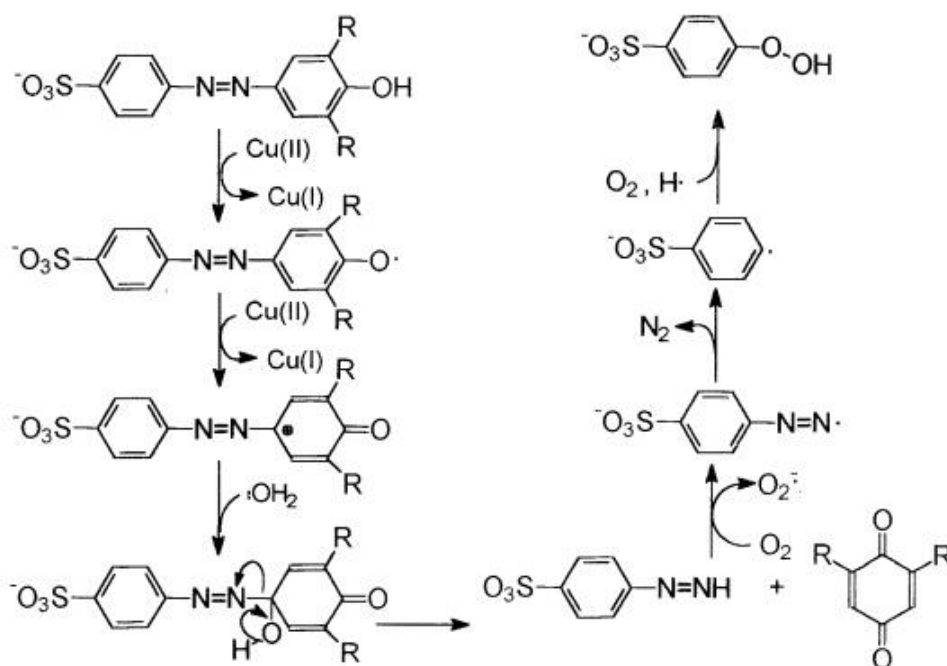


**Figure 1.14:** Possible mechanism of degradation of azo dyes by laccase (Chivukula and Renganathan, 1995)

The above products are then subjected to desulfonation, deamination, aromatic ring cleavage depending on the structure of the dye to form less toxic products (Legerská et al., 2016). The extent of degradation and azo bond breakage depends on the redox potential of the laccase. Fungal laccases have higher redox potential than bacterial laccase therefore they can break the azo bond to degrade and mineralize the dyes (Pereira et al., 2009). *T. modesta* laccase was utilised to degrade azo dyes CI Acid Orange 5, CI Acid Orange 52 and CI Direct Blue 71. They observed the rate of degradation was 2 times higher for AO 52 compared to AO5 due to the presence of electron rich methyl group (AO 52) that donate electrons for the catalysing the reaction (Tauber et al., 2008). Thus, inferring that electron rich phenolic rings and functional groups aid in better degradation of the dye. The rate and time taken for degradation of azo dyes depends on the type of laccase and the structure of the azo dyes.

### **1.3.8.3 Laccase catalysed fuel cells**

Apart from bioremediation, laccases have been used as cathode catalysts in fuel cells. While the anode consists of enzymes such as glucose oxidase, alcohol dehydrogenase the commonly used cathode enzyme for oxygen reduction is laccase (Kim et al., 2006). The catalytic efficiency depends on the redox potential of the enzyme. The redox potential of T1 site of different laccases have been determined using various substrates and mediators. It varies from 430 mV vs SHE for *Rhus vernicifera* (tree laccase) to 780 mV vs SHE for *Trametes versicolor* (fungal laccase). High redox potential laccases are efficient in substrate oxidation and are suitable for bioremediation and fuel cell applications (Shleev et al., 2005).

Laccases from *T. versicolor* and *T. hirsuta* can achieve four proton/four electron reduction of oxygen to water at very low over potentials of 30-70 mV (Le Goff et al., 2015). At the cathode, there are two types of electron transfer: direct and mediated electron transfer. Direct electron transfer (DET) is the direct transfer of electrons from the  $\text{Cu}^{2+}$  catalytic site of enzyme to the electrode (Figure 1.15). The T1 catalytic site that is responsible for electron transfer between the electrode and the T2/T3 site should

be close to the electrode to obtain DET. In a fuel cell in the absence of substrates laccase accepts electrons from the electrode for oxygen reduction reaction.

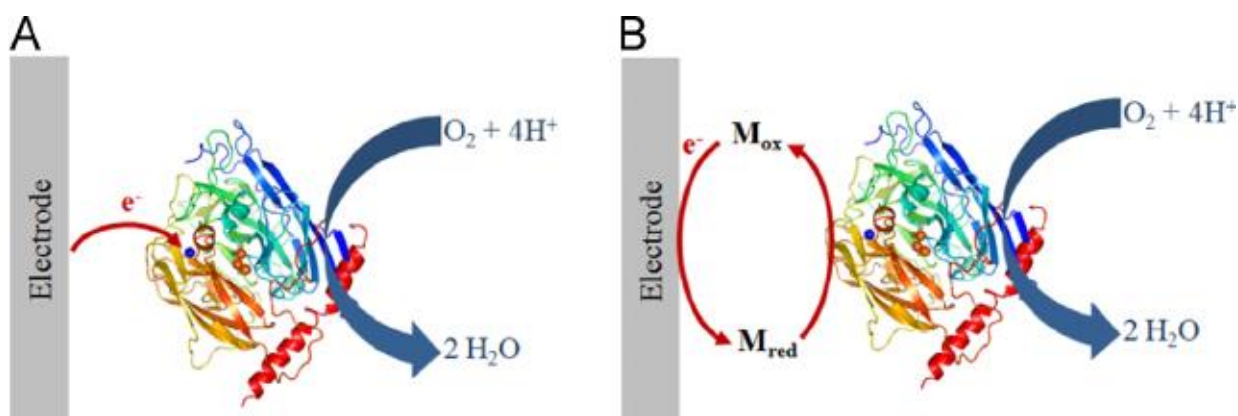


**Figure 1.15:** Direct Electron transfer and Mediated Electron transfer between laccase and electrode in a fuel cell (Le Goff et al., 2015).

Mediated electron transfer (MET) takes place in the presence of redox mediators that shuttle electrons between the electrode and the enzyme catalytic site. The redox mediators are used for laccase that have low redox potential and are unable to perform DET (Figure 1.15). The redox potential of the mediators should be close to the potential of the enzyme active site for higher efficiency (Le Goff et al., 2015). A detailed background on laccase redox mediators are discussed in chapter 6 (Section 6.1).

Laccases from *Trametes* species have been widely used as cathode catalysts in fuel cells due their high redox potentials (Gutiérrez-Sánchez et al., 2012; Lalaoui et al., 2013; Bollella et al., 2018). The culture supernatant of *T. versicolor* laccase was assessed for its electrochemical activity in a half cell configuration. The maximum current density obtained was  $129 \pm 19 \text{ mA cm}^{-2}$  at 400 mV vs SCE (Sané et al., 2013). Similarly, Fokina et al, 2015 have proved that laccase from other fungal source can also exhibit superior performances. The culture supernatant containing laccase from *Pycnoporus sanguineus* produced equivalent current density of  $115.0 \pm 3.5 \text{ } \mu\text{A cm}^{-2}$  at 400 mV vs. SCE at pH 5 (Fokina et al., 2015). Various configuration of fuel cell, electrode materials, redox mediators and protein engineering is carried out constantly to improve performance of laccase-based fuel cells.

#### 1.3.8.4 Laccase as cathode catalyst in Microbial Fuel cells

Biocathodes have been gaining increasing attention in the cathode of microbial fuel cells. There is a need to replace platinum and other metal-based catalyst for oxygen reduction reaction (ORR) to develop cheap MFCs for treatment of effluent wastewater.

Laccase was first employed at the cathode of MFC, by Schaetzle et al, 2009 by immobilizing the enzyme in poly(ethylene glycol) diglycidyl ether hydrogels on a platinum electrode. This biocathode was used in a MFC containing soil and garden compost inoculum in the anode. The maximum power density produced was  $6.8 \text{ mW m}^{-2}$  and on addition of ABTS it increased to  $37 \text{ mW m}^{-2}$  (Schaetzle et al., 2009). Further, laccase from *T. versicolor* was immobilized with ABTS using Nafion polymer on carbon paper electrode and its electrochemical performance was compared to platinum in an MFC. The anode consisted of river sludge inoculum with sodium acetate as the substrate. Lac/ABTS electrode produced a high-power density of  $160 \text{ mW m}^{-2}$  comparable to platinum with  $190 \text{ mW m}^{-2}$ . The enzyme activity in the immobilized laccase was retained even after 800 hours of operation in MFC (Luo et al., 2010).

Another study by Higgins et al, 2011 developed a hybrid MFC with *Shewanella oneidensis* MR-1 at the anode and an air breathing laccase cathode in the absence of mediators. The cathode was prepared by hydraulic pressing of carbon black (Vulcan carbon), PTFE composite and nickel mesh together. Laccase was then added on to the above electrode to be absorbed. The system produced a power density of  $26 \text{ W m}^{-3}$  and the electrode longevity was 4.75 days (Higgins et al., 2011). Although, the above methods of immobilization aided in electron transfer and obtain high power output, the use of mediator and the enzyme immobilization stability in the presence of dye needs to be evaluated if the system is to be employed for bioremediation.

The laccase producing white rot fungus *Coriolus versicolor* has been directly used in MFC cathode to facilitate electron transfer. The fungus was grown at the cathode chamber with respective growth media and the anode chamber was filled with ferricyanide. The maximum power density produced was  $320 \pm 30 \text{ mW m}^{-3}$  which was lower than purified laccase with  $480 \pm 30 \text{ mW m}^{-3}$ . This was due to the fungal adhesion of fungal filaments onto the electrode which inhibited electron transfer (Wu et al., 2012).

### **1.3.8.5 Laccase application in MFC dye decolourization**

A few studies have used laccase in a microbial fuel cell in decolourizing dyes (Bakhshian et al., 2011; Savizi et al., 2012). A 500 U ml<sup>-1</sup> of freely suspended laccase was used at the cathode chamber to decolourize reactive blue dye. The overall dye removal was 87% with a coulombic efficiency of 13.9% after 80 hours of operation (Bakhshian et al., 2011). The same group electropolymerized methylene blue on the electrode and crosslinked with laccase-chitosan (120 U mg<sup>-1</sup> of chitosan) to study decolourization of Reactive Blue dye. They yielded a maximum power density of 58.8 mW m<sup>-2</sup> and a decolourization efficiency of 74% for Reactive Blue 221 dye after 120 hours (Savizi et al., 2012). They observed that immobilization of the enzyme maintained the activity better than free loaded enzyme. Therefore, different immobilization methods need to be considered to enhance laccase stability in dye degradation applications.

The fungal source was directly employed at the cathode to observe decolourization. The fungus *Ganoderma lucidum* was immobilized on the cathode surface to degrade azo dye Acid orange 7. Acid orange 7 dye was used as the carbon source for the fungal growth and they obtained >90% decolourization with a power density of 13.38 mW m<sup>-2</sup> (Lai et al., 2017). Further enhancement in power and decolourization was obtained by using same fungal source in a MFC that contained a super adsorbent polymer mixed with polyvinyl alcohol to develop a new proton exchange membrane for efficient proton transfer from anode to cathode. This air cathode MFC produced a high-power density of 207.74 mW m<sup>-2</sup> with 96.7% decolourization of AO7 (Lai et al., 2017).

The use of fungal based cathodes requires maintaining an aseptic environment and constant media replenishment. The slow growth of the fungi leads to the possibility of contamination by bacteria and the fungal mycelia may also inhibit electron transfer in the electrode. In wastewater treatments an additional step of decontamination is required before reusing or discharging water.

### **1.3.8.6 Challenges in using laccase biocathodes in MFCs**

Although laccase was immobilized in MFC cathodes and used for dye decolourization, there are various factors that lead to the decrease of enzyme activity over time and affecting the MFC performance. Laccases from fungi were shown to be inhibited by environmental factors such as pH and temperatures changes (Madhavi and Lele,

2009). Xu, has studied the pH effect on laccase activity with phenolic and non-phenolic substrates. He concluded that the pH profile is a bell-shaped curve for laccase that varies with individual enzyme irrespective of the substrate. The variation in the pH is due to the difference in the redox potential between the substrate and the T1 Cu<sup>2+</sup> centre or the inhibition of T2/T3 Cu<sup>2+</sup> centres by OH<sup>-</sup> ions in alkaline pH (Xu, 1997). The optimum pH for *T. versicolor* laccase was 4.5 when ABTS was used as the substrate (Stoilova et al., 2010).

A study of *T. versicolor* laccase inhibition profile with heavy metals such as Mn<sup>2+</sup>, Cd<sup>2+</sup> and Zn<sup>2+</sup> revealed that Cd<sup>2+</sup> was a strong inhibitor at high concentrations (80 µM), whereas there was no inhibition observed for Zn<sup>2+</sup> and Mn<sup>2+</sup> using syringaldazine as the substrate (Lorenzo et al., 2005). Other inhibitors include copper chelating agents such as EDTA, citric acid, oxalic acid, malonic acid, sulphamic acid and hydroxylammonium chloride. Lac II from *T. versicolor* was highly stable in the presence of EDTA compared to other chelating agents (Lorenzo et al., 2005). Halides (Cl<sup>-</sup>, F<sup>-</sup>, Br<sup>-</sup>), azides, cyanides and hydroxides inhibit laccase activity and disrupt the internal electron transfer by binding to type 2 and type 3 copper (Madhavi and Lele, 2009).

These factors inhibiting laccase performance in a MFC can be addressed by either maintaining strict conditions in the cathode or by developing robust laccase-based systems by various immobilization methods.

### **1.3.8.7 Microorganisms as cathode catalysts in MFC**

Microbial biocathode is gaining interest due to the low cost, environment friendly and sustainable nature. The aerobic microorganisms at the cathode form biofilm on the electrode and use oxygen as the terminal electron acceptor. Many previous studies have demonstrated the use of microorganisms as catalyst at cathode for oxygen reduction reaction (ORR) in MFCs (Clauwaert et al., 2007; Mu et al., 2015). Mao et al., 2010 have achieved a maximum potential difference of over 600 mV with an external resistance of 100 Ω in a MFC with ferro/manganese-oxidizing bacteria as cathode catalyst and acetate as substrate at the anode. The start-up period was quite slow with maximum voltage obtained after 150 hours (Mao et al., 2010). A minimum period of 20-30 days was required for the acclimation of microorganism to achieve a maximum voltage in a MFC (Clauwaert et al., 2007).

Biocathodes have been explored for their potential in treating wastewater. Antibiotic chloramphenicol containing wastewater was treated using aerobic sludge as catalyst at the cathode with glucose as substrate. There was 96% reduction of chloramphenicol in 24 hours with an applied voltage of 0.5 V (Liang et al., 2013). The bacterial analysis of the biocathodes revealed Proteobacteria as the dominant community. Similarly, a 98% decolourization of Congo red dye was observed in a single chamber BES bioanode-biocathode (activated sludge) with 0.3 V applied voltage (Kong et al., 2014b).

From the above studies it appears that additional voltage is required for the oxidation of dye products. Microorganisms that can function as catalyst in the electron transfer process can also be utilised at the cathode. Manganese and iron are generally used as electron transfer mediators to achieve high electron transfer efficiency under aerobic conditions. These microbes catalyse the oxidation of Mn(II) and Fe (II) and the electrons produced in the process is used for oxygen reduction in the cathode of the fuel cells (He and Angenent, 2006). A few examples of electron accepting microorganisms are listed below:

- a. Iron bacteria (*Acidithiobacillus ferrooxidans*):  $\text{Fe}^{2+} \rightarrow \text{Fe}^{3+} + \text{e}^-$  (He and Angenent, 2006)
- b. Nitrifying bacteria (Nitrobacter):  $\text{NO}^{2-} \rightarrow \text{NO}^{3-} + \text{e}^-$  (Puig et al., 2011)
- c. Manganese oxidising bacteria:  $\text{Mn}^{2+} \rightarrow \text{Mn}^{4+} + 2\text{e}^-$
- d.  $\text{H}_2$  oxidising bacteria (*Ralstonia eutropha*):  $\text{H}_2 \rightarrow 2\text{H}^+ + 2\text{e}^-$

Though biocathodes have the possibility for low cost and sustainable MFCs, further research is required to improve the start-up rate and increase the power output by a factor of 5-10 for its feasibility in commercial use. As suggested by (He et al., 2015) more understanding in mechanisms of electron transfer between electrode, microorganism and electron acceptor in the cathode is required for increased power output.

In recent times, microorganisms capable of accepting electrons from the anode are being developed from soil and sludge sources consisting of mixed microbial community. These are discussed in detail in chapter 7, section 7.1.

## 1.4 Summary

Enzymes and microorganisms have the potential to serve as cathode catalysts as a replacement for platinum, but they are fraught with various limitations that needs to be addressed.

Laccase loss of activity over time requires new ways of preserving the stability e.g. methods for mitigating pH changes in the cathode of MFC and immobilization of laccase was performed to develop effective laccase biocathode for dye decolourization. Some studies reported feeding the dye in the anode chamber while others fed the dye in the cathode chamber but there has been no systematic investigation of the difference in the efficiency/mechanisms of degradation between the two approaches. Redox mediators are often used to mediate electron transfer between substrates and laccase. Artificial mediators however can be toxic at high concentrations (0.5 mM). To improve the laccase dye decolourization and ORR activity natural redox mediators could be employed.

Microbial biocathode performance depends on the source of inoculum and enrichment procedure. A more targeted source of dye degraders e.g. activated sludge system treating textile wastewater would serve as a good source of inoculum and the use of a potentiostatic poised electrode would decrease the time required for enrichment.

## 1.5 Highlights

This work improves our understanding of the potential of using biological catalysts (enzymes and microorganisms) as replacement of platinum catalysts in microbial fuel cells designed for azo dye wastewater treatment. In particular, the work contributes to the importance of maintaining macroenvironment conditions such as pH and salinity for efficient enzyme activity and the role that enzyme immobilisation plays in improving the stability and viability of laccase as an ORR catalyst. Further the efficiency of natural redox mediators for laccase activity and the distinction between anodic microbial-based reduction and cathodic laccase-mediated oxidation of azo dyes have been reported for the first time in this study. The nature of electroautotrophs enriched on a potentiostatically poised electrode as a cathode catalyst has also been observed. The work suggests that laccase and microbial biocathodes have the potential to be excellent catalysts for ORR in MFCs with efficiency equivalent to that of Pt.

## **Chapter 2**

### **Materials and Methods**

## 2.1 Chemicals

The chemicals used for media preparation i.e sodium pyruvate, casein hydrolysate, trace minerals, vitamins; standards for HPLC analysis sulfanilic acid and 1-amino-2-naphthol and the Acid Orange 7 (Orange II sodium salt), Congo Red dye were all analytical grade purchased from Sigma Aldrich (UK).

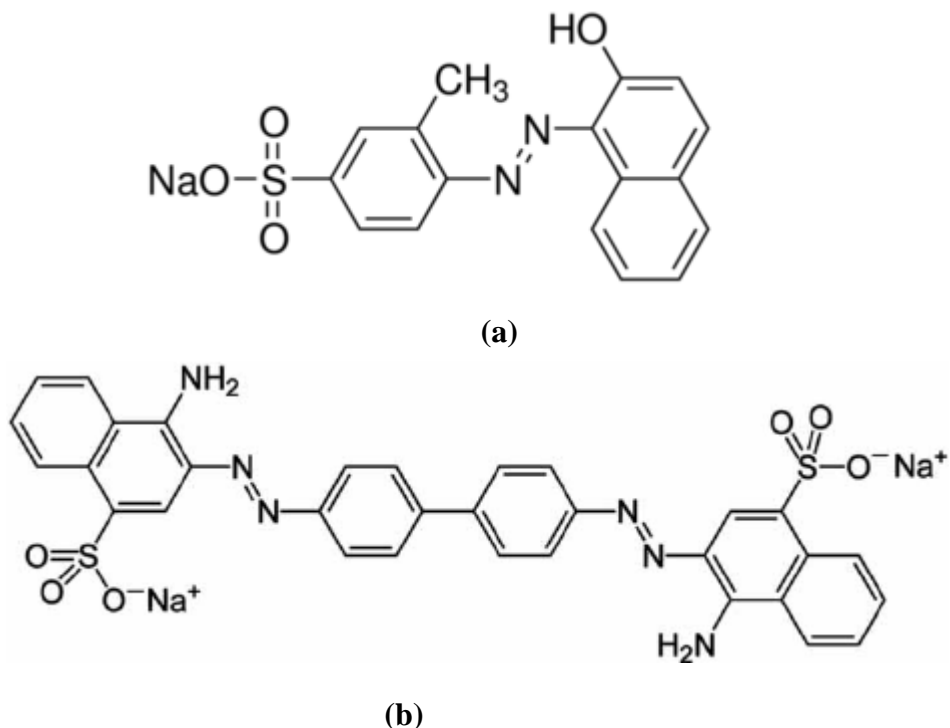


**Figure 2.1:** (a) Structure of Acid Orange 7; (b) Congo Red dye used in the study

The COD reagent Ficodox Plus™ was purchased from Fisher Scientific, UK. Nafion, TBAB, Polyaniline and all the chemicals used for immobilization studies were purchased from Sigma Aldrich and used without further purification.

## 2.2 Bacterial strains

The bacteria in the anode of MFC for all the studies was *Shewanella oneidensis* MR 1 strain (NCIMB: 14063) and for toxicity analysis it was *Vibrio fischeri* strain (NCIMB: 13938). Both the strains were obtained from NCIMB (UK) and the stock cultures were cryopreserved at -80 °C. *Shewanella sp.* was revived and grown in Luria Bertani (LB) broth at 30 °C for a period of 5 hours before inoculating in the anode chamber containing anolyte in all the chapters. The sludge used for enrichment in chapter 7 was obtained from activated sludge tank of Andipalayam common textile effluent treatment plant (CETP), Tiruppur, India and maintained at 30 °C.

### 2.3 MFC Anode media components

The below composition in the anode was the same for all the reactors in all the studies. The anolyte consisted of minimal salts medium containing (per litre): 0.46 g NH<sub>4</sub>Cl, 0.22 g (NH)<sub>2</sub>SO<sub>4</sub>, 0.117 g MgSO<sub>4</sub>, 7.7 g Na<sub>2</sub>HPO<sub>4</sub>.7H<sub>2</sub>O, 2.87 g NaH<sub>2</sub>PO<sub>4</sub> along with 1% (v/v) trace minerals as described by (Marsili et al., 2008) (Table 2.2) and 1% (v/v) vitamin mix as described by (Wolin et al., 1963) (Table 2.1) . The carbon source was pyruvate at a concentration of 1 g L<sup>-1</sup> and casein hydrolysate was added at 500 mg L<sup>-1</sup>. The pH of the anode solution was adjusted to 7. pH and ionic strength were measured using a calibrated benchtop combined pH and ionic strength meter (pH/CON 700 meter, Cole-Parmer, UK).

**Table 2.1** The composition of vitamin mix stock solution (100x) used in this study

Components	Concentration (mg L <sup>-1</sup> )
P-aminobenzoic acid (PABA)	50
L-ascorbic acid	100
Folic acid	50
Riboflavin	10
Nicotinic acid	100
Pantothenic acid	100
Thiamine hydrochloride	10
Biotin	100

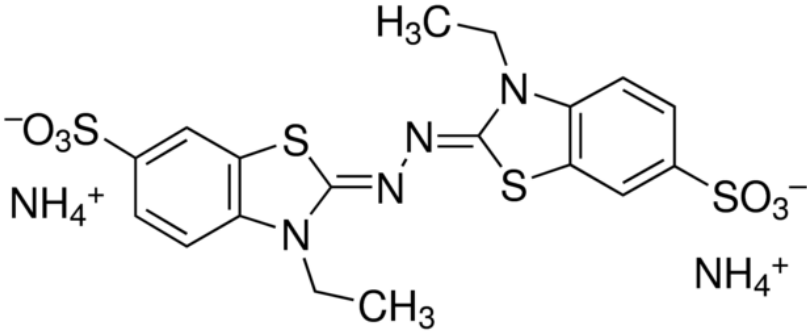
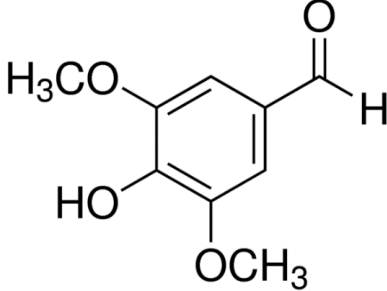
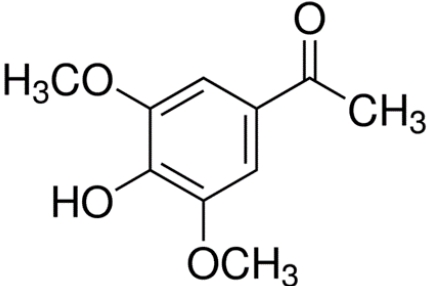
**Table 2.2:** The composition of the trace elements stock solution (100x) used in this study

Components	Concentration (mg L <sup>-1</sup> )
Nitrilotriacetic acid (NTA)	1500
FeSO <sub>4</sub> .7H <sub>2</sub> O	300
CoCl <sub>2</sub> .6H <sub>2</sub> O	170
ZnCl <sub>2</sub>	170
NiCl <sub>2</sub>	120
MnCl <sub>2</sub> .4H <sub>2</sub> O	100
NaSeO <sub>4</sub>	100
NaMoO <sub>4</sub>	90
CuSO <sub>4</sub> .5H <sub>2</sub> O	40
NaWO <sub>4</sub> .2H <sub>2</sub> O	20
AlK(SO <sub>4</sub> ) <sub>2</sub> .12H <sub>2</sub> O	5
H <sub>2</sub> BO <sub>4</sub>	5

## 2.4 MFC Cathode components

Laccase enzyme (EC 1.10.3.2) with 13.6 U mg<sup>-1</sup> of activity from *Trametes versicolor* used in the cathode chamber for chapters 3 and 4 was obtained from Sigma Aldrich (UK). In chapter 5 and 6, a crude commercial fungal laccase with 10 U mg<sup>-1</sup> of activity obtained from Enzyme India Pvt. Ltd, Chennai was used. ABTS and laccase redox mediators syringaldehyde and acetosyringone used in chapter 6 have all been purchased from Sigma Aldrich.

**Table 2.3:** Structure and molecular weights of redox mediators used in chapter 6

<b>Redox Mediators</b>	ABTS (2,2'-azino-bis(3-ethylbenzothiazoline-6-sulphonic acid))	Syringaldehyde	Acetosyringone
<b>Molecular weight (g mol<sup>-1</sup>)</b>	514.7	182.17	196.19
<b>Structure</b>	 <p>The structure shows two 3-ethylbenzothiazoline rings connected by an azo group (-N=N-). Each ring has an ethyl group (-CH<sub>2</sub>CH<sub>3</sub>) on the nitrogen atom and a sulfonate group (-SO<sub>3</sub><sup>-</sup>) on the benzene ring, with an ammonium counterion (NH<sub>4</sub><sup>+</sup>).</p>	 <p>The structure shows a benzene ring with a hydroxyl group (-OH) at the 3-position, a methoxy group (-OCH<sub>3</sub>) at the 4-position, and an aldehyde group (-CHO) at the 1-position.</p>	 <p>The structure shows a benzene ring with a hydroxyl group (-OH) at the 3-position, a methoxy group (-OCH<sub>3</sub>) at the 4-position, and an acetyl group (-COCH<sub>3</sub>) at the 1-position.</p>

## 2.5 Design of bioelectrochemical systems used in this study

The MFC used in all the chapters was the 'H'-type reactor with a working volume of 200 ml in each chamber. The two chambers were clamped together with a metal clip and separated by cation exchange membrane (CMI-7000, Membranes International-USA) (Figure 2.2). The electrodes were constructed from carbon fibre (non-woven) with a surface area of 25 cm<sup>2</sup> connected to a tin-coated copper wire. The connections were coated with non-conductive epoxy for insulation. An external load of 2000  $\Omega$  was used for experiments in chapters 3,4,5,6 and 200  $\Omega$  in chapter 7 and the potential across the resistor was recorded using the Picolog ADC-24 (Pico Technology, UK) online data logging system. The aeration for the cathode chamber was supplied through an air stone fitted to an oxygen pump.

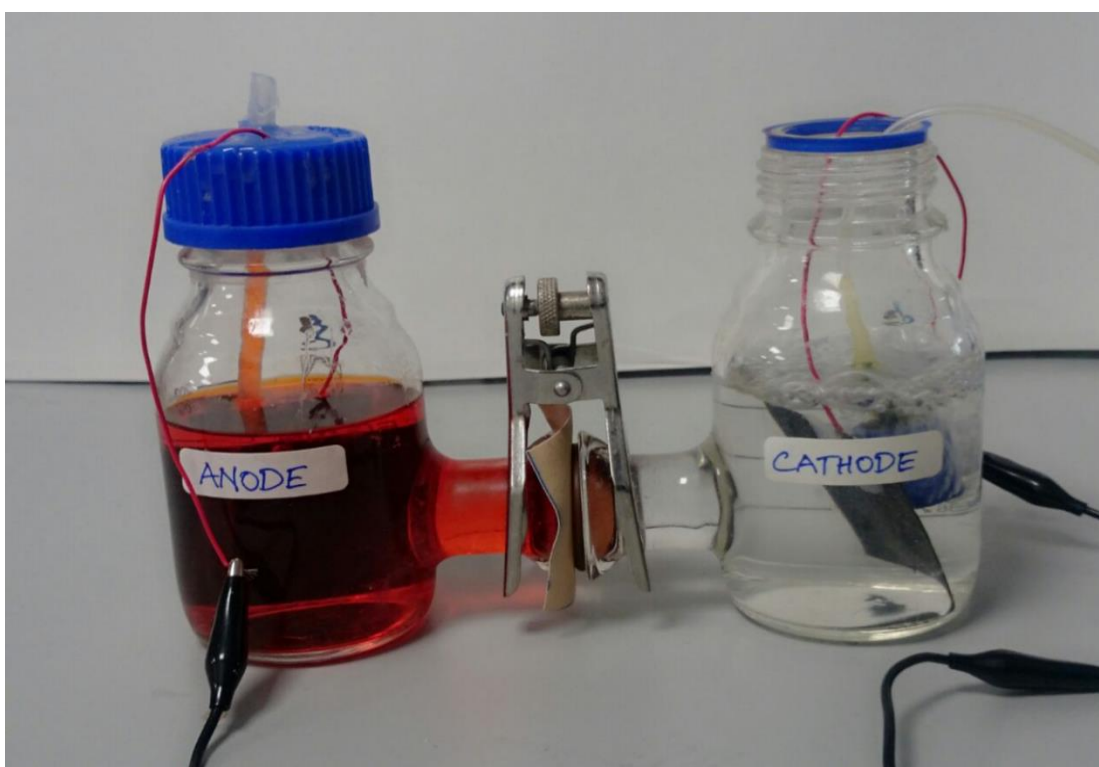


**Figure 2.2** : A H-type microbial fuel cell used in this study

## 2.6 Analytical Procedures

The analytical methods used in the study and the rationale for employing them have been discussed in this section.

### 2.6.1 Acid Orange 7 Decolourization

The decolourization of AO7 in the anode in chapter 3,7 and at the cathode in chapter 4,5,6 was measured at various time intervals using a UV-visible spectrophotometer at a wavelength of 484 nm which is the maximum absorption wavelength for the dye.

The decolourization efficiency (DE) was calculated by

$$DE (\%) = \frac{A_0 - A_t}{A_0} \times 100$$

$A_0$  and  $A_t$  are the absorbance units at the initial and each time point respectively. A time series was plotted for the absorbance values measured.

### 2.6.2 Electrochemical Analysis

The voltage across the system was recorded every 10 minutes using a data acquisition system Picolog (Pico Technology, UK). The current through the unit was calculated using Ohm's Law:

$$\text{Current } (I) = \frac{\text{Voltage } (V)}{\text{Resistance } (\Omega)}$$

The power produced was calculated using the following formula:

$$P = I \times V$$

where  $P$  is power in Watts,  $I$  is current in amperes and  $V$  is the electric potential in volts.

The power and current per surface area of electrode (25 cm<sup>2</sup> and 31 cm<sup>2</sup> in chapter 7) was used to calculate the power and current density. To carry out polarisation tests, each MFC unit was connected to various external resistances ranging from 10  $\Omega$  to 1 M $\Omega$  and the potential measured using a multimeter. The slope of the current vs voltage plot was used to determine the internal resistance of the system.

### 2.6.3 Coulombic efficiency (CE)

CE is the efficiency of the system to convert the electrons produced by the bacterial metabolism into electric current. The number of coulombs recovered is high if the microorganism at the anode completely oxidizes the organic substrates to produce electrons. The CE was calculated by the following formula (Logan et al., 2006):

$$CE (\%) = \frac{M \int_0^t I dt}{b * F * V_{anode} * \Delta COD}$$

where M is the molecular weight of oxygen (32),  $\int_0^t I dt$  is the integration of current over the time period in an experiment (C), b number of electrons exchanged per mole of oxygen (4), F is Faraday constant (96485 C mol<sup>-1</sup>), V<sub>anode</sub> is working volume of anode and COD is change in COD over time (g L<sup>-1</sup>).

### 2.6.4 Chemical Oxygen Demand (COD)

COD is defined as the amount of oxygen required to oxidize organic matter present in the wastewater. It was measured by the standard closed reflux titrimetric method described by Environment Agency (UK), based on APHA method 5220D. This method utilizes a strong oxidant potassium dichromate (K<sub>2</sub>Cr<sub>2</sub>O<sub>7</sub>) to oxidize the organics under acidic (H<sub>2</sub>SO<sub>4</sub>) conditions. Silver is added to catalyse the oxidation of alcohols and low molecular weight acids.

#### a. Procedure

The samples obtained from the MFC were centrifuged at 8000 rpm for 10 mins and the supernatant was then filtered through 0.2 µm filter to remove suspended biomass. To 2 ml of appropriately diluted samples 4 ml of COD reagent- Ficodox (Fisher Scientific) containing sulphuric acid, K<sub>2</sub>Cr<sub>2</sub>O<sub>7</sub>, Ag<sub>2</sub>SO<sub>4</sub> was added and digested at 150°C for two hours. The samples were then titrated against Ferrous Ammonium Sulphate (0.025 M) by adding 2 drops of Ferroin indicator to determine the residual K<sub>2</sub>Cr<sub>2</sub>O<sub>7</sub> present.

The COD was calculated by the following formula:

$$COD = \frac{8000 * (V_b - V_s) * DF * M}{\text{Volume of Sample}}$$

where, DF is the dilution factor, M is the molarity of FAS (0.025),  $V_b$  and  $V_s$  are the titrant volumes of FAS for blank and substrate.

The percentage COD removal was calculated as follows:

$$\text{COD Removal (\%)} = \frac{\text{COD}_I - \text{COD}_S}{\text{COD}_I} \times 100$$

Where,  $\text{COD}_I$  is the initial and  $\text{COD}_S$  is the sample COD values at various time points respectively.

### 2.6.5 Laccase Enzyme Activity

The activity of laccase was measured using ABTS (2,2'-azino-bis(3-ethylbenzothiazoline-6-sulphonic acid)) as a substrate. A solution of 2 ml acetate buffer (100 mM, pH 4.5), 1 ml ABTS (0.5 mM) and 1 ml of enzyme was used for freely suspended enzyme in all the chapters. The oxidation of ABTS by laccase was observed by a change in colour (light to dark blue) and measured using a UV spectrophotometer at 420 nm. The enzyme activity unit (U) was defined as the amount of enzyme required to oxidize 1.0  $\mu\text{mol}$  ABTS  $\text{min}^{-1}$  at 25°C (Eggert et al., 1996).

#### a. Enzyme Immobilization yield

The immobilization yields of the enzyme in chapter 4 was calculated by:

$$\text{Immobilization yield (\%)} = \frac{\text{Amount of Enzyme immobilized}}{\text{Total Enzyme used in immobilization}} \times 100$$

The amount of enzyme immobilized was calculated by ABTS enzyme assay.

### 2.6.6 Detection of metabolites by chromatographic methods

High Performance liquid Chromatography (HPLC) is an analytical method used to separate a mixture of compounds to identify and quantify individual compound from that mixture. The separation is based on the stationary phase and the mobile phase. As the analyte is passed through the column together with the mobile phase, the components with strong interaction to the stationary phase will move slowly through the column with longer retention time and vice versa. The resulting elutant is then passed through an UV detector to produce a chromatogram to identify and quantify the sample based on the standards. The most commonly used is reverse phase HPLC that consists of a non-polar stationary phase (silica-based column) and polar mobile

phase (water + water miscible solvents). In RP-HPLC the principle is based on hydrophobic interaction with less polar molecules having a higher retention time than the polar components that are eluted quickly (Bélanger et al., 1997).

#### **a. Detection of AO7 decolourization products by RP-HPLC**

The decolourized products of the AO7 by *S. oneidensis* in Chapter 3 was detected using RP-High Performance Liquid Chromatography. The HPLC system (DIONEX GS50) was equipped with a Phenomenex Gemini C18 reversed phase column (5 $\mu$ m, 150 x 4.6 mm). Aromatic compounds were quantified using HPLC with standard reductive compounds of AO7, sulfanilic acid and 1-amino-2-naphthol which were detected at wavelengths 248 nm and 284 nm respectively. The mobile phase consists of 50% methanol and 50% 33 mM (pH 7) phosphate buffer with a flow rate of 1 ml min<sup>-1</sup>. The presence of degradation products from the sample was confirmed by the retention times ( $R_t$ ) of the standards (Fernando et al., 2012).

#### **b. Quantification of Pyruvate consumption by Ion-exchange Chromatography**

The principle of Ion-exchange chromatography is based on the attraction between the charges of the stationary phase and the sample. The components that are same charge as the column are excluded from binding while the oppositely charged compounds are bound to the column. They are eluted by changing the pH of the mobile phase based on the charge (cation or anion) of the ion exchange column. Anion exchange chromatography is commonly used for detection of proteins, carbohydrates, sugars amino acids etc. The negatively charged molecules bind to the positively charged column and these molecules are then eluted out with either low or high pH mobile phase based on the charge of the compound analysed.

##### **i) Procedure**

In chapter 5, pyruvate consumption at various time intervals was quantified anion exchange chromatography. The HPLC system (Thermo Scientific: Dionex Ultimate 3000) was equipped with Phenomenex Rezex ROA-Organic Acid H<sup>+</sup> (8%) (300 x 7.8 mm) column. Pyruvate utilization was quantified using sodium pyruvate standard. The mobile was an isocratic solution of 1% Phosphoric acid (H<sub>3</sub>PO<sub>4</sub>) with a flow rate of 0.2 ml min<sup>-1</sup> and the volume of sample was 10  $\mu$ l. The samples were detected with a Photodiode Array (PDA) detector at 210 nm and 214 nm.

### **2.6.7 Morphological characterisation using Scanning Electron Microscopy (SEM)**

Scanning electron microscopy is used to study the morphological characteristics of a sample on a nano-scale level by scanning its surface with a beam of electrons. As the electrons excite the atoms in the sample, secondary electrons are emitted on the surface of the sample that are collected through a detector to produce an image. The electron beams can be easily ionised in air and lose their energy; therefore, the imaging is performed under vacuum.

SEM provides useful information on the morphology and topography of the samples on solid surface. In some studies, it is equipped with Energy-dispersive X-Ray Spectroscopy (EDS), to provide the elemental composition. SEM is widely used for characterization of enzymes immobilized solid surfaces. It provides input on the morphological changes occurring on the surface during each immobilization step and to confirm the outcome of the procedure. The physical stability of the immobilized electrode i.e. peeling, sloughing, tearing etc. can also be easily visualized using this technique.

The topology of laccase immobilized on various support materials have been widely characterized by SEM (Nogala et al., 2008; Sadighi and Faramarzi, 2013).

#### **a. SEM procedure for immobilized laccase electrodes**

In chapter 4, PANI, Nafion and Cu-alg laccase were subjected to SEM analysis to determine the morphological characteristics. The samples were mounted on to aluminium stubs using double side sticky carbon tape. A thin layer of gold was coated on the surface of the samples to enhance conductivity. The samples were then examined in an Inspect-F scanning electron microscopy (SEM) equipped with EDS at a vacuum of  $5.0 \times 10^{-5}$  torr and an accelerating voltage of 30 kV.

### **2.6.8 Functional group identification by Fourier-transform infrared spectroscopy (FTIR)**

FTIR is a sensitive technique that is used to identify the presence of certain functional groups in an organic/inorganic material. The principle relies on the absorption of IR radiation by the chemical bonds present in the sample. As the sample is irradiated by IR rays, the bonds present in the molecule vibrates at various frequencies depending on their type and elements present. The frequencies are represented as wavenumbers

in the FTIR spectra; therefore transmission/absorbance vs wavenumber ( $\text{cm}^{-1}$ ) is plotted. The wavenumbers range from ( $400 \text{ cm}^{-1}$  to  $4000 \text{ cm}^{-1}$ ) for organic molecules and they correspond to the functional groups present. Various vibrations of the bonds such as stretching, stoking, bending, puckering etc can also be inferred from the spectra. The spectra produced by these groups may vary from strong to weak, sharp to broad depending on the vibrational frequency of functional group.

Attenuated total reflection- Fourier transform infrared (ATR-FTIR) is variation of FTIR for solid samples that uses IR radiation through a crystal (diamond) with high total internal reflection for obtaining the spectra. It is widely used method to study immobilization of the enzymes on solid materials as it provides a concise information during each steps of functionalization. The nature of chemical bonds formed during the immobilization, their stability and their orientation can be analysed (Morhardt et al., 2014). The immobilization of laccase by various methods such as adsorption, cross-linking and encapsulated have been widely validated by FTIR (Ahn et al., 2007; Gahlout et al., 2017; Zhang et al., 2018).

#### **a. FTIR procedure for laccase electrodes**

In chapter 4, PANI and Nafion laccase electrodes were subjected to FTIR analysis to determine the presence of functional groups on immobilization. Perkin Elmer Spectrum Two FTIR-ATR Spectrometer was used at a resolution of  $8 \text{ cm}^{-1}$  for 25 scans from the range  $400$  to  $4000 \text{ cm}^{-1}$ . Plain carbon electrode was used as the background.

### **2.6.9 Identification of metabolites from laccase dye degradation by Gas Chromatography/Mass Spectrometry (GC-MS)**

GC-MS is the combination of Gas chromatography that is used to separate the individual compounds from a mixture and Mass spectrometry used to identify and quantify the compounds. This is a powerful technique to detect substances at very low concentration ( $< 0.1 \text{ ppm}$ ) and it is suitable for volatile and semi-volatile compounds.

The sample mixture is injected through the GC inlet, where it is vapourised at high temperature and carried through the GC column by a stream of carrier gas (Helium,  $\text{N}_2$ ). The compounds in the mixture are separated based on the interaction with the stationary phase (column) and elute at various retention times. These compounds then enter the MS where they are ionised and detected. There are various ionisation

methods depending on the ion source i.e. electron ionisation (EI) that uses electrons, chemical ionisation that utilizes a reagent gas (methane, ammonia).

In EI the separated compounds are hit by a stream of electrons that results in the fragmentation and ionisation of the molecules. Ionisation causes loss of electron that creates a radical cation with a positive charge  $M^+$ . The mass ( $m$ ) of the fragments divided by their charge ( $z$ )  $m/z$  represents the molecular weight of the compounds. After ionisation these fragments enter a detector where they are scanned against a broad range of mass fragments to determine the  $m/z$  values of each compound. The  $m/z$  values are compared with a library (NIST) containing the spectra of all compounds to identify them individually (Sneddon et al., 2007). The presence of a library is very helpful in identifying unknown components.

GC-MS is widely used in environmental applications, forensic analysis, perfume analysis, medical purposes etc. In the environment it is used to identify pollutants in soil or water samples.

In chapter 5 we have utilised GC-MS to identify the products acid orange 7 dye degraded by laccase. As discussed in Section 1.3.8.2 laccase degradation of the dye is through a non-specific free radical mechanism. The resulting products were unknown therefore, GC-MS was ideal for this study.

#### **a. GC-MS Analysis Procedure**

The dye degradation products from both the anode and cathode chamber were analysed through GC-MS. Since the samples were of aqueous in nature, they were extracted into organic solvent to make it suitable for the analysis.

The samples were extracted with dichloromethane (DCM) using liquid:liquid extraction at a combination of pHs (acidic, neutral and basic). This modification of pH effectively neutralises any charged compounds (e.g. phenolics, amines etc.) and allows a better partition into the organic solvent. For the extraction 2ml of sample (various pH) was added to 2 ml dichloromethane (DCM) to allow the compounds to separate from the aqueous phase to organic phase. The sample at pH 7 was best extracted into DCM.

The extracted sample was introduced into the GC-MS (Agilent) equipped with Restek Rxi-5ms (20 m x 180 $\mu$ m x 0.18 $\mu$ m) column. The initial temperature was held at 40 °C

for 1 minute, and then ramped at 10 °C min<sup>-1</sup> until 340 °C which was then held for 10 mins. The interface temperature was 280 °C. A 1µl sample was injected on a pulsed splitless injection at 250 °C. The flow rate of carrier gas helium was at 1.1 ml min<sup>-1</sup>. Electron ionisation (EI) was used with MS source temperature at 230 °C and Quad temperature at 150 °C. The m/z range selected was from 25 to 750 amu. The products were identified using NIST mass spectra database. Internal standards were injected in between the samples to validate the method used.

### 2.6.10 Microtox toxicity analysis

Microtox assay is a method that utilizes the bioluminescent bacteria *Vibrio fischeri* to detect toxic pollutants in water, air, soil etc. *V.fischeri* possesses luminescence as a part of their cellular respiration and when exposed to toxic substances they inhibit the respiration thereby decreasing the luminescence. The rate of change in luminescence is directly correlated with the toxicity of the substance (Johnson, 2005). Microtox is used to test the toxicity of drinking water, lake and river sediments, industrial effluents etc.

#### a. Procedure

This assay was performed to determine the toxicity of AO7 decolourized samples in chapter 3 and chapter 5. Freeze dried *Vibrio fischeri* (NCIMB strain 13938) was revived by growing them in NCIMB growth medium 1537 (Oceanibulbus medium).

**Table 2.4:** Composition of Oceanibulbus medium for *Vibrio fischeri*

Component	Concentration (g L <sup>-1</sup> )
Tryptone	10
Yeast extract	5
NaCl	10
Sigma Aldrich sea salts ready mixture (S9983)	14

*V. fischeri* was grown in the above medium for 48 hours (22 °C, 150 rpm), the cells were harvested by centrifuging at 4000 g, washed twice with sterile phosphate buffer

(100 mM, pH 7.1) and suspended in 2% NaCl before starting the assay. The dye decolourization products of *Shewanella* (anode) in chapter 3 and 5; the autooxidation products of *Shewanella* sp. and laccase dye degradation (cathode) in chapter 5 were analysed for their toxicity through Microtox Assay. Serial dilutions of the samples with 2% NaCl in the presence of the *V. fischeri* cell suspension was carried out in a 96 well plate. The plate was incubated at 15°C for 10 mins and the luminescence was measured using a Fluostar Optima plate reader. The absolute light units were recorded and IC<sub>50</sub>, a concentration which inhibits 50% of light was calculated for each sample. The IC<sub>50</sub> concentrations were expressed as the COD equivalent of the samples in chapter 1.

### **2.6.11 Cyclic Voltammetry**

Electrochemical methods are important in understanding the surface reactions on the electrode most notably the oxidation-reduction process. These techniques are usually carried out in a three-electrode set-up. The electrode to be analysed is referred to as the working electrode. To measure the potential, a reference electrode is used whose potential is well established. Some of the commonly used reference electrodes are Standard hydrogen electrode (SHE) with potential of ~0 mV (IUPAC, 1997), Ag/AgCl electrode +197 mV vs SHE and Standard Calomel electrode (SCE) +248 mV vs SHE etc. The current is measured between the working and a third electrode called counter electrode which carries out the counter reaction to the working. This three-electrode set-up with a potentiostat is widely used in electrochemistry to study the interface reactions in fuel cells. One of the commonly used method for studying the electrode redox reaction is cyclic voltammetry (CV). CV involves sweeping the potential of the electrode between a wide potential range and measuring the corresponding current obtained (Figure 2.3). The speed at which the potential is scanned (scan-rate) is critical as the peak current obtained is dependent on it. The scan rate is dependent on the rate of the reaction to be observed with chemical reactions usually requiring a faster scan rate compared to biological reactions.

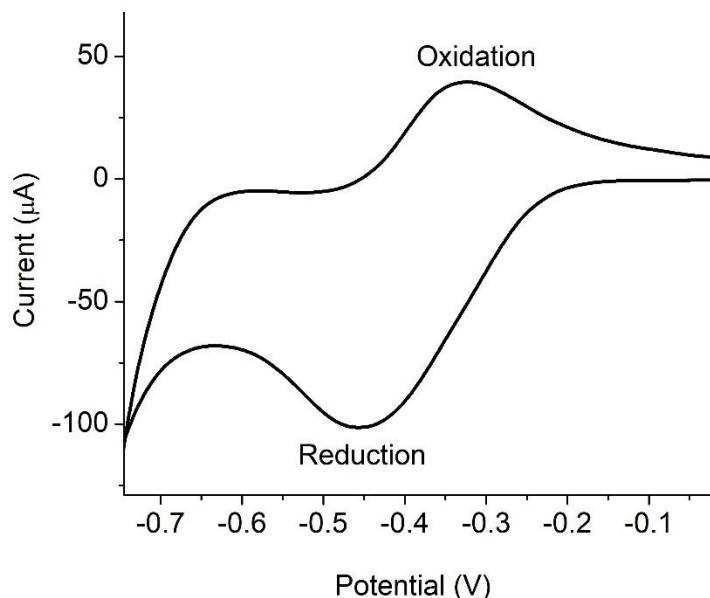


**Figure 2.3:** A CV of Flavin adenine dinucleotide (0.1 mM) at scan rate of  $50 \text{ mV s}^{-1}$  from  $-0.7 \text{ V}$  to  $-0.1 \text{ V}$ .

The oxidation/anodic reaction is characterized by a peak in the forward scan direction (negative to positive) and a reduction/cathodic reaction is observed by a negative current peak in the reverse scan direction (positive to negative). In the above reaction oxidation occurs at a potential of  $-0.3 \text{ V}$  and reduction at  $-0.45 \text{ V}$  (Figure 2.3). A CV can also provide information about multiple redox reactions through multiple peaks and reversibility of the process through presence or absence of the peaks. Laccase has been studied extensively using CV to understand the electron transfer mechanism (Le Goff et al., 2015).

#### **a. Laccase immobilized electrodes CV procedure**

In chapter 4, the cyclic voltammetry (CV) measurements for activity of laccase was performed in a three-electrode system with the working electrode as the PANI laccase/Nafion laccase electrode, platinum as the counter and Ag/AgCl as reference electrode. The CV was carried out in pH 4.5 acetate buffer (100 mM) using a potentiostat Keysight B2900A by cycling between potentials of  $1 \text{ V}$  to  $1.5 \text{ V}$  at  $20 \text{ mV s}^{-1}$ .

#### **b. Dye degradation products CV**

In chapter 5, CV measurements were carried out for standards 1-Amino-2-Naphthol, sulfanilic acid, acid orange 7 dye and the dye degradation products. A three-electrode

system with the working electrode as glassy carbon, platinum as the counter and Ag/AgCl as reference electrode was used. The three standard compounds were prepared in deionised water at a concentration of 100 mg L<sup>-1</sup>. The dye degradation products were filtered to remove any bacterial cells to prevent interference. CV was carried out using a potentiostat Keysight B2900A by cycling between potentials of -1 V to 1.5 V at 50 mV s<sup>-1</sup>.

### **c. CV of redox mediators in the presence and absence of laccase**

In chapter 6, CV measurements of redox mediators ABTS, syringaldehyde and acetosyringone in the presence and absence of laccase was performed. A three-electrode system with the working electrode as glassy carbon, platinum as the counter and Ag/AgCl as reference electrode was used. The three mediators were prepared in deionised water at a concentration of 50 µM. CV was carried out using a CH 660A potentiostat (CH Instruments, USA ) by cycling the potential between -1 V to 1 V at 50 mV s<sup>-1</sup>.

## **2.6.12 Chronoamperometry (CA)**

Chronoamperometry involves the application of constant potential to the working electrode over a period of time and subsequent measurement of the current produced. The current obtained follows the Cottrell's equation as given by:

$$i = nFAD^{1/2} C_0 \Pi^{-1/2} t^{-1/2}$$

where  $i$  is the steady state current,  $n$  is the number of electrons transferred,  $D$  is the diffusion coefficient,  $F$  is the Faradays constant,  $A$  is the area of electrode,  $C_0$  is the concentration of the analyte and  $t$  is the time. In CA the current decreases with time because of depletion in the concentration of the analyte. In case of microbial cathode, the current tends to increase with time due to increased microbial metabolism in presence of substrate. On depletion of substrate the current gradually decreases. These alternate steps continue until a stable biofilm is obtained beyond which a steady state current is obtained independent of the substrate concentration. CA is widely used to enrich electrogenic microorganisms by forming biofilms on electrode surfaces. By applying anodic/cathodic potential to the electrode, bacteria that can donate or accept electrons for their metabolism are selected from the mixed microbial community.

### a. Microbial enrichment procedure using CA

In chapter 7, chronoamperometry technique was using in a three-electrode system to enrich electrogenic bacteria. A three-electrode system with Ag/AgCl as the reference electrode, graphite rod of 45 cm<sup>2</sup> as the counter and graphite rod 31 cm<sup>2</sup> as the working electrode was used for the enrichment of a microbial consortia. The electrodes were connected to a Uniscan (PG581) potentiostat with an applied voltage of -0.1 V and the current was recorded every 20 minutes with a UiEChem software in chronoamperometry mode.

### 2.6.13 Microbial community analysis by PCR-DGGE

The microbial community in chapter 6 was analysed by PCR, DGGE and sequencing of the 16s ribosomal DNA (rDNA) gene of the bacteria.

#### a. Importance of 16srDNA

The advent of PCR and gene sequencing have given rise to phylogenetic studies among various genes, species or populations. The 16s rDNA is a gene segment that codes for 16s rRNA that is highly conserved among different species of bacteria and archaea. It has been observed that even distantly related bacteria share a high functional similarity of 16s rRNA (Tsukuda et al., 2017). The sequencing of these genes provides the genus and species information of unidentifiable bacteria from a microbial community. This enables the identification and classification of various species in an environment. The 16s rRNA is 1.5 kb in length with 9 hyper variable regions (V1-V9) (Figure 2.4).

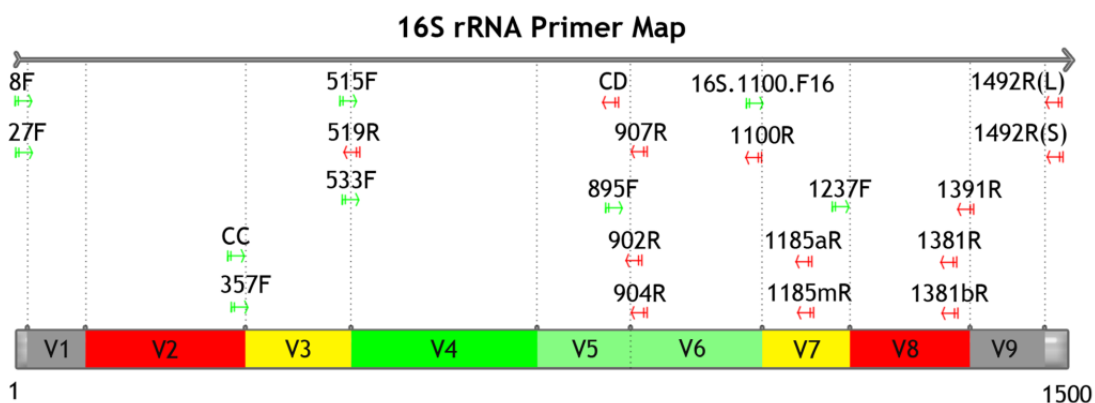


**Figure 2.4:** The hypervariable regions of 16s rRNA with V3 and V4 highly targeted region for PCR amplification (Yang et al., 2016).

## **b. Amplification by PCR**

Polymerase Chain Reaction (PCR) is the commonly used technique to amplify a targeted DNA fragment for further analysis. It is a DNA replication process carried out *in vitro* that requires template DNA, primers for the target region, nucleotides (A, T, G and C) and DNA polymerase. During the reaction, in the first step the temperature is increased above the melting point of DNA to separate the complementary double strands, a process called denaturation. The temperature is then lowered to allow the primers bind to the target region and this process is called annealing. Finally, the temperature is raised again for the DNA polymerase to add nucleotides and extend the primers to form a double stranded DNA (Garibyan and Avashia, 2013). Each cycle doubles the number of DNA copies. This process is repeated for a specified number of cycles to get the desired DNA concentration. The 16s rRNA has universal set of primers for V3-V4 regions.

## **c. Denaturing Gradient Gel Electrophoresis (DGGE)**

DGGE is a molecular fingerprinting technique used to separate a mixture of PCR products based on their sequence composition. It is based on the stability of the nucleotide bonds, as adenine and thymine are bound together by two hydrogen bonds while guanine and cytosine are stronger with three hydrogen bonds. During the DGGE, a high temperature (60 °C) is maintained while the DNA migrates through a polyacrylamide gel containing increasing concentrations of denaturants (urea and formamide). The high temperature is to aid in melting the DNA and to slow its movement through the gel. As the DNA strands reach the concentrations of denaturants the strand unwinds by breaking the bonds between the nucleotides and this denaturing slows the mobility of DNA in the gel. They are then separated by variation in the sequences of the DNA i.e. fragments with higher G-C content would be denatured slowly due to the strong hydrogen bonding compared to A-T nucleotides. The different melting temperatures cause the sequences to migrate at different rates to form bands at various positions the gel (Strathdee and Free, 2013). Each band represents an individual gene, species or population from a mixed community. A G-C clamp is usually placed at the 5' end of the forward primer during PCR to prevent complete unwinding of the DNA to single strands.

#### **d. Microbial community analysis procedure of the enriched biofilm**

In chapter 7, the initial sludge used for enrichment and the enriched samples were subjected to PCR-DGGE and sequencing to identify the species.

The DNA from the sludge sample and three (Plank, EB, EW) sample was extracted with Sigma Aldrich GenElute soil DNA isolation kit. The extracted DNA was tested for purity with A260/A280 ratio and quantified using a Nano-Drop (Nano-1000, Thermo Scientific, USA) spectrophotometer. The presence of DNA was then verified on 1% (w/v) agarose gel and then subjected to PCR.

The PCR reaction mixture (50  $\mu$ l) consisted of the following components (Fernando, 2014):

2X PCR master mix (Thermo Scientific)	25 $\mu$ L
Nuclease free water	22 $\mu$ L
Forward and Reverse primers	1 $\mu$ L each
Template whole genomic DNA	1 $\mu$ L

The V3 region of the 16s rRNA was amplified using the primer sequences: F357-GC (5'-CGC CCG CCG CGC GCG GCG GGC GGG GCG GGG GCA CGG GGG GCC TAC GGG AGG CAG CAG-3') and R518 (5'-ATT ACC GCG GCT GCT GG-3') (Fernando, 2014).

The PCR was performed using Quiagen Rotor-Gene instrument with the following settings: initial temperature at 95 °C for 5 mins; followed by 45 cycles of 95 °C for 0.5 min, 58 °C for 1 min, 72 °C for 1 min, and finally at 72 °C for 7 mins. The size of the PCR products was confirmed by running through 1% (w/v) agarose gel.

DGGE was performed using a CBS Scientific DASG-250 universal mutation detection system. The PCR products were loaded on 8% polyacrylamide gel with the a 30%-60% range of denaturing gradient.

**Table 2.5:** The components of the denaturing gradient gel used in this study (Fernando, 2014).

Components	0%	30%	60%
Tris acetate EDTA (TAE) buffer 50X stock (ml)	0.5	0.5	0.5
Acrylamide (40% 37.5:1 stock) (ml)	5	5	5
Deionised Formamide (ml)	-	3	6
Urea (gm)	-	3.15	6.3
Glycerol (ml)	0.5	0.5	0.5

The gel was cast using the gradient deliver system and the samples loaded with 6X – Promega tracking dye. Electrophoresis was carried out at 120 V for 4 hours in 1X TAE buffer. After electrophoresis the gel was stained by SYBR Safe Red DNA stain (Sigma) and viewed on a Safe Imager 2.0 Blue Light Transilluminator. The individual bands of interest were then excised and placed in 50 µl nuclease free water for 48 hours to elute the DNA from the gel. The DNA was subjected to another round of PCR using universal primer set F338 (5'-ACT CCT ACG GGA GGC AGC AG-3') and R518 with the same PCR conditions as before. The PCR samples were then loaded on 1.5% agarose gels for verification. After verification the remaining PCR product was purified using QIAquick (QIAGEN) PCR Purification Kit and sent for Sanger sequencing to Eurofins GATC Biotech, Germany.

#### **2.6.14 Metagenomic analysis by Illumina Next Generation Sequencing (NGS) method**

Next generation sequencing was performed on the samples to identify the microbial community. Illumina is a high throughput NGS technique that uses the sequencing by synthesis method. In this method, fluorescent labelled deoxyribonucleotide triphosphates (dNTPs) are incorporated into the DNA template during each synthesis cycle by a DNA polymerase. These nucleotides are identified by their fluorescence signal during each cycle. The process of adding each nucleotide and reading the signal is carried out in parallel across millions of fragments. These fragments are then compared against a library to identify and generate a sequence. Illumina sequencing has advantage over Sanger sequencing as it provides in-depth analysis of the genes

and produces error-free reads with high accuracy (<https://emea.illumina.com>). Amplicon sequencing is used to target a particular region or a subset of genes. Illumina-NGS is widely used for diverse metagenomic samples as it alleviates the need for DGGE separation, and the mixed microbial samples can be analysed directly by amplifying the 16s rRNA sequence.

#### **a. Sample preparation for NGS**

The initial sludge referred as “sludge”, planktonic cells referred as “plank”, biofilm on the graphite rod denoted as “EB” and biofilm on the wired connection known as “EW” were prepared for amplicon sequencing. The genomic DNA from the sludge sample and three (Plank, EB, EW) samples was extracted with Sigma Aldrich GenElute soil DNA isolation kit (Sigma Aldrich, UK). The extracted DNA was tested for purity with A260/A280 ratio and quantified using a Nano-Drop (Nano-1000, Thermo Scientific, USA) spectrophotometer. The samples were sent to NovoGene Genome Sequencing Company, China for 16s rRNA amplicon sequencing.

#### **b. Sequencing preparation carried out by NovoGene**

The DNA concentration and purity were monitored on 1% agarose gel and the concentration of DNA was diluted to  $1\text{ ng } \mu\text{L}^{-1}$  using sterile water. PCR amplification was carried out with Phusion High-Fidelity PCR Master Mix (New England Biolabs) for the 16s V4 region using 515F-806R primers. The PCR products were then quantified on 2% agarose gel and the samples that produced bright bands in the 400-450 bp region were used for subsequent analysis. The PCR products were purified using Qiagen Gel Extraction Kit (Qiagen, Germany). The libraries were generated on NEBNext Ultra DNA Library Prep Kit for Illumina and the quality assessed on Qubit 2.0 Fluorometer (Thermo Scientific) and Agilent Bioanalyser 2100 system. The samples were sequenced on Hiseq 2500 platform to generate 250 bp paired-end reads.

#### **c. Bioinformatics Analysis by NovoGene**

The data analysis to produce Operational Taxonomic Units (OTU) clusters was performed with Uparse software (Uparse v7.0.1001) for all the effective tags. For species annotation at each taxonomic rank Mothur software was performed against the small subunit ribosomal ribonucleic acid (SSU rRNA) sequences against the SILVA Database (<http://www.arb-silva.de/>) (Threshold:0.8~1). Phylogenetic relationship in

the samples was established by multiple sequence alignment using the MUSCLE software (Version 3.8.31). Alpha and Beta diversity analysis for Observed-species, Shannon and PCA (Principle Component Analysis) was calculated using QIIME (Version 1.7.0) and displayed with R software (Version 2.15.3). The detailed method of data analysis and the software used is given in the Appendix 4.

### **2.6.15 Statistical analysis**

All experimental data indicated in the text and graphs are the means of triplicate experiments unless otherwise stated. The error bars in the graphs and values in the text represent the standard deviation of the mean (SD). The two tailed t-test was performed using SPSS statistical software package.

## **Chapter 3**

**Decolourization of Acid orange 7 in MFC with a laccase-based biocathode: Influence of mitigating pH changes in the cathode chamber**

## **3.1 Background**

Laccases from fungi have the potential to be inhibited by number of environmental factors such as salinity, pH (Madhavi and Lele, 2009). The pH optima for fungal laccase with ABTS as substrate is in the range of 3-5. pH affects the total net charge of enzymes and the distribution of charges on their exterior surfaces and these changes affect the activity and structural stability of the enzyme.

In a MFC the oxidation of substrate by the microorganisms in the anode produces protons and electrons. The incomplete transfer of protons across the membrane results in an acidic environment at the anode and the movement of cations to the cathode increases both the salinity and pH in the cathode chamber. pH gradients have adverse effects on the performance of MFCs by interfering with metabolic activity in the anode and increasing potential losses at the cathode. According to the Nernst equation, these pH gradients cause high anodic equilibrium potential and/or low cathodic equilibrium potential that significantly lowers the cell voltage and causes a loss of ~60 mV per unit pH change (Rozendal et al., 2008; Popat et al., 2012). Fokina et al, 2015 have observed that increase in pH by one unit caused a decrease in oxygen reduction potential in the range of 30-80 mV in a biofuel cell using laccase as cathode catalyst (Fokina et al., 2015). Changes in charges with pH can also affect the activity, structural stability and solubility of enzymes. Salinity affects the movement of charged groups and the solubility (hence activity and stability) of enzymes.

In order to increase the stability of laccase in MFC cathodes and improve MFC performance various strategies (Section 3.2.1) to mitigate pH changes in the cathode chamber were explored in this study. The investigation was carried out in the context of treatment of azo dye containing wastewater.

## **3.2 Materials and Methods**

### **3.2.1. Experimental design**

The MFC used in the study was the 'H'-type reactor with a working volume of 200 ml in each chamber. The electrodes were constructed from carbon fibre (non-woven) with a surface area of 25 cm<sup>2</sup>. Four systems were set up to mitigate pH changes in the cathode chamber. System 1 which will be referred to as 'Nafion' involved using Nafion 117 as the ion exchange membrane. System 2 referred to as 'pH control'

involved automatically controlling the pH in the cathode through feedback control by addition of acid or base. System 3 referred to as ‘buffer strength’ involved using a buffer of higher strength 200 mM compared to other systems have used 100 mM acetate buffer (pH 4.5) as buffer. System 4 referred to as ‘CEM’ involved using CMI7000 membrane as the ion exchange membrane. These conditions are summarised in Table 3.1 including a rationale for each.

**Table 3.1:** Summary of variables employed in this study along with the rationale for employing them

<b>MFC System</b>	<b>pH mitigation measure</b>	<b>Other conditions</b>	<b>Rationale</b>
[1] Nafion	Nafion 117 membrane	Buffer in cathode chamber 100 mM acetate pH 4.5	High proton affinity and transport (Scholz, 2008).
[2] pH control	Automatic pH control by acid (HCl) or base (NaOH) addition (0.1 M)	Buffer in cathode chamber 100 mM acetate pH 4.5 to begin with; CMI7000 membrane	Tight control of pH.
[3] Buffer strength	Buffer strength increase	Buffer in cathode chamber 200 mM acetate pH 4.5; CMI7000 membrane.	Decouples effects due to pH changes from those due to salinity changes.
[4] CEM	CMI7000 membrane	Buffer in cathode chamber 100 mM acetate pH 4.5	Cheap and commonly used membrane.

### 3.2.2 Operating conditions

The composition in the anode was the same for all the reactors. The anode media components and their concentrations are detailed in Chapter 2, Section 2.3. Nafion 117 membrane was pre-treated by heating in each of the following solutions at 60 °C for 60 minutes: 0.1 M H<sub>2</sub>SO<sub>4</sub>, 0.1 M H<sub>2</sub>O<sub>2</sub> and finally in deionised water. CMI7000 ion exchange membrane was soaked in 5% NaCl for 12 hours prior to use. The anode and cathode were connected to a resistor of 2 K $\Omega$ . The anode was inoculated with 10% v/v *S. oneidensis* MR-1 culture previously grown in Luria Bertani broth to log phase (OD

of 0.4) and the dye Acid Orange 7 was added at a concentration of 150 mg L<sup>-1</sup>. The anode chamber was sparged for 10 minutes with nitrogen gas to remove any dissolved oxygen and maintain an anaerobic environment. The cathode chamber consisted of commercial laccase (Sigma Aldrich, UK) from *Trametes versicolor* (13.6 U mg<sup>-1</sup>) in a buffer solution. In systems 1, 2 and 4 300 U L<sup>-1</sup> of laccase was added to 100 mM acetate buffer with pH 4.5 and in system 3 300 U L<sup>-1</sup> of laccase was added to 200 mM of acetate buffer at pH 4.5. The cathode chamber was maintained in aerobic conditions by supplying air through an air stone at a rate of 200 ml min<sup>-1</sup>. Experiments were conducted at a temperature of 30 °C over a period of 10 days.

### **3.2.3 Analytical Procedures**

The chapter 2, analytical procedures (Section 2.6) details the procedures used for each chapter and the rationale behind performing the tests. The analytical procedures followed in this study were AO7 decolourization (Section 2.6.1), electrochemical tests (Section 2.6.2), Coulombic efficiency (Section 2.6.3), COD (Section 2.6.4), laccase enzyme activity (Section 2.6.5), Detection of AO7 decolourization products by RP-HPLC (Section 2.6.6(a)), *Vibrio* toxicity profile (Section 2.6.10) and statistical analysis (Section 2.6.15). pH and ionic strength were measured using a calibrated benchtop combined pH and ionic strength meter (pH/CON 700 meter, Cole-Parmer, UK).

## **3.3 Results and Discussion**

### **3.3.1 AO7 decolourization**

The decolourization of Acid Orange 7 was measured at the maximum absorption wavelength for the dye (484 nm). The overall dye removal efficiency was 89% in the reactor containing Nafion compared to 82% in system 2 (pH automatically controlled), 80% in system 3 (increased buffer strength) and 78% in system 4 (CEM). There was greater than 50% colour removal within 48 hours for Nafion-containing and automatically controlled pH systems (Figure 3.1). At the end of the runs there was 78% COD reduction in the Nafion reactor followed by 76% in both pH control and buffer strength reactors. The CEM reactor showed a 74% COD reduction.

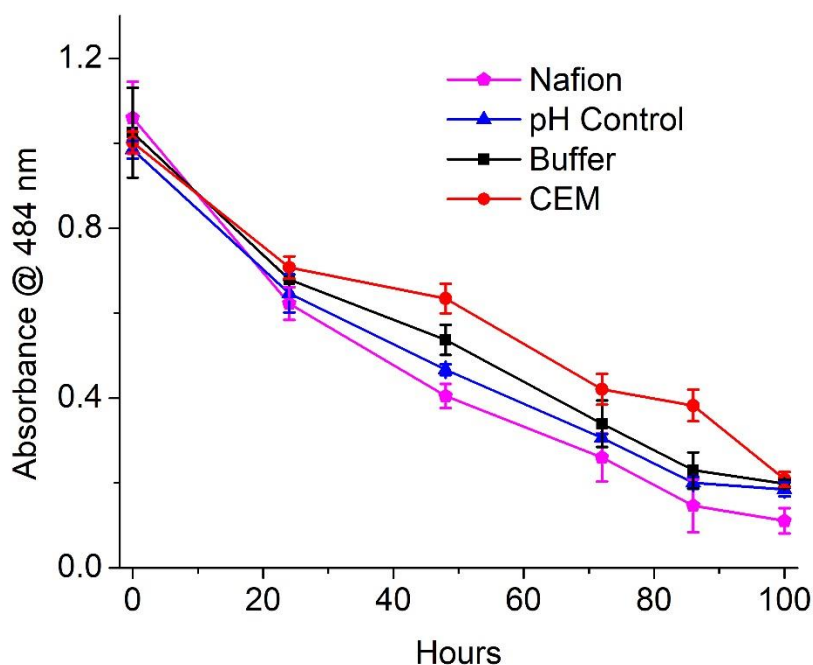


**Figure 3.1:** Comparison of Acid orange 7 decolourization rates in the various MFC systems over a period of 100 hours

A combination of increased proton transport, mitigated pH changes in the cathode chamber (see section 3.3.2) resulted in a better performance in Nafion system which is also evident by a high COD reduction. Biologically, the azo bond is thought to be cleaved under anaerobic conditions in the anode chamber leading to decolourization, but the mechanism is not clear. Since azo dyes are large and usually charged, they are likely to be reduced extracellularly. It has been suggested that the decolourization process is a fortuitous one where azo dye might act as an electron acceptor supplied by carriers of the electron transport chain. There also suggestions that decolourization is due to non-specific extracellular reactions occurring between reduced compounds of anaerobic metabolism e.g. sulphides and the azo dyes. Others suggest that anaerobic reductive cleavage of the azo bond is aided by azoreductases, the electron shuttling being aided by soluble redox mediators e.g. flavins (Saratale et al., 2011; Fernando, 2014).

### 3.3.2 pH and salinity changes in the cathode chamber

The initial pH was 4.5 in all the reactors and 2.5 mS cm<sup>-1</sup> ionic strength. The MFC with 200 mM buffer had an initial ionic strength of 5.32 mS cm<sup>-1</sup>. From Figure 3.2 it can be observed that the nafion-MFC had a better catholyte pH control with pH

changing from 4.5 to 5.5 as compared to CEM-MFC where the pH increased to 8.6. The increase in pH and the ionic strength in the cathode chamber of Nafion setup suggest the migration of cations to the cathode. Nafion is a sulfonated tetrafluoroethylene copolymer that consists of a hydrophobic fluorocarbon backbone ( $-\text{CF}_2-\text{CF}_2-$ ) to which hydrophilic sulfonate groups ( $\text{SO}_3^-$ ) are attached (Mauritz and Moore, 2004). The negatively charged  $\text{SO}_3^-$  groups have high levels of proton conductivity that allows  $\text{H}^+$  ions to be transported to the cathode chamber of a MFC. Rozendal et al, 2006 suggested that although the diffusion coefficient of the metal ions are much smaller than the protons for Nafion membrane, the concentration of these ions is  $10^5$  higher than the protons in a MFC (Rozendal et al., 2006). Increase in both pH and ionic strength in CEM-MFC as compared to Nafion MFC may be explained in terms of higher cation transport as compared to proton transport. Nafion had a better control over the metal ion transport from anode to cathodic chamber as compared to the CEM. This is evident in this study where there is an increase in ionic strength from  $2.5 \text{ mS cm}^{-1}$  to  $6.25 \text{ mS cm}^{-1}$  in Nafion-MFC whereas CEM-MFC has an increase of  $2.5 \text{ mS cm}^{-1}$  to  $22.5 \text{ mS cm}^{-1}$ . The difference between Nafion and CEM ionic strength was statistically significant ( $p < 0.05$ ) as observed by independent sample t-test. The increase in ionic strength in Nafion-MFC is due to cation transport from anode as Nafion possesses undesired affinity for cation species other than protons (Rozendal et al., 2006).

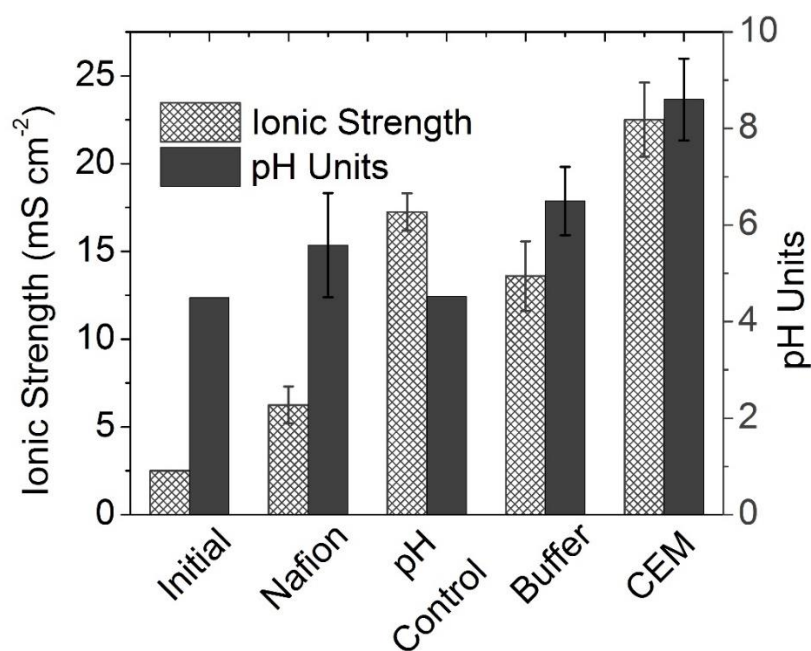


**Figure 3.2:** Initial (time 0) and final (10 days) pH and ionic strength in each setup over a period of 7 days

The increase in buffer strength from 100 mM to 200 mM maintained a similar pH range as the Nafion system suggesting that the increased salinity relative to the Nafion system may be the reason for its poorer dye decolourization efficiency and lower maximum power density.

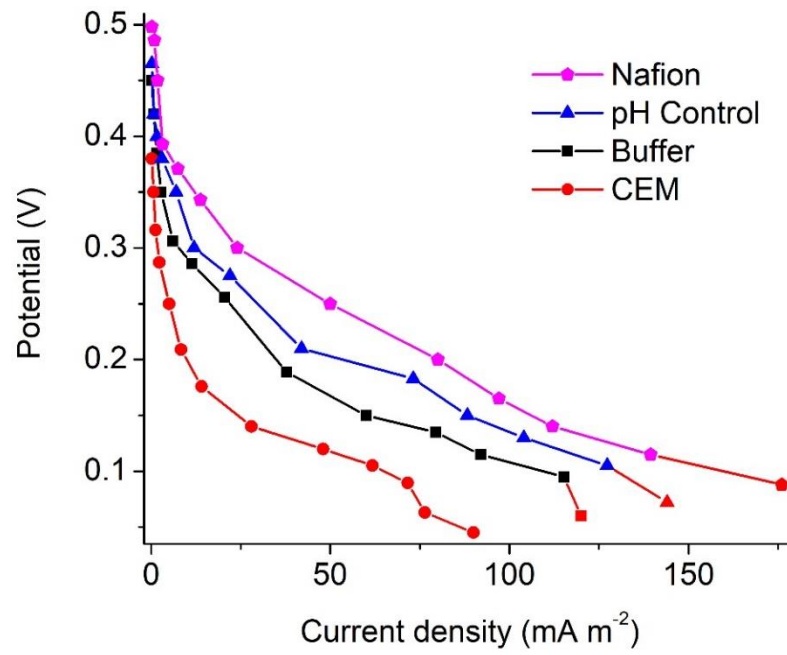
### 3.3.3 Current and Power generation

The maximum voltage recorded was 250 mV for the Nafion system. The other three systems recorded a much lower voltage with CEM showing the lowest voltage of 140 mV. Polarisation tests indicated a maximum power output of 16 mW m<sup>-2</sup> for Nafion, 13.3 mW m<sup>-2</sup> in pH-controlled system, 11 mW m<sup>-2</sup> and 6.5 mW m<sup>-2</sup> for Buffer strength and CEM systems respectively (Figure 3.3 (a)). The internal resistances of the MFCs was calculated from the potential vs current density graph (Figure 3.3 (b)). Nafion produced the lowest internal resistance of 0.860±0.075 kΩ followed by pH control 1±0.12 kΩ; buffer strength 1.2±0.15 kΩ and CEM 1.3±0.17 kΩ. The power density and internal resistances followed the trend observed by Kim et al, 2007 with Nafion performing better than CEM (Kim et al., 2007). The Coulombic efficiency for Nafion was 1.13%; for pH control 1.07%; for buffer strength 0.895% and for CEM 0.71%. The low coulombic efficiency could be due to the consumption of electrons for the reduction of azo dye and accumulation of incompletely oxidised metabolites like acetate under anaerobic condition (Newton et al., 2009).

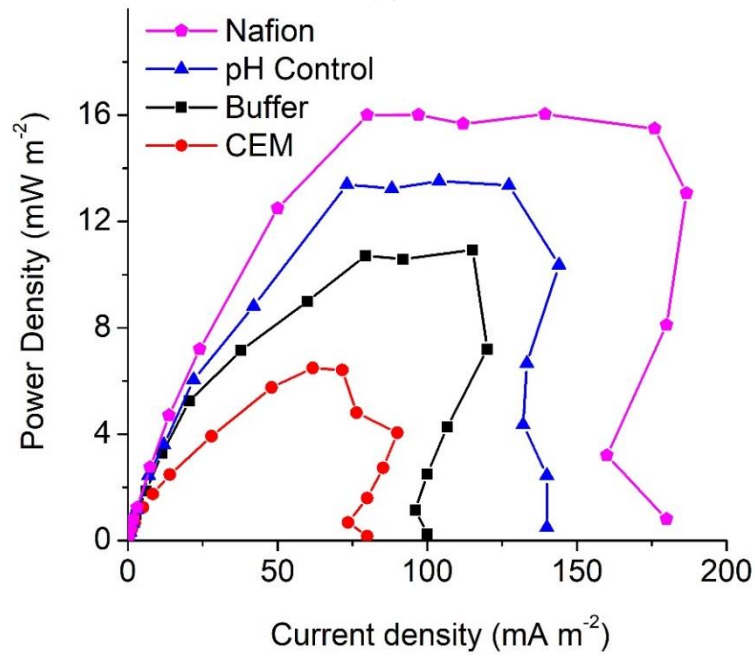
The improved power density in the Nafion system could be due to the reduction of metal ions migration and higher proton transport to the cathode minimising pH changes compared to other systems. This correlates with study by Harnisch, 2008 which suggests that number of protons transported across Nafion is higher than CEM, thereby maintaining the pH equilibrium in Nafion system (Harnisch, 2008). A similar system with 195 mg L<sup>-1</sup> Acid Orange 7 (AO 7) as dye, Pt as catalyst and CMI 7000 as ion exchange membrane gave a Pmax value of 24 mW m<sup>-2</sup> (Fernando et al., 2012).

Although the pH control MFC had better control over catholyte pH as compared to other systems, there was a significant increase in the ionic strength of the system. Based on salinity values the power density values for the pH control system would be expected to be intermediate between CEM and buffer strength systems. The fact that the power density of the pH control system was higher than that of the buffer strength CEM system

suggests that maintaining optimal pH value in the cathode chamber to be more important to power generation than the differences in salinity in the systems tested.



(a)



(b)

**Figure 3.3:** (a) Polarisation curves for each system (b) Power density curve with P<sub>max</sub> for each system obtained by varying the external resistance from 10Ω-1MΩ at day 3.

### 3.3.4 Laccase Enzyme Activity at the cathode

Figure 3.4 shows the trend for enzyme activity in all the systems over time. Nafion 117 membrane was able to limit salinity and pH changes in the cathode chamber leading to prolonged enzyme activity in comparison to other systems ( $p < 0.05$ ). Popat et al., 2012 argue that the ORR at pH 7 takes the form  $O_2 + 2H_2O + 4e \rightarrow 4OH^-$  and not  $O_2 + 4H^+ + 4e \rightarrow H_2O$  as is widely assumed. They suggest that the poor buffering of the catholyte and/or sluggish diffusion of hydroxide causes high cathodic overpotentials and is the main limiting factor of power production in MFCs (Popat et al., 2012). The poor performance of the buffer and CEM systems with regard to enzyme activity is attributed to the production of  $OH^-$  ions which have been known to hamper electron transfer from T1 to T2/T3 Cu sites in laccase (Xu, 1996).

Increasing the buffer strength from 100 mM to 200 mM improved enzyme activity (Figure 3.4). This has also been observed in *Pleurotus ostreatus* laccase in which buffer strengths up to 100 mM increased the rate of enzyme activity (Hassan et al., 2012). In the case of CEM a large shift in pH as compared to the other systems, probably causes a big shift in the standard reduction potential of the ORR reaction which might lead to  $H_2O_2$  formation (instead of water) causing negative feedback inhibition of laccase. The effect of  $H_2O_2$  inhibition was observed by (Milton et al., 2013) in a single chamber enzymatic fuel cell employing laccase for  $O_2$  reduction.

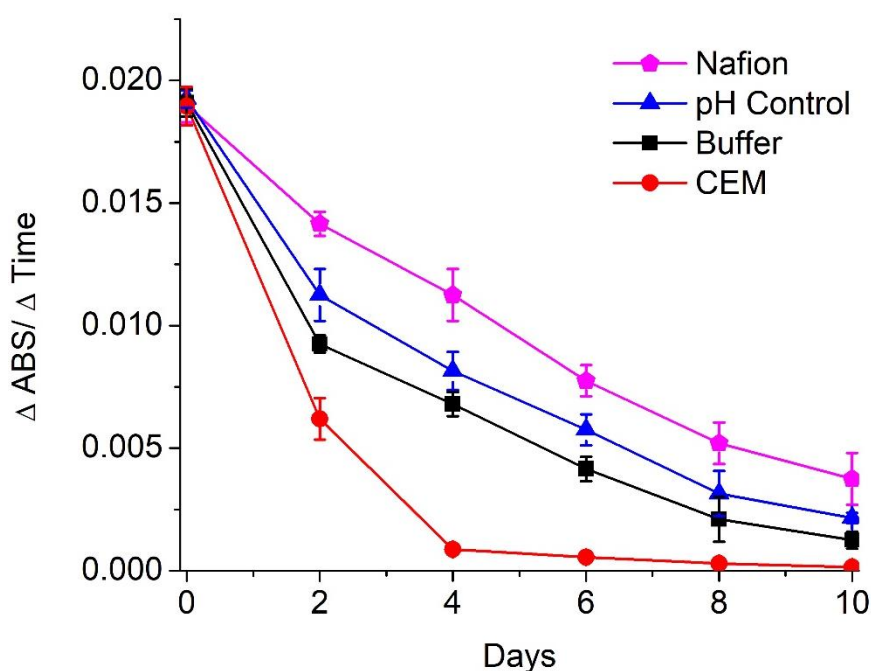


**Figure 3.4:** Laccase Activity indicating the change in absorbance over time for a period of 10 days

The pH profile for *Trametes versicolor* laccase is a bell shaped curve with optimum activity at 4.5 and decreasing gradually as the pH increases (Stoilova et al., 2010). This might explain the better performance of the pH control system over the buffer strength and CEM systems. pH affects the total net charge of enzymes and the distribution of charges on their exterior surfaces and these changes affect the activity and structural stability of the enzyme.

The laccase activity in this study in the nafion system remained stable for a period of 24 hours after that constant loss in activity each day was observed. Incubated laccase from *T. versicolor* in citrate buffer (pH 5) remained stable for 48 hours after which there was constant deactivation with a half-life of 7 days (Rubenwolf et al., 2012).

### 3.3.5 Detection of degradation products through HPLC

HPLC analysis revealed the presence of Sulfanilic acid and 1- amino-2-naphthol, the aromatic products of AO7 degradation (Figure 6). The retention times were Sulfanilic acid  $R_t= 1.7$  mins and 1-amino-2-naphthol  $R_t= 2.7$  mins respectively (Figure 3.5).

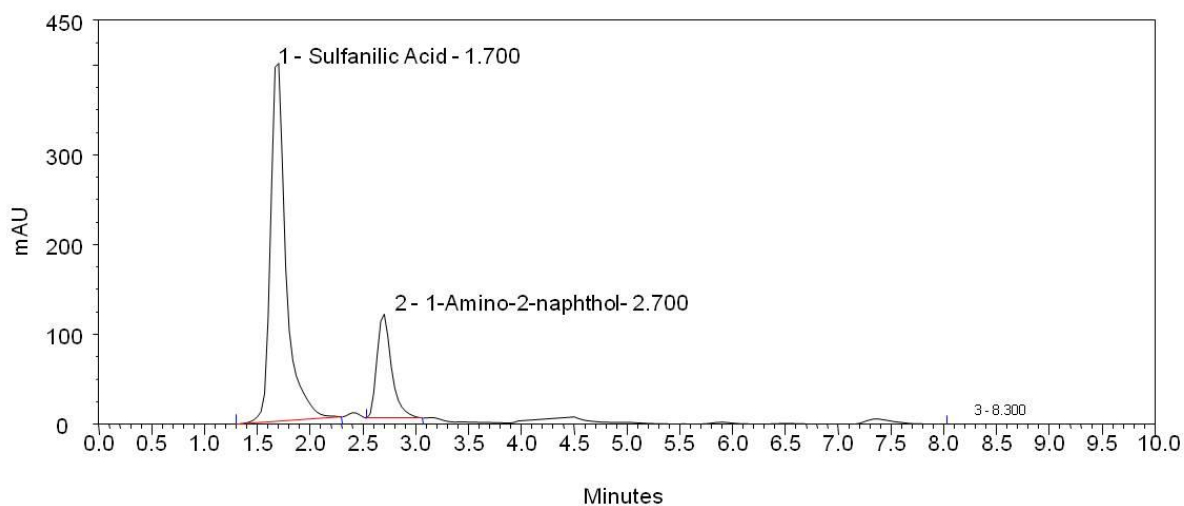


**Figure 3.5:** HPLC analysis of degradation products with peaks representing the dye decolourization products with their retention time

### 3.3.6 Toxicity Testing

The Microtox toxicity assay conducted at the end of the run using *Vibrio fischeri* indicated that the degradation products were toxic. The half maximal inhibitory concentration ( $IC_{50}$ ) for Nafion was at 200 mg COD  $L^{-1}$  and around 150 mg COD  $L^{-1}$  for all other samples ( $p < 0.05$ , Anova) (Figure 3.6). The toxicity and COD are directly

related as high COD indicates higher reduced organic content such as the aromatic amines from dye breakdown (not oxidised completely) that are toxic in nature.

The toxicity of the degradation products sulfanilic acid and 1- amino-2-naphthol is widely reported in various literature but an independent study done in our lab suggests that this can be reduced by using a second aerobic treatment step (Fernando, 2014).

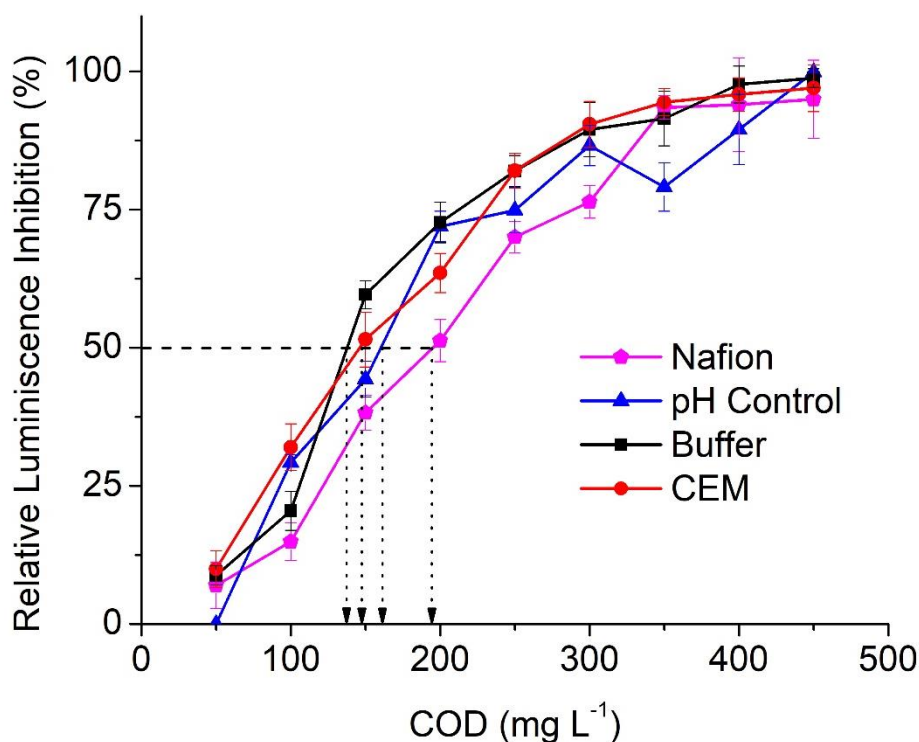


**Figure 3.6:** Relative luminescence inhibition in relationship to COD. There was no statistically significant difference in the levels of toxicity in the systems tested after a run time of 10 days.

### 3.4 Conclusion

This study investigated various ways of mitigating pH changes in the cathode chambers of MFCs and their effect on laccase activity and decolourization of a model azo dye Acid orange 7 in the anode chamber. The methods included using Nafion 117 and CMI7000 as membranes, automatic control of pH in the cathode chamber and using a high strength buffer.

Nafion 117 membrane was able to limit salinity and pH changes in the cathode chamber leading to prolonged enzyme activity and improved performance of the system in comparison to other MFCs. The pH optima for laccase is 4.5 and there is a

gradual decrease in enzyme activity as the pH shifts from the optima. This is evident in MFC with CMI7000 membrane as they had the highest change in pH and ionic strength which contributed to low performance and decreased longevity of enzyme activity. The MFCs with pH control and increased buffer strength (200 mM) had higher power output due to better retention of enzyme activity than one with CMI7000 membrane. Although Nafion performed better than other MFCs, its cost may hinder its usage in wastewater treatments and scaled up reactors.

It is observed that pH control is essential for preserving laccase activity and increasing the performance of a MFC, but it does not guarantee sustained laccase activity that salinity increases also affects the activity and could be mitigated using a proton selective membrane. Therefore, it is essential to decouple pH and salinity to develop efficient biocathodes for MFCs. Moreover, laccase has the versatility of being engineered to improve the efficiency. With the advent of protein engineering, immobilization strategies etc. laccase holds potential to be an efficient cathode catalyst for oxygen reduction reaction.

## **Chapter 4**

**Laccase immobilization strategies for application as a cathode catalyst in microbial fuel cells for azo dye decolourization**

## **4.1 Background**

### **4.1.1 Immobilization for stability and better direct electron transfer (DET)**

The use of enzymatic cathodes is limited by the short lifetime and stability of the enzymes in the system. In a fuel cell the lifetimes of the enzymes typically vary from 7-10 days due to their fragile nature (Cooney et al., 2008). The deactivation of laccase from *T. versicolor* in citrate buffer (pH 5) at room temperature was studied by Rubenwolf et al. (2012) who observed that the enzyme remained stable for 2 days after which there was constant deactivation rate with a half- life of 7 days (Rubenwolf et al., 2012). In our previous study we have observed that maintaining strict conditions at the cathode can preserve laccase activity to some extent. These conditions cannot guarantee sustained activity and the enzyme cannot be reused. The previous study maintains the macro environment to provide optimal conditions for enzyme activity. The loss of enzyme activity over time is due to the loss of enzyme co-factors or disruption in the charges of amino acids that might result in enzyme denaturation. For sustained activity the enzyme must be protected from the environmental changes. Enzymes in the immobilized form are stable, resistant to changes in environmental factors e.g. pH and can be reused.

Immobilization offers enzymes the structural stability, retention of activity, prevention from deactivation and protects it from external inhibitors. The immobilized enzymes can be reused to reduce the cost of the system. There are various types of immobilization depending on the enzyme, choice of support material and their applications. Immobilization of laccase on different support material with different methods have been explored widely (Davis and Burns, 1992; Lalaoui et al., 2013; Le Goff et al., 2015).

### **4.1.2 Types of enzyme immobilization**

#### **4.1.2.1 Adsorption**

The most simple and straight forward method of immobilization in which the enzyme is physically adsorbed onto the solid support. Adsorption is based on weak Van der Waals force, hydrophobic interaction and hydrogen bonds (Jesionowski et al., 2014). Since these are weak bonds the immobilization is reversible, where in the solid support can be reused several times even after the enzyme has been decayed. The method

involves immersing and incubating the solid support in the enzyme solution for a specific amount of time until adsorption has occurred (Mohamad et al., 2015).

For applications in fuel cells, laccase enzyme from *P. sanguineus* was adsorbed on to buckypaper cathode and its electrochemical activity studied. The cathode polarization produced current density of  $115.0 \pm 3.5 \mu\text{A cm}^{-2}$  at 400 mV vs. SCE (Fokina et al., 2015). Similarly, a hybrid microfluidic fuel cell containing Laccase/ABTS adsorbed on carbon to develop a Lac/ABTS/C cathode electrode. This electrode was tested in a fuel cell containing AuAg/C anode and produced a maximum power density of  $0.45 \text{ mW m}^{-2}$  (López-González et al., 2014).

Although adsorption is a cheap, simple and easy method of immobilization, the bonding is very weak to prevent the enzyme from leaching out and losing its activity.

#### 4.1.2.2 Covalent bonding

This is the most commonly used method for immobilization due to the strong bonding and irreversible enzyme attachment. This method utilizes the functional groups amino (lysine), carboxylic (aspartic, glutamic acid), thiol (cysteine) of the enzymes to form covalent bonds with the support material (Guisan, 2006) (Figure 4.1).

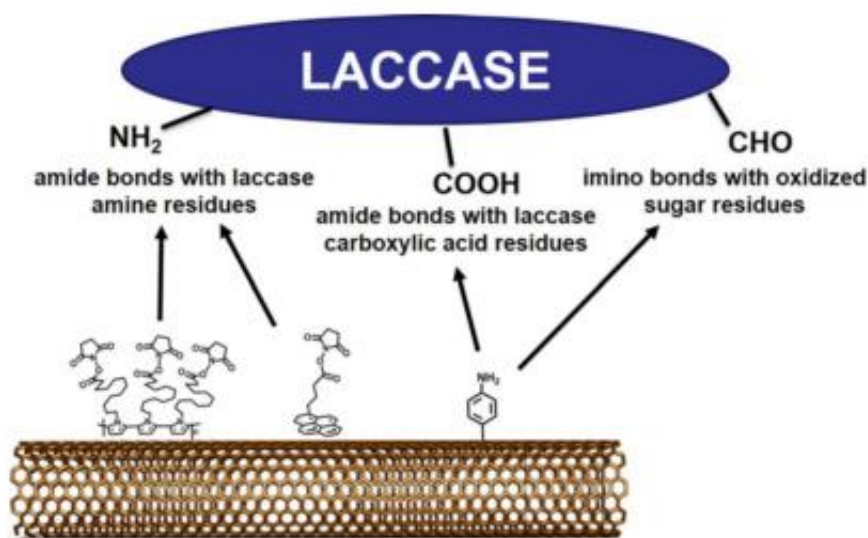


**Figure 4.1:** Laccase formation of covalent bonds on carbon nano tubes (Le Goff et al., 2015)

Carbon nanotubes (CNT) are widely used for laccase immobilization for their good conductivity, nano-structure that provides effective direct electron transfer and the

large surface area for high enzyme loading (Le Goff et al., 2015) (Figure 4.1). Functionalized CNTs and nanoparticles are also used to immobilize laccase for dye decolourization, effluent treatment, chlorophenol degradation applications. They help in retaining enzyme activity in the presence of the pollutants to make it reusable for various cycles (Dai et al., 2016; Othman et al., 2016; Taheran et al., 2017). MWCNTs on cellulose nitrate support was used for covalent bonding of laccase to study the decolourization of Reactive Black (RB5) dye. There was 84% decolourization in the presence of 1-hydroxybenzotriazole (HBT) as mediator and 95% of its activity was retained for 10 cycles of reaction (Othman et al., 2016).

Cross linking is a method of immobilizing enzymes on the electrode through use of cross-linking agent namely glutaraldehyde. It forms covalent bonds between the amine group (lysine) of the enzymes and any external polymers (Mohamad et al., 2015). A novel biocathode was fabricated by Zhang et al, 2015 using laccase coated with polymer polyethylenimine (PEI) followed by crosslinking with glutaraldehyde for decolourization of Acid Orange 7 dye. PEI has large number of amino groups that enables easy crosslinking with the enzyme. This biocathode had higher decolourization kinetics and enzyme stability compared to free laccase solution (Zhang et al., 2015).

#### **4.1.2.3 Entrapment**

In this method the enzyme is caged in a porous matrix by covalent or non-covalent bonds (Datta et al., 2013). The matrix would physically limit the enzyme from leaching out and shields the enzyme from potential inhibitors. Polymers are suitable entrapment matrices as there is control over the polymerization process, modification of functional groups and easy co-immobilization of enzymes. The simplest form of entrapment is the gelation of poly anionic or cationic polymers in the presence of counter ions. Polymer matrix commonly used are alginate, carrageenan, collagen, polyacrylamide, gelatin etc. (Guisan, 2006; Mohamad et al., 2015). Entrapment of laccase in polymers is the most widely used method for dye decolourization application (Chhabra et al., 2015; Koklukaya et al., 2016; Bagewadi et al., 2017). Laccase from *Trametes versicolor* was entrapped within a chitosan grafted polyacrylamide hydrogel to study its durability on degrading dye Malachite Green. The half-life of hydrogel immobilized laccase was 13 times longer than free laccase and there was greater than 90% colour removal in both systems. The enzyme was reusable for 6 cycles (Sun et

al., 2015). In recent years redox polymers have been used for entrapping laccase to aid in DET to the electrode for fuel cell applications (Ackermann et al., 2010). Osmium ( $[\text{Os}(2,2'\text{-bipyridine})_2(\text{polyvinylimidazole})_{10}\text{Cl}]^{+}/2^{+}$ ) based hydrogels have been developed to entrap laccase from *Melanocarpus albomyces* for reduction of oxygen. They have produced a current density of  $3.8 \text{ mA cm}^{-2}$  at  $0.2 \text{ V}$  vs Ag/AgCl (Kavanagh et al., 2008).

#### **4.1.2.4 Encapsulation**

In this type of immobilization, the enzyme is caged in micelles of polymer that have hydrophobic interior and hydrophilic exterior. These micelles increase the enzyme stability compared to water or buffer (Cooney et al., 2008). Since the enzymes are pH dependent the micelles create a perfect environment for laccase to prevent enzyme denaturation from pH changes. Various dehydrogenase enzymes have been encapsulated by Nafion modified with tetraalkylammonium bromides. Nafion micelles helps in retention of enzyme activity by providing a protective outer shell. The dehydrogenase enzymes immobilized in Nafion and tetrabutylammonium bromide (TBAB) had retained activity for over 45 days (Moore et al., 2004). Laccase from *Rhus vernificera* was immobilized with Nafion modified TBAB and used as air breathing biocathode in a 40% direct methanol fuel cell (DMFC). The system produced a maximum current density of  $50 \text{ mA cm}^{-2}$  and a power density of  $8.5 \text{ mW cm}^{-2}$ . The lifetime of the laccase biocathode was 290 hours in the DMFC (Gellett et al., 2010).

Each immobilization method has their advantages and limitations (Table 4.1) depending on the enzyme used and the application.

**Table 4.1:** Types of enzyme immobilization with their advantages and disadvantages

Type of immobilization	Method	Advantage	Disadvantage
Adsorption	Enzymes are adhered to surface of carrier matrix through ionic, hydrophobic or van der Waals interaction (Jesionowski et al., 2014)	<ol style="list-style-type: none"> <li>1. Relatively simple</li> <li>2. Reduces conformational changes or denaturation of enzymes</li> <li>3. Suitable for wide variety of carriers (Huang and Cheng, 2008)</li> </ol>	<ol style="list-style-type: none"> <li>1. Weak bonding (Cooney et al., 2008)</li> <li>2. Exposed to microenvironment (pH, Temperature)</li> <li>3. Depends on affinity between enzyme and carrier matrix</li> </ol>
Covalent bonding (Cross-linking)	Enzyme is attached to the matrix by covalent bonds (Guisan, 2006) .	<ol style="list-style-type: none"> <li>1. Strong Bonding</li> <li>2. No leakage</li> <li>3. Higher stability (Romo-Sánchez et al., 2014)</li> </ol>	<ol style="list-style-type: none"> <li>1. Enzyme loading limited by matrix functional group density (Cooney et al., 2008)</li> <li>2. Structural and conformational change</li> <li>3. Diffusional limitation to the active site of the enzyme</li> </ol>
Encapsulation	Enzyme is caged micelles of polymer having hydrophobic interior and hydrophilic exterior (Moehlenbrock and Minter, 2017)	<ol style="list-style-type: none"> <li>1. Retains native enzyme structure</li> <li>2. Minimal enzyme requirement</li> <li>3. No chemical modification</li> </ol>	<ol style="list-style-type: none"> <li>1. Not suitable for large substrates</li> <li>2. Diffusional limitation (Cooney et al., 2008)</li> <li>3. Microcapsules are sensitive to surrounding medium to like pH, ionic strength etc.</li> </ol>
Entrapment	Enzyme is caged in a porous matrix by covalent or non-covalent bonds (Datta et al., 2013)	<ol style="list-style-type: none"> <li>1. Retains native enzyme structure</li> <li>2. Minimal enzyme requirement</li> <li>3. No chemical modification</li> </ol>	<ol style="list-style-type: none"> <li>1. The polymer used in entrapment might be charged resulting in lower activity.</li> <li>2. Difficult to control the pore size</li> <li>3. Enzyme leaching</li> <li>4. Diffusional barrier</li> </ol>

### **4.1.3 Types of laccase immobilization used in this study**

Immobilizing enzymes on the electrode provides direct electron transfer and higher power output (Cooney et al., 2008). Monomers of conducting polymers like Poly Aniline (PANI) can be electropolymerized to form conductive layers of desired thickness on the surface of the base electrode. PANI has the advantage of possessing an exposed amine group that can be used for the cross linking with the enzyme. Laccase and glucose oxidase enzymes have been immobilized on polyaniline nanofibres for biofuel cell applications (Kim et al., 2014, 2011).

Another method of immobilizing the enzyme is the entrapment in to beads. This method has advantage of retaining the native structure of enzyme as compared to that of cross-linking method. Laccase is a copper-dependent enzyme and immobilizing in copper alginate beads will retain more activity compared to other methods. Teerapatsakul et al. 2007 have observed that the immobilization yield and enzyme activity was higher when  $\text{CuSO}_4$  was used as crosslinking solution compared to  $\text{CaCl}_2$  (Teerapatsakul et al., 2007).

The third method of immobilization was encapsulation of laccase in Nafion micelles formed by modifying the polymer with an alkyl ammonium salt such as tetrabutylammonium bromide (TBAB) (Meredith et al., 2012). The quaternary ammonium cations modify the Nafion to less acidic form by replacing the protons and counteracting the sulfonate groups. They also increase the size of micelles and channels which should result in favourable enzyme immobilization. Meredith et al, 2012 have developed this relatively new method to immobilize various enzymes and observed an increase in enzyme activity (Meredith et al., 2012).

Platinum is the most commonly used cathode catalyst for high performance fuel cells. In recent years there has been a transition to PGM (Platinum Group Metals) free catalysts for oxygen reduction reactions with metal compounds impregnated with Nitrogen doped Carbon (N-C) serving as a good replacement for Pt. Masa et al, 2013 have impregnated trace (1.05%) levels of Fe with nitrogen doped carbon (NC) and observed electrochemically that the ORR activity of Fe-N/C matched that of Pt/C (Masa et al., 2013).

In this study, laccase in the three immobilized states (Cross-linking, entrapment in beads and micellar encapsulation) was compared with freely suspended enzyme with

respect to dye decolourization, enzyme activity retention, power production and reusability in the cathode of a microbial fuel cell. This study aims to emphasize the effect of immobilization on laccase ability to perform as efficient cathode catalyst. The performance of the laccase electrode was evaluated against platinum and Fe-N/C catalysts.

## **4.2 Materials and Methods**

### **4.2.1 Chemicals**

The Fe-N/C catalyst was obtained from Dr. J. Masa from Ruhr-University Bochum in Germany. The laccase used was commercial laccase (Sigma Aldrich, UK) from *Trametes versicolor* (13.6 U mg<sup>-1</sup>).

### **4.2.2 Laccase Immobilization**

#### **a. Polyaniline laccase**

Polyaniline (PANI) immobilization was carried out by electropolymerization of 0.1 M Aniline in 1 M Sulphuric acid with carbon fibre (2.5 cm<sup>2</sup>) as working electrode, titanium wire as counter electrode and Ag/AgCl as reference using Keysight B2900A potentiostat. A current density of 4.5 mA cm<sup>-2</sup> for 50 seconds was used for electropolymerization of aniline on to bare carbon electrodes. After electropolymerization, PANI was functionalised using 1.25% glutaraldehyde at 37 °C for 15 mins. This was followed by the addition of laccase enzyme 1 U ml<sup>-1</sup> (60 Units) to the solution for cross linking for 15 mins. Enzyme assay (Section 2.6.5) of the laccase solution was carried out before and after cross linking to get an estimate of amount of laccase immobilized.

#### **b. Copper Alginate Beads**

The Cu-Alginate immobilization procedure was adapted from (Teerapatsakul et al., 2007). A 3% w/v Sodium alginate was dissolved in 40 ml of water. A total activity of 60 Units of laccase was added to the alginate solution. The above mixture was passed through a 21-gauge syringe into 0.15 M cross-linker copper sulphate solution. The beads were allowed to rest for 45 minutes after which they were washed with and incubated in acetate buffer. Enzyme assay (Section 2.6.5) was performed on the beads, the cross-linking solution to determine the immobilization yield (2.6.5(a)).

### **c. Nafion micelles preparation**

The salt modified Nafion micelles was prepared according to the method developed by (Meredith et al., 2012). A 2 ml of 5% w/v Nafion solution (Sigma) was added to 78.3 mg of TBAB (tetrabutylammonium bromide) and vortexed at 1500 rpm for 10 minutes. The solution was poured in a weighing boat and the solvent was allowed to evaporate. After 18 hours a yellow transparent film was formed at the bottom on the weighing tray. The tray was then filled with 18 M $\Omega$  deionised (DI) water and soaked for 24 hours to remove the excess alkyl ammonium bromide salts and HBr. The water was removed, and the polymer rinsed with DI water was allowed to dry. The resulting dry film was suspended in 2 ml ethanol.

Immobilization of laccase in Nafion micelles was performed by dissolving the enzyme in 10 ml acetate buffer (pH 4.5) to achieve a total activity of 60 Units. 1 ml of the ethanol-polymer suspension was added to 2 ml of the enzyme solution and vortexed. The resultant mixture was poured on to the electrode and the solvent allowed to evaporate, thus forming a film on the electrode surface.

### **4.2.3 Platinum and Fe–N/C Electrode Preparation**

The cathode contained a Pt catalyst layer with a Pt loading of 0.5 mg cm<sup>-2</sup>. Pt powder for the cathode was mixed with carbon black powder (Sigma Aldrich, UK) for a 10% (w/w) mixture. This mixture was suspended in Nafion solution (Sigma Aldrich) and the suspension was applied as a uniform coating on the cathode electrodes using a paint brush and allowed to air dry. The same approach was used for Fe–N/C catalyst electrode preparation.

### **4.2.4 Experimental design**

The MFC used in the study was the 'H'-type reactor with a working volume of 200 ml in each chamber. The electrodes were constructed from carbon fibre (non-woven) with a surface area of 25 cm<sup>2</sup>. Cation exchange membrane CMI7000 ion exchange membrane was soaked in 5% NaCl for 12 hours prior to use.

Four systems were setup with laccase in the cathode chamber and one without enzyme: System 1 with Polyaniline crosslinked to laccase electrode referred to as "PANI laccase" to reduce ohmic loss; System 2 with laccase entrapped in copper alginate beads referred to as "Cu-Alg Laccase" to reduce enzyme denaturation; System 3 with

laccase freely suspended in the buffer referred to as "Free laccase"; System 4 with laccase immobilized in Nafion micelles is referred to as "Nafion Laccase" to maintain activity and System 5 referred to as "Control" which consisted of dye and buffer in the absence of laccase. Free laccase was added at  $0.3 \text{ U ml}^{-1}$  (60 Units/200 ml) in the cathode chamber. The total of 60 Units was maintained initially for all laccase immobilized systems.

The immobilized and free enzymes were suspended in 200 ml of 100 mM acetate buffer (pH 4.5) with  $100 \text{ mg L}^{-1}$  of Acid Orange 7 dye. The cathode chamber was maintained in aerobic conditions by supplying air through an air stone at a rate of  $200 \text{ ml min}^{-1}$ . For platinum comparison System 1 with platinum coated electrode is referred as "Platinum and System 2 with Fe-N/C coated electrode is referred to as "Fe-N/C". The immobilized enzymes, platinum and Fe-N/C electrode were suspended in 200 ml of 100 mM acetate buffer (pH 4.5).

#### **4.2.5 Operation of the Microbial fuel cell**

The composition in the anode was the same for all the reactors. The anode media components and their concentrations are detailed in Chapter 2, Section 2.3. The pH of the anolyte was initially adjusted to 7. The anode and cathode were connected to a resistor of  $2 \text{ k}\Omega$ . The anode was inoculated with 10% v/v *S. oneidensis* MR-1 culture previously grown in Luria Bertani broth to log phase (OD:0.4). The anode chamber was sparged for 10 minutes with nitrogen gas to remove any dissolved oxygen and maintain an anaerobic environment. Experiments were conducted at a temperature of  $30 \text{ }^\circ\text{C}$ . One cycle in this study represents 5 days. The experiments were carried out in triplicates.

#### **4.2.6 Analytical Procedures**

The analytical procedures followed in this study were AO7 decolourization (Section 2.6.1), electrochemical tests (Section 2.6.2), laccase enzyme activity and immobilization yield (Section 2.6.5 & 2.6.5(a)), Morphological characterisation using Scanning Electron Microscopy (SEM) of immobilized laccase electrodes (Section 2.6.7), functional group analysis of immobilized electrodes by FTIR (Section 2.6.8), Cyclic voltammetry (CV) of the laccase electrodes (Section 2.6.11 (a)) and statistical analysis (Section 2.6.15).

## 4.3 Results and Discussion

### 4.3.1 Characterization of immobilized laccase biocathode system

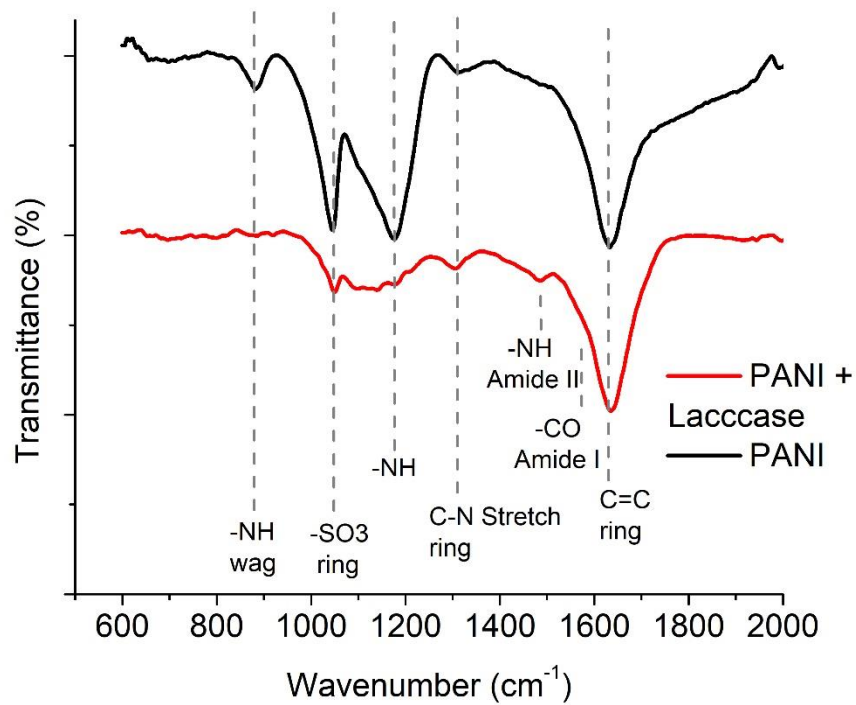
The immobilized laccase cathodes were analysed for their functional, morphological and electrochemical characteristics using FTIR, SEM and cyclic voltammetry (CV) respectively.

#### 4.3.1.1 Functional group analysis of Laccase biocathodes by FTIR

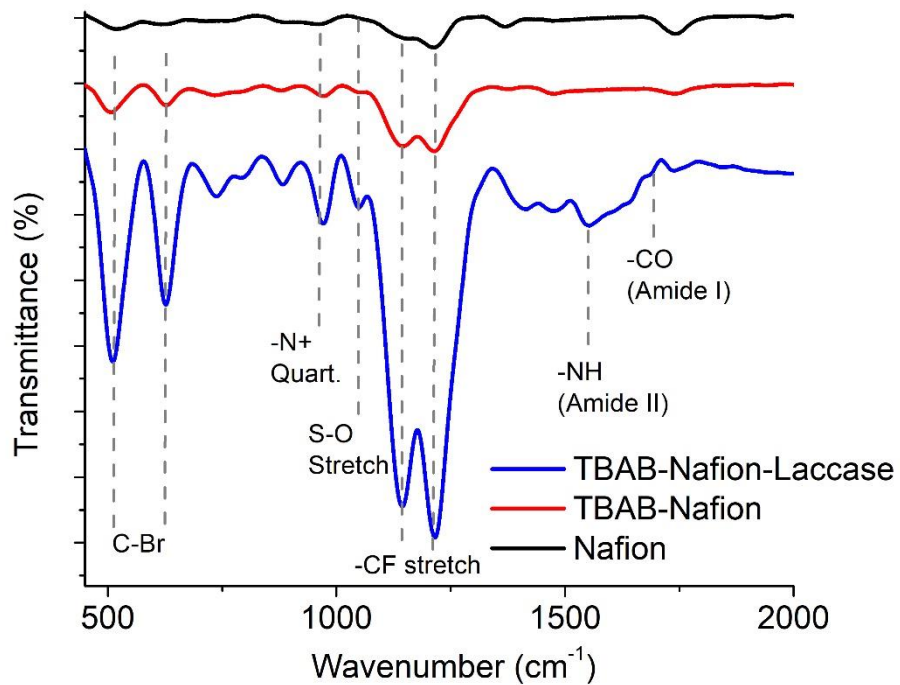
Functional group analysis was performed for polymer-based laccase immobilized biocathodes viz. PANI-laccase and Nafion-laccase. As both the immobilizations were multi-step procedures it was necessary to understand the modifications in the polymer during each step and the robustness of the laccase on immobilization.

FTIR was carried out to confirm the presence of PANI functionalization on the electrode (Figure 4.2a). The  $1314\text{ cm}^{-1}$  is typical of PANI (emeraldine base) attributed to C-N stretch vibration of the quinoid ring. The peak at  $1175\text{ cm}^{-1}$  indicates the vibration mode of  $-\text{NH}^+$  of the charged polymer. After the glutaraldehyde cross linking this mode disappears due to the crosslinking with laccase. This mode in PANI is responsible for the delocalized electron and hence the conductivity. The peak at  $882\text{ cm}^{-1}$  corresponds to the N-H wag of the  $1^\circ$  and  $2^\circ$  amine which disappears on cross-linking with the enzyme (Figure 4.2(a)). Another peak characteristic of the PANI deposited in sulphuric acid was observed at  $1047\text{ cm}^{-1}$  which is due to the sulphonation of the ring due to the substitution of the  $\text{SO}_3^-$  in place of  $\text{NH}_3^+$  (Figure 4.2a). The strong peak observed at  $1627\text{ cm}^{-1}$  is due to the C=C in vibration within the ring (Stejskal and Gilbert, 2006).

The Nafion functional group showed a CF stretch at  $1134\text{ cm}^{-1}$  and  $1213\text{ cm}^{-1}$  which is characteristic of tetrafluoroethylene backbone (Figure 4.2b). The mild peak at  $1048\text{ cm}^{-1}$  indicates the sulfonated terminal of the tetrafluoroethylene chain (Kunimatsu et al., 2010). On functionalization with TBAB, a peak appeared at  $978\text{ cm}^{-1}$  which indicated the presence of  $4^0\text{ N}^+$  embedded within the polymer (Figure 4.2b) (Hu et al., 2016). The laccase was characterized by the peaks at  $1559\text{ cm}^{-1}$  and  $1959\text{ cm}^{-1}$  which indicates the amine and carboxylic moiety of its amino acids (Figure 4.2b). For both PANI and Nafion immobilization, laccase was characterized by the presence of Amide I ( $1600\text{-}1690\text{ cm}^{-1}$ ) and Amide II ( $1480\text{-}1575\text{ cm}^{-1}$ ) for  $-\text{CO}$  and  $-\text{NH}$  stretch respectively (Kong and Yu, 2007).



(a)



(b)

**Figure 4.2:** FTIR spectra indicating the presence of functional groups of the polymer and immobilized laccase (a) PANI/Laccase (b) TBAB/Nafion/laccase

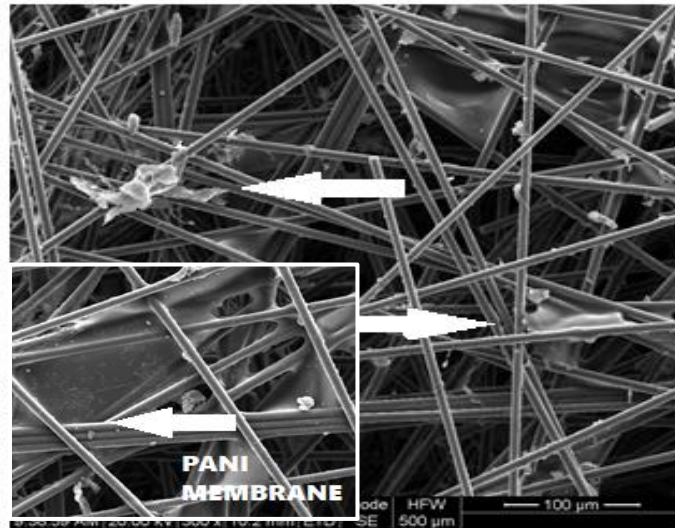
#### **4.3.1.2 Morphological analysis of the immobilized laccase biocathode using SEM**

Morphological analysis was performed for PANI laccase, Cu-Alg laccase and Nafion laccase electrodes. The main significance of this study was to understand the porosity of the Cu-Alg electrode and structural changes in the polymer (PANI, Nafion) on immobilization of the laccase.

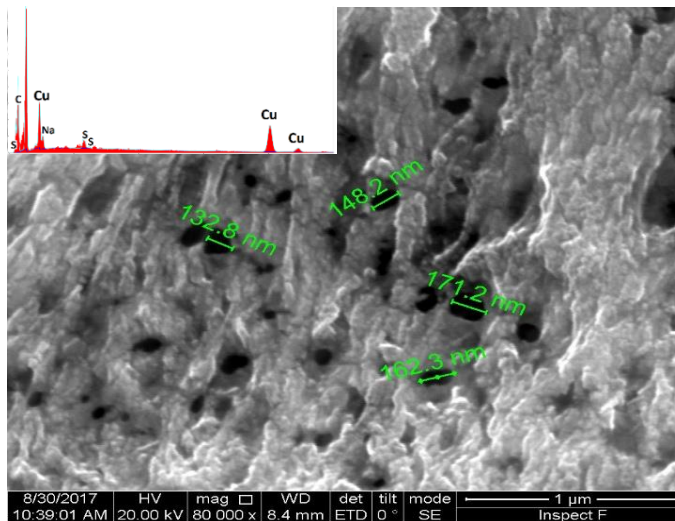
SEM images reveal the PANI fibres on the carbon electrode and the immobilized laccase (Figure 4.3 a-Inset). PANI appears as a polymer sheath formed over the carbon fibres. It is deposited primarily at close knit fibers of carbon due to higher charge density, with dimensions in the range of 30 x 50  $\mu\text{M}$ . Crosslinking causes slight disruption of the membrane with the globular structure more prominent after laccase immobilization (Figure 4.3a). The adhesion of the globular laccase aggregates can be seen more prominently on the carbon fiber filaments, and thus is expected to have a low charge transfer resistance during the oxygen reduction reaction (ORR).

The beads were found to have a porous morphology with pore size of around 130 nm to 170 nm in diameter (Figure 4.3b). EDS (Energy-dispersive X-ray spectroscopy) results obtained through EDS indicates the presence of  $\text{Cu}^{2+}$  in the beads (Figure 4.3b-inset). The large size of the pores might have resulted in continuous release of laccase into the solution.

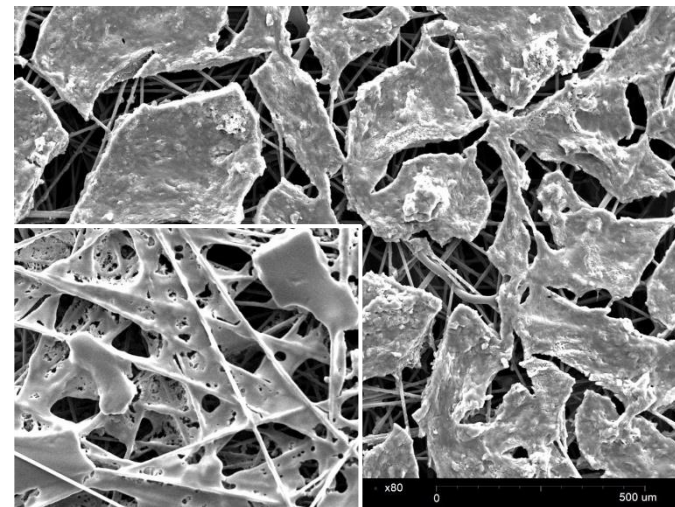
TBAB modified Nafion was found to coalesce to form a film on the electrode surface (Figure 4.3c-Inset). Unlike PANI film, the Nafion membrane is evenly distributed over the carbon filaments. The porosity of the electrode was found to be decreased on the film formation, which might affect the charge density. A gelation of the Nafion polymer is seen on addition of TBAB. In the presence of laccase, the film appears to be a thick layer of membrane compared to bare TBAB Nafion (Figure 4.3c). Unlike PANI-Laccase, Nafion-laccase film was seen to be restricted to the surface of the electrode. In addition, the aggregate size of the enzyme-polymer was larger compared to PANI-laccase.



(a)



(b)



(c)

**Figure 4.3:** SEM image of (a) Laccase-PANI Arrows indicate laccase, Inset-PANI (b) Cu-Alg-Laccase, Inset: EDS spectra (c) Nafion-Laccase, Inset-Nafion-TBAB

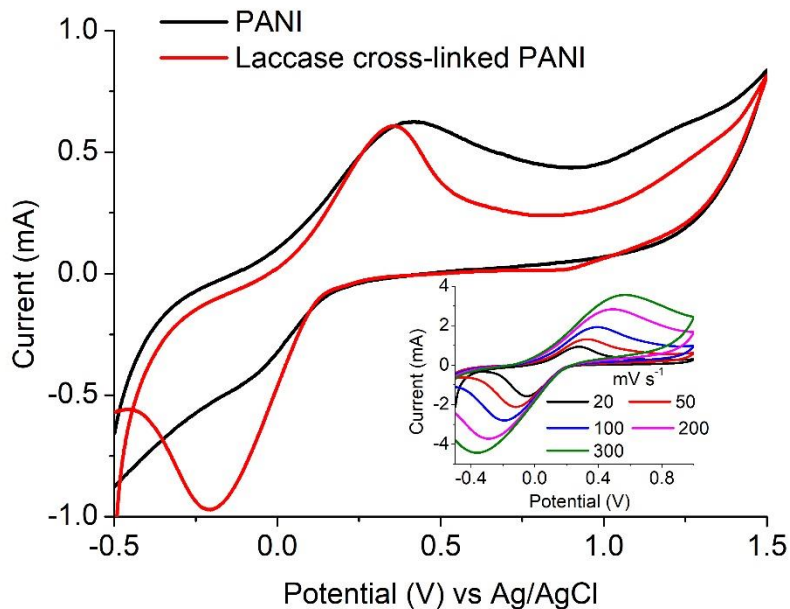
### 4.3.1.3 Electrochemical analysis of PANI and Nafion Laccase electrodes

The electrochemical analysis of the immobilized laccase biocathodes were limited to the PANI-laccase and Nafion-laccase biosystems because of the conductivity of the polymer used.

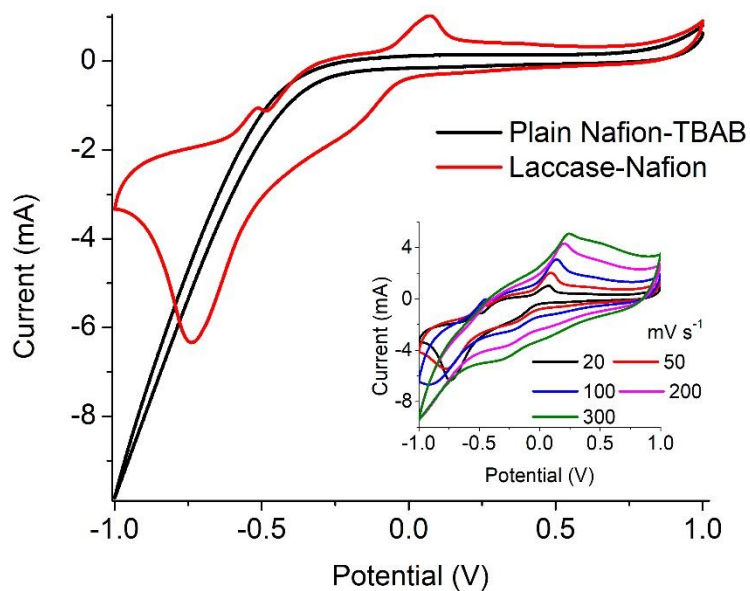
The redox property of the PANI-Laccase biocathode was analysed by cyclic voltammetry. An oxidation peak at 0.2 V indicates the presence of polyaniline on the electrode surface (Figure 4.4a).

PANI did not display the multiple peaks usually observed in strong acids, as the electrolyte used in this study was a weak acetate buffer (Hassan et al., 2012). This indicates the differential ionisation state of PANI under buffered conditions. On cross-linking with laccase an additional peak was observed at -0.32 V which might indicate oxygen reduction reaction (Le Goff et al., 2015). With increasing scan rate the rise in cathodic peak current was proportional to the square root of scan rate, indicating oxygen diffusion limited process (Figure 4.4a inset). Thus, the laccase catalytic activity was preserved on cross-linking with PANI (Figure 4.4a).

Nafion polymer alone did not show any characteristic peaks due to absence of the characteristic redox moiety. In presence of laccase the ORR takes place on the surface and the reduction peak appears at -0.6 V limited by oxygen diffusion (Figure 4.4b-Inset). Nafion-laccase showed an overpotential compared to the PANI laccase, which might be due poor electron conductivity of the Nafion (Figure 4.4b).



(a)



(b)

**Figure 4.4:** Cyclic voltammetry of immobilized electrodes at  $20 \text{ mV s}^{-1}$  of (a) PANI and PANI cross-linked with laccase (b) Nafion-TBAB and Nafion-TBAB laccase system. Insets: Immobilized laccase at different scan rates.

### 4.3.2 Power generation of Laccase biocathodes

The maximum voltage of  $480\pm 20$  mV was recorded across  $2\text{ k}\Omega$  in the MFC with PANI laccase followed by freely suspended laccase ( $420\pm 14$  mV), Nafion-laccase at  $405\pm 30$  mV and Cu-Alginate laccase at  $350\pm 25$  mV. The higher voltage of PANI/laccase MFCs compared to those with freely suspended laccase was probably due to the decreased proximity between the catalytic sites and the electrode, thus decreasing the ohmic and mass transfer resistance. Moreover, PANI is a conducting polymer, it decreases the charge transfer resistance of the electrode thus permitting the easy electron transfer. Although Nafion is also a conducting polymer, it is known to be an ionic conductor rather than an electron conductor (Heitner-Wirguin, 1996). In this study, laccase embedded in the Nafion without any mediators was less efficient in transferring electrons from the electrode to the enzyme compared to PANI. The low voltage of Cu-Alg laccase system was probably due to the high diffusion barrier imposed by beads to both oxygen and electron transfer from the electrode. This agreed with the maximum power density which was  $38.2\pm 1.7\text{ mW m}^{-2}$  for MFCs with PANI and  $28\pm 1\text{ mW m}^{-2}$  for freely suspended laccase,  $25.6\pm 2.08\text{ mW m}^{-2}$  for Nafion and  $14.7\pm 1.04\text{ mW m}^{-2}$  for laccase entrapped in beads (Figure 4.5). A maximum power density of only  $6.5\text{ mW m}^{-2}$  was observed by Schaetzle et al. (2009) when laccase was immobilized in hydrogels due to the reduced electron transfer of the enzyme hydrogels (Schaetzle et al., 2009). Thus, it is evident that the distance between the enzyme and the electrode is critical in achieving good oxygen reduction and higher power output. PANI/laccase, Nafion/laccase and freely suspended enzyme have better contact with the electrode compared to the beads. The OCV for PANI laccase reached up to  $900\pm 35$  mV while for free laccase it was  $700\pm 20$  mV,  $640\pm 48$  mV for Nafion and  $500\pm 32$  mV for laccase in Cu-alginate beads. The control MFC without enzyme at the cathode had low power density ( $0.6\pm 0.08\text{ mW m}^{-2}$ ) due to the absence of catalyst for the oxygen reduction reaction. The internal resistance for MFCs with PANI was  $1.4\pm 0.15\text{ k}\Omega$  which was the lowest compared to  $2.1\pm 0.12\text{ k}\Omega$  for free laccase and  $7.5\pm 1\text{ k}\Omega$  for the beads which was directly related to the above factors of ohmic and diffusion barrier. The internal resistance for Nafion laccase was  $5.3\pm 0.5\text{ k}\Omega$  which might account for the low power output compared to PANI laccase. The coulombic efficiency was quite

low for all systems with PANI-laccase highest at  $4.65 \pm 0.18\%$ , Nafion with  $4.23 \pm 0.45\%$ , Free laccase  $3.83 \pm 0.11\%$  and the lowest was Cu-Alg with  $2.97 \pm 0.16\%$ .

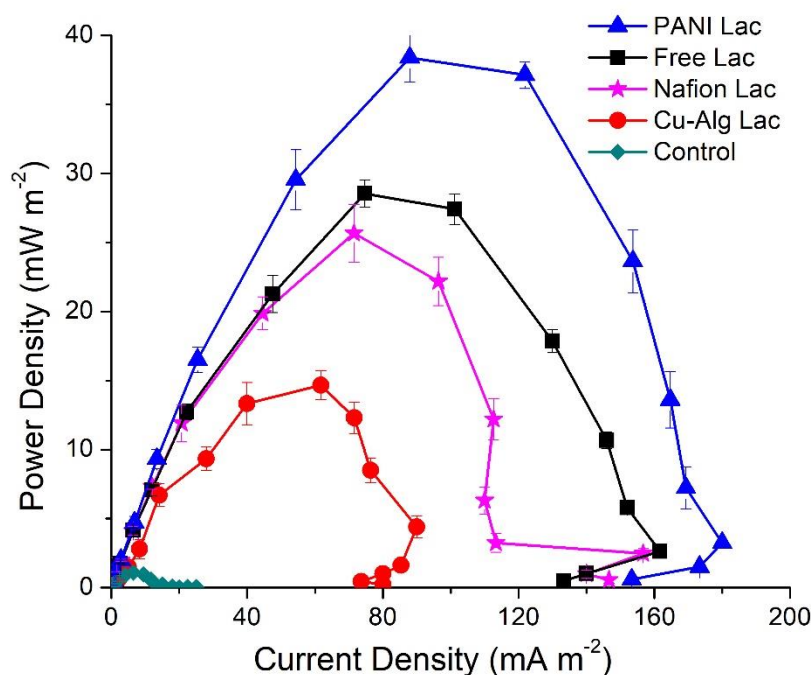


**Figure 4.5:** Comparison of  $P_{max}$  (Maximum power density) for the different laccase based biocathode systems obtained by varying the external resistance from  $10\Omega$ - $1M\Omega$  on day 3.

### 4.3.3 Dye decolourization in laccase biocathodes

There was  $85 \pm 3\%$  decolourization by MFC with enzyme in the freely suspended form compared to  $75.6 \pm 2.1\%$  for PANI laccase and  $73 \pm 2\%$  Nafion laccase over a period of 5 days (Figure 4.6a). The decolourization in MFCs with Cu-Alg beads laccase was  $81 \pm 4\%$ . There was  $>50\%$  decolourization in the first 24 hours for free and Cu-Alg laccase. Freely suspended laccase has the freedom of movement to interact with the dye and bring about better decolourization. On immobilization the protein becomes restricted to interact with the dye (Zille, 2006). In addition, the amount of enzyme cross-linked on the PANI laccase was lower (Section 4.3.4) than that of freely suspended enzyme due to the functional group density limitation of glutaraldehyde which also contributes to lower decolourization. Similarly, for Nafion-laccase limitation of the dye movement to the active site of the enzyme might have resulted in

lower decolourization compared to free laccase and Cu Alg-Laccase. The initial rapid decolourization is due to the high enzyme activity initially; the rate of decolourization decreases gradually as the enzyme activity decreases as shown in the enzyme activity graphs (Section 4.3.4). There was significant amount of dye adsorbed on the alginate beads which indicates that part of decolourization is due to adsorption (Figure 4.6b). Control beads without laccase showed  $8.2 \pm 0.5\%$  decolourization of the dye.

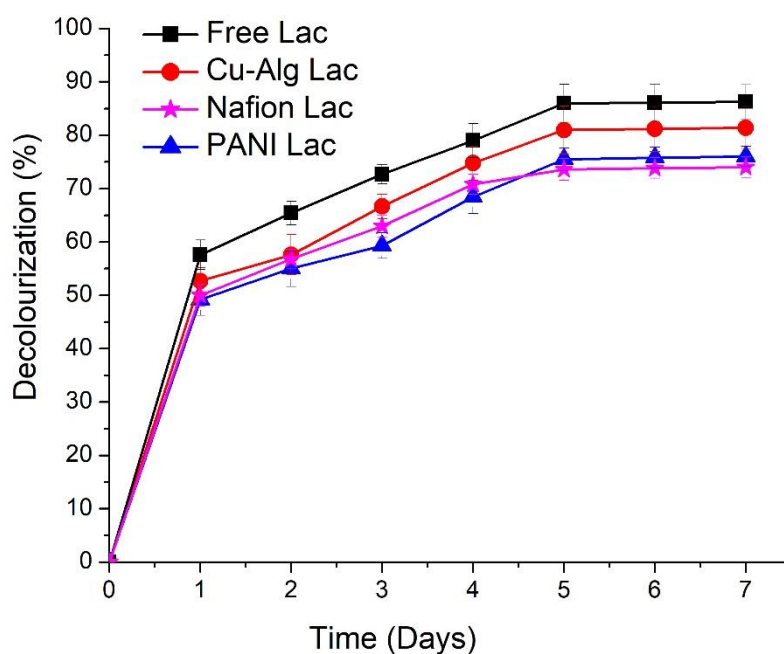


**Figure 4.6(a):** Comparison of decolourization rates of AO7 in the different laccase based MFC systems over a period of 7 days



**Figure 4.6(b):** Dye adsorption in copper alginate beads. Blue - Initial bead colour, Green- On adsorption of dye.

Similar results were observed by Daâssi et al, 2014 where 34% and 24% of dyes Reactive Black and Lanset Grey was adsorbed on calcium alginate beads with laccase (Daâssi et al., 2014). The laccase beads were reusable for two more cycles with the decolourization decreasing gradually each cycle (69% and 57%). There was no further decolourization observed after 120 hours in any of the systems.

#### **4.3.4 Enzyme activity of the laccase biocathodes in MFC**

The immobilization yield of the laccase immobilized systems was obtained by comparing the activity prior and after the immobilization. The immobilization efficiency was highest in Cu-Alg laccase with  $73\pm 8\%$  yield followed by Nafion and PANI with  $57\pm 2\%$  and  $38\pm 1\%$  respectively.

The enzyme activity was determined by ABTS assay for freely suspended laccase and for Cu-Alginate laccase. The relative decrease in activity for PANI-laccase and Nafion laccase on the electrodes were measured through cyclic voltammetry by comparing the cathodic peak current ( $I_{pc}$ ) each day to the initial peak current (Figure 4.7). Cyclic voltammetry of PANI laccase/Nafion-Laccase indicated a decrease in peak current ( $I_{pc}$ ) with the number of days. (Figure 4.7- Inset).

The relative percentage decrease in enzyme activity for each electrode compared to their initial activity is shown in Figure 4.8. PANI Laccase retained  $81\pm 2\%$  activity after one MFC cycle (5 days), while freely suspended enzyme retained only  $23.8\pm 1.8\%$  activity after the first MFC cycle (5 days). The rate of enzyme deactivation was highest for freely suspended laccase with about  $15.2\pm 0.12\%$  decrease in relative enzyme activity per day. The enzyme activity was also observed to be decreasing in Nafion-laccase with loss of activity at the rate of  $6.2\pm 0.39\%$  per day in Nafion laccase compared to PANI laccase with just  $3.8\pm 0.6\%$  per day. There was greater than  $69\pm 4\%$  enzyme activity retained in Nafion-laccase after one cycle (5 days) (Figure 4.8). The immobilization of Nafion-laccase on to the electrode is through adsorption on the surface and this method involves weak interaction with the support material compared to crosslinking by PANI. This leaves a possibility of enzyme leaching out into the solution and losing its activity. The laccase activity was 5 times higher when immobilized with Nafion-TBAB compared to plain Nafion. Similar results was observed by Meredith et al, 2012 for certain enzymes immobilized with Nafion modified with TBAB (Meredith et al., 2012).

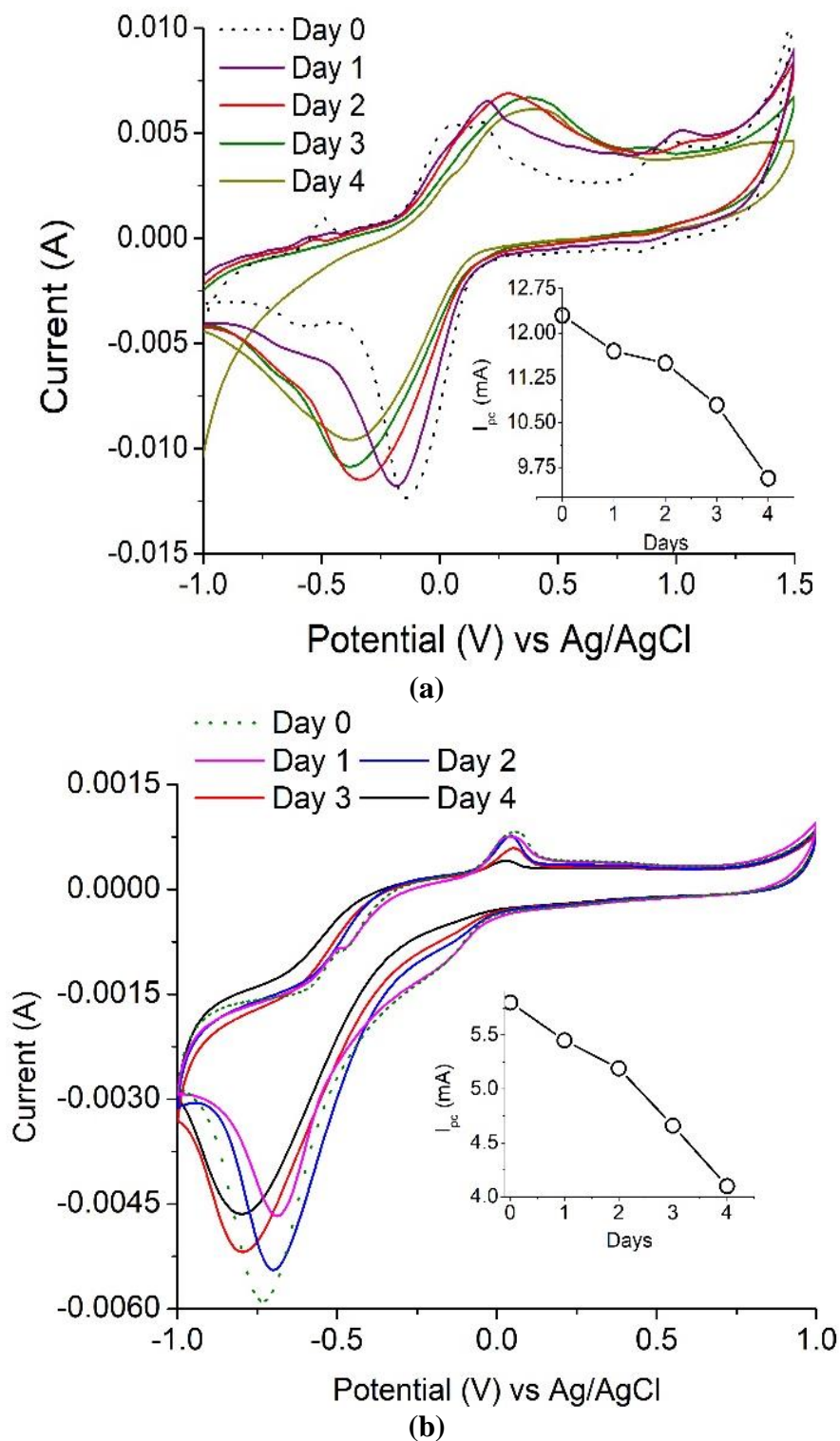


**Figure 4.7:** Laccase electrochemical activity with time **(a)** PANI-Laccase **(b)** Nafion-Laccase. Inset: Cathodic peak current vs time at  $20 \text{ mV s}^{-1}$

The laccase entrapped in Cu-alginate beads had an initial burst release of  $25 \pm 0.8\%$  within the 24 hours of immobilization in the catholyte of MFC; following this, per day  $4.3 \pm 0.6\%$  for Cu-Alg Beads with retention of  $61.5 \pm 2.5\%$  after 5 days (Figure 4.8). The

burst release might be due to repulsion between the negatively charged alginate (-29 mV) and laccase (-6 mV) at pH of 4.5 as observed with the zeta potential. Mohan et al. 2005 observed that Horse-Radish Peroxidase (HRP) immobilized in alginate had poor performance due to the ionic interaction between the enzyme and alginate. Thus the activity retention was highest in PANI because of decrease in the entropy of the enzyme usually caused by the exposure of the hydrophobic residues to the water, thus lowering denaturation (Wong and Wong, 1992). Nafion polymer laccase retained better activity compared to Cu-Alg due to lower leaching of the enzyme and well protected microenvironment in the polymer micelle.

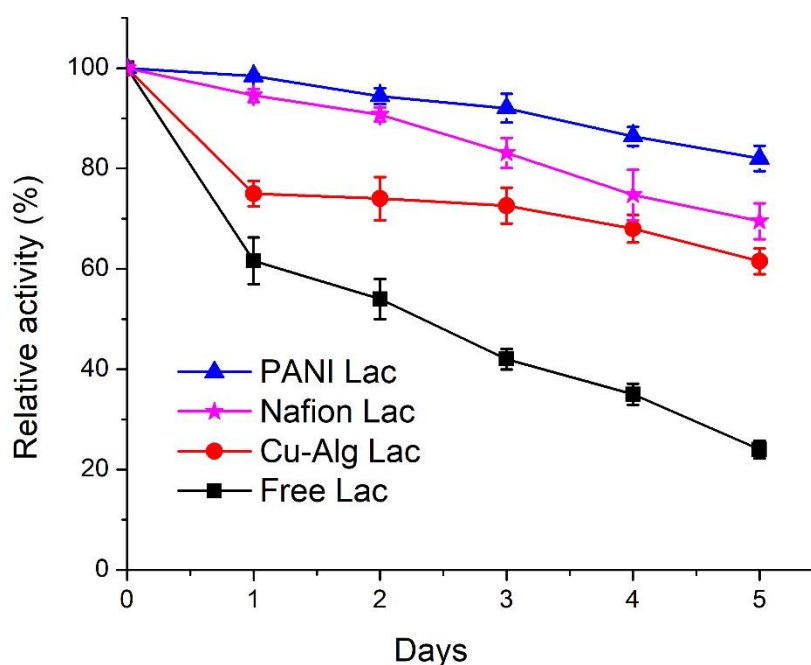


**Figure 4.8:** Comparison of relative enzyme activity for each immobilized and free laccase system for a period of 5 days.

#### 4.3.5 Comparison of laccase system with the conventional Pt and Fe impregnated catalyst (Fe-N/C)

The laccase biocathode MFC systems above were compared with the traditional Pt and Fe impregnated N-doped carbon catalyst for the power density in *Shewanella oneidensis*-based MFC. Pt and Fe-N/C produced a power density of  $80 \pm 2 \text{ mW m}^{-2}$  and  $54.7 \pm 2.4 \text{ mW m}^{-2}$  respectively (Figure 4. 9).

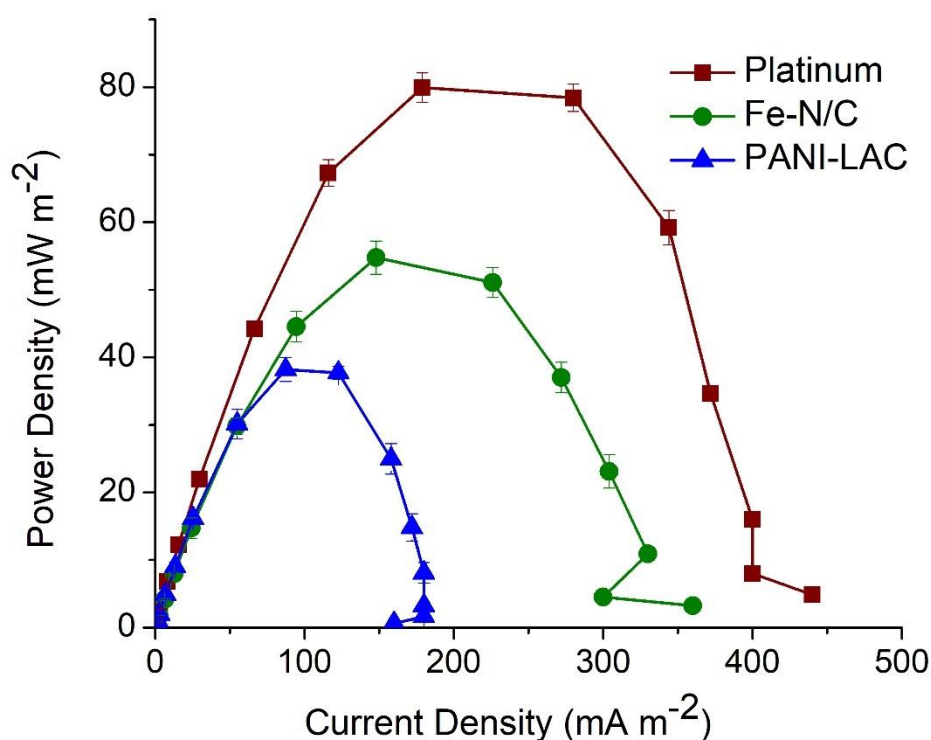


**Figure 4.9:** Comparison of maximum power density for Pt catalyst, Fe-N/C and PANI-Laccase.

The highest power density produced by laccase biocathode (PANI-Laccase) ( $38.2 \pm 1.7$   $\text{mW m}^{-2}$ ) was much lower than Pt ( $80 \pm 2$   $\text{mW m}^{-2}$ , Figure 4.9), but factors such as cost of the enzyme and its concomitant dye decolourization rates serve as a major advantage. The cost of platinum is 2.5 times higher than laccase. 1 gm of platinum costs £198 (Sigma Aldrich) compared to laccase at £70/gm. Enzyme loading in our study is much less compared to other studies (Teerapatsakul et al., 2007; Savizi et al., 2012). The normalised power output for platinum was 0.04  $\text{mW}/\text{£}$  and 0.07  $\text{mW}/\text{£}$  for laccase. Laccase has 1.75 times higher power output per pound compared to platinum.

The use of platinum electrodes in wastewater treatment has resulted in biofouling of the electrode and reduced power density (An et al., 2011). Fe-N/C and other metal oxides-based catalysts have shown to be cost effective and their performance is comparable to platinum. The possible leaching of the metal into wastewater, their toxicity and the environmental impacts should be taken into consideration.

Laccase serves a dual purpose in decolourizing the dye and carrying out the oxygen reduction reaction. Immobilization plays a key role in maintaining the stability, activity and reusability of the enzymes. The orientation of enzyme after immobilization is necessary for substrate oxidation and oxygen reduction. From the above results, PANI laccase maintained high activity and produced the highest power in a MFC. However, the decolourization was much less compared to the freely suspended enzyme. Nafion on being treated with TBAB was favourable for laccase immobilization. The dye decolourization observed in Nafion laccase is due the mixture casting of the Nafion suspension which allows the dye to pass through the membrane to reach the enzyme. This was observed by Schrenk et al, 2002 in a study which detected and quantified erythromycin on quaternary ammonium salt treated Nafion mixture suspensions compared to no detection in plain Nafion suspension (Schrenk et al., 2002). The immobilization has the drawback of restricting protein movement and making it less accessible to the substrate. Similar results were obtained by Savizi *et al.* 2012 with laccase in MFC, where freely suspended enzyme decolourized 77% of Reactive blue 221 dye compared to 70% in immobilized laccase (Savizi et al., 2012).

PANI laccase electrodes were reusable for up to 3 cycles with the power and activity decreasing each cycle. Nafion and Cu-Alg laccase were reusable for two more cycles (Data in Appendix 1, Table A1&A2). Although copper alginate beads were proven to effectively decolourize and be reusable for greater than 10 cycles (Palmieri et al., 2005; Teerapatsakul et al., 2017), in this study the performance of the beads were poor producing the lowest power density of  $14.7 \pm 1.04 \text{ mW m}^{-2}$ . The colour change (blue) in the anode indicated that there was movement of copper across the cation exchange membrane from cathode to anode which might have hindered the bacterial growth and decreasing the overall performance of the system. A comparison of Cu-Alg beads with Calcium alginate (Ca-Alg) beads was performed to evaluate the enzyme activity and power production. The Ca-Alg system produced better power ( $20.5 \text{ mW m}^{-2}$ ) than Cu-Alg probably due to calcium not being a heavy metal that inhibits bacterial growth even on migration to anode (Appendix 2, Figure A1). The enzyme activity was retained better with Cu-Alg beads (Appendix 2, Figure A2). The type of immobilization procedure is important as it affects the protein conformation and the ionic state of enzyme and its environment (Akertek and Tarhan, 1995). The use of laccase enzyme

provides better power and more versatility in water treatment applications as compared to using a fungal culture in a MFC (Lai et al., 2017).

Thus, laccase cross-linked with PANI served as an effective system striking the right balance between enzyme activity, dye decolourization and power output in an MFC (Table 4.2). These factors make it a suitable robust catalyst in MFCs compared to Pt and other metal-based catalyst which are expensive and difficult to maintain.

**Table 4.2:** Summary of the measured parameters for each system and the normalized power output

Laccase immobilization methods	Max. Power Density (mW m <sup>-2</sup> )	Dye decolourization (%)	Relative Enzyme Activity after 1 cycle (%)	Coulombic Efficiency (%)	Power density per unit of enzyme per mg of dye decolourized (mW m <sup>-2</sup> mg <sup>-1</sup> U <sup>-1</sup> ) **
PANI Lac	38.2±1.7	75.6±2.1	81±2	4.65±0.18	0.11±0.003
Nafion Lac	25.6±2.08	73±2	69±4	4.23±0.45	0.05±0.006
Cu-Alg Lac	14.7±1.04	81±4	61.5±2.5	2.97±0.16	0.02±0.001
Free Lac	28±1	85±3	23.8±1.8	3.83±0.112	0.03±0.0009

\*\*Power density (mW m<sup>-2</sup>) normalized with the amount of enzyme immobilized (U) with the amount of dye decolourized (mg) by each laccase immobilized systems. From the above table, PANI laccase shows the best performance when normalized with amount of enzyme immobilized and the amount of dye decolourized.

#### 4.4 Conclusion

In this study, different methods of immobilization of the laccase were investigated with regards to their application as biocathodes in *Shewanella* based MFC. Four different systems were used, viz. laccase cross-linked with PANI to reduce ohmic loss, laccase entrapped in Cu alginate beads and encapsulated in Nafion micelles to maintain activity and free laccase for comparison. Cu-Alg laccase showed better retention in activity after initial burst release but poor performance in power generation

due to high ohmic loss. Although both PANI and Nafion are conducting polymer, PANI was a better electron conductor and aided transfer of electrons from electrode to laccase efficiently compared to Nafion. PANI laccase showed a higher power density as compared to both Cu-alginate beads and freely suspended laccase due to the proximity of the enzyme to the surface of the electrode. The decolourization was highest in free laccase due to less orientation restriction of the active site, and lowest in PANI may be due to low amount of enzyme immobilized and unfavourable orientation for dye interaction. The Cu-alg and Nafion decolourization efficiency was median between free laccase and PANI laccase. Overall PANI laccase showed best performance and can be concluded to be economical due to its superior power and reusability with lower amount of enzyme as compared to Cu-alginate, Nafion and free laccase. Many studies have used large enzyme loadings of 500 U ml<sup>-1</sup> to 2000 U ml<sup>-1</sup> and mediators for dye decolourization and higher power output in MFC. In this study, we have utilised much less enzyme loading (maximum 0.3 U ml<sup>-1</sup> for free laccase) in the absence of mediators to bring about decolourization of dyes and produce a good power output which served as major advantage compared to Pt and metal oxide catalyst-based cathodes. The unstable nature of biological cathodes to wastewater is the major drawback for its efficiency in microbial fuel cells. Laccase has the versatility of being engineered for immobilization to extend their active lifetimes and a catalyst for ORR to provide the comparable efficiency to that of Pt.

## **Chapter 5**

**Degradation of Acid orange 7 in a microbial fuel cell:  
comparison between feeding the dye in the anode vs  
the cathode**

## 5.1 Background

In a MFC there are two modes of decolourization, at anode and at cathode. At the anode under anaerobic conditions the -N=N- bond of the azo dye is cleaved in the presence of microorganisms to form toxic aromatic amines (Hou et al., 2011; Fernando et al., 2012). These aromatic amines are recalcitrant in nature and do not undergo further degradation in that environment. They can be further reduced to less toxic products in the aerobic stage.

Laccase has been widely used for various types of dye decolourization studies (Abadulla et al., 2000; Daâssi et al., 2013; Ramírez-Montoya et al., 2015). The major advantage of laccase is that it degrades the dye by non-specific free radical mechanism to form phenolic products thereby avoiding the formation of aromatic amines (Chivukula and Renganathan, 1995). In MFC, laccase was employed at cathode for oxygen reduction reaction (ORR) and dye degradation by (Bakhshian et al., 2011; Savizi et al., 2012). The aerobic degradation by laccase yielded products that are less toxic than the original dye.

The individual decolourization in anode and at cathode was discussed in detail in literature review Section 1.3.7.3.

Though the above studies have investigated azo dye decolourization in the anode and others in the cathode, it is not clear which approach is the best as different studies used different organisms, operating conditions, cathode catalyst etc, making a direct comparison of decolourization rates for each system difficult (Table 5.1). Therefore, this study aims to understand the mechanism of dye decolourization in both the processes (anode & cathode), and the nature of products formed, while operating under same conditions.

This study compared the performance of MFCs treating Acid Orange 7 under anaerobic condition in the presence of bacteria at the anode of MFC and in aerobic condition in the presence of laccase enzyme at the cathode of MFC. The rate of dye decolourization, power density, COD reduction, degradation products and their toxicity were used as performance indicators.

**Table 5.1:** Features of dye degradation in the anode vs cathode of MFCs.

Anode dye degradation	Cathode dye degradation
<p>I. Microbially mediated</p> <p>II. Reductive process forming aromatic amines</p> <p>III. Mechanism not clear- Azo reductase or reduction by exogenous mediators or reduction by sulphides (Section 1.3.6 c)</p> <p>IV. Microbes can be inhibited by parent dye or the dye degradation products.</p> <p>V. Complete mineralisation of dye is unlikely.</p>	<p>I. Electrochemically mediated if the dye possesses a high redox potential or applying external power to the system</p> <p>II. Can involve oxidation of dye by laccase or other enzymes with oxygen as the terminal electron acceptor</p> <p>III. Dye or contaminants in wastewater may inhibit the enzyme activity</p> <p>IV. Complete mineralisation of dye is possible.</p>

## 5.2 Materials and Methods

### 5.2.1 Experimental Design

The MFC used in the study was the 'H'-type reactor with a working volume of 200 ml in each chamber. The electrodes were constructed from carbon fibre (non-woven) with a surface area of 25 cm<sup>2</sup>. Three MFC systems were setup. System 1 was dye in the anode with *Shewanella oneidensis* MR1 and laccase enzyme in the cathode, subsequently to be referred to as "MFC Dye Anode". System 2 was with *S. oneidensis* in the anode and laccase in the presence of dye in cathode, subsequently to be referred to as "MFC Dye Cathode" and System 3 with absence of dye in both chambers known as MFC<sub>Control</sub>. Crude commercial laccase enzyme (10 Units mg<sup>-1</sup>) obtained from Enzyme India Pvt. Ltd, Chennai was used at an activity of 0.3 U ml<sup>-1</sup> freely suspended in 200 ml of 100 mM acetate buffer (pH 4.5).

## 5.2.2 Operating conditions

The anode media components and their concentrations are detailed in Chapter 2, Section 2.3. The anode and cathode were connected to a resistor of 2 k $\Omega$ . The anode was inoculated with 10% v/v *S. oneidensis* MR-1 culture previously grown in Luria Bertani broth to log phase (OD: 0.4). The anode chamber was sparged for 10 minutes with nitrogen gas to remove any dissolved oxygen and maintain an anaerobic environment.

The cathode chamber was maintained in aerobic conditions by supplying air through an air stone at a rate of 200 ml air per min. Experiments were conducted at a temperature of 30 °C. All experiments were performed in triplicates.

## 5.2.3 Analytical procedures

The methods section details the analytical procedures and the rationale behind performing the tests. The analytical procedures followed in this study were AO7 decolourization (Section 2.6.1), electrochemical tests (Section 2.6.2), Coulombic efficiency (Section 2.6.3), COD (Section 2.6.4), quantification of pyruvate consumption by Ion-exchange chromatography (Section 2.6.6 (b)), GC-MS analysis of dye degradation products (2.6.9), *Vibrio* toxicity profile (Section 2.6.10), Cyclic voltammetry of anode decolourized products (Section 2.6.11(b)), and statistical analysis (Section 2.6.15).

## 5.3 Results and Discussion

### 5.3.1 Power Generation and COD reduction

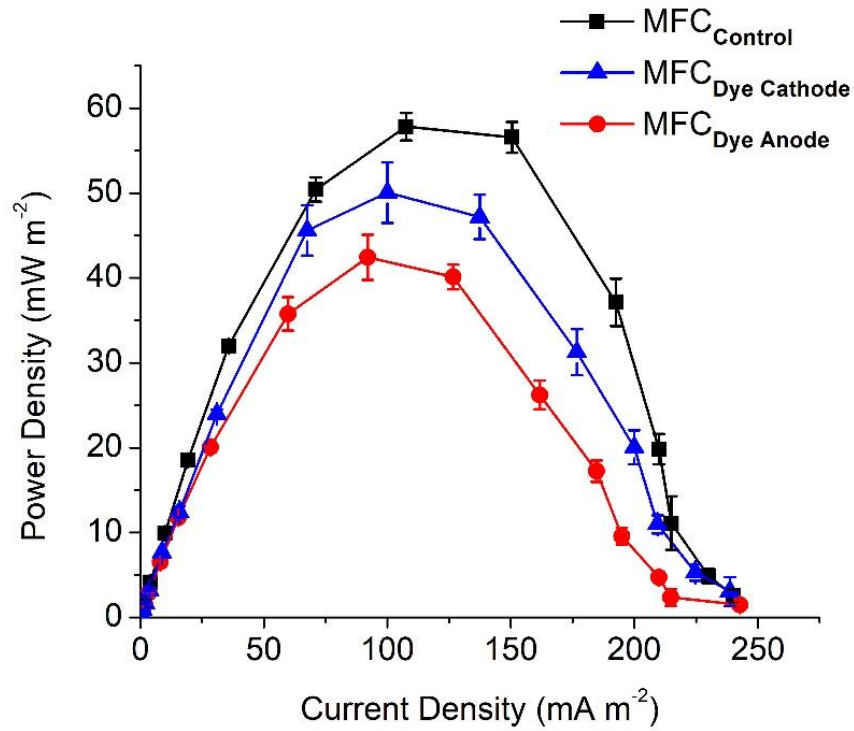
The open circuit voltage (OCV) was highest for MFC<sub>Control</sub> with 1.3 V followed by MFC<sub>Dye Cathode</sub> with 950 mV and 930 mV for MFC<sub>Dye Anode</sub>. The maximum power density obtained from MFC<sub>Dye Anode</sub> was 42.5 $\pm$ 2.6 mW m<sup>-2</sup> and 50 $\pm$ 4 mW m<sup>-2</sup> for MFC<sub>Dye Cathode</sub> and 57.8 $\pm$ 1.6 mW m<sup>-2</sup> for MFC<sub>Control</sub>. (Figure 5.1). The lower power density in case of dye in the anode indicates that the presence of AO7 had a significant effect on the growth rate of *S. oneidensis*. One of the major reasons affecting the cell viability might be the accumulation of anaerobic degradation products of azo dyes such as aromatic amines which are known to be toxic to the bacteria. Moreover, it has

been reported that the reduction of azo dyes by *S. oneidensis* under anaerobic condition is enhanced by mediators such as flavins and quinones (von Canstein et al., 2008; Le Laz et al., 2014). These flavins produced by *Shewanella* are also responsible for the extracellular electron transfer to the electrode at the anode (Marsili et al., 2008). The competition of electrons from the flavins between dye and electrode might result in lower power in the MFC<sub>Dye Anode</sub>. Another possible mechanism for lower power is as suggested by Sun et al., 2013, that in biological decolourization of dyes in MFCs a portion of the available electrons are transported to electrode while another portion of electrons are used for reductive decolourization of dyes. The absence of dye in both chambers increased the power in MFC<sub>Control</sub> due to bacteria shuttling electrons to the electrode rather than the dye and at cathode the electrode is the sole electron donor to laccase. The internal resistance of MFC<sub>Control</sub> was lowest with  $1.5 \pm 0.07$  k $\Omega$  followed by the MFC<sub>Dye Anode</sub> with  $1.72 \pm 0.11$  k $\Omega$  and highest for MFC<sub>Dye Cathode</sub> with  $1.9 \pm 0.13$  k $\Omega$ . The presence of dye in both the chambers, decreases the overall ionic conductivity of the solution due to the low diffusion coefficient of the dye compared to other ions, thus increasing the internal resistance (Hori et al., 1987).

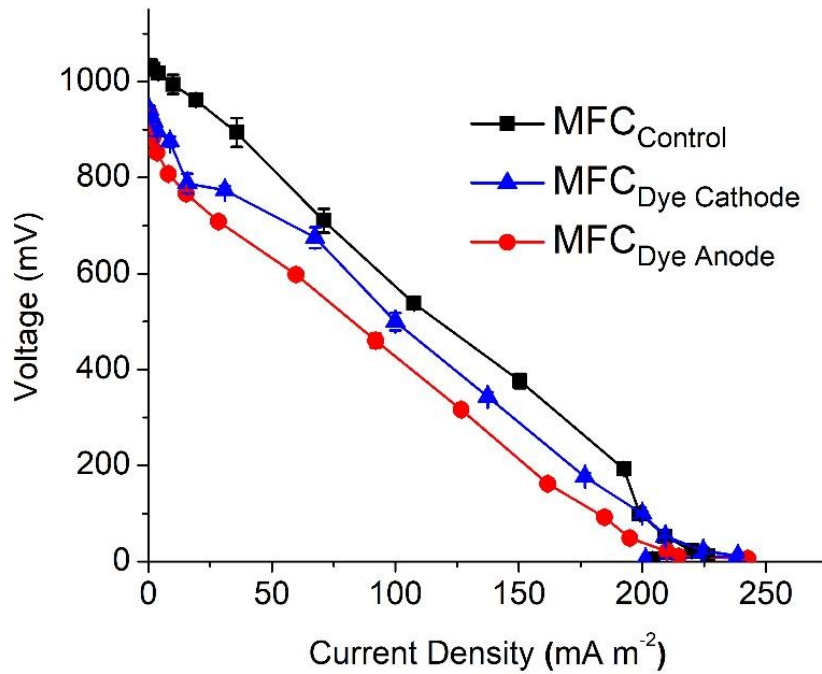
There was  $80.4 \pm 1.2\%$  reduction in COD for MFC<sub>Dye Cathode</sub> which was closely followed by the control system with  $79.2 \pm 1.3\%$  reduction for MFC<sub>Control</sub> and finally  $69 \pm 2\%$  for MFC<sub>Dye Anode</sub>. The Coulombic efficiency (CE) of the systems also followed the trend with 5% for MFC<sub>Control</sub>, 4.7% and 3.6% for MFC<sub>Dye Cathode</sub> and MFC<sub>Dye Anode</sub> respectively. Overall, on comparing the voltage, CE, power density and COD MFC<sub>Control</sub> performance was the best.

In the absence of dye at cathode, laccase accepts electrons from the electrode for oxygen reduction reaction. The redox potential of the dye (0.653 V vs SHE) is lower than that of laccase at 0.78 V vs SHE, therefore, in the system MFC<sub>Dye Cathode</sub> the dye is oxidized easily for electrons that are used for ORR. The lower power in MFC<sub>Dye Cathode</sub> than MFC<sub>Control</sub> might be due to the inhibition of the enzyme activity by the dye or its degradation products (Appendix 3, Figure A3). Since the bacterial electron transfer is quite slow, the anode reaction acts as a rate limiting step in the MFC. As a result, whilst there is competition between the dye and electrode for electron transfer

to laccase or inhibition of laccase by the dye, the power is not significantly affected by the cathode reaction.



(a)



(b)

**Figure 5.1:** (a) Comparison of MFC performance for all MFC systems obtained by varying the external circuit resistance (10Ω –1MΩ) (b) Polarisation curves for all the systems used in the study conducted on day 3.

### 5.3.2 AO7 dye decolourization

The decolourization of Acid Orange 7 was measured at the maximum absorption wavelength for the dye (484 nm). The rate of decolourization was faster in the MFC<sub>Dye Cathode</sub> compared to MFC<sub>Dye Anode</sub>. There was >80% decolourization within the first 24 hours for laccase compared to 20% for MFC<sub>Dye Anode</sub> (Figure 5.2). The overall dye decolourization in 96 hours was 97±2% for MFC<sub>Dye Anode</sub> and 98±3% for MFC<sub>Dye Cathode</sub>. The enzyme activity graph in Appendix 3 indicates a decrease in 20% activity in the first 24 hours. In case of laccase the decrease in activity over time contributes to high decolourization during the initial period which then gradually decreases. In MFC<sub>Dye Anode</sub>, the bacteria have an initial lag phase (slower decolourization) followed by a log phase where there is an increased decolourization rate. Hence the time taken to reach maximum power density was also slower in case of dye in the anode as compared to the dye in the cathode.

Anaerobic treatment of azo dyes involves the reductive cleavage of the N=N to form colourless aromatic amines. In the anode, azo dye under anaerobic conditions is reduced by *Shewanella* via azoreductase enzyme or by the Mtr respiratory pathway. Initially an azo reductase enzyme was speculated to be responsible for degradation of azo dyes by *Shewanella*, but these enzymes were effective only with cell extracts and not with intact cells. Thus, establishing that decolourization is mainly an extracellular process (Brigé et al., 2008; Hong and Gu, 2010). Recent studies have shown that Mtr respiratory pathway in *S. oneidensis* MR1 is responsible for azo dye reduction under anaerobic condition in which OmcA/MtrC plays the role of “azo reductase”. Flavins have been reported to aid and enhance the decolourization process (Cai et al., 2012). This is in concurrence with the lower power obtained for dye in anode due to the dye being the alternative electron acceptor to the electrode.

The decolourization by laccase follows an entirely different mechanism than the bacteria. There is production of free radicals by laccase enzyme that carries out non-specific attack of the dye at various positions to yield a number of products. The mechanism of laccase dye degradation is given in details with schematics in the introduction Section 1.3.8.2 and the degradation products are discussed in the GC-MS section 5.3.6. The dye decolourization was faster with enzyme due to the faster reaction kinetics of enzyme compared to the bacteria.

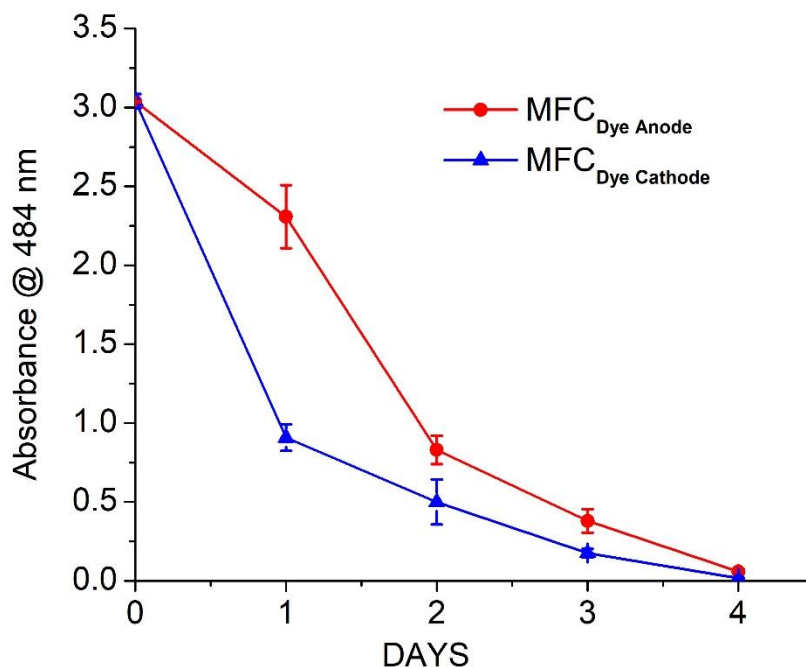
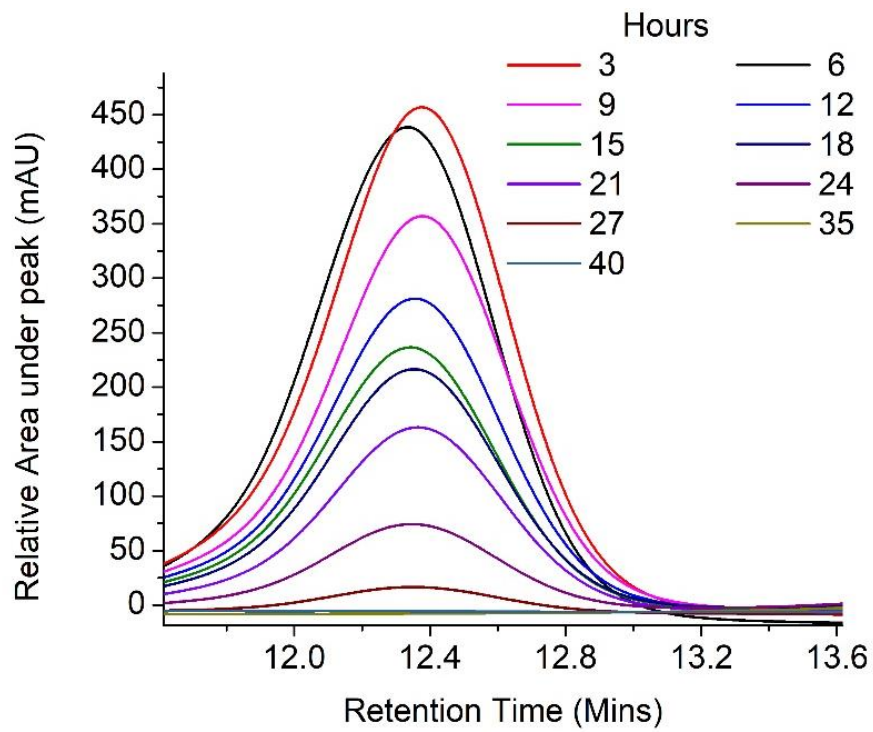


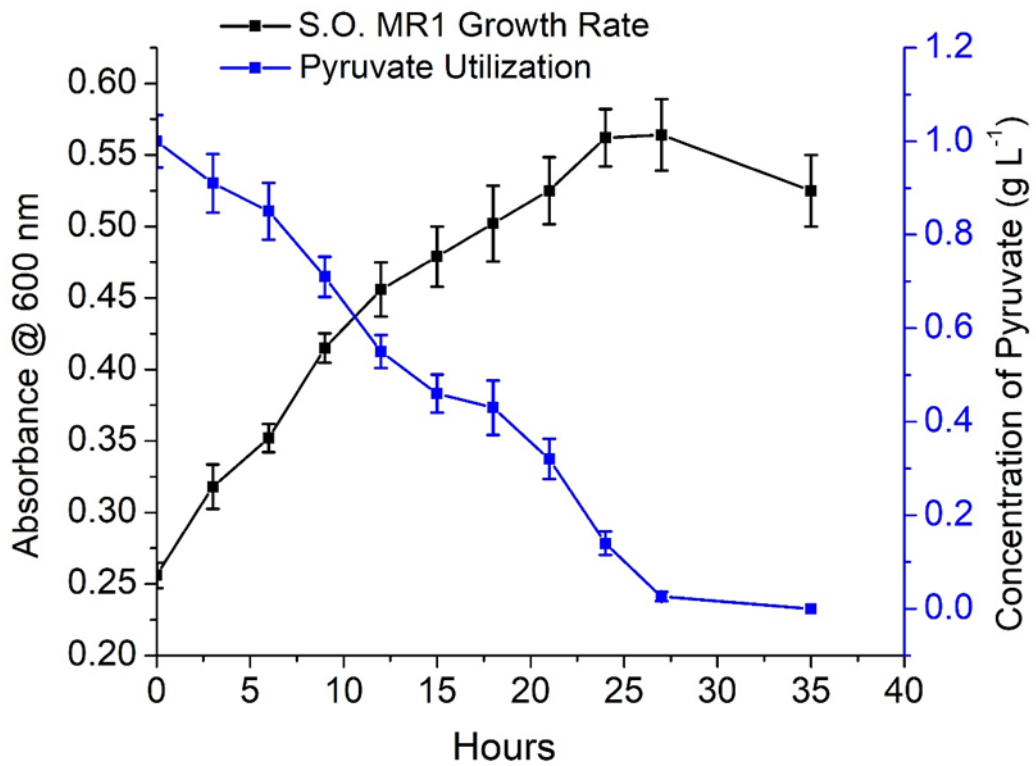
**Figure 5.2:** Decolourization of AO7 in the anode (*S. oneidensis*) and cathode (Laccase) of MFC over a period of 4 days

### 5.3.3 Pyruvate consumption and growth curve of *S. oneidensis* MR1

The rate of pyruvate consumption by *Shewanella oneidensis* MR1 at the anode was measured by Ion Chromatography to establish the relationship between utilization of carbon source, bacterial growth and the dye degradation. The concentration of pyruvate ( $R_t:12.4$ ) decreased rapidly every three hours (Figure 5.3(a)). The lag phase in the first six hours is due to the bacterial acclimatization to the new media, from 9hrs there is rapid decrease in the pyruvate concentration until it is negligible by 35 hours (Figure 5.3(a)). The growth curve for *S. oneidensis* MR 1 (*S.O.* MR 1) indicates the log phase increasing consistently with the pyruvate consumption and by 24 hours it has reached the stationary phase (Figure 5.3 (b)). The growth rate of *S. oneidensis* is slower in the anaerobic condition compared to the aerobic state (Wang et al., 2010).



(a)



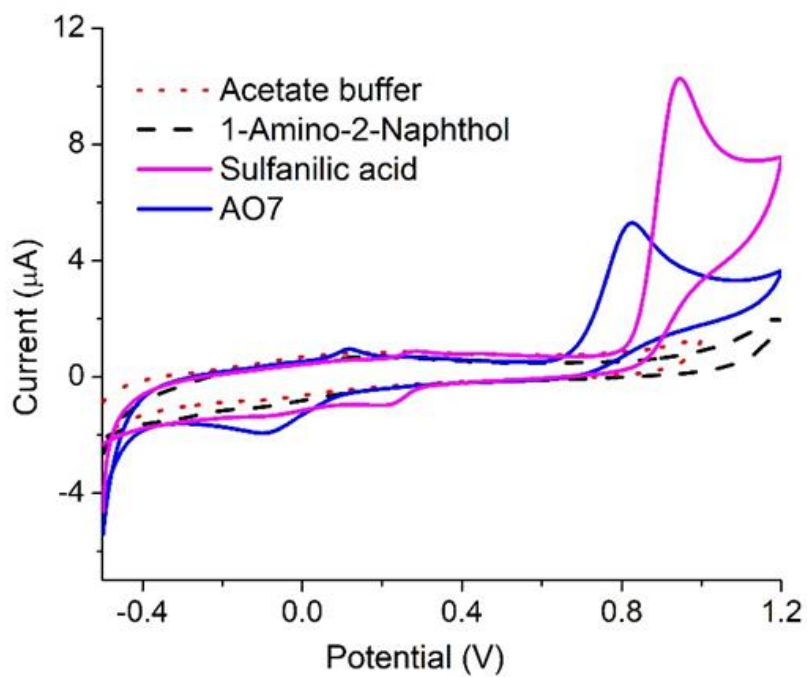
(b)

**Figure 5.3:** (a)HPLC analysis of Pyruvate consumption by MR1 for each time interval (b) Comparison of MR 1 growth rate with pyruvate concentration.

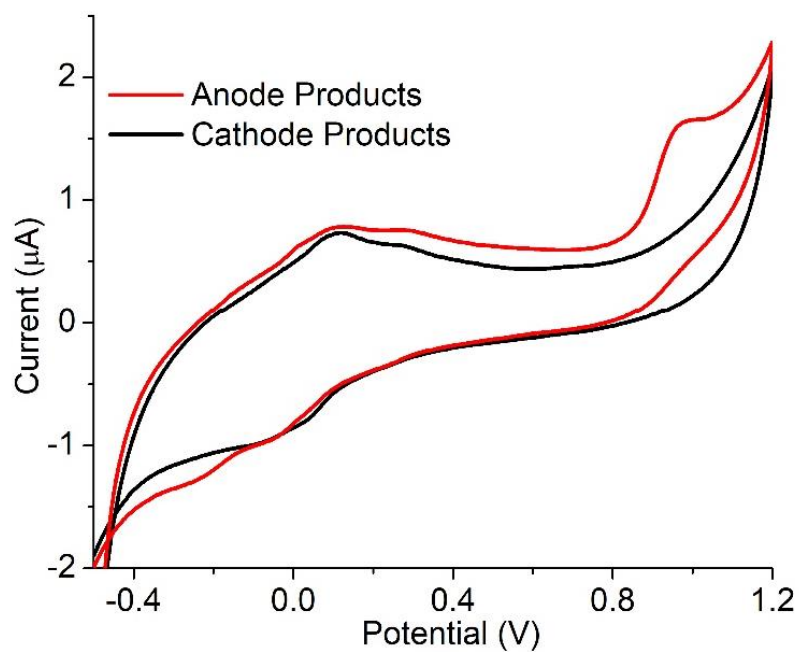
There was gradual reduction of dye during the first 24 hours, but the rate of dye reduction was not concomitant with the bacterial growth rate (Figure 5.2 & 5.3 (b)). This suggests that the dye is not utilized by the bacteria for carbon source and the decolourization is a fortuitous one that happens during the bacterial metabolism reactions. The increase in dye reduction after 24 hours indicates the pyruvate metabolism by bacteria might have yielded reducing equivalents capable of dye reduction. The catabolism of pyruvate by *S. oneidensis* MR1 (*S.O.* MR1) produces NADH, flavin mononucleotide (FMN), riboflavins that aid in the extracellular electron transfer (EET) pathway (Kouzuma et al., 2015; Marsili et al., 2008). The reductive cleavage of the azo bond by “azoreductases” is aided by electron shuttling through soluble redox mediators e.g. flavins (Gomaa et al., 2017). The reduction of dye after pyruvate metabolism indicates these redox mediators produced might have aided in the decolourization. This also correlates with the low power for dye anode as part of electrons were shuttled to the dye rather than the electrode.

#### **5.3.4 Electrochemical analysis of dye degradation products**

The anode dye degradation products were analysed using cyclic voltammetry for the presence of reduction end products. The CV was compared with the standard compounds viz. acid orange 7, sulfanilic acid (SA) and 1-amino-2-naphthol (1-A-2-N). Standard sulfanilic acid showed strong oxidation/reduction peaks at 0.94 V/0.811 V and a weak oxidation/reduction couple at 0.27 V/0.211 V vs Ag/AgCl (Figure 5.4 (a)). The CV of initial AO7 dye produced a redox couple at 0.89 V/0.7 V and 0.11 V /-0.08 V vs Ag/AgCl respectively (Figure 5.4 (a)). The shift in the peak potential is due to the presence of both SA and 1-A-2-N in the parent dye. The *S. oneidensis* degraded dye product showed a characteristic peak at 0.96 V indicating the presence of sulfanilic acid (Figure 5.4 (b)). There was no peak observed for 1-A-2-N, which might be the result of limited solubility of the compound in water. Thus, it can be inferred that mechanism of dye degradation in anode is through the cleavage of the N=N azo bond separating the two rings. On the other hand, the laccase dye degradation at the cathode did not show any characteristic redox peaks indicating a completely different mechanism (Figure 5.4(b)). Since the redox peaks for both AO7 and sulfanilic acid were absent it can be presumed that the degradation involves a ring cleavage thus releasing the characteristic functional groups



(a)



(b)

**Figure 5.4:** Cyclic Voltammetry of (a) parent dye (AO7), standards SA and 1-A-2-N (b) anode and cathode decolourized products, at  $50 \text{ mV s}^{-1}$  vs Ag/AgCl.

### 5.3.5 Auto-oxidation of *S. oneidensis* (anode) decolourized products

The anaerobic dye degradation products (colourless) on exposure to air regained colour. This phenomenon of colour formation from decolourized products was referred to as auto-oxidation (Figure 5.5).

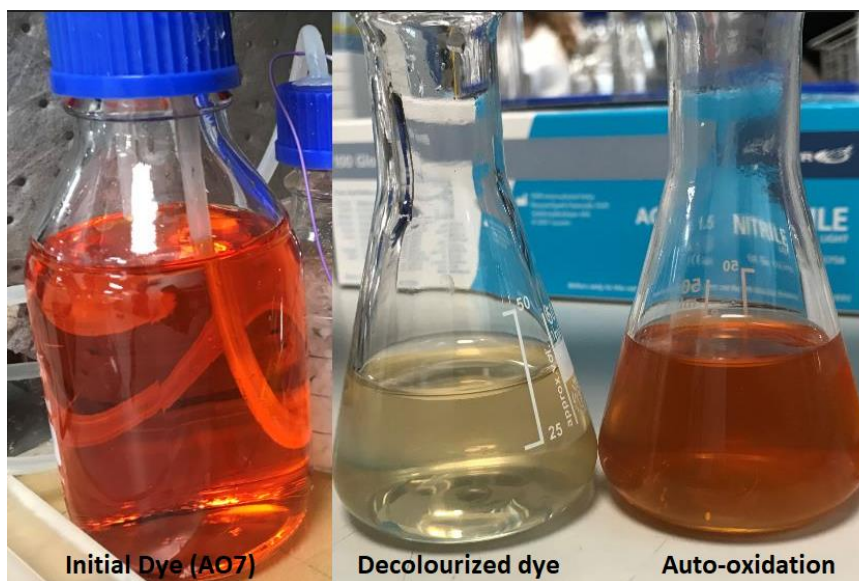


**Figure 5.5:** The depiction of initial coloured dye together with the decolourized products and the coloured auto-oxidation products.

To determine the possibility of auto-oxidation occurring in other azo dyes the anaerobic decolourization of Congo Red (CR), a diazo dye, was carried out in the presence of *S. oneidensis* to observe the stability of the decolourized products. Similar to AO7, the CR decolourized products were also auto-oxidized on exposure to air. Initially it was hypothesized the colour formation might be due to the diazotization (-N=N-) of the auto-oxidized products to form the initial dye. Therefore, a UV-scan of the decolourized products, auto-oxidized products and the initial dye for both AO7 and CR was performed. The scan results revealed that the colour was not due to the formation of -N=N- present in the initial dyes (Figure 5.6).

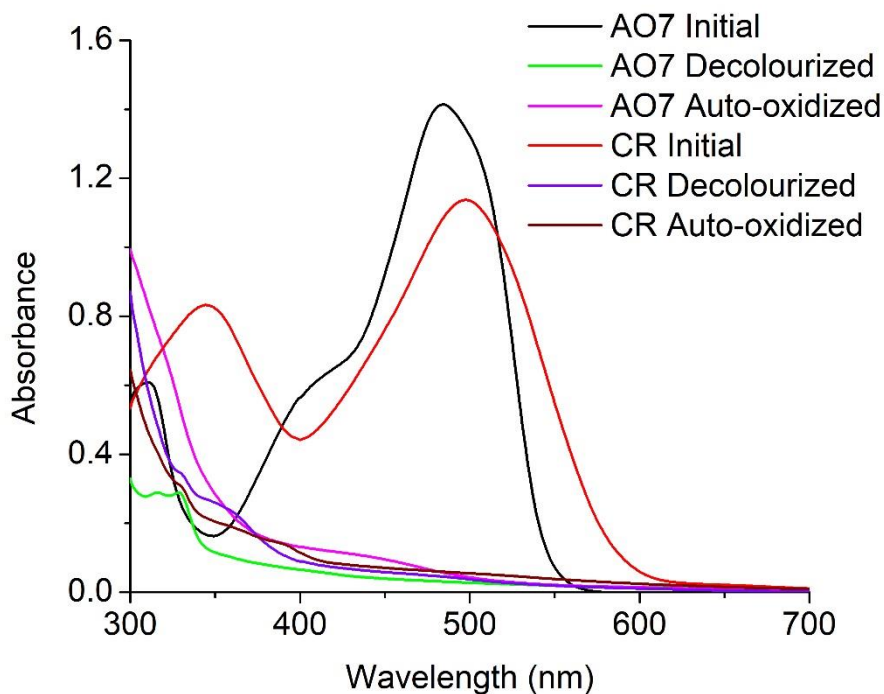


**Figure 5.6:** UV-Scan of AO7 and CR initial dye, decolourized products and Auto-oxidation products indicating the colour in the auto-oxidation products was not a result of diazotization.

The auto-oxidation effect on anaerobic azo dye degradation products was first observed by (Kudlich et al., 1999). They determined that mono and diazo sulfonated dyes that produced aminohydroxynaphthalenesulfonate (AHNS) by-products were unstable, sensitive to oxygen and underwent dimerization to form coloured products. The auto-catalysis of Acid Orange 7 (AO 7) studied by (Carvalho et al., 2008) detected that 1-amino-2-naphthol, formed by reductive cleavage of the dye, when exposed to aerobic conditions yielded products that are brown in colour.

The nature of auto-oxidation products of AO7 has not been discussed in literature thus far. A GC-MS analysis of these products was performed to identify and determine the pathway that leads to the formation of colour.

### 5.3.6 GC-MS analysis of dye degradation products

#### 5.3.6.1 S.O MR1 (anode) dye degradation products

The mechanism of the dye degradation analysed by CV was further confirmed with GC-MS. Under anaerobic condition in MFC<sub>Dye Anode</sub>, *S. oneidensis* was observed to symmetrically cleave the azo bond resulting in the formation of 1-amino-2-naphthalenol (1-A-2-N) ( $M+H^+=159$ ,  $R_t$ : 18.13) and aminobenzene sulfonic acid (sulfanilic acid). Sulfanilic acid (SA) being highly polar molecule was not detected in GC-MS. 2-amino-1-naphthalenol ( $M+H^+=159$ ,  $R_t$ : 18.49) was also present in the degradation products of *Shewanella* indicating the formation of various aromatic amine metabolites during the reductive decolourization of AO7 (Figure 5.7). The presence of aminobenzenes under anaerobic dye decolourization of AO7 was also observed by (Fernando et al., 2012). In chapter 3, HPLC analysis of anode products revealed the presence of 1-A-2-N and SA which corroborates with the GC-MS results.

#### 5.3.6.2 Auto-oxidation products and mechanism

The initial products obtained were the same as in anode dye decolourized i.e., 1-amino-2-naphthalenol (1-A-2-N) ( $M+H^+=159$ ,  $R_t$ : 18.13), aminobenzene sulfonic acid (sulfanilic acid), 2-amino-1-naphthalenol (2-A-1-N) ( $M+H^+=159$ ,  $R_t$ : 18.49). On exposure to oxygen, 2-amino-1-naphthalenol was oxidized to 2-amino-1,4-naphthoquinone (2ANQ) ( $M+H^+=173$ ,  $R_t$ : 15.75) (Figure 5.7). The 2ANQ further underwent substitution reaction with carboxylic acids (acetate from bacterial metabolism) in the reaction medium to produce 2-methoxy-1,4-naphthoquinone (2MNQ) ( $M+H^+=188$ ,  $R_t$ : 14.84) an orange coloured product (Figure 5.7). 2MNQ is an orange colour organic pigment originally derived from the soil (Lambert et al., 1971). The colour formation in the auto-oxidized products might be due to the presence of the above pigment.

The other quinones observed in the GC-MS of auto-oxidation products were 4-quinolinecarboxyaldehyde ( $M+H^+=157$ ,  $R_t$ :11.61) and 4-Thio-methyl-1,2-naphthoquinone ( $M+H^+=176$ ,  $R_t$ :14.43) with 1,2-naphthoquinone being a product of 1-A-2-N oxidation (Figure 5.7). A clear mechanism of sulfanyl group ( $SO^{2-}$ ) addition could not be further explained. Quinones are precursors for anthraquinone dyes and a number of these compounds have a chromophore moiety (Matsuoka, 1990). The production of quinone intermediates during anaerobic degradation of dyes is seen in

number of mono and diazo dyes. In general, quinones possess redox mediating properties and aid in azo dye decolourization by transferring electrons between dye and bacteria (Van der Zee et al., 2000).

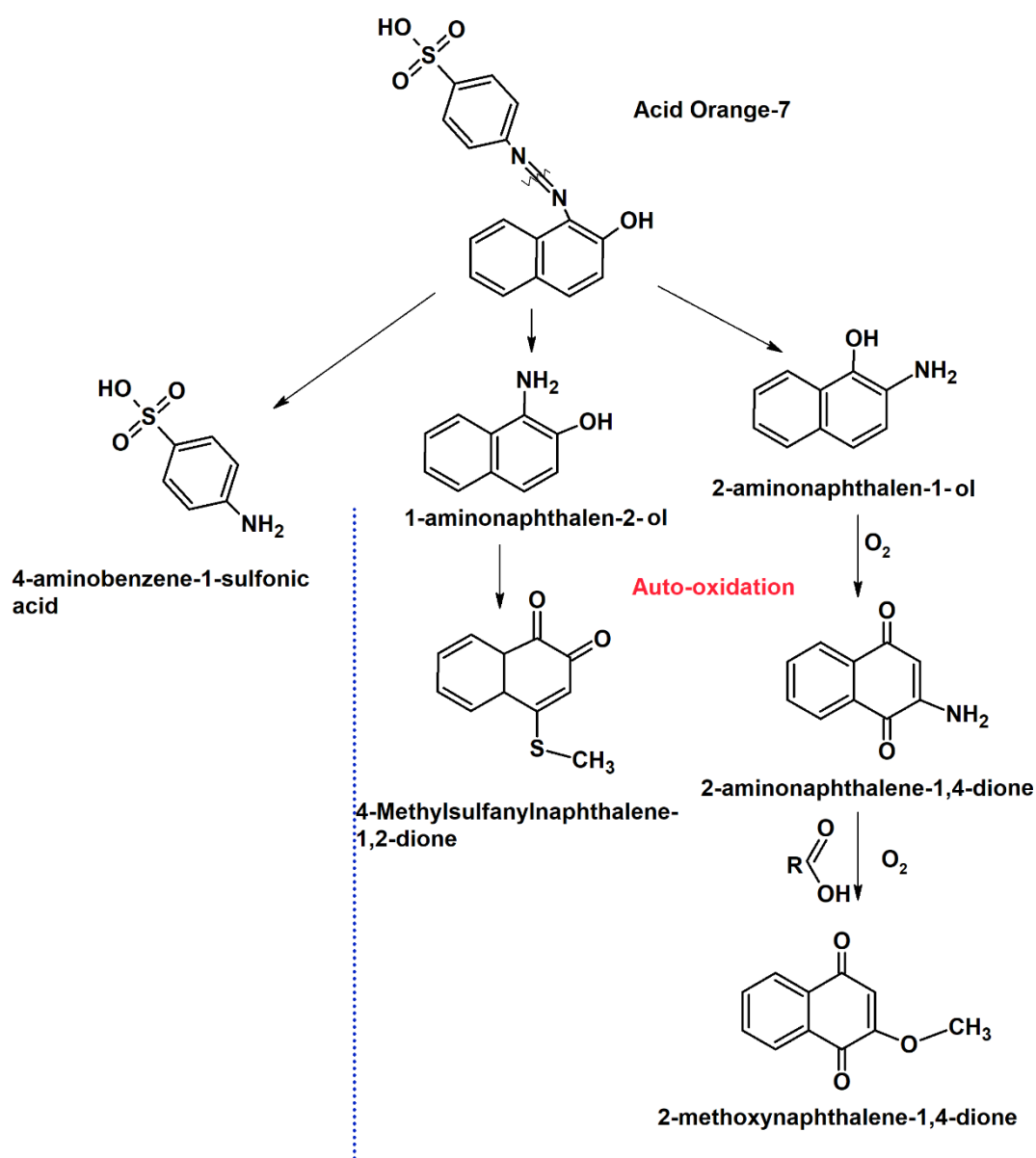


**Figure 5.7:** Putative dye degradation pathway by *S. oneidensis* MR 1 at the anode and the auto-oxidation mechanism based on the intermediate products obtained from GC-MS analysis

The presence of a variety of quinone intermediates and their subsequent conversion products that yield a colour clearly indicates the mechanism of colour formation due to auto-oxidation.

This was also observed by Kudlich et al., (1999) in which the naphthalene derivatives of azo dye degradation underwent auto-oxidation to form dimers which resulted in colour formation. In their study the oxidation of aminohydroxynaphthalenesulfonates (AHNS) to naphthoquinonesulfonates and their subsequent dimerization developed a coloured product. The substitution reaction with carboxylic acid might be similar to that of 5-hydroxy-1,4-naphthoquinone when treated with acetic anhydride to form 5-hydroxy-3-methoxy-1,4-naphthoquinone (Blauenburg et al., 2012).

### 5.3.6.3 Laccase dye degradation products and mechanism

The first step in laccase degradation mechanism for system MFC<sub>Dye Cathode</sub> is the decolourization of the Acid Orange 7 dye by asymmetric cleavage of the -N=N- bond to form intermediates Naphthalen-2-ol and (4-sulfophenyl) diazenyl (Figure 5.8).

The intermediate Naphthalen-2-ol undergoes aromatic ring cleavage to produce 1,2-Benzenedicarboxylic acid (Phthalic acid) ( $M+H^+=149.1$ ,  $R_t:9.50$ ). Phthalic acid functional group is further oxidized to form benzoic acid ( $M+H^+=105$ ,  $R_t: 7.89$ ) (Figure 5.8).

The other intermediate (4-sulfophenyl)diazenyl was subjected to oxidative desulfonation to form phenyldiazenyl. Phenyl diazene radical rapidly loses nitrogen ( $N_2$ ) as gas molecule and the nucleophilic substitution of hydroxyl radical ( $OH^-$ ) on the aromatic ring results in the formation of phenol. Phenols are the natural substrates for laccase therefore the oxidative ring cleavage of phenol ring was carried out to form fatty acid such as hexanoic acid ( $M+H^+=60$ ,  $R_t: 4.95$ ) (Figure 5.8). Hexanoic acid is a non-toxic compound that is present in food products available for human consumption.

The benzoic acid pathway was also observed by (Fernando et al., 2014) for aerobic degradation of AO7 suggesting that mono-oxygenase enzymes from bacteria were capable of the degradation pathway. Due to the slow bacterial metabolism, only the larger intermediate products were observed in their study. The rapid laccase reaction in this study led to the formation of smaller and simple products.

The symmetric and asymmetric cleavage depends on the dye structure and the type of enzyme used. It is suggested that bacterial laccase with low redox potential are not capable of cleaving the azo bond. (Pereira et al., 2009) observed that laccase from *Bacillus subtilis* oxidized mono azo dye Sudan Orange G to produce oligomers and

polymers by radical coupling reactions without the cleavage of the azo bond. Therefore, fungal laccase with high redox potential can effectively cleave the azo bonds to bring about decolourization.

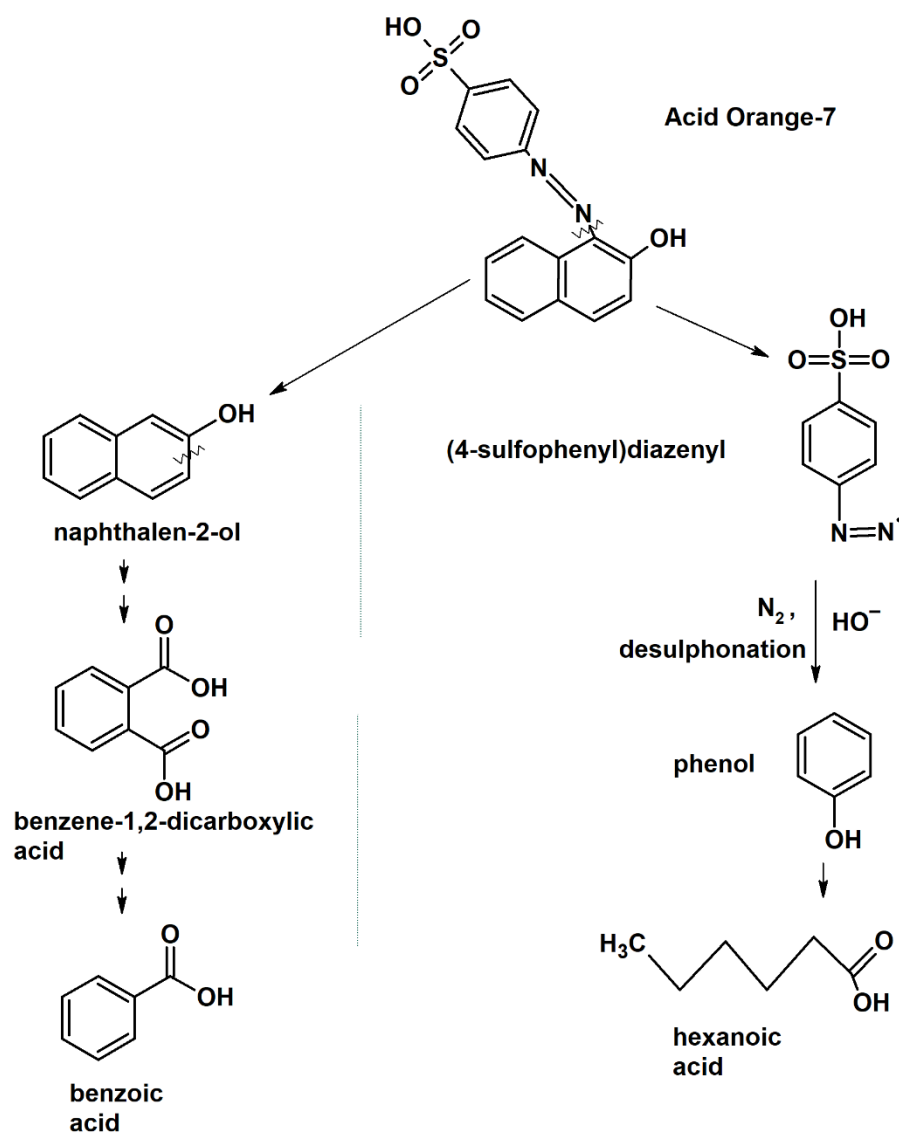


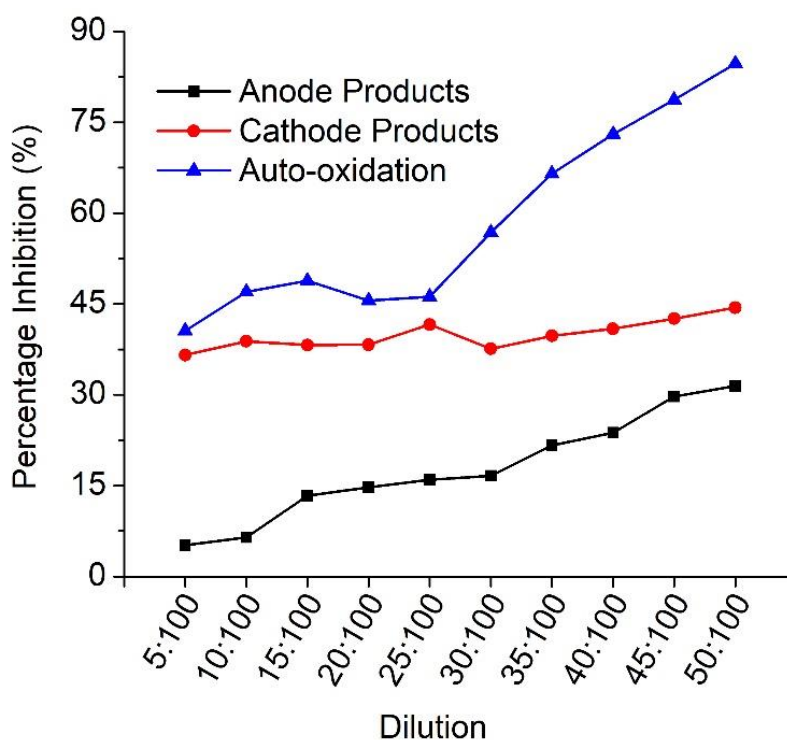
**Figure 5.8:** Putative laccase dye degradation pathway deduced from the intermediates form GC-MS analysis

The azo dye degradation by laccase follows asymmetrical ring cleavage followed by oxidative deamination, desulfonation, demethylation depending on the structure of the ring (Telke et al., 2010). The formation of phenyl diazene radical and loss of  $N_2$  was also observed by (Chivukula and Renganathan, 1995) for degradation of phenolic azo dyes by *P. oryzae* laccase. The attack of dioxygen on phenolic ring cleavage by laccase

is widely seen in oxidation of lignin products and catechol (Crestini and Argyropoulos, 1998; Chen et al., 2017). Laccase oxidation of dye is through highly reactive free radicals that are involved in the above reactions and since they are non-specific a wide number of products are formed. This mechanism produces phenol-based products thereby avoiding the formation of toxic aromatic amines (Figure 5.8).

### 5.3.7 Toxicity Analysis

The toxicity of the samples was analysed by *V. fischeri* toxicity assay to determine the percentage inhibition of the dye degradation products to the bacterial cells. The samples were subjected to dilutions and the corresponding inhibition values were plotted against each dilution (Figure 5.9(a)).



(a)

**Figure 5.9(a):** *V. fischeri* toxicity profile indicating the % inhibition for each dilution for all the products

It is evident that the auto-oxidation products have higher inhibition compared to anode (MFC<sub>Dye Anode</sub>) and cathode (MFC<sub>Dye Cathode</sub>) treated products. In the initial concentration, cathode treated products are comparatively more inhibitive than the

anode products. As seen in the graph on increasing the concentration, the anode products have an upward trend while laccase products are quite constant throughout. As the concentration of the anode effluents increase the toxicity increases. Similar trend was observed for the auto-oxidation products.

Laccase degradation of dye is through a free radical mechanism that produces a huge number of products (phenol, benzoic acid, hexanoic acid) compared to *Shewanella* degradation. These products are monocyclic hydrocarbons that could be degraded readily in next stages of water treatment. The LD<sub>50</sub> concentration of benzoic acid for mammalian cells is 2.3 gm/Kg (MSDS, Sigma Aldrich). The overall concentration of the dye is 100 mg/L in this study. Therefore, the concentration of dye breakdown would be expected to be lower than 100 mg/L, which is a very low concentration to exhibit toxicity. The horizontal curve for cathode products might be due to the formation of phenol-based products by laccase that are toxic to the *V. fischeri* or the consumption of the dissolved oxygen by laccase enzyme that created anoxic conditions for the bacteria. *Vibrio fischeri* is a highly sensitive organism and its EC<sub>50</sub> for phenol is 23 mg L<sup>-1</sup> (Fernando et al., 2014).

In contrast, 1-amino-2-naphthalenol obtained from by reductive cleavage of the dye by *S. oneidensis* is known to be xenobiotic and are classified as possible human carcinogens by the International Agency for Research on Cancer (Group 1 or 2B) and the European Union (Category 1A or 1B). In Japan, 20% of workers involved in the production of aromatic amines developed uroepithelial cancer (Hamasaki et al., 1996). The auto-oxidation of these amines yielded products that are more toxic than the parent amines.

The auto-oxidation products showed highest toxicity to the *Vibrio* cells due to the presence of naphthoquinone intermediates (Figure 5.9 (a) & 5.7). Naphthoquinones are highly reactive oxidative species that are known to cause cellular oxidative stress that affects the signalling pathway in the cells (Klotz et al., 2014). Quinones are used for medicinal purposes due to their anti-fungal, anti-bacterial and antioxidant properties. They are used in cancer drugs due their ability to form Reactive oxygen species (ROS) that attack and destroy the tumour cells (Verrax et al., 2011).

The toxicity measurements are a relative comparison between each system. There are various methods for testing the toxicity depending on the application of the discharged

effluents. In this study, Microtox assay was utilized due to its high level of sensitivity compared to methods like MTT.

## 5.4 Conclusion

There are several azo dye degradation pathways depending on the treatment methods. In the current study two different systems i.e. MFC with dye at the anode in presence of *S. oneidensis* and MFC with dye at cathode in the presence of laccase, were explored for AO7 degradation. A MFC system with absence of dye in both chambers was used as control. The power density was highest for MFC<sub>Control</sub> with  $57.8 \pm 1.6 \text{ mW m}^{-2}$  followed by MFC<sub>Dye Cathode</sub> with  $50 \pm 4 \text{ mW m}^{-2}$  and finally for MFC<sub>Dye Anode</sub> it was  $42.5 \pm 2.6 \text{ mW m}^{-2}$ . The same trend was followed for CE and COD respectively. The time required for decolourization was longer with bacteria (anode) where only 20% decolourization was obtained after 24 h whereas there was >80% for laccase during the same time. The overall decolourization was greater than 95% in both systems. The anode decolourized products were found to be unstable when exposed to oxygen resulting in autooxidation and regaining of the colour. On analysing the dye degradation products in GC-MS, it revealed simpler compounds such as benzoic acid and hexanoic acid for laccase, whereas *S. oneidensis* produced aromatic amines. The colour formation in auto-oxidation was likely due to the presence of quinones produced by oxidation of the aromatic amines. These products were much more toxic than the anode and cathode solutions. Therefore, from this study it was observed that laccase based MFC-dye decolourization systems are best suited for degradation and detoxification of azo dyes while producing good power output. Thus, the current study also provides an insight into the different mechanisms and pathways leading to maximal degradation of the azo dyes. To develop an ideal MFC system for dye degradation, further studies need to be carried out to prevent auto-oxidation of the treated products and feed anode effluents to the cathode or vice-versa to obtain complete degradation of the dyes.

## **Chapter 6**

### **Role of laccase redox mediators in dye decolourization and power production in a MFC**

## 6.1 Background

The redox potential of the substrate should be lower than that of laccase for oxidation to be thermodynamically feasible. The redox potential range for fungal laccase is between 0.4 V-0.8 V vs SHE, which is suitable for oxidation of phenolic substrates. For non-phenolic substrates that have a redox potential  $>1.3\text{V}$  vs SHE and cannot be oxidized directly by laccase; a redox mediator is required (Morozova et al., 2007).

A redox mediator is a small molecular weight compound that is oxidised by the enzyme and reduced by the substrate continuously. They act as electron shuttles for large substrates that cannot access the active site of the enzyme and decrease the steric hindrance (Christopher et al., 2014). In laccase mediator systems (LMS), the enzyme oxidizes the mediators to form stable radicals with high redox potential that diffuse away from the enzyme active site and oxidize the substrates and get reduced in the process. In this way laccase indirectly oxidises substrates that have high redox potential or large size (Figure 6.1) (Kunamneni et al., 2007).

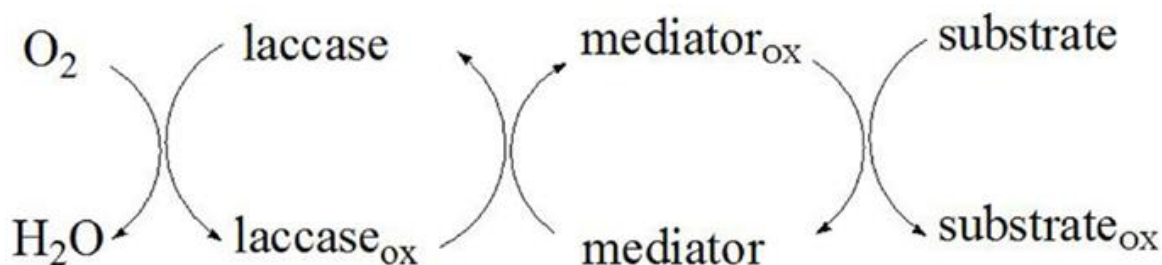


**Figure 6.1:** Laccase substrate oxidation through mediators and subsequent reduction of mediators (Christopher et al., 2014). In a MFC setting the substrate can either be electrode or the dye which acts as an electron source for the mediators.

A redox mediator should ideally be non-toxic, stable and should not inhibit the laccase-mediated reaction in both its oxidized and reduced forms (Morozova et al., 2007). The first synthetic redox mediator reported was 2,2'-azinobis(3-ethylbenzthiazoline-6-sulfonate) (ABTS) for laccase from *T. versicolor* for oxidation of non-phenolic lignin compounds (Bourbonnais and Paice, 1990). ABTS is first oxidised to generate cationic radical ABTS<sup>•+</sup> that is sequentially oxidised to dication ABTS<sup>2+</sup>:



The redox potential of  $\text{ABTS}^{\cdot+}$  is 0.68 V vs SHE and  $\text{ABTS}^{2+}$  is 1.09 V vs SHE respectively (Christopher et al., 2014). ABTS is readily oxidised by various laccases and the mediator is constantly regenerated aiding in the enzyme reaction. The two methods of mediation are Electron transfer (ET) route or radical hydrogen atom transfer (HAT). ABTS follows the ET route of mediation in which only electrons are involved in the formation of free radicals and in oxidation/reduction of the mediator (Section 6.3.3, Figure 6.8). In HAT mechanism, besides an electron, a  $\text{H}^+$  ion is abstracted from hydroxyl groups of the mediators resulting in  $\text{O}^{\cdot}$  free radical that aids in the mediation (Section 6.3.3, Figure 6.7). Another mediator that is involved in laccase lignin degradation and bleaching of kraft pulps is 1-Hydroxybenzotriazole (HBT) (Call and Mücke, 1997). HBT possess N-OH functional group, therefore the oxidation produces a highly reactive nitroxyl radical ( $\text{N-O}^{\cdot}$ ) which then targets the weak C-H bonds in the lignin substrates resulting in their breakdown. Other mediators with the N-OH group are violuric acid (VLA), N-hydroxyacetanilide (NHA), TEMPO (Cañas and Camarero, 2010). Although laccase mediator systems were initially used for delignification and bio bleaching of wood pulps, they have now been widely used for degradation of xenobiotics compounds and dyes.

Soares et al, 2001 have revealed that Remazol Blue was only decolourized when redox mediators violuric acid (VA) and HBT were added to laccase. There was complete decolourization within 20 mins of adding VA as mediator for laccase. On the contrary, high concentrations of HBT (>11 mM) inhibited laccase activity (Soares et al., 2001). Laccase mediator system (LMS) is not required for many low molecular weight dyes. LMS is most commonly used for degradation of contaminants like Chlorophenols and large substrates with high redox potentials (Wu et al., 2008; Zeng et al., 2017).

### **6.1.1 Phenolic Mediators**

Although ABTS and HBT are the most widely used redox mediators for laccase, the artificial mediators are not economically feasible, and they are toxic to the enzymes in the long run. In recent times, natural mediators have been explored for their environmental friendliness and low-cost. These natural mediators are phenolic compounds that exist in nature and mediate lignin oxidation in white rot fungi. The commonly used phenolic mediators are syringaldehyde, acetosyringone, vanillin, acetovanillone, methyl vanillate, p-coumaric acid etc (Cañas and Camarero, 2010).

They have been widely studied for their mediating capabilities in oxidation of dyes and other recalcitrant compounds. The above mediators were compared with ABTS and HBT for decolourization of different dyes with laccase from *T. versicolor* and *P. cinnabarinus*. Syringaldehyde and Acetosyringone showed 100% decolourization of Acid blue 74 with both laccases while there was >85% decolourization for Reactive Black 5 dye in less than 1 hour for both the dyes. There was less than 50% decolourization of Acid Blue 74 by ABTS and HBT in the same time period. The phenolic mediators were more rapid and efficient in oxidation of the dyes than their synthetic counterparts (Camarero et al., 2005). In another study, they have concluded laccase-syringaldehyde as the best system for decolourization of azo dyes Red FN-2BL, Red BWS, Remazol Blue RR and Blue 4BL with efficiency of 98%, 88%, 80% and 78% respectively with the above decolourization achieved in less than 2 hours (Mendoza et al., 2011). The decolourization efficiency of various LMS depends on the dye structure and the competency of the mediator towards a specific functional group. The mechanism of laccase mediation varies between each mediator. It was observed for lignin oxidation (Section 1.3.8.1, Figure 1.13) ABTS/Laccase carried out C $\alpha$  oxidation and coupling of the lignin subunits whereas HBT/laccase polymerized them (Hilgers et al., 2018).

Laccase stability and activity was decreased when incubated with redox mediators ABTS, HBT, TEMPO (2,2,6,6-tetramethylpiperidin-N-oxyl) and VA at concentrations of 0.5 mM (Kurniawati and Nicell, 2007). Even in the absence of any mediator laccase activity decreased from 1000 U L<sup>-1</sup> to 290 U L<sup>-1</sup> in 15 days (Mendoza et al., 2011). It is probably due to this reason that higher enzyme loadings such as 500 U ml<sup>-1</sup> to 2000 U ml<sup>-1</sup> are used in various dye decolourising experiments (Stoilova et al., 2010). Therefore, methods to increase the stability of laccase and decrease the enzyme loading should be further examined.

In this study natural mediators such as syringaldehyde and acetosyringone were studied with relatively low enzyme loadings (300 U L<sup>-1</sup>) to develop a low cost and sustainable laccase-mediator system. As the free radical forming moiety is different in case of natural and synthetic mediators, it was of interest to study the effect it has on the decolourization of AO7. The presence of laccase with natural phenolic mediators such as syringaldehyde and acetosyringone in a microbial fuel cell for dye decolourization has not been reported so far. The aim was to understand the effect of

mediators on dye decolourization and power density in a laccase biocathode MFC. The synergistic effect of dye and mediators as oxidising substrates for laccase was also inferred in this study.

## **6.2 Materials and methods**

### **6.2.1 Experimental Design**

The MFC used in this study was the 'H'-type reactor with a working volume of 200 ml in each chamber. The electrodes were constructed from carbon fibre (non-woven) with a surface area of 25 cm<sup>2</sup>. The cathode chamber consisted of crude commercial laccase (Enzyme India Pvt. Limited, Chennai) from a fungal source (10 U mg<sup>-1</sup>) in acetate buffer (pH 4.5). Seven MFC systems were set up. System 1 was with *S. oneidensis* in the anode and laccase enzyme suspended in the cathode chamber in absence of mediator, subsequently to be referred to as "Control Lac". System 2 was with *S. oneidensis* in the anode and laccase in the presence of ABTS in the cathode, subsequently to be referred to as "ABTS-lac". System 3 was with *S. oneidensis* in the anode and laccase in the presence of syringaldehyde in the cathode, subsequently to be referred to as "Syr-lac". System 4 was with *S. oneidensis* in the anode and laccase in the presence of acetosyringone in the cathode, subsequently to be referred to as "As-lac". System 5 was with *S. oneidensis* in the anode and syringaldehyde in the cathode without laccase, subsequently to be referred to as "Syringaldehyde". System 6 was with *S. oneidensis* in the anode and acetosyringone in cathode without laccase, subsequently to be referred to as "Acetosyringone". System 7 was with *S. oneidensis* in the anode and ABTS in the cathode without laccase, subsequently to be referred to as "ABTS". Laccase enzyme (300 U L<sup>-1</sup>) was freely suspended in 200 ml of 100 mM acetate buffer (pH 4.5) and 100 mg L<sup>-1</sup> of Acid Orange 7 dye was added in the cathode chamber. After subsequent trial experiments the concentration of the mediators were fixed at 50 µM.

### **6.2.2 Operating conditions**

The composition in the anode was the same for all the reactors. The anode media components and their concentrations are detailed in Chapter 2, Section 2.3. The anode and cathode were connected to a resistor of 2 kΩ. The anode was inoculated with 10% v/v *S. oneidensis* MR-1 culture previously grown in Luria Bertani broth to an OD of

0.4. The anode chamber was sparged for 10 minutes with nitrogen gas to remove any dissolved oxygen and maintain an anaerobic environment.

The cathode chamber was maintained in aerobic conditions by supplying air through an air stone at a rate of 200 ml air per min. Experiments were conducted at a temperature of 30 °C. All experiments were performed in triplicates.

### **6.2.3 Analytical procedures**

The analytical procedures followed in this study were AO7 decolourization (Section 2.6.1), electrochemical tests (Section 2.6.2), cyclic voltammetry of the redox mediators (Section 2.6.11(c)) and statistical analysis (Section 2.6.15).

## **6.3 Results and Discussion**

### **6.3.1 Power Generation**

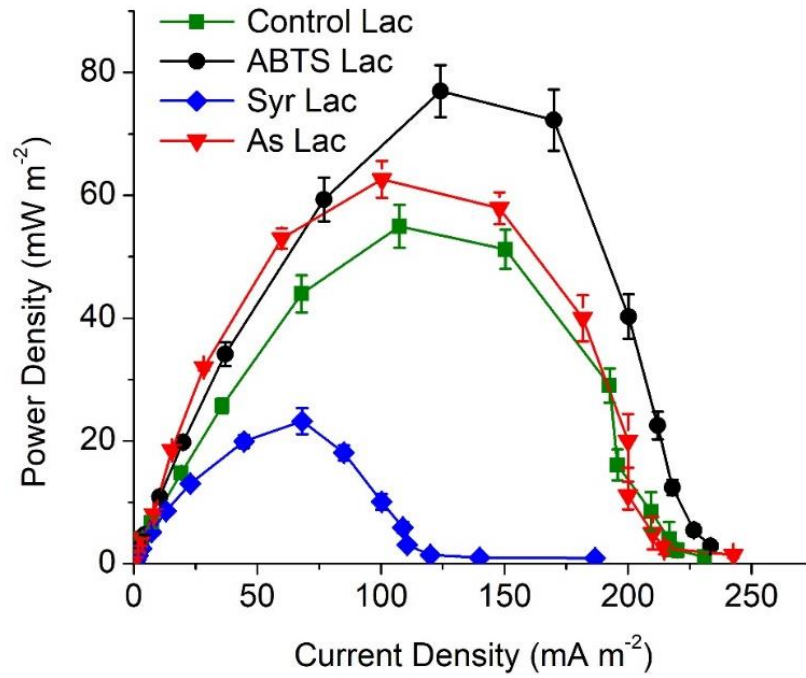
The power density was highest for ABTS-lac cathode with  $77.2 \pm 4.2 \text{ mW m}^{-2}$  compared to control laccase (no mediators) with  $54.7 \pm 3.5 \text{ mW m}^{-2}$  (Figure 6.2(a)). This power density for ABTS-laccase is equivalent to the performance of platinum electrode ( $80 \text{ mW m}^{-2}$ ) reported in chapter 4. Similar results were obtained by Luo et al., 2010 when laccase immobilized with Nafion-ABTS produced a power equivalent to platinum. The power density in this study was much higher than Schaeztle et al., 2009 who obtained  $37 \text{ mW m}^{-2}$  with laccase-ABTS at cathode of a MFC. The power density was lower in their study due to the immobilization of the enzyme in hydrogels which might have created mass transport limitation for diffusion of electrons to the enzyme.

ABTS is oxidised by laccase and it is regenerated (reduced) by receiving electrons from the electrode and the dye. The electrode and dye act as the substrates for ABTS regeneration. It is the most efficient mediator for laccase in fuel cells to produce high current output (Le Goff et al., 2015). The redox potential of the intermediates, ABTS<sup>•+</sup> is 0.68 V and ABTS<sup>2+</sup> is 1.09 V vs SHE respectively (Christopher et al., 2014). The high redox potential of ABTS radical aids laccase in efficient ORR which occurs at a potential of 1.2 V vs SHE.

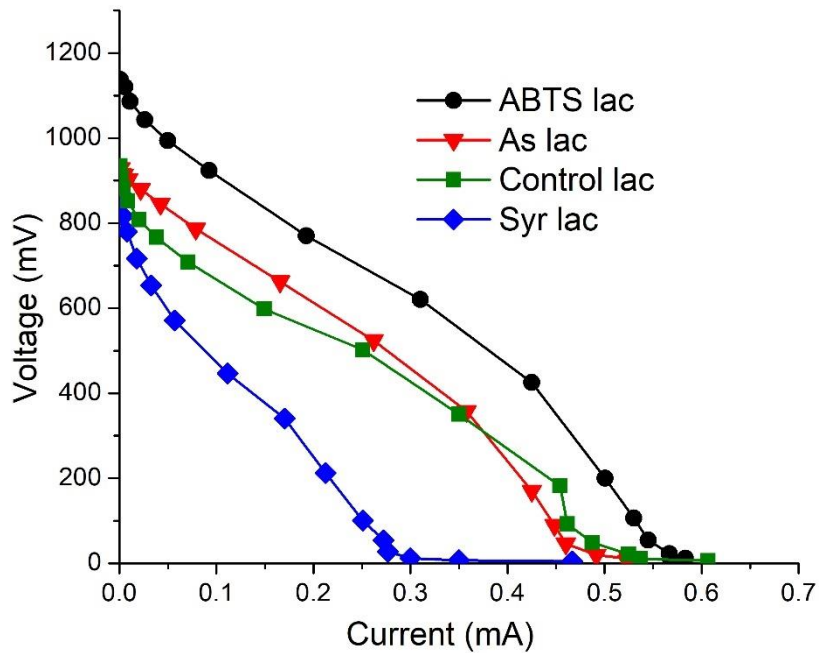
The acetosyringone-lac produced a  $P_{\max}$  of  $62.5 \pm 3.7 \text{ mW m}^{-2}$  and for Syr-lac it was  $23.2 \pm 2.1 \text{ mW m}^{-2}$  (Figure 6.2 (a)). The power density was higher for As-lac than control laccase without any mediators and it was vice versa for Syr-lac. The low power produced by syringaldehyde is probably due to it acting as substrate for laccase rather than mediator. The electron donating groups of the benzene ring in the phenolic compounds lowers their redox potentials which enables laccase to readily oxidizes these substrates for electrons that is used in oxygen reduction reaction (Cañas and Camarero, 2010). Since phenols are natural substrates for laccase they favour accepting electrons from phenol oxidation rather than from the electrode (Section 6.3.3). This reduces the performance of the fuel cells. The higher power density in control laccase indicates that in the absence of mediators the electrons are accepted from the electrode. Although acetosyringone is also a phenolic compound, the power was greater than control laccase as it was efficiently regenerated as a mediator compared to syringaldehyde. The detailed mechanism for the mediation is discussed in section 6.3.3. Thus, from the  $P_{\max}$  it can be observed that acetosyringone is a lower affinity substrate for laccase as compared to syringaldehyde. This study is the first use of phenolic mediators in a MFC for laccase oxidation.

The internal resistance was the lowest for As-lac system with  $1.5 \pm 0.07 \text{ K}\Omega$  compared to  $1.79 \pm 0.09 \text{ K}\Omega$  for control laccase. ABTS-lac system possessed an internal resistance of  $1.89 \pm 0.11 \text{ K}\Omega$ , while Syr-lac system had the highest with  $2.2 \pm 0.15 \text{ K}\Omega$  (Figure 6.2(b)). Acetosyringone was able to decrease the ohmic resistance of a laccase system compared to any other mediators. ABTS is a larger molecule ( $515 \text{ g mol}^{-1}$ ) with higher molecular weight and higher diffusion co-efficient ( $2.5 \times 10^{-10} \text{ m}^2 \text{ s}^{-1}$ ) compared to acetosyringone ( $196 \text{ g mol}^{-1}$ ) which is smaller molecule with lower diffusion co-efficient ( $3.4 \times 10^{-10} \text{ m}^2 \text{ s}^{-1}$ ) (Srinivas and King, 2011; Preedy and Patel, 2012). This might have contributed to the difference in the internal resistance between the two mediators.

In absence of laccase the power density for cathodes containing syringaldehyde and acetosyringone was  $8.6 \text{ mW m}^{-2}$  and  $7.5 \text{ mW m}^{-2}$  respectively.



(a)



(b)

**Figure 6.2:** (a) Maximum Power density for mediator based and control MFCs obtained by varying the external resistance from  $10\Omega$ - $1M\Omega$  (b) Voltage vs Current plot (Slope=internal resistance) on day 3.

### 6.3.2 Acid Orange 7 decolourization

The decolourization rate of AO7 was highest in case of As-lac followed by Syr-lac and finally unmediated laccase biocathode. There was greater than 87% decolourization in As-lac within 18 hours of addition of dye. Laccase without mediator was slightly slower with less than 80% decolourization in 18 hours (Figure 6.3). Overall there was > 90% decolourization for all laccase-based systems. Similar trend was observed for acetosyringone with Reactive Blue dye where >80% decolourization was observed in 2 hours (Camarero et al., 2005). As the two mediators are phenolic compounds that are substrates for laccase they are rapidly oxidised by the enzyme to produce phenoxy radicals that aid in dye decolourization (Camarero et al., 2005). In the presence of AO 7 dye, the mediated laccase prefers the oxidation of dye for electrons rather than the anodic electron source with redox potential of -0.2 mV (Marsili et al., 2008). The mediators are regenerated by abstraction of  $H^+$  from the dye and  $e^-$  from the electrode respectively. Syringaldehyde and acetosyringone have been reported to have redox potential of 0.660 V and 0.580 V vs SHE (Pardo et al., 2013; Baker et al., 2014). In the absence of laccase, the mediators have lower redox potential than the dye (0.693 V vs SHE), therefore no decolourization was observed (Figure 6.3).

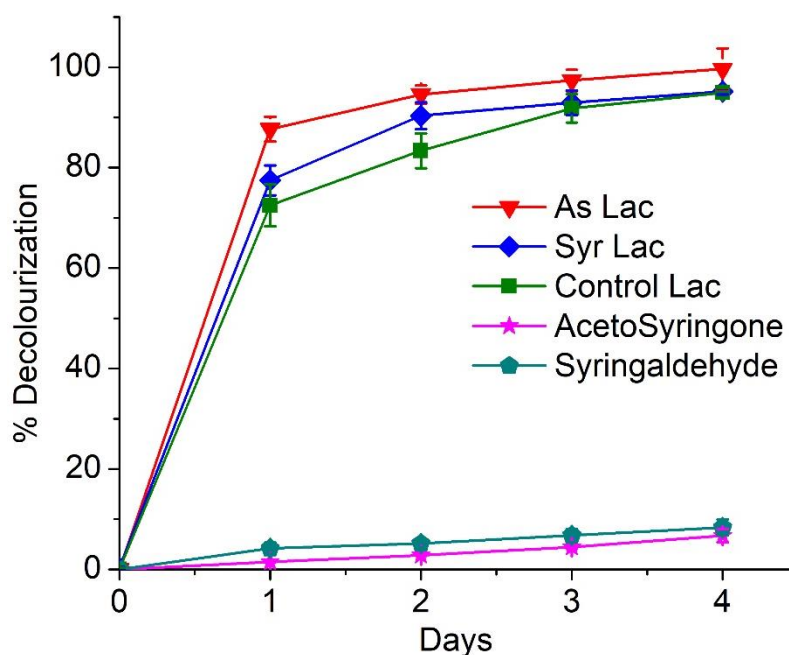


**Figure 6.3:** Decolourization of AO7 dye by laccase in the presence and absence of mediators over a period of 4 days.

The decolourization through ABTS-Laccase system was also attempted for comparison. Due to heavy interference with the colour of ABTS in the presence of laccase (blue), the decolourization could not be studied effectively.

### 6.3.3 Electrochemical activity of the laccase-mediator systems

To understand the reaction mechanism of the laccase-mediator systems, cyclic voltammetry (Section 2.6.11(c)) was performed. Syringaldehyde revealed a very weak oxidation peak at 0.73 V without any quantifiable cathodic current (Figure 6.4). In presence of laccase the oxidation peak was further decreased indicating its reduction reaction with the enzyme. There was absence of any redox peaks that are characteristics to redox mediators that indicates their regeneration. This might be due to laccase oxidizing syringaldehyde to syringic acid while producing phenoxy radicals and syringic acid further oxidizing to 2,6-dimethoxy-1,4-benzoquinone (DMBQ) (Lin et al., 2014; Volkova et al., 2012) (Figure 6.5). Due to the subsequent oxidation of syringaldehyde it is not regenerated and available as a mediator. The lower power density in Syr-lac might be a result of syringaldehyde oxidation products inhibiting laccase enzyme activity.

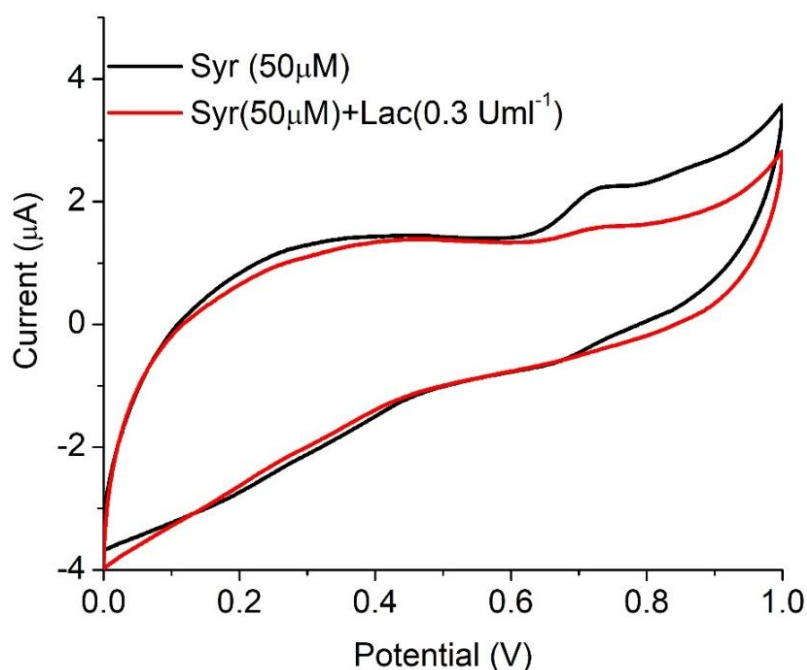


**Figure 6.4:** Cyclic voltammetry of syringaldehyde in the presence and absence of laccase at a scan rate of 50 mV s<sup>-1</sup>.



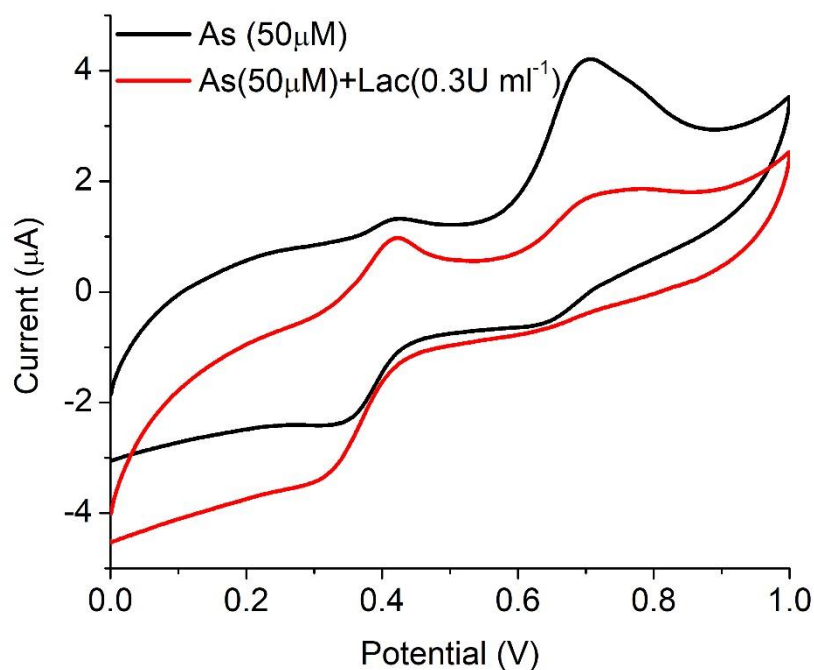


**Figure 6.6:** CV of acetosyringone indicating the oxidation/reduction peak in the presence and absence of laccase at a scan rate of  $50 \text{ mV s}^{-1}$

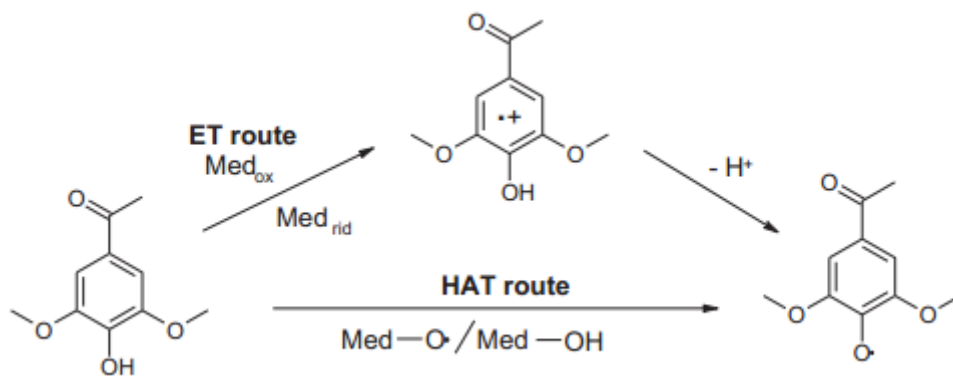


**Figure 6.7:** Electron transfer (ET) and Hydrogen atom transfer (HAT) oxidation mechanisms of acetosyringone mediated by laccase (Martorana et al., 2013).

In case of ABTS, there were two redox couples, first at  $0.9 \text{ V} / 0.67 \text{ V}$  and second at  $0.63 \text{ V} / 0.45 \text{ V}$  (Figure 6.8 (b)). ABTS oxidation is a two-step mechanism where first it is oxidised to generate cationic radical ( $\text{ABTS}^{\cdot+}$ ) that is sequentially oxidised to dication ( $\text{ABTS}^{2+}$ ) (Figure 6.8 (a)) (Bourbonnais et al., 1998). ABTS is readily oxidised by laccase and the mediator is constantly regenerated by accepting electrons from the electrode and the dye. The mechanism of ABTS mediation is through electron transfer (ET) route between enzyme and the substrate (Figure 6.8 (a))

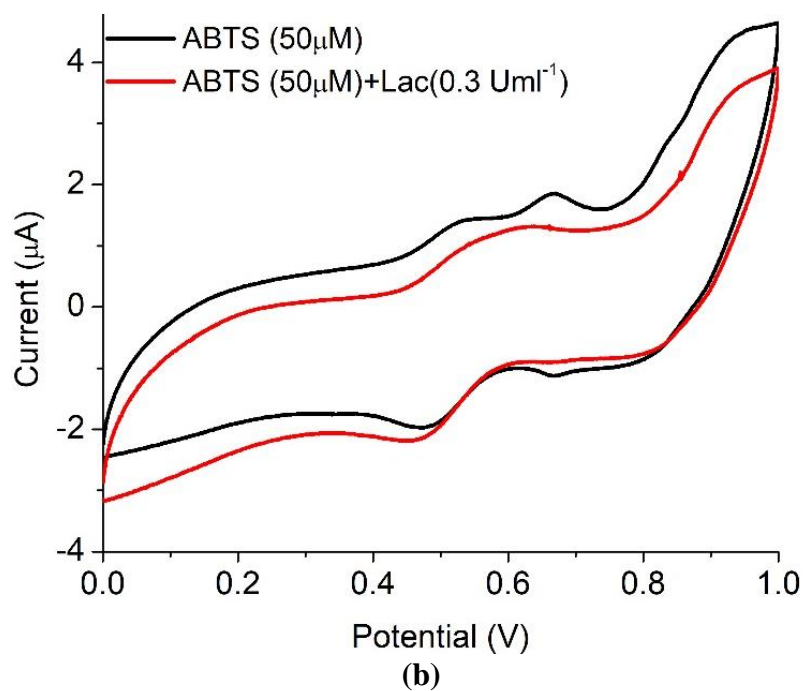
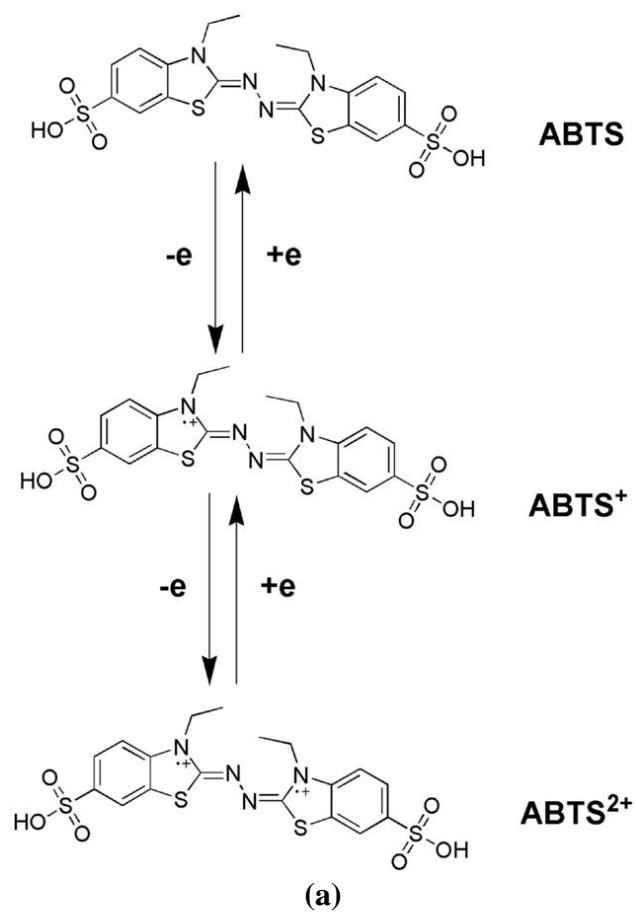


**Figure 6.8:** (a) Two step oxidation of ABTS (Christopher et al., 2014) (b): CV of ABTS with and without laccase at  $50 \text{ mV s}^{-1}$ .

The effect of laccase-mediator reaction on the reduction current was further tested by chronoamperometry. The electrode was poised at a constant potential of 0.7 V with 50  $\mu\text{M}$  mediator in the solution. A constant amount ( $0.03 \text{ U ml}^{-1}$ ) of laccase was added to the solution to observe the effect on the current. It was observed that ABTS system gave the highest cathodic current of 600  $\mu\text{A}$ , whereas syringaldehyde and acetosyringone system produced 150 and 125  $\mu\text{A}$  respectively (Figure 6.9).

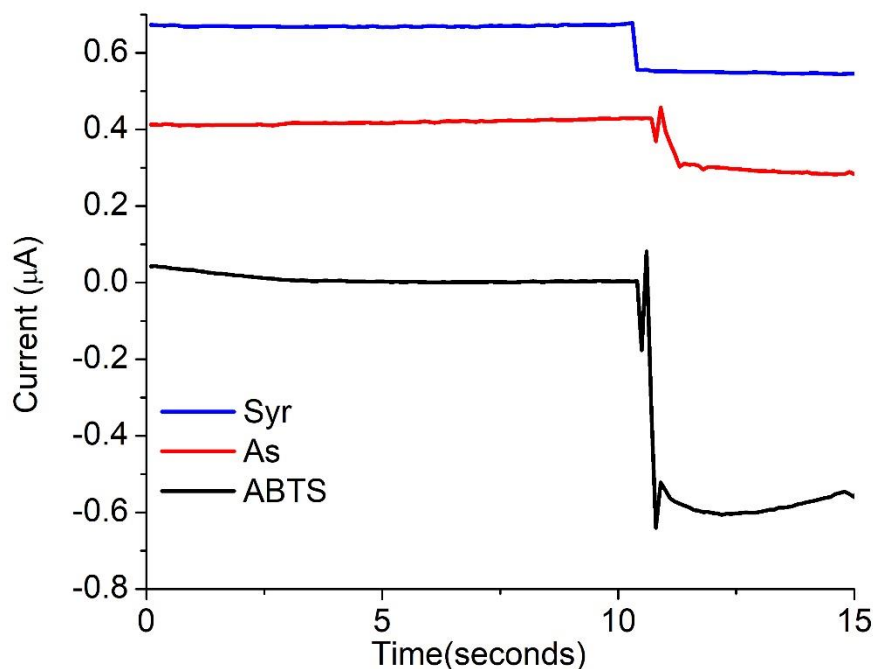


**Figure 6.9:** Chronoamperometry depicting the reduction current for each mediator at a concentration of 50  $\mu\text{M}$ .

Although ABTS was the best mediator in terms of power production, acetosyringone performed comparably with an added advantage of dye decolourization. It is much cheaper and sustainable than ABTS. Syringaldehyde was the best substrate for laccase and was completely oxidized thus it did not act as a mediator to improve the performance of the MFC. Overall, acetosyringone-lac system can be preferred for dye decolourization and power production in a MFC.

## 6.4 Conclusion

Mediators are known to improve the power density and efficiency of dye decolourization when used with laccase in the cathode of a MFC. For reasons regarding environment and economic advantage in the present study natural mediators such as syringaldehyde and acetosyringone was compared for their effectiveness to that of a synthetic mediator like ABTS. The presence of mediators increased the power density: ABTS-lac cathode produced a  $P_{\max}$  of  $77.2 \pm 4.2 \text{ mW m}^{-2}$  while As-lac gave  $62.5 \pm 3.7 \text{ mW m}^{-2}$ . The control system without mediators produced  $54.7 \pm 3.5 \text{ mW m}^{-2}$  while the power density was quite low for Syr-lac with  $23.2 \pm 2.1 \text{ mW m}^{-2}$ . There was increase in decolourization by 20% with addition of mediators as compared to laccase in absence of mediators with As-lac achieving greater than 85% decolourization in 18 hours. Electrochemical analysis performed to determine the redox properties of the mediators, revealed syringaldehyde did not produce any redox peaks thus inferring it was oxidized by laccase to syringic acid and further to quinone, making it unavailable as a mediator, while acetosyringone and ABTS revealed two redox couples demonstrating the redox behaviour of these compounds. Thus, acetosyringone served as an efficient mediator for laccase, aiding in increased rate of dye decolourization and power production in a MFC.

## **Chapter 7**

**Enrichment of microbial biocathodes to replace platinum catalyst in microbial fuel cells**

## 7.1 Background

In recent times, microorganisms capable of accepting electrons from the electrode are being developed from soil and sludge sources consisting of mixed microbial community. This eliminates the need to use large quantities of Mn and Fe as terminal electron acceptors. The bacteria in the mixed community are identified through DGGE and 16srRNA sequencing. The aerobic biocathodes isolated from the various sources mainly belong to species from Alphaproteobacteria, Betaproteobacteria, Gamma proteobacteria, Bacteroidetes, Planctomycetes etc (Xia et al., 2012; Wang et al., 2013; Strycharz-Glaven et al., 2013; Du et al., 2014; Milner et al., 2016). The enrichment of electroactive bacteria takes place either in a three-electrode system known as half-cell (electron supplied externally) or a MFC (electron supplied from the anode). To reduce the internal resistance and maximize the voltage produced a new biocathode was developed from dairy manure waste by (Zhang et al., 2012). The MFC anode consisted of anaerobic sludge from wastewater and the cathode contained soil mixed with dairy manure and operated for 102 days. The maximum power density produced was  $15.1 \text{ W m}^{-3}$  with an internal resistance of  $31 \text{ } \Omega$ . Microbial community analysis revealed highest presence of species from *Alcaligenaceae* family (38.3%), followed by *Xanthomonadaceae* (6.0%), *Brucellaceae* (5.1%), *Bradyrhizobiaceae* (4.2%), Enterobacteriaceae (4.0%) etc (Zhang et al., 2012).

Rabaey and co-workers compared the efficiency of mixed microbial population with that of individual isolates for reducing oxygen in a MFC. The biofilm was obtained from a mixture of samples from river, pond and activated sludge plant after 212 days of incubation in MFC conditions. These biocathodes produced a maximum power density of  $303 \text{ mW m}^{-2}$ . Analysis of the cathode microbial community revealed *Sphingobacterium*, *Acinetobacter* and *Acidovorax* sp. as dominant species. These isolates tested individually as cathode catalysts obtained maximum power of only  $49 \text{ mW m}^{-2}$ . Therefore, mixed populations seemed to produce significantly higher power than pure cultures due to the population density and the co-metabolic activity. The *Sphingobacterium* and *Acinetobacter* species were able to readily switch to hydrogen metabolism after few days incubation in  $\text{H}_2/\text{O}_2$  environment indicating their adaptability to various substrates (Rabaey et al., 2008).

Although the start-up time is quite slow compared to chemical or enzyme catalyst, microbial cathodes can be regenerated and are suitable for long term usage. In an MFC, biocathodes produced a power density of  $62 \mu\text{W cm}^{-2}$  which was comparable to platinum at  $70 \mu\text{W cm}^{-2}$  (Milner et al., 2016). A decrease in activation overpotential was observed when the biocathodes were used in an MFC, suggesting that the bacteria act as true catalysts for oxygen reduction (Rabaey et al., 2008). As suggested by He and Angenent 2006, more understanding in mechanisms of electron transfer between electrode, microorganisms and electron acceptors at the cathode is required for increased power output. The source of inoculum, the enrichment method (half-cell, MFC) and the potential used can affect the type of microbial community selected (Table 7.1).

**Table 7.1:** BES employed in development of microbial biocathode and the dominant microbial communities identified.

<b>Cathode Material</b>	<b>Source of inoculum</b>	<b>Enrichment method/Potential</b>	<b>Microbial community</b>	<b>References</b>
Carbon paper	Aerobic sludge	MFC (-0.1 V vs SCE)	80% Uncultured Bacteroidetes 13% <i>Thiorhodospira</i> sp. ( $\gamma$ -Proteobacteria)	(Xia et al., 2012)
Carbon fibre Brush	Nitrifying sludge	MFC (1000 $\Omega$ )	38.8% <i>Nitrosomonas</i> sp., 2% Nitrate oxidizing bacteria; 34.7% <i>Alkalilimnicola</i> sp. (Proteobacteria)	(Du et al., 2014)
Stainless Steel	River water	OCP	Actinobacter, Firmicutes, Bacteroidetes, $\alpha$ , $\beta$ and $\gamma$ - Proteobacteria	(Lyautey et al., 2011)
Graphite fibre brush/graphite granules	Top soil	MFC (500 $\Omega$ )	<i>Nitrobacter</i> sp., <i>Achromobacter</i> sp., <i>Acinetobacter</i> sp. (Proteobacteria) Bacteroidetes	(Zhang et al., 2011)

Cathode Material	Source of inoculum	Enrichment method/Potential	Microbial community	References
Graphite fibre brush	Sulphur reducing bacteria sludge (SRB)	MFC (-0.8 V vs SHE)	<i>Desulfovibrio</i> sp., <i>Thiomonas</i> sp., <i>Sulfuricurvum</i> sp. and <i>Thiobacillus</i> sp.	(Blázquez et al., 2017)
Graphite plate	Acclimated SRB+ Magnetite particles	MEC (0.8 V)	72.2% <i>Desulfovibrio</i> sp., 14.2% <i>Acetobacterium</i> sp.	(Hu et al., 2018)
Graphite granules	Denitrifying sludge	MEC	<i>Escherichia/Shigella</i> spp., <i>Actinotalea</i> sp., <i>Desulfitobacterium</i> sp. (Fe reducing bacteria); <i>Petrimonas</i> , <i>Thermomonas</i> , <i>Chelatococcus</i> (Denitrifying bacteria) species	(Zhao et al., 2018)
Carbon cloth	Aerobic sludge	MFC (-0.3 V vs Ag/AgCl)	39.9% Proteobacteria, 29.9% Planctomycetes, 13.3% Bacteroidetes	(Wang et al., 2013)
Carbon felt	Activated sludge	Half cell (0.1 V vs Ag/AgCl)	23.3%-44.3% Unidentified $\gamma$ - Proteobacteria	(Milner et al., 2016)

As seen above various inoculum sources and enrichment methods produce different microbial communities capable of carrying out reactions such as oxygen reduction, denitrification etc at the cathode of MFC. In this study, aerobic sludge from activated sludge tank of textile water treatment plant in India was used to develop a cathodic biofilm capable of oxygen reducing reaction (ORR). The catalytic efficiency of this biofilm was compared to Platinum in the cathode of a microbial fuel cell. The Acid orange 7 dye was added in the anode to compare the rate of dye decolourization in each system. The sequencing and bioinformatics analysis of the biofilm was carried out to identify the dominant species responsible for electrochemical activity by comparing it with other forms of growth (planktonic) observed in the study. The aim was to isolate new strains of bacteria capable of performance equivalent to that of platinum in a MFC.

## **7.2 Materials and Methods**

### **7.2.1 Preparation of half-cell for enrichment**

A three-electrode system with Ag/AgCl as the reference electrode, graphite rod of 45 cm<sup>2</sup> (14 cm x 0.5 cm) as the counter and graphite rod 31 cm<sup>2</sup> (12 cm x 0.4 cm) as the working electrode was used for the enrichment of microbial consortia. The counter electrode (CE) and working electrode (WE) were prepared by connecting a tin-coated Cu wire (0.2 mm) to the graphite rods. A small hole (size) was drilled into the graphite rods and the wire was threaded into the hole with a screw. The screw was tightened to keep the wire in place and in contact with the graphite rods. The screw and the wire end connected to the electrode was coated with non-conductive epoxy for insulation. The resistance of both the electrodes was measured to ensure conductivity. To prevent poisoning of Ag/AgCl electrode by the sludge, an agar bridge was constructed using a syringe and a glass capillary tube (Fig 7.1). A 10 cm length glass capillary tube was connected to the bottom of a 5 ml syringe with a rubber tubing to establish a firm connection. The plunger of the syringe was removed and 1.5% agar in 1M KCl was poured until it flowed through the full length of the glass capillary leaving approximately 2-3 ml in the syringe. It was allowed to cool and solidify. The remaining volume of syringe was filled with 1M KCl and the reference electrode was placed in the syringe to be floating in the KCl. The wires of both CE and WE were threaded through a hole pierced in the middle of a rubber septum in the screw cap of glass stoppers. Similarly, the bottom end of the capillary was passed through a hole pierced

in a larger rubber septum in the screw cap of glass stopper. These glass stoppers were sealed tightly in the inlets of the glass set-up. The glass-setup had five inlets, of which three were used for the electrodes, one for sampling and the other for aeration. For the aeration one end of the tube was connected to an air pump, it was passed through a syringe filter (0.2  $\mu\text{m}$ ) before entering the glass setup, and other end to an air stone. Another tube was connected to a syringe filter for air outlet. Both the air coming in and out were filter sterilized to avoid possible contamination.

### 7.2.2 Operation of the half-cell

The working volume for the electrochemical setup was 300 ml of minimal salts medium (MSM) containing (per litre): 0.46 g  $\text{NH}_4\text{Cl}$ , 0.22 g  $(\text{NH})_2\text{SO}_4$ , 0.117 g  $\text{MgSO}_4$ , 7.7 g  $\text{Na}_2\text{HPO}_4 \cdot 7\text{H}_2\text{O}$ , 2.87 g  $\text{NaH}_2\text{PO}_4$  along with 1% (v/v) trace minerals as described by (Marsili et al., 2008) and 1% (v/v) vitamin mix as described by (Wolin et al., 1963). There was no organic carbon source added. A 10% w/v sludge, from activated sludge tank of Andipalayam common textile effluent treatment plant (CETP) in Tirupur, India was used as the source of inoculum. The electrodes were connected to a Uniscan (PG581) potentiostat, the whole setup was placed in the dark at 30 °C and aeration was supplied through an air pump. The voltage applied was -0.1 V and the current was recorded every 20 minutes with a UiEChem software in chronoamperometry mode.



**Figure 7.1:** Three electrode electrochemical set-up used in this study

The half-cell was operated in batch mode for 2 months with periodic change in the media until a stable current was obtained from the biofilm formed. The WE was placed at the cathode of MFC to assess its oxygen reduction efficiency. The enrichment was performed in the dark without additional carbon source to eliminate heterotrophs and photoautotrophs to select for electroactive bacteria capable of accepting electrons from the electrode for their metabolism.

### **7.2.3 Platinum Electrode Preparation**

The cathode of one MFC contained a platinum catalyst layer with a Pt loading of 0.5 mg cm<sup>-2</sup>. Pt powder was mixed with carbon black powder (Sigma Aldrich, UK) for a 10% (w/w) mixture. This mixture was dissolved in Nafion solution (Sigma Aldrich) and the suspension was applied on a graphite rod of 31 cm<sup>2</sup> (12 cm x 0.4 cm) surface area.

### **7.2.4 Experimental design**

The MFC used in the study was the 'H'-type reactor with a working volume of 200 ml in each chamber. Cation exchange membrane CMI7000 ion exchange membrane was soaked in 5% NaCl for 12 hours prior to use.

Three systems were setup with the same conditions in the anode for all the reactors while changing the cathode electrodes. System 1 referred to as “Plain graphite MFC” consisted of a plain graphite as the cathode electrode in the absence of any catalyst. System 2 termed as “Platinum MFC” contained a platinum-coated graphite rod as the cathode catalyst. System 3 referred to as “Biocathode MFC” consisted of the biofilm enriched electrode at the cathode of the MFC. The MFC systems were connected across 200 Ω resistor. A 200 Ω was utilised based on the average resistance (142 Ω) calculated from average current (0.0007 V) and voltage (0.1 V) from the chronoamperometry used in the enrichment. One cycle in this study represents 7 days.

### **7.2.5 Operation of the Microbial fuel cell**

#### **7.2.5.1 Anode of the Microbial fuel cell**

The anode electrode was a 31 cm<sup>2</sup> (12 cm x 0.4 cm) graphite rod connected to a tin coated Cu wire. The anode media components and their concentrations are detailed in Chapter 2, Section 2.3. The anode was inoculated with 10% v/v *S. oneidensis* MR-1 culture previously grown in Luria Bertani broth to log phase (OD: 0.4) and the dye Acid Orange 7 was added at a concentration of 100 mg L<sup>-1</sup>. The anode chamber was sparged for 10 minutes with nitrogen gas to remove any dissolved oxygen and maintain an anaerobic environment.

### 7.2.5.2 Cathode of the microbial fuel cell

The three cathode electrodes used were biofilm enriched, platinum coated, and plain graphite rod. The catholyte was kept constant for all MFCs and it consisted of the same MSM, vitamins, trace minerals used in the half-cell (Section 7.2.2). The cathode chamber was maintained in aerobic conditions by supplying air through an air stone at a flow rate of 200 ml min<sup>-1</sup>.

### 7.2.6 Analytical Procedures

The analytical procedures followed in this study were spectrophotometry to determine AO7 decolourization (Section 2.6.1), electrochemical tests (Section 2.6.2), chronoamperometry (Section 2.6.12), microbial community analysis DGGE (Section 2.6.13), Illumina Next Gen sequencing (Section 2.6.14) and statistical analysis (Section 2.6.15).

## 7.3 Results and Discussion

### 7.3.1 Enrichment of electron-accepting microbes using chronoamperometry

A stable current was obtained from the biofilm after a period of 70 days. A stable current is defined by a phase where there is no sharp increase in current on replacement of the catholyte. The average peak current produced was -0.7 mA at -0.1 V vs Ag/AgCl. (Figure 7.2).

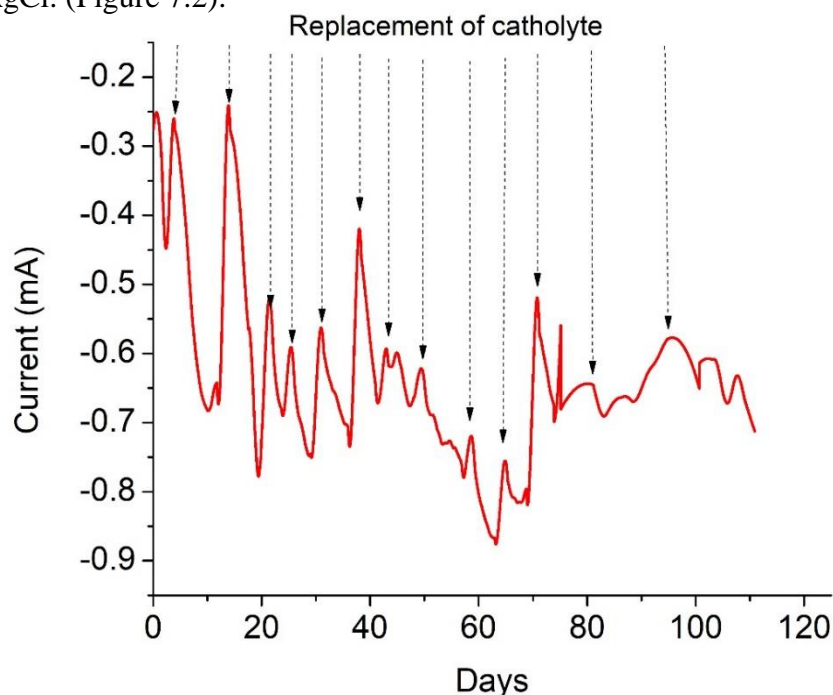


**Figure 7.2:** Chronoamperometry of biofilm showing the peak current for each cycle

The increase in the reduction current suggests the formation of electroactive biofilm on the electrode surface (Figure 7.2). The current started to increase 5 days after the inoculation and reached the maximum after 20 days. The start-up time varies depending on the potential applied and the substrate used. Biocathodes poised at different potentials produce different microbial communities (Table 7.1). In this study, -0.1 V used for enrichment decreased the start-up time and produced current at a faster rate.

Many studies utilized an organic carbon source (glucose, acetate) for the first few cycles to accelerate the formation of biofilm or a previously acclimated inoculum to decrease the start-up time (Xia et al., 2012; Zaybak et al., 2013). The activated sludge used in this study acclimated faster to the new media in the absence of organic carbon to form a biofilm. At day 60 there was an increase in current to a maximum of 0.9 mA after which it decreased to a steady state. The sustained current production for a period of 70 days indicates the electroactive behaviour of the biofilm.

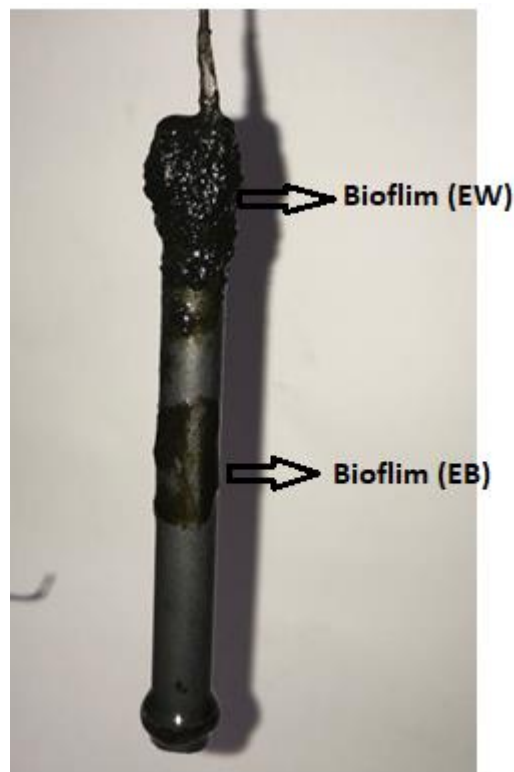


**Figure 7.3** : Enriched biofilm after 70 days of chronoamperometry with arrows indicating the two types of biofilm formed i.e. near the wired connection and at centre of the electrode.

A biofilm formation was also observed on the connection between the wire and the graphite rod which suggests that the microorganisms are electrophilic and depend on the electrons for their respiration and other metabolic activities (Figure 7.3). The average resistance of the system was 142  $\Omega$ , varying depending on the current produced.

Apart from biofilms on the electrodes, there was planktonic cells in the media and on the glass walls of the electrochemical set-up. The characteristics of the biofilm and planktonic cells were analysed by sequencing the microbial community.

### **7.3.2 Power Density**

The maximum voltage (OCV) obtained was highest for Platinum MFC with 950 mV, 890 mV for biocathode and 400 mV for plain graphite. The acclimated biocathode achieved a cell potential equivalent to Platinum MFC in 4-5 hours. The prior acclimation eliminates the start-up lag in MFC as observed by (Clauwaert et al., 2007; Mao et al., 2010). A steady voltage was maintained for 7 days after which the media was replenished.

The polarization tests revealed a maximum power density of  $72.7 \pm 1.2 \text{ mW m}^{-2}$  for Platinum MFC followed by  $64.6 \pm 3.5 \text{ mW m}^{-2}$  for Biocathode MFC and  $4.3 \pm 0.1 \text{ mW m}^{-2}$  for plain graphite MFC (Figure 7.4). The major limiting factor in a MFC is the high overpotentials at the electrodes and oxygen mass transfer at the cathode. The three losses to be considered are activation losses (AL) caused by high overpotential at electrodes, ohmic losses (OL) due to reactor design and the mass transfer losses (ML) due to low oxygen diffusion at cathode. Platinum is the golden standard for catalytic activity due to the rapid rate of oxygen reduction reaction (ORR). The biocathode in this study decreased the activation over potential at the cathode and performed at a rate comparable to platinum. This was confirmed by voltage vs current density graph, where Pt MFC showed a steeper potential drop at lower current densities indicating a higher activation loss compared to the biocathode MFC (Figure 7.4 inset). Similar results were observed by (Rabaey et al., 2008) suggesting that the bacteria act as true catalysts for cathode reduction reaction. The instant start-up time and the high voltage of cathode is limited by the slow onset of anode reaction in this study. The internal resistance of the cell with biocathode MFC was  $680 \pm 32.2 \Omega$  and with platinum it was  $655 \pm 43.1 \Omega$  MFC. The internal resistance depends on several factors such as reactor

design, electrode configurations, type of catalyst etc. The distance between the electrodes is large (~13 cm) in the ‘H’ type reactor used in this study and this accounts for potential losses and high ohmic resistance. (Zhang et al., 2012) developed a novel tubular MFC with graphite brush electrodes (~2-3 cm distance between the electrodes) that produced a low internal resistance of only 30  $\Omega$  with a bioanode and biocathode. Therefore, with improvement in the reactor design the ohmic losses could be considerably reduced. The oxygen diffusion is low in aqueous solutions and the lack of stirring in anode contributes to the mass transfer losses. Due to the presence of biological catalysts at both anode and cathode the rate of electron transfer is compatible with each other. Therefore, biocathode is able to reduce the fuel cell losses and acts as an efficient catalyst in a MFC.

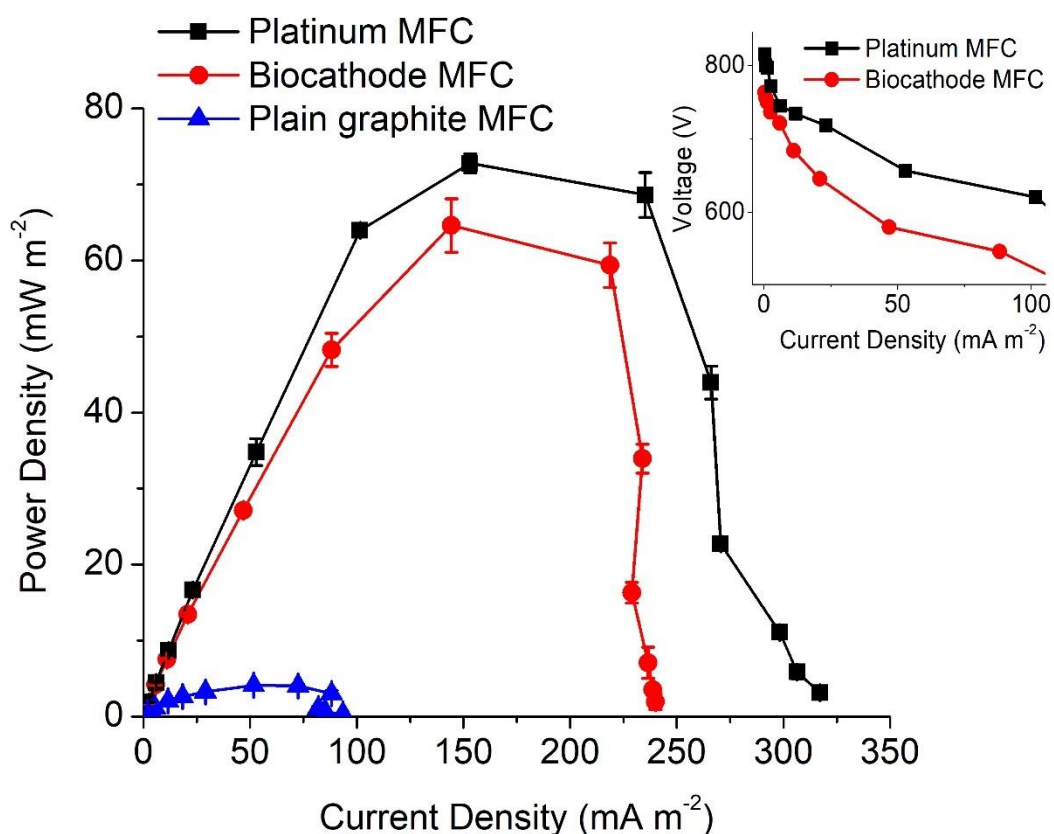


**Figure 7.4:** Maximum power density for each cathode catalysts. Inset: Voltage/current graph for the cathodes indicating the losses.

### 7.3.3 Dye Decolourization

The rate of dye decolourization at the anode of MFC employing different cathode catalysts was assessed by adding 100 mg L<sup>-1</sup> of Acid orange 7 dye in the anode

chamber. As the biofilm was enriched solely without a carbon source, introduction of dye in the cathodic chamber would have drastically shifted the microbial community due to the bacteria switching to the organic dye for its metabolism. The anodic decolourization of AO7 by *S. oneidensis* was observed to be at equivalent rate in both Pt and biocathode based MFC with >95% decolourization being obtained on the 5<sup>th</sup> day (Figure 7.5).

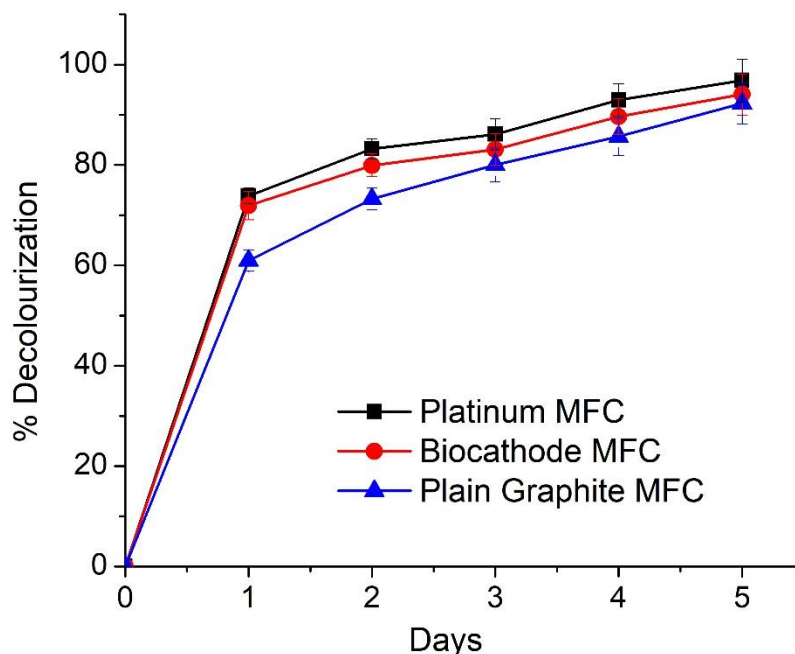


**Figure 7.5:** Anodic dye decolourization in *Shewanella oneidensis* based MFC for different cathode catalysts.

The similar rate of decolourization for all the systems indicate the dye decolourization at the anode is independent of the cathode reaction. The decolourization by the bacteria (*S. oneidensis*) is likely solely dependent on the enzymes and mediators produced during the bacterial metabolism.

### 7.3.4 Microbial community analysis

The microbial community analysis was carried out at the end of the study after the biofilm electrode was tested for its efficiency as cathode catalyst in a MFC. For better understating of the microbial biodiversity, the initial sludge and the biofilms formed were analysed by DGGE and Illumina-Next generation sequencing. The DGGE

analysis produced short partial sequences which could not be further analysed (Appendix 5). Therefore, Illumina NGS was performed on the samples. Four different types of samples were analysed viz. Sludge- Initial sludge used for enrichment, EB- biofilm on the graphite electrode, EW- biofilm on the connecting copper wires and plank- planktonic cells formed on the walls of the enrichment set-up. The 16s region of the whole genome was amplified and subjected to sequencing by synthesis. The amplified tags were then identified based on the DNA match >97% and were clustered as operational taxonomic units (OTU). Sludge had OTUs of 1044 and after enrichment EB had an OTUs of 889, whereas EW and Plank had 930 and 822 respectively (Figure 7.6 inset). These OTUs were compared with SILVA database to identify the consortia of species and annotate each of the samples. The number of observed species in sludge was 1044, which on enrichment decreased to ~765 for EW, less than 710 for EB and 624 for plank (Figure 7.6). These results contradict (Wang et al., 2013) who obtained a higher number of species in planktonic compared to biofilm. The higher number of species near the electrode wire (EW) suggests these bacteria are electrophilic and strive to accept the electrons for their metabolism.

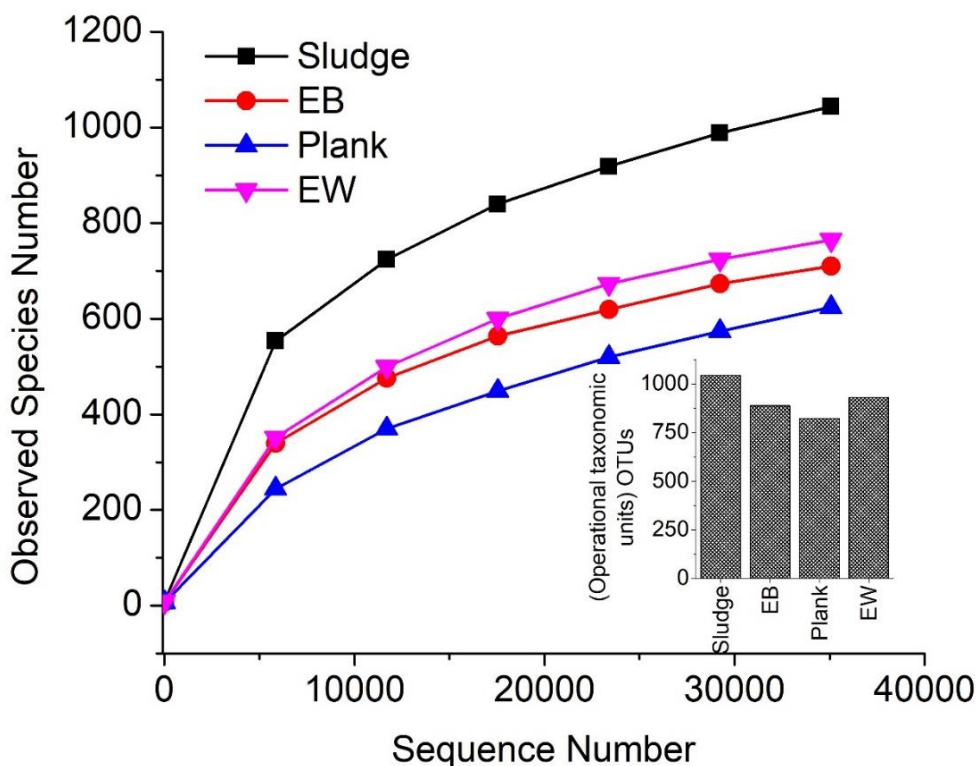


**Figure 7.6:** Observed number of species in each sample. Inset: OTUs obtained from each of the samples.

Shannon index provides an estimate of the diversity and variance among the species population within a sample. A high diversity in the sample is characterized by a higher Shannon index. Sludge had a Shannon index of 6.648, highest among all the samples, indicating a highly diverse population (Figure 7.7). As the sample was obtained from activated sludge tank of a common textile effluent treatment plant, the organisms present will be dominantly aerobic or facultative aerobic Gram-negative organism tolerant to toxic dyes. As these dyes have complex structures a diverse population of organisms might thrive exhibiting synergism, syntrophy, co-metabolism etc. Shannon index was significantly reduced for EB and plank with 5.102 and 4.394 respectively (Figure 7.7). This indicates that the population within the enriched sample belonged to related groups carrying out similar metabolic function. On enrichment chemolithotroph group or similar group of organisms might have been enriched resulting in loss of other species. As these enriched organisms have similar function, the diversity in the samples was reduced.

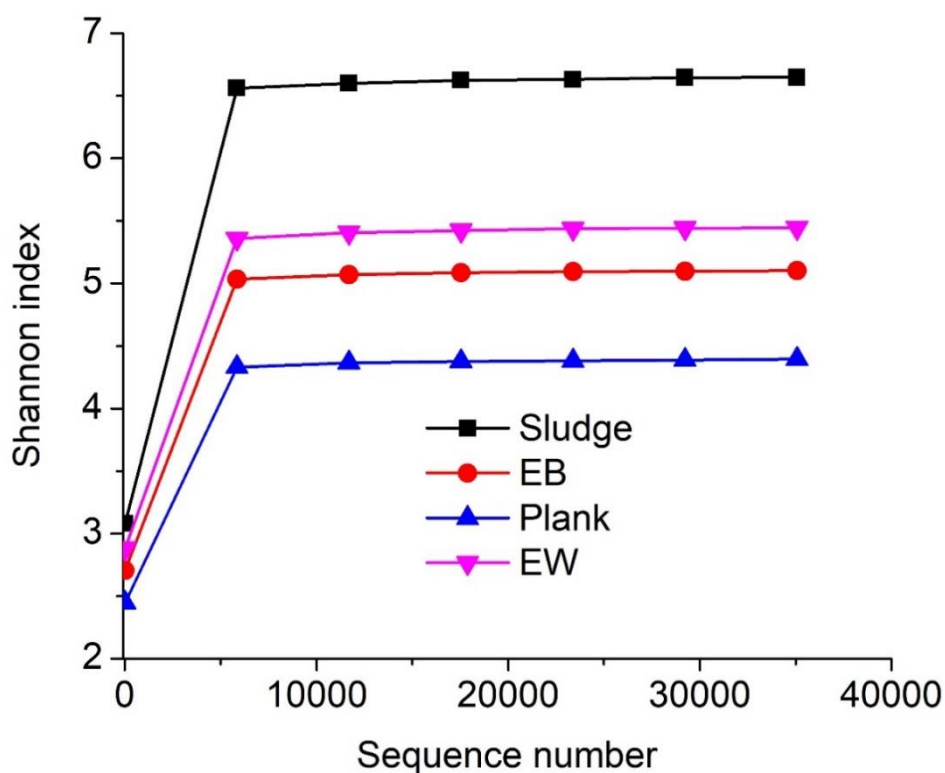


**Figure 7.7:** Shannon index for diversity variance among the species population in each sample

The relationship between various species in different samples were analysed by PCoA based on Unweighted Unifrac similarity. The analysis showed that the EB, EW and plank species were very closely related than those present in the initial sludge inoculum. Further, among the enriched samples, EW and EB share a close resemblance compared to the planktonic species (Figure 7.8).

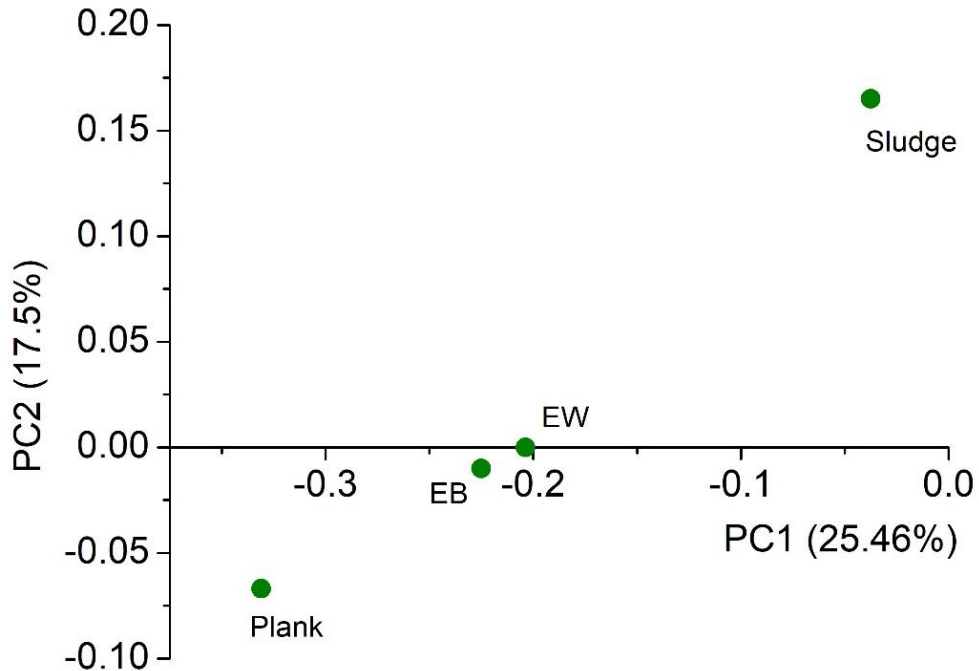


**Figure 7.8:** PCoA analysis of all the samples based on Unweighted Unifrac similarity

The dominant phylum for all the samples were Bacteroidetes, Proteobacteria, Firmicutes, Actinobacteria and Acidobacteria. There was variation in the relative amount of species between sludge and the enriched samples. The sludge sample had the following dominant class  $\alpha$ -Proteobacteria (24%),  $\gamma$ -Proteobacteria (15%) and Sphingobacteriia (12%) of Bacteroidetes phylum. On enrichment  $\alpha$ -Proteobacteria (Plank 32%, EW 31% and EB 29%) was further increased and Sphingobacteriia was replaced with Flavobacteriia as the dominant class in that phylum (Figure 7.9).

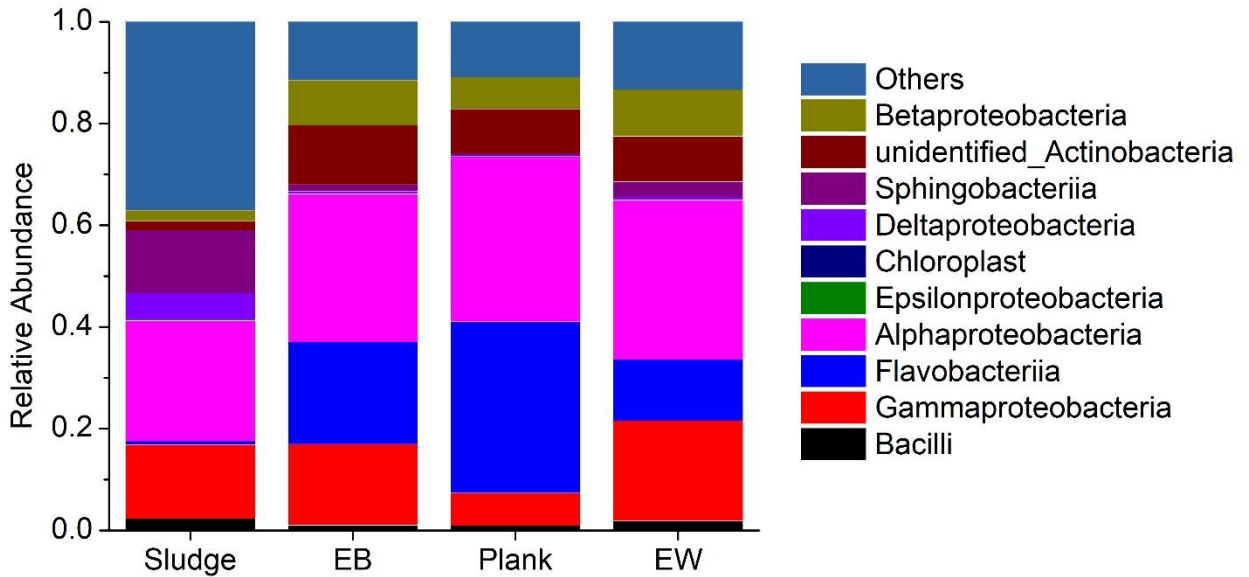


**Figure 7.9:** The relative abundance for the dominant class in each phylum for all samples.

A Ternary plot between the orders of sludge, EB and plank sample show a significant increase in Flavobacteriales (Bacterioidetes) and Rhizobiales ( $\alpha$ -Proteobacteria) in the enriched samples (EB, Plank) which was initially outnumbered by Sphingobacteriales and Rhodospirillales in the same phylum for sludge (Figure 7.10). Sphingomonadales is another order of  $\alpha$ -Proteobacteria that is in high number in the enriched samples. In  $\gamma$ -Proteobacteria phylum, species of Xanthomonadales order increased from 8% in sludge to 12% in EB, while it decreased to 5% in plank. Further among Actinobacteria phylum, order of Cornyebacteriales was specially enriched in EB (11%), plank (8%) and EW (7%) samples (Figure 7.10).

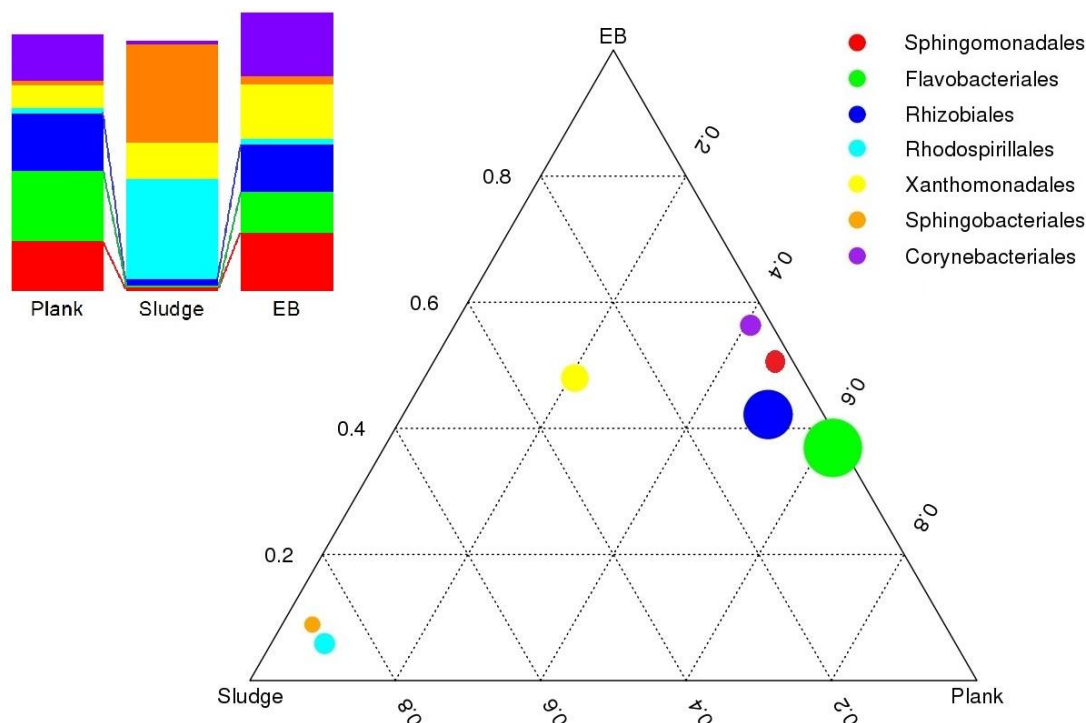


**Figure 7.10:** Ternary plot for the Orders between Sludge, EB and Plank samples

*Rhodospirillaceae* (15%) (Order-Rhodospirillales) the dominant family of Alphaproteobacteria class in sludge drastically diminished after enrichment (EB- 0.3%, Plank- 0.2%) (Figure 7.11). At genus level, *Defluviicoccus* sp. was present in highest number in that family. *Defluviicoccus* sp. exhibits an anaerobic metabolism with the ability of glycogen accumulation (Dai et al., 2007). It is a heterotrophic organism that exhibits sugar metabolism in the presence of glucose, acetate propionate etc. Other species of Rhodospirillales order are known to be phototrophic bacteria that utilise light for their metabolism. As these organisms require organic carbon source or light for their survival, it is possible that they diminished on enrichment under no organic carbon or light environment in this study.

Another dominant order in sludge that decreased on enrichment was Spingobacteriales (12%) which contained (10%) *Lentimicrobiaceae* family (Figure 7.11&7.12). *Lentimicrobiaceae* family consists of species that are found in anaerobic methanogenic high strength starch based wastewater (Sun et al., 2016). Further evidence of enrichment comes from the disappearance of *Ignavibacterium* genus (order-Igvanibacteriales) present in significant number in sludge (Figure 7.11 & 7.12). *Ignavibacterium* genus contains species that are chemoheterotroph, which relies on sugars and amino acid present in the media for metabolism and growth (Liu et al., 2012). Therefore, it can be concluded that the enrichment conditions (no organic

carbon source, no light and presence of oxygen) enhanced the selection of microbial community capable thriving by accepting electrons from the electrode.

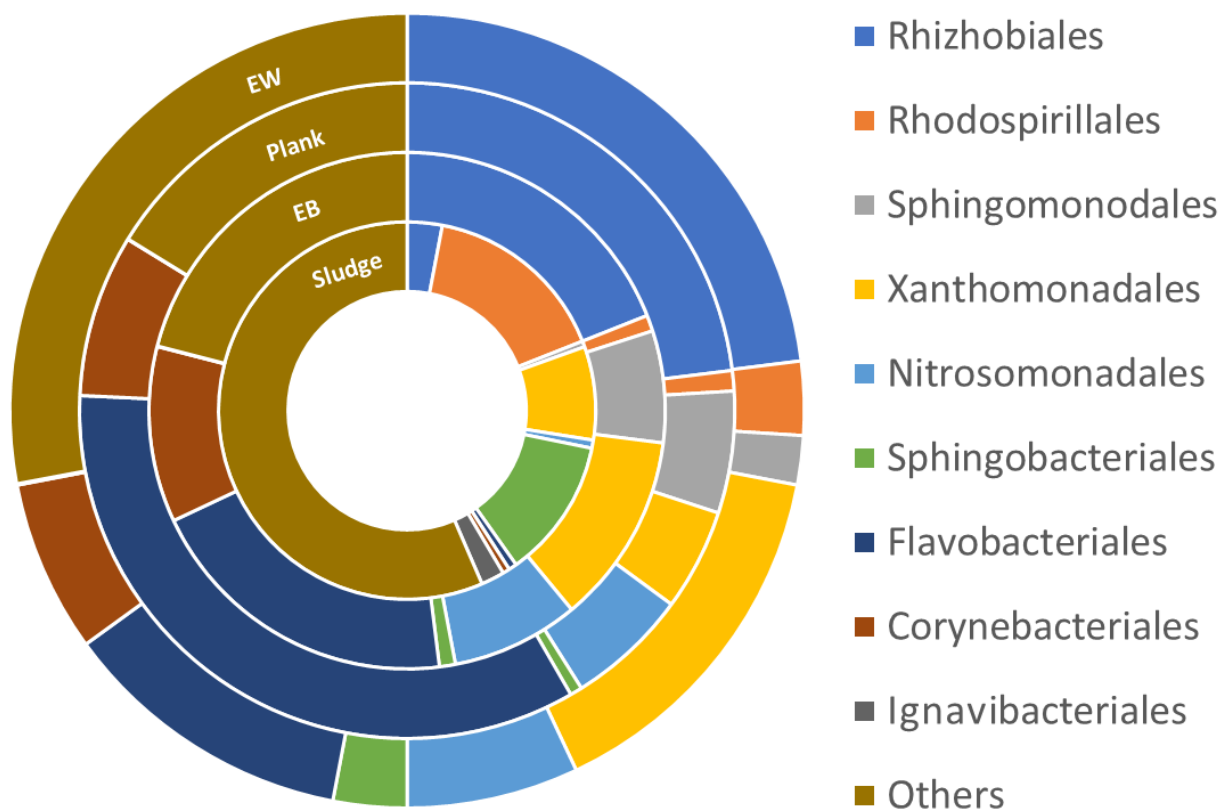


**Figure 7.11:** Representation of microbial orders present in all the samples

On enrichment, species of Flavobacteriales order and *Flavobacteriaceae* family formed the major population among the Bacteroidetes phylum in samples (EB- 20%, Plank-34%, EW- 12%) (Figure 7.11 & 7.12). *Moheibacter* was the dominant genus from the above family. *Moheibacter sediminis*, a species of *Moheibacter* genus, was isolated from river sediment and was found to be catalase and oxidase positive (Zhang et al., 2014). The good performance of biocathode in MFC might be due to the catalase present in the bacteria that decomposes the  $H_2O_2$  produced as a by-product of ORR and protect the bacterial cells from oxidative damage by reactive oxygen species (ROS).

There was increased species of order Rhizobiales (23%-Plank, 19%-EB) and Sphingomonadales (6%-Plank, 7%- EB) in enriched samples, which was initially present in very low amounts in Sludge (3% and 0.5% respectively) (Figure 7.11). The species of order Rhizobiales have been found to be dominant in MFC biocathode (Zhang et al., 2011) which accounts for its higher abundance in enriched samples compared to sludge. *Bradyrhizobiaceae* family (Rhizobiales-Order) are known for nitrogen assimilation and carbon dioxide fixation and hence are chemoautolithotrophs (Figure 7.12). *Rhodopseudomonas palustris* a species of the *Bradyrhizobiaceae* family has been utilized in a microbial fuel cell to produce electricity (Xing et al., 2008). It can fix CO<sub>2</sub> and switch between four modes of metabolism (Larimer et al., 2004). The versatile nature of *Rhodopseudomonas* and its ability to produce electric current makes it an ideal biocathode for MFC applications. *Nitrobacter spp.* of *Bradyrhizobiaceae* family present in the samples is also a known CO<sub>2</sub> fixer. This indicates the presence of dominant autolithotrophs in the enriched samples. Thus, biofilm established has several bacteria that have electrogenic properties and utilise carbon dioxide in the air for their metabolism.

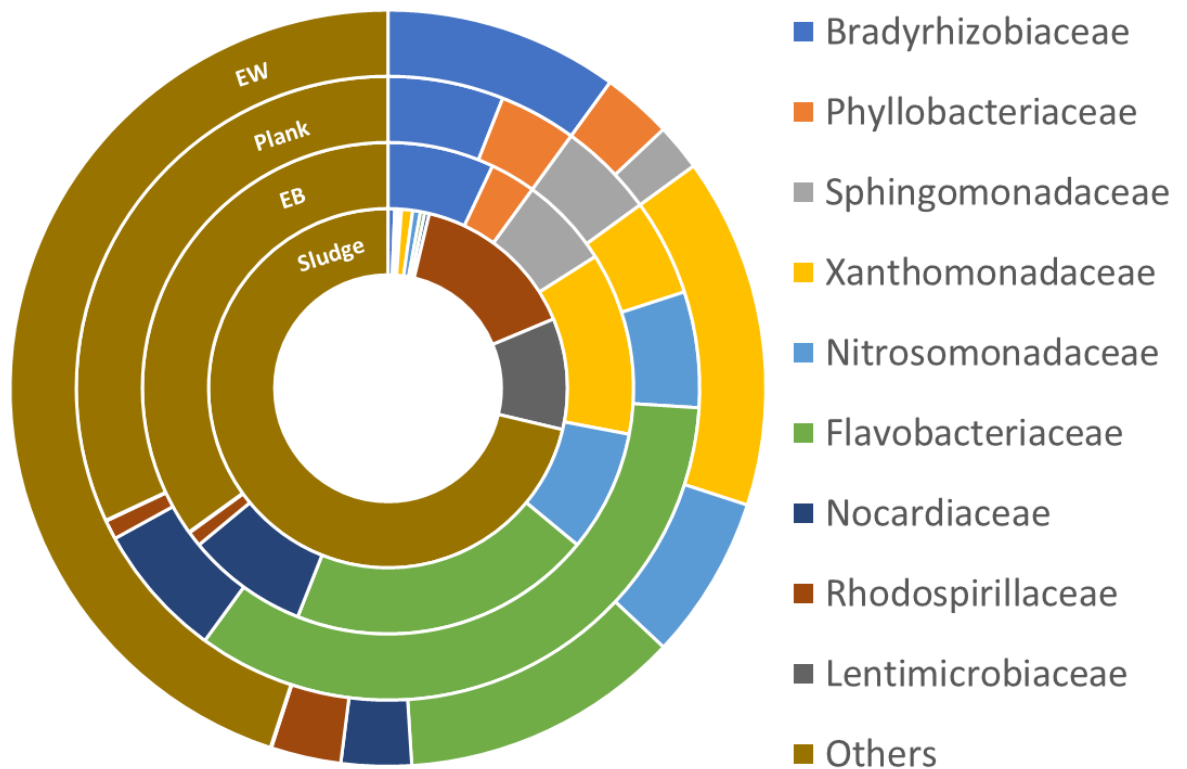


**Figure 7.12:** Representation of microbial families present in all the samples

The dominant species present in their respective families (*Nitrosomonas europaea* from *Nitrosomonadeceae* family; *Sphingobium aminese* from *Sphingomonadaceae* family; *Nitratireductor indicus* from *Phyllobacteriaceae* family and *Gordonia polyisoprenivorans* from *Nocardiaceae* family (Corynebacteriales order)) could be clearly observed on ternary plot between EB, EW and Plank samples (Figure 7.13). *Nitrosomonas europaea* was one of the prominent species that was enriched in all the biofilms, and hence it could be spotted at the centre of the ternary plot (Figure 7.13). *N. europaea* is a chemolithoautotroph, deriving its energy from oxidation of ammonium ions to nitrite (Laanbroek et al., 2002). The source of ammonia could be the ammonium chloride and ammonium sulphate present in the enrichment media. The nitrite produced by this species would have been utilised by *Nitrobacter sp.* as it obtains energy from oxidation of nitrite ions to nitrate ions (Grundmann et al., 2000). *N. europaea* also has the ability to fix CO<sub>2</sub> through Calvin cycle to form sugars that can be utilized by other organisms in the biofilm (Chain et al., 2003). A species from phylum Actinomycetes, namely *Gordonia polyisoprenivorans* was seen to be enriched specifically in EB and plank biofilm. It was first isolated from automobile tyres and is one of the few available latex degrading microbes (Ding et al., 2017). The detailed metabolic pathway for this species is well established and is known to have benzoate degradation pathway where it can metabolize compounds such as amino-benzoate, toluene, chlorobenzene etc (Linos et al., 1999; Hiessl et al., 2012) which are known precursor and intermediates for various dyes. In addition, *G. polyisoprenivorans* converts sugars to extracellular polysaccharides which is responsible for the formation of biofilms (Fusconi et al., 2006). One of the few chemoheterotrophs enriched on biofilms were *Sphingobium aminese*, which was present specifically on EB and plank samples (Figure 7.13). This species is capable of utilizing only organic carbon source for its metabolism. It was isolated from the soil and is known to degrade Nonylphenol an endocrine disrupting compound (Ushiba et al., 2003). The sugars formed by *N. europaea* through Calvin cycle might have acted as the carbon source for *S. aminese*. Only subtle differences were observed between Plank and EB samples. Plank had a higher population of *Mesorhizobium sp.* and *Paracoccus pantotrophus*. *P. pantotrophus* has nitrate reductase which can convert nitrate to nitrite (Sears et al., 2000). In addition, *P. pantotrophus* has the ability to fix CO<sub>2</sub> through ribulose biphosphate pathway (Bardischewsky and Friedrich, 2001). The primary microbe that might be responsible for the cathodic current is *Nitratireductor indicus* through the

process of denitrification. Although it's an enzymatic process, the source of electron for the periplasmic enzyme might be through the cascade between graphite and biofilm. *Nitratireductor indicus* has the ability to degrade crude oil and was isolated from the deep-sea water of the Indian ocean and it reduces nitrate to nitrite (Lai et al., 2011). A dominant genus observed in *Xanthomonadaceae* family was *Luteimonas* that was high in EB (11%) and EW(14%) compared to Plank (4%). Some species of this genus are capable of nitrate reduction to nitrite (Young et al., 2007) (Figure 7.12). The dominance of *Luteimonas* EB and EW indicates that it follows similar mechanism as *Nitratireductor indicus* to contribute to the current produced.

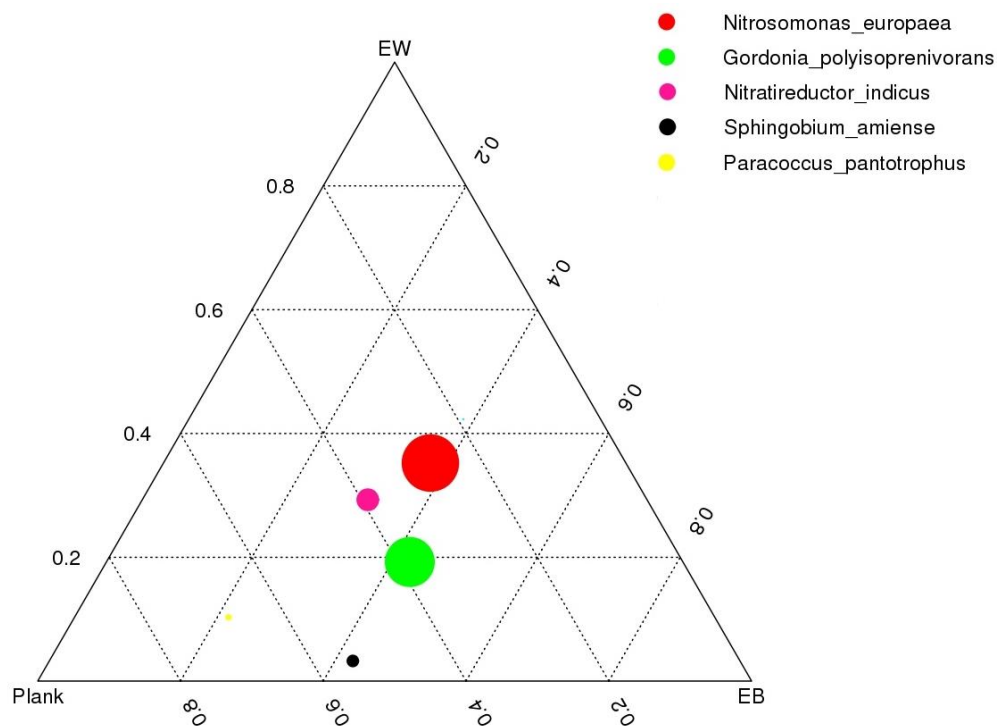


**Figure 7.13:** Ternary plot indicating the dominant species in the enriched samples

*Luteimonas*, the nitrate reducing bacteria is known to utilize organic acids and certain amino acids as the organic substrates. These metabolites are the by-products of other types of bacterial metabolism. Thus, the overall consortia of the microbes established in the biofilm had complementary metabolic roles leading to a formation of chemolithotrophic community. The overall schematic for the enriched biofilm is given below (Figure 7.14).

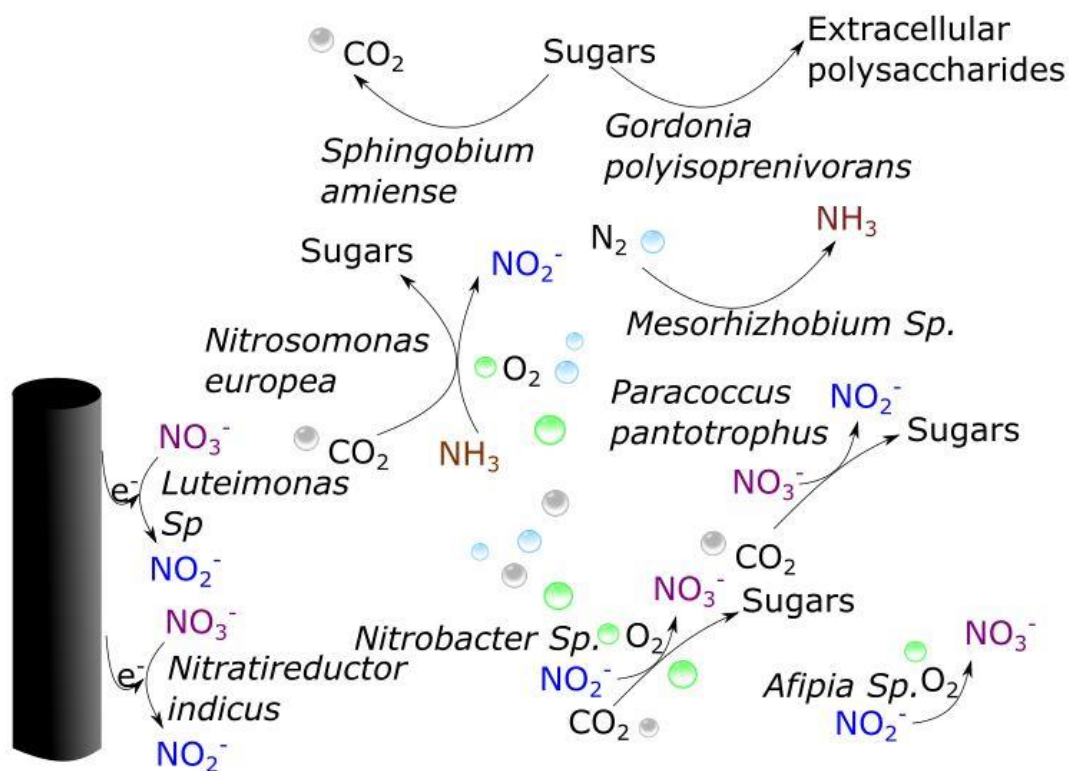


**Figure 7.14:** Schematic representation of metabolic activity between the microbes enriched in the biofilm

Figure 7.14 depicts the metabolic interactions that are vital for maintaining the microbial community. These microbial interactions are widely seen in biofilms and planktonic bacteria. The  $\text{CO}_2$  fixers in the samples fix carbon dioxide to sugars that is utilized by other nitrate reducing species. *Gordonia* sp. utilizes sugars to form extracellular polysaccharides that aids in biofilm formation. The nitrate reducing bacteria accept electrons from the electrode to complete the reduction process at the cathode and produce current. The biofilm reaction is multi-trophic and the current produced in the MFCs is a combination of all bacterial interactions. There was no nitrates or nitrites source present in the media. The presence of ammonium salts in the buffered media enhanced the selection of nitrifying and denitrifying bacteria. Since the enrichment was initiated to select for microbes that carry out ORR at the cathode, no nitrogen gas measurements were carried out to confirm the occurrence of complete denitrification cycle.

Nitrates have been used as terminal electron acceptor at the cathode of MFCs. Biocathodes equipped for reduction of nitrate from wastewater produced a low power density of 9.4 mW m<sup>-2</sup> in a MFC (Lefebvre et al., 2008). In this study, the power output of biocathode (64.6±3.5 mW m<sup>-2</sup>) was comparable to platinum (72.7±1.2 mW m<sup>-2</sup>) and it had lower activation overpotential than platinum. Therefore, it can be concluded that biocathodes utilising alternative terminal electron acceptors (nitrates) together with oxygen could be used to achieve a high-power output at the cathode of MFC.

Several species present in the samples (*Gordonia* sp., *S. aminese*, *Nitratireductor indicus*) are capable of degrading environmental pollutants. The role of the species in nitrate reduction, pollutant removal and power production in a MFC is a perfect combination to develop an ideal MFC for bioremediation applications.

## 7.4 Conclusion

In this study, electroactive bacteria were enriched from textile wastewater for utilising as cathode catalyst in a MFC. The biofilm produced an average peak current of 0.7 mA during the enrichment and produced a maximum power density of 64.6±3.5 mW m<sup>-2</sup> comparable to platinum (72.7±1.2 mW m<sup>-2</sup>) when employed in a MFC. The acclimated biocathode eliminated the start-up lag and decreased the activation over potential at the cathode and performed at a rate comparable to platinum. The voltage vs current density graph revealed a higher activation loss for platinum compared to the biocathode, suggesting that the bacteria act as true cathode catalysts. The microbial community analysis of initial sludge sample and the enriched samples (plank, EB, EW) revealed the selection of chemolithoautotrophic organisms that fix CO<sub>2</sub> for their metabolism. The most dominant order of species was Flavobacteriales (Bacterioidetes) and Rhizhobiales (Alphaproteobacteria) in the enriched samples. A nitrogen cycle micro-environment was observed with the presence of *Nitrosomonas* and *Nitratireductor* species. The metabolic interaction between CO<sub>2</sub> fixers and reduction of nitrate to nitrite contributes to the biofilm formation and current production.

## **Chapter 8**

### **Concluding Remarks**

The aim of the study was to develop enzyme and microbial biocathode systems for efficient ORR and dye decolourization in MFC.

The use of enzyme cathode was expected to be limited by poor stability of the enzymes in the system and environmental factors such as pH, salinity, metal ions etc. In Chapter 3, various ways of mitigating pH changes in the cathode of MFCs and their effect on laccase activity and decolourization of a model azo dye Acid orange 7 in the anode chamber were investigated. Experiments were run with catholyte pH automatically controlled via feedback control, by using acetate buffers (pH 4.5) of various strength (100 mM and 200 mM), with CMI7000 as the cation exchange membrane and Nafion 117 membrane. Results showed that using Nafion 117 membrane limits salinity and pH changes in the cathode (100 mM acetate buffer as catholyte) leading to prolonged laccase activity and faster AO7 decolourization compared to using CMI7000 as a membrane; similarly, automatic pH control in the cathode chamber was found to be better than using higher strength (200 mM) acetate buffer. MFCS with Nafion membrane produced the highest power of 16 mW m<sup>-2</sup>. The results suggested that while pH control in the cathode chamber is important, it does not guarantee sustained laccase activity; that salinity increases affect the activity but could be mitigated using a cation selective membrane such as Nafion.

In view of the above findings, strategies to prolong laccase activity were needed. Therefore, suitable immobilization techniques to maintain the activity and increase longevity of the enzyme were employed (Chapter 4). Laccase was immobilized using three different approaches, i.e. crosslinking with electropolymerized polyaniline (PANI), entrapment in copper alginate beads (Cu-Alg) and encapsulation in Nafion micelles (Nafion), in the absence of redox mediators. These laccase systems were employed in a cathode of MFCs for decolourization of Acid orange 7 (AO7) dye with electrons generated from *Shewanella oneidensis* MR-1 oxidation of pyruvate in the anode chamber. The enzyme in the immobilized states was compared with freely suspended enzyme with respect to dye decolourization at the cathode, enzyme activity retention, power production and reusability. PANI laccase showed the highest stability and activity, producing a power density of 38.2±1.7 mW m<sup>-2</sup> compared to 25.6±2.08 mW m<sup>-2</sup> for Nafion laccase, 14.7±1.04 mW m<sup>-2</sup> for Cu-Alg laccase and 28±1 mW m<sup>-2</sup> for the freely suspended enzyme. There was 81% enzyme activity retained after 1

cycle (5 days) for PANI laccase compared to 69% for Nafion and 61.5% activity for Cu-alginate laccase and 23.4% activity retention for the freely suspended laccase compared to initial activity. The dye decolourization was highest for freely suspended enzyme with over 85% decolourization whereas for PANI it was 75.6%, Nafion 73% and 81% Cu-alginate systems respectively. All the immobilized laccase systems were reusable for more than two cycles. Cost comparisons revealed that on a per pound basis, power production from laccase-based MFCs (0.07 mW/£) was 1.75 times better than those based on platinum (0.04 mW/£).

On establishing laccase potential for catalysing the ORR, it was of interest to compare and understand the mechanism of Acid Orange 7 dye degradation by bacteria (*S. oneidensis*) at the anode and laccase at the cathode (Chapter 5). A comparison of the two approaches was made in this study in which Acid orange 7 dye was loaded in the anode chamber in the presence of *Shewanella oneidensis* species or in cathode chamber in the presence of laccase. The systems were compared in terms of power production, dye decolourization, COD reduction, degradation products and their toxicity. The power density was higher with  $50\pm 4$  mW m<sup>-2</sup> for dye cathode and  $42.5\pm 2.6$  mW m<sup>-2</sup> for dye anode. The decolourization was slower with *Shewanella* species where only 20% decolourization was obtained after 24 h whereas with laccase >80% decolourization was obtained within 24 h of operation. The anode decolourized products were unstable and underwent autooxidation to produce colour. GC-MS analysis revealed simpler compounds such as benzoic acid and hexanoic acid for laccase degradation products, whereas *Shewanella* species produced aromatic amines. The colour formation in autooxidation was due to the presence of quinones produced by oxidation of the aromatic amines. These products were more toxic than anode and cathode products. Therefore, the power and decolourization rate of dye was better for the system with dye in cathode in the presence of laccase enzyme. Thus, the study provided an insight into the different mechanisms and pathways leading to maximal degradation of the azo dyes.

To further enhance the dye decolourization and power production of laccase biocathodes redox mediators were utilised in a subsequent study (Chapter 6). ABTS is the most widely used redox mediator for laccase but synthetic mediators are costly, and they are toxic to the enzymes in the long run. Therefore, natural mediators such as syringaldehyde and acetosyringone were explored for their environmental friendliness

and low-cost. These natural mediators are phenolic compounds that exist in nature and mediate lignin oxidation in white rot fungi. The presence of ABTS and acetosyringone increased the power density from  $54.7 \pm 3.5 \text{ mW m}^{-2}$  (control laccase without mediators) to  $77.2 \pm 4.2 \text{ mW m}^{-2}$  and  $62.5 \pm 3.7 \text{ mW m}^{-2}$  respectively. The power decreased to  $23.2 \pm 2.1 \text{ mW m}^{-2}$  for laccase with syringaldehyde. There was increase in decolourization by 20% with addition of mediators as compared to laccase in absence of mediators. Cyclic voltammetry analysis revealed the redox nature of the mediators by producing oxidation/reduction peaks for acetosyringone and ABTS. Syringaldehyde did not show any redox peaks in their CV. Laccase oxidized syringaldehyde to syringic acid and subsequently to quinones thus making it unavailable as a mediator. Although the power produced was highest for ABTS, dye decolourization could not be studied due to strong colour interference from laccase-ABTS reaction. Therefore, acetosyringone acted as an efficient mediator for laccase aiding in increasing the rate of dye decolourization and power production.

To determine whether microorganisms could be used as cathode catalysts in MFCs, activated sludge from a textile treatment plant was enriched by potentiostatic method for a period of 70 days (Chapter 7). The enrichment conditions were set to eliminate heterotrophic or photoautotrophic growth and select for electroactive bacteria capable of accepting electrons for their respiration only from the cathode. The biofilm formed generated an average current of 0.7 mA during the enrichment. The biofilm was employed in the cathode of MFC with *Shewanella oneidensis* MR1 anode and compared with platinum. The maximum power density obtained was  $72.7 \pm 1.2 \text{ mW m}^{-2}$  for platinum and  $64.6 \pm 3.5 \text{ mW m}^{-2}$  for biocathode. The biocathode in this study decreased the activation over potential at the cathode and performed at a rate comparable to platinum. The activation losses were lower for biocathode compared to platinum. The microbial community analysis of initial sludge sample and the enriched samples (plank, EB, EW) revealed the selection of chemolithoautotrophic organisms that fix  $\text{CO}_2$  for their metabolism. The most dominant order of species was Flavobacteriales (Bacteroidetes) and Rhizobiales (Alphaproteobacteria) in the enriched samples. A nitrogen cycle micro-environment was observed with the presence of *Nitrosomonas* and *Nitratireductor* species. The metabolic interaction between  $\text{CO}_2$  fixers and reduction of nitrate to nitrite contributes to the biofilm formation and current production. From the microorganism selected in this study, it

was observed that the cathode reaction was a combination of nitrate reduction and oxygen reduction reactions. These results prove that biocathodes utilising alternative terminal electron acceptors (nitrates, sulphates) together with oxygen can provide an efficient power output comparable to platinum at the cathode of MFC.

Overall, from the above studies for laccase-based MFCs, acetosyringone mediated laccase produced the highest power density ( $62.5 \pm 3.7 \text{ mW m}^{-2}$ ) together with faster decolourization of Acid Orange 7 dye. The crude laccase used in this study produced comparable power ( $50 \pm 4 \text{ mW m}^{-2}$ ) and dye degradation (98%) to mediated laccase. Microbial biocathode ( $64.6 \pm 3.5 \text{ mW m}^{-2}$ ) was the most efficient cathode catalyst performing at a rate equivalent to platinum ( $72.7 \pm 1.2 \text{ mW m}^{-2}$ ).

## **Chapter 9**

### **Future Work**

From this study it is evident that biocathodes are a suitable alternative to platinum as cathode catalysts. They have an added advantage of dye decolourization together with power production. To develop a more robust model for azo dye degradation using biocathodes further research can be conducted.

## **9.1 Enhancement of power production in microbial biocathode**

In Chapter 7, an aerobic biofilm was enriched that performed equivalent to platinum as cathode catalyst in a MFC. To further enhance the power production, individual species can be isolated from the biofilm and tested for their electrogenic activity. Due to time and equipment constraints we were unable to perform more electrochemical analysis of the biofilm. Cyclic voltammetry (CV) provides information on the kinetics of electron transfer between the electrode and the biofilm. It also helps to determine the reversibility of the reaction, the presence of any redox reaction intermediates and the redox potential of the reaction. Electrochemical impedance spectroscopy (EIS) is used to deduce the resistance between the electrode/biofilm and resistance within the biofilm that will aid in understanding the electron transfer pathway in the microorganisms. These techniques aid in characterizing the biofilm and their electrogenic properties, to further improve the catalytic activity.

A selection of microbial community can be developed by varying the enrichment methods and parameters to develop a biocathode producing higher power than platinum. The method of enrichment can be varied i.e. open or closed circuit MFC enrichment, poised potential in MFC, poised potentiostat (this study) etc. The parameters such as different poised potentials, resistors and electrodes can also be varied to obtain electroactive biofilms. Alternatively, versatile bacteria such as *Rhodospseudomonas palustris* that can switch between four modes of metabolism can be employed at cathode of MFC. It can switch between: photoautotrophic, photoheterotrophic, chemoautotrophic and chemoheterotrophic modes (Larimer et al., 2004). *R. palustris* have been observed to decolourize (reactive red 195 dye) and bring about complete mineralisation of the dye under anaerobic conditions (Çelik et al., 2012). The bacteria has also been used in MFCs for power production (Xing et al., 2008). Therefore, the adaptable nature could be exploited for developing *R. palustris*

based biocathode system for dye decolourization and power production. During the individual species selection, the substrate provided will depend on the inherent metabolic nature of the species. Eg: *P. pantothropus* will be tested in presence of nitrate, *Nitrobacter* in presence of nitrate and *Sphingobium* in presence of sugars.

The dye decolourization in the presence of microorganisms at the cathode of MFCs have been carried out by applying external voltage (Kong et al., 2014; Yang et al., 2016). The dye molecules are large therefore bacteria are unable to degrade them under aerobic conditions. Therefore, the sludge could be enriched in the presence of dye and the number of species capable of dye degradation under aerobic conditions can be isolated. These can be combined with the electrogenic bacteria from biofilm to develop a bioelectrochemical system that can degrade the dye and produce a good power output.

## **9.2 Use of crude laccase extracts in MFC**

The fungal strain *Trametes versicolor* could be utilised to produce crude laccase that can be used in bioreactors. There are two types of fermentation to produce laccase from white rot fungi 1) solid state fermentation (SSF) 2) submerged fermentation. In SSF, the fungi are grown on solid supports that also acts as the carbon source. Under these conditions it mimics the natural growth environment and the production of the enzyme is greatly increased. In SF, a liquid media is used to grow the fungi (Stoilova et al., 2010). In both types of fermentation, the enzyme production is high with the presence of an inducer such as phenol-based products. The use of crude enzyme would reduce the cost, provide better activity and stability due to the presence of natural enzyme stabilizers in the fungal source. As laccase is an extracellular enzyme the crude extracts present in the spent media could be used directly which reduces the cost of purification. In dye decolourization studies the crude extracts of laccase aid in better decolourization due to the synergistic action of manganese peroxide, laccase and other lignolytic enzymes (Sen et al., 2016). The crude extracts have several advantage such as the presence of natural laccase mediators, various metabolites and residual macronutrients that can stabilise the crude enzyme (Zeng et al., 2011).

Crude extracts were not used in this study due to the presence of the above interferents that would hinder true laccase activity studies. Commercial laccase has been utilised to establish various proof of concepts for factors mitigating laccase activity,

immobilization techniques and use of redox mediators. These concepts can be further validated using crude enzyme extracts for dye decolourization and power production in MFCs.

### 9.3 Photosynthetic biocathodes as cathode catalysts

Photosynthetic bacteria are a group of microorganisms that utilise sunlight as a source of energy to produce oxygen through photosynthesis. *Chlorella vulgaris*, one of the fastest growing microalgae has been used in a microbial fuel cell for power generation and in-situ oxygen production. Algae are responsible for producing 72% of the world's oxygen. The use of these organisms at the cathode to produce oxygen in-situ can eliminate the use of mechanical aeration (Zou et al., 2009; Velasquez-Orta et al., 2009; Zhou et al., 2012).

The sequestration of carbon dioxide from anode to cathode chamber to assist the growth of algae in a MFC was studied by (Wang et al., 2010). A microbial carbon capture cell (MCC) was constructed in which CO<sub>2</sub> produced from glucose oxidation at the anode was fed into the cathode for photosynthesis by algae. The peak power density obtained was 4.1 to 5.6 W m<sup>-3</sup> with Pt coated electrodes and 94% of the carbon input was captured by the MCC. (He et al., 2014) have utilised an immobilised (sodium alginate + CaCl<sub>2</sub>) *Chlorella vulgaris* at the cathode in the absence of platinum to treat wastewater and simultaneously produce electricity. Anaerobic sludge with glucose as the substrate was used at the anode and the CO<sub>2</sub> from the anode was fed into the cathode. The maximum power density was 2.57 W m<sup>-3</sup> with COD removal efficiency of 92.1 % and a 14.1% coulombic efficiency.

Algae and cyanobacteria have been previously studied for their decolourization and degradation of azo dyes (Acuner and Dilek, 2004; El-Sheekh et al., 2009). *Chlorella vulgaris*, *Oscillatoria rubescens*, *Elkatohrix viridis* showed > 90% degradation of Basic Fuschin dye. The azo reductase in the algae breaks down the azo bond to form aromatic amines (El-Sheekh et al., 2009). A proposed mechanism of azo degradation pathway by algae in stabilisation ponds by (Jinqi and Houtian, 1992) (Figure 9.1).

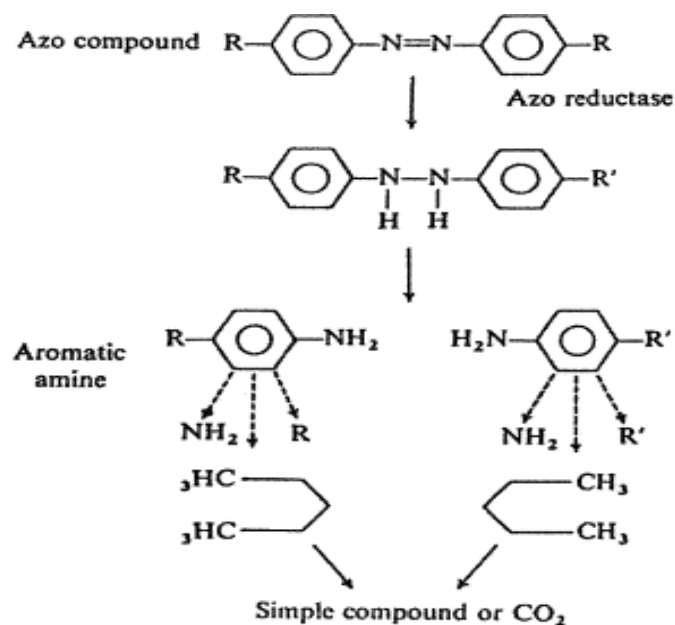


**Figure 9.1 :** Suggested mechanism of of azo dyes degradation by algae (Jinqi and Houtian, 1992).

Considering the power production and the dye degradation capabilities of algae it would be interesting to develop a photosynthetic MFC for dye degradation. These biocathodes would prove as renewable source of energy while operating using natural sunlight.

## References

- Abadulla, E., Tzanov, T., Costa, S., Robra, K.H., Cavaco-Paulo, A. and Gübitz, G.M. (2000) Decolorization and detoxification of textile dyes with a laccase from *Trametes hirsuta*. *Applied and environmental microbiology*. 66 (8), 3357–62.
- Abrahart, E.N. (1977) *Dyes and Their Intermediates*. New York, Chemical Publishing, 1–12.
- Ackermann, Y., Guschin, D.A., Eckhard, K., Shleev, S. and Schuhmann, W. (2010) Design of a bioelectrocatalytic electrode interface for oxygen reduction in biofuel cells based on a specifically adapted Os-complex containing redox polymer with entrapped *Trametes hirsuta* laccase. *Electrochemistry Communications*. 12 (5), 640–643.
- Acuner, E. and Dilek, F.B. (2004) Treatment of tectilon yellow 2G by *Chlorella vulgaris*. *Process Biochemistry*. 39 (5), 623–631.
- Aeschbacher, M., Sander, M. and Schwarzenbach, R.P. (2010) Novel Electrochemical Approach to Assess the Redox Properties of Humic Substances. *Environmental Science & Technology*. 44 (1), 87–93.
- Ahn, M.-Y., Zimmerman, A.R., Martínez, C.E., Archibald, D.D., Bollag, J.-M. and Dec, J. (2007) Characteristics of *Trametes villosa* laccase adsorbed on aluminum hydroxide. *Enzyme and Microbial Technology*. 41 (1–2), 141–148.
- Akertek, E. and Tarhan, L. (1995) Characterization of immobilized catalases and their application in pasteurization of milk with H<sub>2</sub>O<sub>2</sub>. *Applied Biochemistry and Biotechnology*. 50 (3), 291–303.
- Aljamali, N.M. (2015) Review in Azo Compounds and its Biological Activity. *Biochemistry & Analytical Biochemistry*. 04 (02), 169.
- Allen, R.L.M. (1971) *Colour Chemistry*. Springer US, 1-336.
- An, J., Jeon, H., Lee, J. and Chang, I.S. (2011) Bifunctional Silver Nanoparticle Cathode in Microbial Fuel Cells for Microbial Growth Inhibition with Comparable Oxygen Reduction Reaction Activity. *Environmental Science &*

*Technology*. 45 (12), 5441–5446.

- Anjaneyulu, Y., Sreedhara Chary, N. and Samuel Suman Raj, D. (2005) Decolourization of Industrial Effluents -- Available Methods and Emerging Technologies -- A Review. *Reviews in Environmental Science and Bio/Technology*. 4 (4), 245–273.
- de Aragao Umbuzeiro, G., Freeman, H.S., Warren, S.H., de Oliveira, D.P., Terao, Y., Watanabe, T. and Claxton, L.D. (2005) The contribution of azo dyes to the mutagenic activity of the Cristais River. *Chemosphere*. 60 (1), 55–64.
- Atteke, C., MOUNGUENGUI, S., SAHA TCHINDA, J.-B., NDIKONTAR, M.K., IBRAHIM, B., GELHAYE, E. and GELHAYE, E. (2013) Biodegradation of Reactive Blue 4 and Orange G by *Pycnoporus sanguineus* Strain Isolated in Gabon. *J Bioremed Biodeg*. 4 (206), 2155–6.199.
- Bagewadi, Z.K., Mulla, S.I. and Ninnekar, H.Z. (2017) Purification and immobilization of laccase from *Trichoderma harzianum* strain HZN10 and its application in dye decolorization. *Journal of Genetic Engineering and Biotechnology*. 15 (1), 139–150.
- Baker, C.J., Mock, N.M., Whitaker, B.D., Hammond, R.W., Nemchinov, L., Roberts, D.P. and Aver'yanov, A.A. (2014) Characterization of apoplast phenolics: Invitro oxidation of acetosyringone results in a rapid and prolonged increase in the redox potential. *Physiological and Molecular Plant Pathology*. 8657–63.
- Bakhshian, S., Kariminia, H.-R. and Roshandel, R. (2011) Bioelectricity generation enhancement in a dual chamber microbial fuel cell under cathodic enzyme catalyzed dye decolorization. *Bioresource Technology*. 102 (12), 6761–6765.
- Bardischewsky, F. and Friedrich, C.G. (2001) The shxVW locus is essential for oxidation of inorganic sulfur and molecular hydrogen by *Paracoccus pantotrophus* GB17: A novel function for lithotrophy. *FEMS Microbiology Letters*. 202 (2), 215–220.
- Barragán, B.E., Costa, C. and Carmen Márquez, M. (2007) Biodegradation of azo dyes by bacteria inoculated on solid media. *Dyes and Pigments*. 75 (1), 73–81.

- Bélanger, J.M.R., Jocelyn Paré, J.R. and Sigouin, M. (1997) 'Chapter 2 High performance liquid chromatography (HPLC): Principles and applications', in J.M.R. Bélanger J.R.J. Paré (ed.) *Techniques and Instrumentation in Analytical Chemistry*. [Online]. Elsevier. pp. 37–59.
- Blánquez, A., Rodríguez, J., Brissos, V., Mendes, S., Martins, L.O., Ball, A.S., Arias, M.E. and Hernández, M. (2018) Decolorization and detoxification of textile dyes using a versatile *Streptomyces* laccase-natural mediator system. *Saudi Journal of Biological Sciences* (In Press).
- Blauenburg, B., Metsä-Ketelä, M. and Klika, K.D. (2012) Formation of 5-Hydroxy-3-methoxy-1,4-naphthoquinone and 8-Hydroxy-4-methoxy-1,2-naphthoquinone from Juglone. *ISRN Organic Chemistry*.1–7.
- Blázquez, E., Gabriel, D., Baeza, J.A. and Guisasola, A. (2017) Evaluation of key parameters on simultaneous sulfate reduction and sulfide oxidation in an autotrophic biocathode. *Water Research*. 301–310.
- Blumel, S., Busse, H.J., Stolz, A. and Kampfer, P. (2001) *Xenophilus azovorans* gen. nov., sp. nov., a soil bacterium that is able to degrade azo dyes of the Orange II type. *International Journal of Systematic and Evolutionary Microbiology*. 51 (5), 1831–1837.
- Bokulich, N.A., Subramanian, S., Faith, J.J., Gevers, D., Gordon, J.I., Knight, R., Mills, D.A. and Caporaso, J.G. (2013) Quality-filtering vastly improves diversity estimates from Illumina amplicon sequencing. *Nature methods*. 10 (1), 57–9.
- Bollella, P., Fusco, G., Stevar, D., Gorton, L., Ludwig, R., Ma, S., Boer, H., Koivula, A., Tortolini, C., Favero, G., Antiochia, R. and Mazzei, F. (2018) A Glucose/Oxygen Enzymatic Fuel Cell based on Gold Nanoparticles modified Graphene Screen-Printed Electrode. Proof-of-Concept in Human Saliva. *Sensors and Actuators B: Chemical*. 256, 921–930.
- Bond, D.R., Strycharz-Glaven, S.M., Tender, L.M. and Torres, C.I. (2012) On Electron Transport through *Geobacter* Biofilms. *ChemSusChem*. 5 (6), 1099–1105.

- Bourbonnais, R., Leech, D. and Paice, M. (1998) Electrochemical analysis of the interactions of laccase mediators with lignin model compounds. *Biochimica et Biophysica Acta*. 1379381–390.
- Bourbonnais, R. and Paice, M.G. (1990) Oxidation of non-phenolic substrates. *FEBS Letters*. 267 (1), 99–102.
- Brigé, A., Motte, B., Borloo, J., Buyschaert, G., Devreese, B. and Van Beeumen, J.J. (2008) Bacterial decolorization of textile dyes is an extracellular process requiring a multicomponent electron transfer pathway. *Microbial biotechnology*. 1 (1), 40–52.
- Brüschweiler, B.J. and Merlot, C. (2017) Azo dyes in clothing textiles can be cleaved into a series of mutagenic aromatic amines which are not regulated yet. *Regulatory Toxicology and Pharmacology*. 88, 214–226.
- Cai, P.J., Xiao, X., He, Y.R., Li, W.W., Chu, J., Wu, C., He, M.X., Zhang, Z., Sheng, G.P., Lam, M.H.W., Xu, F. and Yu, H.Q. (2012) Anaerobic biodecolorization mechanism of methyl orange by *Shewanella oneidensis* MR-1. *Applied Microbiology and Biotechnology*. 93 (4), 1769–1776.
- Call, H.P. and Mücke, I. (1997) History, Overview and Application of mediated lignolytic systems, especially lacasse-mediator-systems (Lignozyme®-process). *Journal of Biotechnol.* 53, 163–202.
- Camarero, S., Ibarra, D., Martinez, M.J. and Martinez, A.T. (2005) Lignin-Derived Compounds as Efficient Laccase Mediators for Decolorization of Different Types of Recalcitrant Dyes. *Appl. Environ. Microbiol.* 71 (4), 1775–1784.
- Cañas, A.I. and Camarero, S. (2010) Laccases and their natural mediators: Biotechnological tools for sustainable eco-friendly processes. *Biotechnology Advances*. 28 (6), 694–705.
- von Canstein, H., Ogawa, J., Shimizu, S. and Lloyd, J.R. (2008) Secretion of flavins by *Shewanella* species and their role in extracellular electron transfer. *Applied and environmental microbiology*. 74 (3), 615–23.
- Cao, Y., Hu, Y., Sun, J. and Hou, B. (2010) Explore various co-substrates for simultaneous electricity generation and Congo red degradation in air-cathode

single-chamber microbial fuel cell. *Bioelectrochemistry*. 79 (1), 71–76.

Caporaso, J.G., Kuczynski, J., Stombaugh, J., Bittinger, K., Bushman, F.D., Costello, E.K., Fierer, N., Peña, A.G., Goodrich, J.K., Gordon, J.I., Huttley, G.A., Kelley, S.T., Knights, D., Koenig, J.E., Ley, R.E., Lozupone, C.A., McDonald, D., Muegge, B.D., Pirrung, M., Reeder, J., Sevinsky, J.R., Turnbaugh, P.J., Walters, W.A., Widmann, J., Yatsunenko, T., Zaneveld, J. and Knight, R. (2010) QIIME allows analysis of high-throughput community sequencing data. *Nature methods*. 7 (5), 335–6.

Carvalho, M.C., Pereira, C., Gonçalves, I.C., Pinheiro, H.M., Santos, A.R., Lopes, A. and Ferra, M.I. (2008) Assessment of the biodegradability of a monosulfonated azo dye and aromatic amines. *International Biodeterioration & Biodegradation*. 62 (2), 96–103.

Casas, N., Parella, T., Vicent, T., Caminal, G. and Sarrà, M. (2009) Metabolites from the biodegradation of triphenylmethane dyes by *Trametes versicolor* or laccase. *Chemosphere*. 75 (10), 1344–1349.

Casieri, L., Varese, G.C., Anastasi, A., Prigione, V., Svobodová, K., Filippello Marchisio, V. and Novotný, Č. (2008) Decolorization and detoxication of reactive industrial dyes by immobilized fungi *Trametes pubescens* and *Pleurotus ostreatus*. *Folia Microbiologica*. 53 (1), 44–52.

Çelik, L., Öztürk, A. and Abdullah, M.I. (2012) Biodegradation of reactive red 195 azo dye by the bacterium *Rhodopseudomonas palustris* 51ATA. *African Journal of Microbiology Research*. 6 (1), 120–126.

Chain, P., Lamerdin, J., Larimer, F., Regala, W., Lao, V., Land, M., Hauser, L., Alan, H., Klotz, M., Norton, J., Sayavedra-Soto, L., Arciero, D., Hommes, N., Whittaker, M. and and Arp, D. (2003) Complete Genome Sequence of the Ammonia-Oxidizing Bacterium and Obligate Chemolithoautotroph *Nitrosomonas europaea* Complete Genome Sequence of the Ammonia-Oxidizing Bacterium and Obligate Chemolithoautotroph *Nitrosomonas europaea* †. *Journal of Bacteriology*. 185 (9), 2759–2773.

Chakraborty, J.N. (2011) '13 – Metal-complex dyes', in *Handbook of Textile and Industrial Dyeing*. [Online]. pp. 446–465.

- Chen, M., Wang, L., Tan, T., Luo, X.C., Zheng, Z., Yin, R.C., Su, J.H. and Du, J.F. (2017) Radical mechanism of laccase-catalyzed catechol ring-opening. *Wuli Huaxue Xuebao/ Acta Physico - Chimica Sinica*. 33 (3), 620–626.
- Cheng, S., Liu, H. and Logan, B.E. (2006) Power densities using different cathode catalysts (Pt and CoTMPP) and polymer binders (Nafion and PTFE) in single chamber microbial fuel cells. *Environmental Science and Technology*. 40 (1), 364–369.
- Chhabra, M., Mishra, S. and Sreekrishnan, T.R. (2015) Immobilized laccase mediated dye decolorization and transformation pathway of azo dye acid red 27. *Journal of environmental health science & engineering*. 1–9.
- Chivukula, M. and Renganathan, V. (1995) Phenolic Azo Dye Oxidation by Laccase from *Pyricularia oryzae*. *Applied and environmental microbiology*. 61 (12), 4374–7.
- Christopher, L.P., Yao, B. and Ji, Y. (2014) Lignin Biodegradation with Laccase-Mediator Systems. *Frontiers in Energy Research*. 212.
- Chung, K.T. and Cerniglia, C.E. (1992) Mutagenicity of azo dyes: Structure-activity relationships. *Mutation Research/Reviews in Genetic Toxicology*. 277 (3), 201–220.
- Clark, M. (2011) *Principles, processes and types of dyes*. Woodhead Pub.
- Clauwaert, P., Van Der Ha, D., Boon, N., Verbeken, K., Verhaege, M., Rabaey, K. and Verstraete, W. (2007) Open air biocathode enables effective electricity generation with microbial fuel cells. *Environmental Science and Technology*. 41 (21), 7564–7569.
- Cohen, B. (1931) The Bacteria Culture as an Electrical Half-Cell. *Journal of Bacteriology*. 21, 18–19.
- Cooney, M.J., Svoboda, V., Lau, C., Martin, G. and Minteer, S.D. (2008) Enzyme catalysed biofuel cells. *Energy & Environmental Science*. 1 (3), 320.
- Couto, S.R. and Toca-herrera, J.L. (2006) Lacasses in the textile industry. *Biotechnology and Molecular Biology Review*. 1 (December), 115–120.

- Crestini, C. and Argyropoulos, D.S. (1998) The early oxidative biodegradation steps of residual kraft lignin models with laccase. *Bioorganic & Medicinal Chemistry*. 6 (11), 2161–2169.
- Crini, G. (2006) Non-conventional low-cost adsorbents for dye removal: A review. *Bioresource Technology*. 97 (9), 1061–1085.
- Daâssi, D., Rodríguez-Couto, S., Nasri, M. and Mechichi, T. (2014) Biodegradation of textile dyes by immobilized laccase from *Coriolopsis gallica* into Ca-alginate beads. *International Biodeterioration and Biodegradation*. 90, 71–78.
- Daâssi, D., Zouari-Mechichi, H., Frikha, F., Martinez, M.J., Nasri, M. and Mechichi, T. (2013) Decolorization of the azo dye Acid Orange 51 by laccase produced in solid culture of a newly isolated *Trametes trogii* strain. *3 Biotech*. 3 (2), 115–125.
- Dai, Y., Yao, J., Song, Y., Liu, X., Wang, S. and Yuan, Y. (2016) Enhanced performance of immobilized laccase in electrospun fibrous membranes by carbon nanotubes modification and its application for bisphenol A removal from water. *Journal of Hazardous Materials*. 317, 485–493.
- Dai, Y., Yuan, Z., Wang, X., Oehmen, A. and Keller, J. (2007) Anaerobic metabolism of *Defluviococcus vanus* related glycogen accumulating organisms (GAOs) with acetate and propionate as carbon sources. *Water Research*. 41, 1885–1896.
- Datta, S., Christena, L.R. and Rajaram, Y.R.S. (2013) Enzyme immobilization: an overview on techniques and support materials. *3 Biotech*. 3 (1), 1–9.
- Davis, S. and Burns, R. (1992) Covalent immobilization of laccase on activated carbon for phenolic effluent treatment. *Applied Microbiology and Biotechnology*. 37 (4), 474–479.
- DeSantis, T.Z., Hugenholtz, P., Larsen, N., Rojas, M., Brodie, E.L., Keller, K., Huber, T., Dalevi, D., Hu, P. and Andersen, G.L. (2006) Greengenes, a chimera-checked 16S rRNA gene database and workbench compatible with ARB. *Applied and environmental microbiology*. 72 (7), 5069–72.
- Ding, X., Yu, Y., Chen, M., Wang, C., Kang, Y., Li, H. and Lou, J. (2017)

- Bacteremia due to *Gordonia polyisoprenivorans*: Case report and review of literature. *BMC Infectious Diseases*. 17 (1), 1–4.
- Diniz, P.E., Lopes, A.T., Lino, A.R. and Serralheiro, M.L. (2002) Anaerobic reduction of a sulfonated azo dye, Congo Red, by sulfate-reducing bacteria. *Applied biochemistry and biotechnology*. 97 (3), 147–63.
- Du, Y., Feng, Y., Dong, Y., Qu, Y., Liu, J., Zhou, X. and Ren, N. (2014) Coupling interaction of cathodic reduction and microbial metabolism in aerobic biocathode of microbial fuel cell. *RSC Adv*. 4 (65), 34, 350–355.
- Durand, F., Gounel, S., Kjaergaard, C.H., Solomon, E.I. and Mano, N. (2012) Bilirubin oxidase from *Magnaporthe oryzae*: an attractive new enzyme for biotechnological applications. *Applied microbiology and biotechnology*. 96 (6), 14, 89–98.
- Lambert, E.N., Seaforth, C. E., and Ahmad, N. (1971) The Occurrence of 2-Methoxy-1,4-Naphthoquinone in Caribbean Vertisols. *Soil Science Society Of America*. 35 (1), 7–8.
- Edgar, R.C. (2004) MUSCLE: multiple sequence alignment with high accuracy and high throughput. *Nucleic Acids Research*. 32 (5), 1792–1797.
- Edgar, R.C. (2013) UPARSE: highly accurate OTU sequences from microbial amplicon reads. *Nature Methods*. 10 (10), 996–998.
- Edgar, R.C., Haas, B.J., Clemente, J.C., Quince, C. and Knight, R. (2011) UCHIME improves sensitivity and speed of chimera detection. *Bioinformatics (Oxford, England)*. 27 (16), 2194–200.
- Eggert, C., Temp, U. and Eriksson, K.L. (1996) The Ligninolytic System of the White Rot Fungus *Pycnoporus cinnabarinus* : Purification and Characterization of the Laccase. *Appl. Environ. Microbiol.* 62 (4), 1151–1158.
- El-Sheekh, M.M., Gharieb, M.M. and Abou-El-Souod, G.W. (2009) Biodegradation of dyes by some green algae and cyanobacteria. *International Biodeterioration & Biodegradation*. 63 (6), 699–704.
- Erable, B., Feron, D. and Bergel, A. (2012) Microbial Catalysis of the Oxygen Reduction Reaction for Microbial Fuel Cells : A Review. *ChemSusChem*. 5,

975–987.

- Falade, A.O., Nwodo, U.U., Iweriebor, B.C., Green, E., Mabinya, L. V and Okoh, A.I. (2017) Lignin peroxidase functionalities and prospective applications. *MicrobiologyOpen*. 6 (1), 1-14 .
- Feng, Y., Wang, X., Logan, B.E. and Lee, H. (2008) Brewery wastewater treatment using air-cathode microbial fuel cells. *Applied Microbiology and Biotechnology*. 78 (5), 873–880.
- Fernández, J.L.M. (2011) Laccases from new fungal sources and some promising applications. PhD thesis, Lund University, Sweden.
- Fernando, E. (2014) Treatment of azo dyes in industrial wastewater using microbial fuel cells. PhD thesis, University of Westminster, UK.
- Fernando, E., Keshavarz, T. and Kyazze, G. (2014) Complete degradation of the azo dye Acid Orange-7 and bioelectricity generation in an integrated microbial fuel cell, aerobic two-stage bioreactor system in continuous flow mode at ambient temperature. *Bioresource technology*. 156, 155–162.
- Fernando, E., Keshavarz, T. and Kyazze, G. (2012) Enhanced bio-decolourisation of acid orange 7 by *Shewanella oneidensis* through co-metabolism in a microbial fuel cell. *International Biodeterioration & Biodegradation*. 72, 1–9.
- Fokina, O., Eipper, J., Winandy, L., Kerzenmacher, S. and Fischer, R. (2015) Improving the performance of a biofuel cell cathode with laccase-containing culture supernatant from *Pycnoporus sanguineus*. *Bioresource Technology*. 175, 445–453.
- Forootanfar, H., Moezzi, A., Aghaie-Khozani, M., Mahmoudjanlou, Y., Ameri, A., Niknejad, F. and Faramarzi, M.A. (2012) Synthetic dye decolorization by three sources of fungal laccase. *Iranian journal of environmental health science & engineering*. 9 (1), 27.
- Fusconi, R., Leal Godinho, M.J., Cruz Hernández, I.L. and Segnini Bossolan, N.R. (2006) *Gordonia polyisoprenivorans* from groundwater contaminated with landfill leachate in a subtropical area: Characterization of the isolate and exopolysaccharide production. *Brazilian Journal of Microbiology*. 37 (2), 168–

- Gahlout, M., Rudakiya, D.M., Gupte, S. and Gupte, A. (2017) Laccase-conjugated amino-functionalized nanosilica for efficient degradation of Reactive Violet 1 dye. *International Nano Letters*. 7 (3), 195–208.
- Galhaup, C. and Haltrich, D. (2001) Enhanced formation of laccase activity by the white-rot fungus *Trametes pubescens* in the presence of copper. *Applied Microbiology and Biotechnology*. 56 (1–2), 225–232.
- Garibyan, L. and Avashia, N. (2013) Polymerase chain reaction. *The Journal of investigative dermatology*. 133 (3), 1–4.
- Gellett, W., Schumacher, J., Kesmez, M., Le, D. and Minteer, S.D. (2010) High Current Density Air-Breathing Laccase Biocathode. *Journal of The Electrochemical Society*. 157 (4), B557.
- Giménez, J., Curcó, D. and Marco, P. (1997) Reactor modelling in the photocatalytic oxidation of wastewater. *Water Science and Technology*. 35 (4), 207–213.
- Glaze, W.H., Kang, J.-W. and Chapin, D.H. (1987) The Chemistry of Water Treatment Processes Involving Ozone, Hydrogen Peroxide and Ultraviolet Radiation. *Ozone: Science & Engineering*. 9 (4), 335–352.
- Le Goff, A., Holzinger, M. and Cosnier, S. (2015) Recent progress in oxygen-reducing laccase biocathodes for enzymatic biofuel cells. *Cellular and Molecular Life Sciences*. 72 (5), 941–952.
- Gogate, P.R. and Pandit, A.B. (2004) A review of imperative technologies for wastewater treatment II: hybrid methods. *Advances in Environmental Research*. 8 (3), 553–597.
- Golob, V., Vinder, A. and Simonič, M. (2005) Efficiency of the coagulation/flocculation method for the treatment of dyebath effluents. *Dyes and Pigments*. 67 (2), 93–97.
- Gomaa, O.M., Fapetu, S., Kyazze, G. and Keshavarz, T. (2017) The role of riboflavin in decolourisation of Congo red and bioelectricity production using *Shewanella oneidensis*-MR1 under MFC and non-MFC conditions. *World Journal of Microbiology and Biotechnology*. 33 (3), 56.

- Gomaa, O.M., Linz, J.E. and Reddy, C.A. (2008) Decolorization of Victoria blue by the white rot fungus, *Phanerochaete chrysosporium*. *World Journal of Microbiology and Biotechnology*. 24 (10), 2349–2356.
- Gong, X.-B., You, S.-J., Wang, X.-H., Zhang, J.-N., Gan, Y. and Ren, N.-Q. (2014) A novel stainless steel mesh/cobalt oxide hybrid electrode for efficient catalysis of oxygen reduction in a microbial fuel cell. *Biosensors and Bioelectronics*. 55, 237–241.
- Gorby, Y.A., Yanina, S., McLean, J.S., Rosso, K.M., Moyles, D., Dohnalkova, A., Beveridge, T.J., Chang, I.S., Kim, B.H., Kim, K.S., Culley, D.E., Reed, S.B., Romine, M.F., Saffarini, D.A., Hill, E.A., Shi, L., Elias, D.A., Kennedy, D.W., Pinchuk, G., Watanabe, K., Ishii, S., Logan, B., Nealson, K.H. and Fredrickson, J.K. (2006) Electrically conductive bacterial nanowires produced by *Shewanella oneidensis* strain MR-1 and other microorganisms. *Proceedings of the National Academy of Sciences of the United States of America*. 103 (30), 11358–11363.
- Gouterman, M. (1978) *Optical spectra and electronic structure of porphyrins and related rings*. In Dolphin, D. (ed.) *The porphyrins*. Vol. III, New York, Academic Press, 1–165.
- Grundmann, G.L., Neyra, M. and Normand, P. (2000) High-resolution phylogenetic analysis of NO<sub>2</sub>--oxidizing Nitrobacter species using the rrs-rrl IGS sequence and rrl genes. *International Journal of Systematic and Evolutionary Microbiology*. 50 (5), 1893–1898.
- Guisan J M (2006) *Immobilization of Enzymes and Cells*. Methods in Biotechnology™. Jose M. Guisan (ed.). Vol. 22. Totowa, NJ: Humana Press.
- Gulrajani, M.L. (2011) '10 – Disperse dyes', in *Handbook of Textile and Industrial Dyeing*. [Online]. pp. 365–394.
- Gutiérrez-Sánchez, C., Jia, W., Beyl, Y., Pita, M., Schuhmann, W., De Lacey, A.L. and Stoica, L. (2012) Enhanced direct electron transfer between laccase and hierarchical carbon microfibers/carbon nanotubes composite electrodes. Comparison of three enzyme immobilization methods. *Electrochimica Acta*. 82, 218–223.

- Haas, B.J., Gevers, D., Earl, A.M., Feldgarden, M., Ward, D. V., Giannoukos, G., Ciulla, D., Tabbaa, D., Highlander, S.K., Sodergren, E., Methe, B., DeSantis, T.Z., Petrosino, J.F., Knight, R., Birren, B.W. and Birren, B.W. (2011) Chimeric 16S rRNA sequence formation and detection in Sanger and 454-pyrosequenced PCR amplicons. *Genome Research*. 21 (3), 494–504.
- Hamasaki, T., Aramaki, K., Hida, T., Inatomi, H., Fujimoto, N., Okamura, T., Ozu, K. and Sugita, A. (1996) Clinical study of occupational uroepithelial cancer. *Journal of UOEH*. 18 (4), 247–59.
- Harnisch, F., Schroder, U., Scholz, F. (2008) The Suitability of Monopolar and Bipolar Ion Exchange Membranes as Separators for Biological Fuel Cells. *Environmental Science & Technology*. 42 (5), 1740–1746
- Hassan, H.K., Atta, N.F. and Galal, A. (2012) Electropolymerization of aniline over chemically converted graphene-systematic study and effect of dopant. *International Journal of Electrochemical Science*. 7, 11161–11181.
- Hassan, M.M., Elshafei, A.M., Haroun, B.M., Elsayed, M.A. and Othman, A.M. (2012) Biochemical Characterization of an Extracellular Laccase From *Pleurotus ostreatus* ARC280. *Journal of Applied Sciences Research*. 8 (8), 4525-4536.
- He, C.-S., Mu, Z.-X., Yang, H.-Y., Wang, Y.-Z., Mu, Y. and Yu, H.-Q. (n.d.) Electron acceptors for energy generation in microbial fuel cells fed with wastewaters: A mini-review. *Chemosphere*. 140, 12-17.
- He, H., Zhou, M., Yang, J., Hu, Y. and Zhao, Y. (2014) Simultaneous wastewater treatment, electricity generation and biomass production by an immobilized photosynthetic algal microbial fuel cell. *Bioprocess and Biosystems Engineering*. 37 (5), 873–880.
- He, Z. and Angenent, L.T. (2006) Application of Bacterial Biocathodes in Microbial Fuel Cells. *Electroanalysis*. 18 (19–20), 2009–2015.
- Heilmann, J. and Logan, B.E. (2006) Production of Electricity from Proteins Using a Microbial Fuel Cell. *Water Environment Research*. 78 (5), 531–537.
- Heitner-Wirguin, C. (1996) Recent advances in perfluorinated ionomer membranes:

- structure, properties and applications. *Journal of Membrane Science*. 120 (1), 1–33.
- Hiessl, S., Schuldes, J., Thürmer, A., Halbsguth, T., Bröker, D., Angelov, A., Liebl, W., Daniel, R. and Steinbüchel, A. (2012) Involvement of two latex-clearing proteins during rubber degradation and insights into the subsequent degradation pathway revealed by the genome sequence of *Gordonia polyisoprenivorans* strain VH2. *Applied and Environmental Microbiology*. 78 (8), 2874–2887.
- Higgins, S.R., Lau, C., Atanassov, P., Minteer, S.D. and Cooney, M.J. (2011) Hybrid Biofuel Cell : Microbial Fuel Cell with an Enzymatic. *ACS Catalysis*. 994–997.
- Hilgers, R., Vincken, J.-P., Gruppen, H. and Kabel, M.A. (2018) Laccase/Mediator Systems: Their Reactivity toward Phenolic Lignin Structures. *ACS Sustainable Chemistry & Engineering*. 6 (2), 2037–2046.
- Hong, Y.-G. and Gu, J.-D. (2010) Physiology and biochemistry of reduction of azo compounds by *Shewanella* strains relevant to electron transport chain. *Applied microbiology and biotechnology*. 88 (3), 637–43.
- Hongfei, L., Su, J., Ying, L and Yang, L. (2014) Catalytic Conversion of Lignocellulosic Biomass to Value-Added Organic Acids in Aqueous Media. Fangming Jin (ed.). *Springer*. 109-138
- Hori, T., Kojima, H., Rohnert, R.M. and Zollinger, H. (1987) Structure correlation between diffusion and of anionic and cationic dyes in water. 103, 265–270.
- Hou, B., Sun, J. and Hu, Y. (2011a) Simultaneous Congo red decolorization and electricity generation in air-cathode single-chamber microbial fuel cell with different microfiltration, ultrafiltration and proton exchange membranes. *Bioresource technology*. 102 (6), 4433–8.
- Hou, B., Sun, J. and Hu, Y. (2011b) Simultaneous Congo red decolorization and electricity generation in air-cathode single-chamber microbial fuel cell with different microfiltration, ultrafiltration and proton exchange membranes. *Bioresource Technology*. 102 (6), 4433–4438.
- Hou, H., Zhou, J., Wang, J., Du, C. and Yan, B. (2004) Enhancement of laccase production by *Pleurotus ostreatus* and its use for the decolorization of

- anthraquinone dye. *Process Biochemistry*. 39 (11), 1415–1419.
- Hsueh, C.-C., Wang, Y.-M. and Chen, B.-Y. (2014) Metabolite analysis on reductive biodegradation of reactive green 19 in *Enterobacter cancerogenus* bearing microbial fuel cell (MFC) and non-MFC cultures. *Journal of the Taiwan Institute of Chemical Engineers*. 45 (2), 436–443.
- Hu, J., Zeng, C., Liu, G., Luo, H., Qu, L. and Zhang, R. (2018) Magnetite nanoparticles accelerate the autotrophic sulfate reduction in biocathode microbial electrolysis cells. *Biochemical Engineering Journal*. 13396–105.
- Hu, X., Lin, X., Zhao, H., Chen, Z., Yang, J., Li, F., Liu, C. and Tian, F. (2016) Surface functionalization of polyethersulfone membrane with quaternary ammonium salts for contact-active antibacterial and anti-biofouling properties. *Materials*. 9 (5), 1–12.
- Huang, L. and Cheng, Z.-M. (2008) Immobilization of lipase on chemically modified bimodal ceramic foams for olive oil hydrolysis. *Chemical Engineering Journal*. 144 (1), 103–109.
- Huang, W., Chen, J., Hu, Y., Chen, J., Sun, J. and Zhang, L. (2017) Enhanced simultaneous decolorization of azo dye and electricity generation in microbial fuel cell (MFC) with redox mediator modified anode. *International Journal of Hydrogen Energy*. 42 (4), 2349–2359.
- Jayaprakash, J., Parthasarathy, A. and Viraraghavan, R. (2016) Decolorization and degradation of monoazo and diazo dyes in *Pseudomonas* catalyzed microbial fuel cell. *Environmental Progress & Sustainable Energy*. 35 (6), 1623–1628.
- Jesionowski, T., Jakub, Z. and Krajewska, B. (2014) Enzyme immobilization by adsorption: a review. *Adsorption*. 20, 801–821.
- Jin, X.-C., Liu, G.-Q., Xu, Z.-H. and Tao, W.-Y. (2007) Decolorization of a dye industry effluent by *Aspergillus fumigatus* XC6. *Applied Microbiology and Biotechnology*. 74 (1), 239–243.
- Jinqi, L. and Houtian, L. (1992) Degradation of azo dyes by algae. *Environmental Pollution*. 75 (3), 273–278.
- Johnson, B.T. (2005) 'Microtox® Acute Toxicity Test', in Christian Blaise & Jean-

- François Férard (eds.) *Small-scale Freshwater Toxicity Investigations: Toxicity Test Methods*. [Online]. Dordrecht: Springer Netherlands. pp. 69–105.
- Kandelbauer, A., Maute, O., Kessler, R.W., Erlacher, A. and Gübitz, G.M. (2004) Study of dye decolorization in an immobilized laccase enzyme-reactor using online spectroscopy. *Biotechnology and Bioengineering*. 87 (4), 552–563.
- Kargi, F. and Eker, S. (2007) Electricity generation with simultaneous wastewater treatment by a microbial fuel cell (MFC) with Cu and Cu–Au electrodes. *Journal of Chemical Technology & Biotechnology*. 82 (7), 658–662.
- Kavanagh, P., Jenkins, P. and Leech, D. (2008) Electroreduction of O<sub>2</sub> at a mediated *Melanocarpus albomyces* laccase cathode in a physiological buffer. *Electrochemistry Communications*. 10 (7), 970–972.
- Khan, R. and Fulekar, M.H. (2017) Mineralization of a sulfonated textile dye Reactive Red 31 from simulated wastewater using pellets of *Aspergillus bombycis*. *Bioresources and Bioprocessing*. 4 (1), 23.
- Kiernan, J. (2001) Classification and naming of dyes, stains and fluorochromes. *Biotechnic & Histochemistry*. 76 (5–6), 261–278.
- Kim, B.H., Kim, H.J., Hyun, M.S. and Park, D.H. (1999) Direct electrode reaction of Fe(III)-reducing bacterium, *Shewanella putrefaciens*. *Journal of Microbiology and Biotechnology*. 9 (2), 127–131.
- Kim, H., Lee, I., Kwon, Y., Kim, B.C., Ha, S., Lee, J. and Kim, J. (2011) Immobilization of glucose oxidase into polyaniline nanofiber matrix for biofuel cell applications. *Biosensors & bioelectronics*. 26 (9), 3908–13.
- Kim, J., Jia, H. and Wang, P. (2006) Challenges in biocatalysis for enzyme-based biofuel cells. *Biotechnology Advances*. 24 (3), 296–308.
- Kim, J.R., Cheng, S., Oh, S.-E. and Logan, B.E. (2007) Power generation using different cation, anion, and ultrafiltration membranes in microbial fuel cells. *Environmental Science and Technology*. 41 (3), 1004–1009.
- Kim, J.R., Jung, S.H., Regan, J.M. and Logan, B.E. (2007) Electricity generation and microbial community analysis of alcohol powered microbial fuel cells. *Bioresource Technology*. 98 (13), 2568–2577.

- Kim, R.E., Hong, S.-G., Ha, S. and Kim, J. (2014) Enzyme adsorption, precipitation and crosslinking of glucose oxidase and laccase on polyaniline nanofibers for highly stable enzymatic biofuel cells. *Enzyme and microbial technology*. 6635–41.
- Klotz, L.O., Hou, X. and Jacob, C. (2014) 1,4-naphthoquinones: From oxidative damage to cellular and inter-cellular signaling. *Molecules*. 19 (9), 14902–14918.
- Knapp, J.S., Newby, P.S. and Reece, L.P. (1995) Decolorization of dyes by wood-rotting basidiomycete fungi. *Enzyme and Microbial Technology*. 17 (7), 664–668.
- Kodali, M., Santoro, C., Serov, A., Kabir, S., Artyushkova, K., Matanovic, I. and Atanasov, P. (2017) Air Breathing Cathodes for Microbial Fuel Cell using Mn-, Fe-, Co- and Ni-containing Platinum Group Metal-free Catalysts. *Electrochimica acta*. 231, 115–124.
- Koklukaya, S.Z., Sezer, S., Aksoy, S. and Hasirci, N. (2016) Polyacrylamide-based semi-interpenetrating networks for entrapment of laccase and their use in azo dye decolorization. *Biotechnology and Applied Biochemistry*. 63 (5), 699–707.
- Kong, F., Wang, A., Cheng, H. and Liang, B. (2014) Accelerated decolorization of azo dye Congo red in a combined bioanode-biocathode bioelectrochemical system with modified electrodes deployment. *Bioresource technology*. 151, 332–9.
- Kong, F., Wang, A., Liang, B., Liu, W. and Cheng, H. (2013) Improved azo dye decolorization in a modified sleeve-type bioelectrochemical system. *Bioresource Technology*. 143, 669–673.
- Kong, J. and Yu, S. (2007) Fourier Transform Infrared Spectroscopic Analysis of Protein Secondary Structures Protein FTIR Data Analysis and Band Assignment. *Acta Biochimica et Biophysica Sinica*. 39 (8), 549–559.
- Kouzuma, A., Kasai, T., Hirose, A. and Watanabe, K. (2015) Catabolic and regulatory systems in *Shewanella oneidensis* MR-1 involved in electricity generation in microbial fuel cells. *Frontiers in Microbiology*. 6, 1–11.
- Kudlich, M., Hetheridge, M.J., Knackmuss, H.-J. and Stolz, A. (1999) Autoxidation

Reactions of Different Aromatic *o*-Aminohydroxynaphthalenes That Are Formed during the Anaerobic Reduction of Sulfonated Azo Dyes. *Environmental Science & Technology*. 33 (6), 896–901.

Kunamneni, A., Ballesteros, A., Plou, F.J. and Alcalde, M. (2007) Fungal laccase – a versatile enzyme for biotechnological applications. *Applied Microbiology*. 233–245.

Kunimatsu, K., Yoda, T., Tryk, D.A., Uchida, H. and Watanabe, M. (2010) In situATR-FTIR study of oxygenreduction at the Pt/Nafion interface. *Phys. Chem. Chem. Phys.* 12 (3), 621–629.

Kurniawati, S. and Nicell, J.A. (2007) Efficacy of mediators for enhancing the laccase-catalyzed oxidation of aqueous phenol. *Enzyme and Microbial Technology*. 41 (3), 353–361.

Kusvuran, E., Gulnaz, O., Irmak, S., Atanur, O.M., Ibrahim Yavuz, H. and Erbatur, O. (2004) Comparison of several advanced oxidation processes for the decolorization of Reactive Red 120 azo dye in aqueous solution. *Journal of Hazardous Materials*. 109 (1), 85–93.

Kwang-Soo, S. and Chang-Jin, K. (1998) Decolorisation of artificial dyes by peroxidase from the white-rot fungus, *Pleurotus ostreatus*. *Biotechnology Letters*. 20 (6), 569–572.

Laanbroek, H.J., Bär-Gilissen, M.J. and Hoogveld, H.L. (2002) Nitrite as a stimulus for ammonia-starved *Nitrosomonas europaea*. *Applied and Environmental Microbiology*. 68 (3), 1454–1457.

Lai, C.-Y., Liu, S.-H., Wu, G.-P. and Lin, C.-W. (2017) Enhanced bio-decolorization of acid orange 7 and electricity generation in microbial fuel cells with superabsorbent-containing membrane and laccase-based bio-cathode. *Journal of Cleaner Production*. 166, 381–386.

Lai, C.-Y., Wu, C.-H., Meng, C.-T. and Lin, C.-W. (2017) Decolorization of azo dye and generation of electricity by microbial fuel cell with laccase-producing white-rot fungus on cathode. *Applied Energy*. 188, 392–398.

- Lai, Q., Yu, Z., Yuan, J., Sun, F. and Shao, Z. (2011) *Nitratireductor indicus* sp. nov., isolated from deep-sea water. *International Journal of Systematic and Evolutionary Microbiology*. 61 (2), 295–298.
- Lalaoui, N., Elouarzaki, K., Goff, A. Le, Holzinger, M. and Cosnier, S. (2013) Efficient direct oxygen reduction by laccases attached and oriented on pyrene-functionalized polypyrrole/carbon nanotube electrodes. *Chemical Communications*. 49 (81), 9281-9283.
- Larimer, F.W., Chain, P., Hauser, L., Lamerdin, J., Malfatti, S., Do, L., Land, M.L., Pelletier, D.A., Beatty, J.T., Lang, A.S., Tabita, F.R., Gibson, J.L., Hanson, T.E., Bobst, C., Torres, J.L.T. y, Peres, C., Harrison, F.H., Gibson, J. and Harwood, C.S. (2004) Complete genome sequence of the metabolically versatile photosynthetic bacterium *Rhodospseudomonas palustris*. *Nature Biotechnology*. 22 (1), 55–61.
- Le Laz, S., Kpebe, A., Lorquin, J., Brugna, M. and Rousset, M. (2014) H<sub>2</sub>-dependent azoreduction by *Shewanella oneidensis* MR-1: involvement of secreted flavins and both [Ni–Fe] and [Fe–Fe] hydrogenases. *Applied Microbiology and Biotechnology*. 98 (6), 2699–2707.
- Lefebvre, O., Al-Mamun, A. and Ng, H.Y. (2008) A microbial fuel cell equipped with a biocathode for organic removal and denitrification. *Water Science and Technology*. 58 (4), 881–885.
- Legerská, B., Chmelová, D. and Ondrejovič, M. (2016) Degradation of synthetic dyes by laccases - A mini-review. *Nova Biotechnologica et Chimica*. 15 (1), 90–106.
- Legrini, O., Oliveros, E. and Braun, A.M. (1993) Photochemical processes for water treatment. *Chemical Reviews*. 93 (2), 671–698.
- Liang, B., Cheng, H.-Y., Kong, D.-Y., Gao, S.-H., Sun, F., Cui, D., Kong, F.-Y., Zhou, A.-J., Liu, W.-Z., Ren, N.-Q., Wu, W.-M., Wang, A.-J. and Lee, D.-J. (2013) Accelerated Reduction of Chlorinated Nitroaromatic Antibiotic Chloramphenicol by Biocathode. *Environmental Science & Technology*. 47 (10), 5353–5361.

- Liang, C.-Z., Sun, S.-P., Li, F.-Y., Ong, Y.-K. and Chung, T.-S. (2014) Treatment of highly concentrated wastewater containing multiple synthetic dyes by a combined process of coagulation/flocculation and nanofiltration. *Journal of Membrane Science*. 469306–315.
- Liao, C.-H., Kang, S.-F. and Wu, F.-A. (2001) Hydroxyl radical scavenging role of chloride and bicarbonate ions in the H<sub>2</sub>O<sub>2</sub>/UV process. *Chemosphere*. 44 (5), 1193–1200.
- Li, Z., Zhang, X., Lin, J., Han, S. and Lei, L (2010) Azo dye treatment with simultaneous electricity production in an anaerobic–aerobic sequential reactor and microbial fuel cell coupled system. *Bioresource Technology*. 101(12), 4440-4445.
- Linos, A., Steinbuchel, A., Sproer, C. and Kroppenstedt, R.M. (1999) *Gordonia polyisoprenivorans* sp. nov., a rubber-degrading actinomycete isolated from an automobile tyre. *International Journal of Systematic Bacteriology*. 49, 1785–1791.
- Liu, L., Li, F.B., Feng, C.H. and Li, X.Z. (2009) Microbial fuel cell with an azo-dye-feeding cathode. *Applied Microbiology and Biotechnology*. 85 (1), 175–183.
- Liu, R.-H., Sheng, G.-P., Sun, M., Zang, G.-L., Li, W.-W., Tong, Z.-H., Dong, F., Hon-Wah Lam, M. and Yu, H.-Q. (2011) Enhanced reductive degradation of methyl orange in a microbial fuel cell through cathode modification with redox mediators. *Applied Microbiology and Biotechnology*. 89 (1), 201–208.
- Liu, Y., Huang, J. and Zhang, X. (2009) Decolorization and biodegradation of remazol brilliant blue R by bilirubin oxidase. *Journal of Bioscience and Bioengineering*. 108 (6), 496–500.
- Liu, Z., Frigaard, N., Vogl, K., Iino, T., Ohkuma, M. and Overmann, J. (2012) Complete genome of *Ignavibacterium album*, a metabolically versatile, flagellated, facultative anaerobe from the phylum Chlorobi. *Frontiers in Microbiology*. 3 (May), 1–15.
- Logan, B.E., Hamelers, B., Rozendal, R., Schroder, U., Keller, J., Freguia, S., Aelterman, P., Verstraete, W. and Rabaey, K. (2006) Microbial fuel cells:

- Methodology and technology. *Environmental Science and Technology*. 40 (17), 5181–5192.
- Logan, B.E., Murano, C., Scott, K., Gray, N.D. and Head, I.M. (2005a) Electricity generation from cysteine in a microbial fuel cell. *Water Research*. 39 (5), 942–952.
- Logan, B.E., Murano, C., Scott, K., Gray, N.D. and Head, I.M. (2005b) Electricity generation from cysteine in a microbial fuel cell. *Water Research*. 39 (5), 942–952.
- López-González, B., Dector, A., Cuevas-Muñiz, F.M., Arjona, N., Cruz-Madrid, C., Arana-Cuenca, A., Guerra-Balcázar, M., Arriaga, L.G. and Ledesma-García, J. (2014) Hybrid microfluidic fuel cell based on Laccase/C and AuAg/C electrodes. *Biosensors and Bioelectronics*. 62, 221–226.
- Lorenzo, M., Moldes, D., Rodríguez Couto, S. and Sanromán, M.A. (2005) Inhibition of laccase activity from *Trametes versicolor* by heavy metals and organic compounds. *Chemosphere*. 60 (8), 1124–1128.
- Luo, H., Jin, S., Fallgren, P.H., Park, H.J. and Johnson, P.A. (2010) A novel laccase-catalyzed cathode for microbial fuel cells. *Chemical Engineering Journal*. 165 (2), 524–528.
- Luo, Y., Zhang, R., Liu, G., Li, J., Qin, B., Li, M. and Chen, S. (2011) Simultaneous degradation of refractory contaminants in both the anode and cathode chambers of the microbial fuel cell. *Bioresour Technol*. 102 (4), 3827–3832.
- Lyautey, E., Cournet, A., Morin, S., Boulétreau, S., Etcheverry, L., Charcosset, J.-Y., Delmas, F., Bergel, A. and Garabetian, F. (2011) Electroactivity of phototrophic river biofilms and constitutive cultivable bacteria. *Applied and environmental microbiology*. 77 (15), 5394–401.
- Madhavi, V. and Lele, S.S. (2009) Laccase: Properties and applications. *BioResources*. 4 (4), 1694–1717.
- Magoč, T. and Salzberg, S.L. (2011) FLASH: fast length adjustment of short reads to improve genome assemblies. *Bioinformatics (Oxford, England)*. 27 (21), 2957–2963.

- Manohar, A.K. and Mansfeld, F. (2009) The internal resistance of a microbial fuel cell and its dependence on cell design and operating conditions. *Electrochimica Acta*. 54 (6), 1664–1670.
- Mao, Y., Zhang, L., Li, D., Shi, H., Liu, Y. and Cai, L. (2010) Power generation from a biocathode microbial fuel cell biocatalyzed by ferro/manganese-oxidizing bacteria. *Electrochimica Acta*. 55 (27), 7804–7808.
- Marsili, E., Baron, D.B., Shikhare, I.D., Coursolle, D., Gralnick, J.A. and Bond, D.R. (2008) *Shewanella* secretes flavins that mediate extracellular electron transfer. *PNAS*. 105 (10), 6–11.
- Martorana, A., Sorace, L., Boer, H., Vazquez-Duhalt, R., Basosi, R. and Baratto, M.C. (2013) A spectroscopic characterization of a phenolic natural mediator in the laccase biocatalytic reaction. *Journal of Molecular Catalysis B: Enzymatic*. 97, 203–208.
- Masa, J., Xia, W., Sinev, I., Zhao, A., Sun, Z., Grütze, S., Weide, P., Muhler, M. and Schuhmann, W. (2014) Mn(x)O(y)/NC and Co(x)O(y)/NC nanoparticles embedded in a nitrogen-doped carbon matrix for high-performance bifunctional oxygen electrodes. *Angewandte Chemie (International ed. in English)*. 53 (32), 8508–12.
- Masa, J., Zhao, A., Xia, W., Sun, Z., Mei, B., Muhler, M. and Schuhmann, W. (2013) Trace metal residues promote the activity of supposedly metal-free nitrogen-modified carbon catalysts for the oxygen reduction reaction. *Electrochemistry Communications*. 34, 113–116.
- Matsuoka, M. (1990) 'Quinone Dyes', in *Infrared Absorbing Dyes*. [Online]. Boston, MA: Springer US. pp. 35–43.
- Mauritz, K.A. and Moore, R.B. (2004) State of understanding of Nafion. *Chemical Reviews*. 104 (10), 4535–4585.
- Mendoza, L., Jonstrup, M., Hatti-Kaul, R. and Mattiasson, B. (2011) Azo dye decolorization by a laccase/mediator system in a membrane reactor: Enzyme and mediator reusability. *Enzyme and Microbial Technology*. 49 (5), 478–484.
- Meredith, S., Xu, S., Meredith, M.T. and Minter, S.D. (2012) Hydrophobic Salt-

- modified Nafion for Enzyme Immobilization and Stabilization. *Journal of Visualized Experiments*. (65), 1–6.
- Milner, E.M., Popescu, D., Curtis, T., Head, I.M., Scott, K. and Yu, E.H. (2016) Microbial fuel cells with highly active aerobic biocathodes. *Journal of Power Sources*. 324, 8–16.
- Milton, R.D., Giroud, F., Thumser, A.E., Minteer, S.D. and Slade, R.C.T. (2013) Hydrogen peroxide produced by glucose oxidase affects the performance of laccase cathodes in glucose/oxygen fuel cells: FAD-dependent glucose dehydrogenase as a replacement. *Physical chemistry chemical physics : PCCP*. 15 (44), 19371–19379.
- Min, B., Kim, J., Oh, S., Regan, J.M. and Logan, B.E. (2005) Electricity generation from swine wastewater using microbial fuel cells. *Water Research*. 39 (20), 4961–4968.
- Moehlenbrock, M.J. and Minteer, S.D. (2017) Introduction to the Field of Enzyme Immobilization and Stabilization, *Methods in Molecular Biology*, Humana Press, New York, 1–7.
- Mohamad, N.R., Marzuki, N.H.C., Buang, N.A., Huyop, F. and Wahab, R.A. (2015) An overview of technologies for immobilization of enzymes and surface analysis techniques for immobilized enzymes. *Biotechnology, biotechnological equipment*. 29 (2), 205–220.
- Mohan, S.V., Prasad, K.K., Rao, N.C. and Sarma, P.N. (2005) Acid azo dye degradation by free and immobilized horseradish peroxidase (HRP) catalyzed process. *Chemosphere*. 58 (8), 1097–1105.
- Moore, C.M., Akers, N.L., Hill, A.D., Johnson, Z.C. and Minteer, S.D. (2004) Improving the environment for immobilized dehydrogenase enzymes by modifying nafion with tetraalkylammonium bromides. *Biomacromolecules*. 5 (4), 1241–1247.
- Morhardt, C., Ketterer, B., Heißler, S. and Franzreb, M. (2014) Direct quantification of immobilized enzymes by means of FTIR ATR spectroscopy – A process analytics tool for biotransformations applying non-porous magnetic enzyme

- carriers. *Journal of Molecular Catalysis B: Enzymatic*. 107, 55–63.
- Morozova, O. V., Shumakovich, G.P., Shleev, S. V. and Yaropolov, Y.I. (2007) Laccase-mediator systems and their applications: A review. *Applied Biochemistry and Microbiology*. 43 (5), 523–535.
- Mu, Y., Rabaey, K., Rozendal, R.A., Yuan, Z. and Keller, J. (2009) Decolorization of Azo Dyes in Bioelectrochemical Systems. *Environmental Science & Technology*. 43 (13), 5137–5143.
- Mu, Y., Rabaey, K. and Yuan, Z. (2015) Decolourization of Azo Dyes in Bioelectrochemical Systems Decolorization of Azo Dyes. *Bioelectrochemical Systems*. 43 (13), 5137–5143.
- Murty, M.N. and Kumar, S. (2011) Water Pollution in India: An economic appraisal. *India Infrastructure Report*. 285–298.
- Newton, G.J., Mori, S., Nakamura, R., Hashimoto, K. and Watanabe, K. (2009) Analyses of current-generating mechanisms of *Shewanella loihica* PV-4 and *Shewanella oneidensis* MR-1 in microbial fuel cells. *Applied and Environmental Microbiology*. 75 (24), 7674–7681.
- Niu, C.-G., Wang, Y., Zhang, X.-G., Zeng, G.-M., Huang, D.-W., Ruan, M. and Li, X.-W. (2012) Decolorization of an azo dye Orange G in microbial fuel cells using Fe(II)-EDTA catalyzed persulfate. *Bioresource technology*. 126,101–106.
- Nogala, W., Burchardt, M., Opallo, M., Rogalski, J. and Wittstock, G. (2008) Scanning electrochemical microscopy study of laccase within a sol–gel processed silicate film. *Bioelectrochemistry*. 72 (2), 174–182.
- Noori, M.T., Ghangrekar, M.M. and Mukherjee, C.K. (2016) V2O5 microflower decorated cathode for enhancing power generation in air-cathode microbial fuel cell treating fish market wastewater. *International Journal of Hydrogen Energy*. 41 (5), 3638–3645.
- Nyanhongo, G., Gomes, J., Gübitz, G., Zvauya, R., Read, J. and Steiner, W. (2002) Decolorization of textile dyes by laccases from a newly isolated strain of *Trametes modesta*. *Water Research*. 36 (6), 1449–1456.
- Oh, S. and Logan, B.E. (2005) Hydrogen and electricity production from a food

- processing wastewater using fermentation and microbial fuel cell technologies. *Water Research*. 39 (19), 4673–4682.
- Oh, S.E. and Logan, B.E. (2006) Proton exchange membrane and electrode surface areas as factors that affect power generation in microbial fuel cells. *Applied Microbiology and Biotechnology*. 70 (2), 162–169.
- Ooi, T., Shibata, T., Sato, R., Ohno, H., Kinoshita, S., Thuoc, T.L. and Taguchi, S. (2007) An azoreductase, aerobic NADH-dependent flavoprotein discovered from *Bacillus* sp.: functional expression and enzymatic characterization. *Applied Microbiology and Biotechnology*. 75 (2), 377–386.
- Othman, A.M., González-Domínguez, E., Sanromán, Á., Correa-Duarte, M. and Moldes, D. (2016) Immobilization of laccase on functionalized multiwalled carbon nanotube membranes and application for dye decolorization. *RSC Advances*. 6 (115), 114690–114697.
- Palmieri, G., Giardina, P. and Sanna, G. (2005) Laccase-Mediated Remazol Brilliant Blue R Decolorization in a Fixed-Bed Bioreactor. *Biotechnology Progress*. 21 (5), 1436–1441.
- Pandey, A., Singh, P. and Iyengar, L. (2007) Bacterial decolorization and degradation of azo dyes. *International Biodeterioration & Biodegradation*. 59 (2), 73–84.
- Pardo, I., Chanagá, X., Vicente, A.I., Alcalde, M. and Camarero, S. (2013) New colorimetric screening assays for the directed evolution of fungal laccases to improve the conversion of plant biomass. *BMC biotechnology*. 13 (1), 90.
- Park, D.H., Kim, S.K., Shin, I.H. and Jeong, Y.J. (2000) Electricity production in biofuel cell using modified graphite electrode with Neutral Red. *Biotechnology Letters*. 22 (16), 1301–1304.
- Pazarlıoğlu, N.K., Sariışık, M. and Telefoncu, A. (2005) Laccase: production by *Trametes versicolor* and application to denim washing. *Process Biochemistry*. 40 (5), 1673–1678.
- Pereira, L., Coelho, A. V., Viegas, C.A., Santos, M.M.C. dos, Robalo, M.P. and Martins, L.O. (2009) Enzymatic biotransformation of the azo dye Sudan Orange

- G with bacterial CotA-laccase. *Journal of Biotechnology*. 139 (1), 68–77.
- Pizzolato, T., Carissimi, E., Machado, E. and Schneider, I.A. (2002) Colour removal with NaClO of dye wastewater from an agate-processing plant in Rio Grande do Sul, Brazil. *International Journal of Mineral Processing*. 65 (3), 203–211.
- Popat, S.C., Ki, D., Rittmann, B.E. and Torres, C.I. (2012) Importance of OH-transport from cathodes in microbial fuel cells. *ChemSusChem*. 5 (6), 1071–1079.
- Potter, M.C. (1911) Electrical Effects Accompanying the Decomposition of Organic Compounds. *Proceedings of the Royal Society B: Biological Sciences*. 84 (571), 260–276.
- Preedy, V. and Patel, V. (2012) Biosensors and Environmental Health. CRC Press. DOI: 10.1201/b12775.
- Puig, S., Serra, M., Vilar-Sanz, A., Cabré, M., Bañeras, L., Colprim, J. and Balaguer, M.D. (2011) Autotrophic nitrite removal in the cathode of microbial fuel cells. *Bioresource Technology*. 102 (6), 4462–4467.
- Rabaey, K., Boon, N., Höfte, M. and Verstraete, W. (2005) Microbial phenazine production enhances electron transfer in biofuel cells. *Environmental science & technology*. 39 (9), 3401–8.
- Rabaey, K., Read, S.T., Clauwaert, P., Freguia, S., Bond, P.L., Blackall, L.L. and Keller, J. (2008) Cathodic oxygen reduction catalyzed by bacteria in microbial fuel cells. *ISME Journal*. 2 (5), 519–527.
- Ramalingam, Saraswathy, N., Shanmugapriya, S., Shakthipriyadarshini, S., Sadasivam, S. and Shanmugaprasath, M. (2010) Decolorization of textile dyes by *Aspergillus tamarii*, mixed fungal culture and *Penicillium purpurogenum*. *Journal of Scientific and Industrial Research*. 69 (2), 151–153.
- Ramírez-Montoya, L.A., Hernández-Montoya, V., Montes-Morán, M.A., Jáuregui-Rincón, J. and Cervantes, F.J. (2015) Decolorization of dyes with different molecular properties using free and immobilized laccases from *Trametes versicolor*. *Journal of Molecular Liquids*. 212, 30–37.

- Rashed, N.M. (2013). Adsorption Technique for the Removal of Organic Pollutants from Water and Wastewater, Organic Pollutants, IntechOpen, DOI: 10.5772/54048. Available from: <https://www.intechopen.com/books/organicpollutants-monitoring-risk-and-treatment/adsorption-technique-for-theremoval-of-organic-pollutants-from-water-and-wastewater>
- Rawat, D., Mishra, V. and Sharma, R.S. (2016) Detoxification of azo dyes in the context of environmental processes. *Chemosphere*. 155, 591–605.
- Regalado, C., García-Almendárez, B.E. and Duarte-Vázquez, M.A. (2004) Biotechnological applications of peroxidases. *Phytochemistry Reviews*. 3 (1–2), 243–256.
- Reguera, G., McCarthy, K.D., Mehta, T., Nicoll, J.S., Tuominen, M.T. and Lovley, D.R. (2005) Extracellular electron transfer via microbial nanowires. *Nature*. 435 (7045), 1098–1101.
- Rincón, R. a., Masa, J., Mehrpour, S., Tietz, F. and Schuhmann, W. (2014) Activation of oxygen evolving perovskites for oxygen reduction by functionalization with Fe–Nx/C groups. *Chem. Commun.* 50 (94), 14760–14762.
- Rismani-Yazdi, H., Carver, S.M., Christy, A.D. and Tuovinen, O.H. (2008) Cathodic limitations in microbial fuel cells: An overview. *Journal of Power Sources*. 180 (2), 683–694.
- Robinson, T., McMullan, G., Marchant, R. and Nigam, P. (2001) Remediation of dyes in textile effluent: a critical review on current treatment technologies with a proposed alternative. *Bioresource Technology*. 77 (3), 247–255.
- Rodrigues da Silva, M.E., Firmino, P.I.M. and dos Santos, A.B. (2012) Impact of the redox mediator sodium anthraquinone-2,6-disulphonate (AQDS) on the reductive decolourisation of the azo dye Reactive Red 2 (RR2) in one- and two-stage anaerobic systems. *Bioresource Technology*. 121, 1–7.
- Romo-Sánchez, S., Camacho, C., Ramirez, H.L. and Arévalo-Villena, M. (2014) Immobilization of Commercial Cellulase and Xylanase by Different Methods

- Using Two Polymeric Supports. *Advances in Bioscience and Biotechnology*. 05 (06), 517–526.
- Rozendal, A., Hamelers, H.V.M., Rabaey, K., Keller, J. and Buisman, C.J.N. (2008) Towards practical implementation of bioelectrochemical wastewater treatment. *Trends in biotechnology*. 26 (8), 450–459.
- Rozendal, R. a., Hamelers, H.V.M. and Buisman, C.J.N. (2006) Effects of Membrane Cation Transport on pH and Microbial Fuel. *Environmental science & technology*. 40 (17), 5206–5211.
- Rubenwolf, S., Sané, S., Hussein, L. and Kestel, J. (2012) Prolongation of electrode lifetime in biofuel cells by periodic enzyme renewal Theoretical background. *Bioenergy and Biofuels*. 96, 841–849.
- Russ, R., Rau, J. and Stolz, A. (2000) The function of cytoplasmic flavin reductases in the reduction of azo dyes by bacteria. *Applied and environmental microbiology*. 66 (4), 1429–34.
- Russo, M.E., Giardina, P., Marzocchella, A., Salatino, P. and Sannia, G. (2008) Assessment of anthraquinone-dye conversion by free and immobilized crude laccase mixtures. *Enzyme and Microbial Technology*. 42 (6), 521–530.
- Sadighi, A. and Faramarzi, M.A. (2013) Congo red decolorization by immobilized laccase through chitosan nanoparticles on the glass beads. *Journal of the Taiwan Institute of Chemical Engineers*. 44 (2), 156–162.
- Sané, S., Jolival, C., Mittler, G., Nielsen, P.J., Rubenwolf, S., Zengerle, R. and Kerzenmacher, S. (2013) Overcoming bottlenecks of enzymatic biofuel cell cathodes: Crude fungal culture supernatant can help to extend lifetime and reduce cost. *ChemSusChem*. 6 (7), 1209–1215.
- Santoro, C., Babanova, S., Atanassov, P. and Li, B. (2013) High Power Generation by a Membraneless Single Chamber Microbial Fuel Cell ( SCMFC ) Using Enzymatic Bilirubin Oxidase ( BOx ) Air-Breathing Cathode. *Journal of The Electrochemical Society*. 160 (10), 720–726.
- Santoro, C., Serov, A., Villarrubia, C.W.N., Stariha, S., Babanova, S., Artyushkova, K., Schuler, A.J. and Atanassov, P. (2015) High catalytic activity and pollutants

- resistivity using Fe-AAPyr cathode catalyst for microbial fuel cell application. *Scientific Reports*. 5 (May), 1–10.
- dos Santos, A.B., Cervantes, F.J. and van Lier, J.B. (2007a) Review paper on current technologies for decolourisation of textile wastewaters: Perspectives for anaerobic biotechnology. *Bioresource Technology*. 98 (12), 2369–2385.
- Saratale, R.G., Saratale, G.D., Chang, J.S. and Govindwar, S.P. (2011) Bacterial decolorization and degradation of azo dyes: A review. *Journal of the Taiwan Institute of Chemical Engineers*. 42 (1), 138–157.
- Sarayu, K. and Sandhya, S. (2012) Current Technologies for Biological Treatment of Textile Wastewater—A Review. *Applied Biochemistry and Biotechnology*. 167 (3), 645–661.
- Savizi, I.S.P., Kariminia, H.R. and Bakhshian, S. (2012) Simultaneous decolorization and bioelectricity generation in a dual chamber microbial fuel cell using electropolymerized-enzymatic cathode. *Environmental Science and Technology*. 46, 6584–6593.
- Schaetzle, O., Barrière, F. and Schröder, U. (2009) An improved microbial fuel cell with laccase as the oxygen reduction catalyst. *Energy Environ. Sci.* 2 (1), 96–99.
- Schliephake, K., Mainwaring, D.E., Lonergan, G.T., Jones, I.K. and Baker, W.L. (2000) Transformation and degradation of the disazo dye Chicago Sky Blue by a purified laccase from *Pycnoporus cinnabarinus*. *Enzyme and Microbial Technology*. 27 (1–2), 100–107.
- Scholz, F. (2008) The Suitability of Monopolar and Bipolar Ion Exchange Membranes as Separators for Biological Fuel Cells. *Energy Environ. Sci.* 42 (5), 1740–1746.
- Schrenk, M.J., Villigam, R.E., Torrence, N.J., Brancato, S.J. and Minteer, S.D. (2002) Effects of mixture casting Nafion® with quaternary ammonium bromide salts on the ion-exchange capacity and mass transport in the membranes. *Journal of Membrane Science*. 205 (1–2), 3–10.
- Schröder, U., Nießen, J. and Scholz, F. (2003) A Generation of Microbial Fuel Cells

with Current Outputs Boosted by More Than One Order of Magnitude.

*Angewandte Chemie International Edition*. 42 (25), 2880–2883.

Sears, H.J., Sawers, G., Berks, B.C., Ferguson, S.J. and Richardson, D.J. (2000) Control of periplasmic nitrate reductase gene expression (napEDABC) from *Paracoccus pantotrophus* in response to oxygen and carbon substrates. *Microbiology*. 146, 2977–2985.

Sekar, N. (2011) '15 – Acid dyes', in *Handbook of Textile and Industrial Dyeing*. [Online], 1<sup>st</sup> ed. WoodHead Publishing, pp. 486–514.

Sen, S.K., Raut, S., Bandyopadhyay, P. and Raut, S. (2016) Fungal decolouration and degradation of azo dyes: A review. *Fungal Biology Reviews*. 30 (3), 112–133.

Shleev, S., Jarosz-wilkolazka, A., Khalunina, A., Morozova, O., Yaropolov, A., Ruzgas, T. and Gorton, L. (2005) Direct electron transfer reactions of laccases from different origins on carbon electrodes. *Bioelectrochemistry*. 67,115–124.

Singh, K. and Arora, S. (2011) Removal of Synthetic Textile Dyes From Wastewaters: A Critical Review on Present Treatment Technologies. *Critical Reviews in Environmental Science and Technology*. 41 (9), 807–878.

Singh, R.P., Singh, P.K. and Singh, R.L. (2014) Bacterial Decolorization of Textile Azo Dye Acid Orange by *Staphylococcus hominis* RMLRT03. *Toxicology international*. 21 (2), 160–6.

Slokar, Y.M. and Majcen Le Marechal, A. (1998) Methods of decoloration of textile wastewaters. *Dyes and Pigments*. 37 (4), 335–356.

Sneddon, J., Masuram, S. and Richert, J.C. (2007) Gas chromatography-mass spectrometry-basic principles, instrumentation and selected applications for detection of organic compounds. *Analytical Letters*. 40 (6), 1003–1012.

Soares, G.M.B., De Amorim, M.T.P. and Costa-Ferreira, M. (2001) Use of laccase together with redox mediators to decolourize Remazol Brilliant Blue R. *Journal of Biotechnology*. 89 (2–3), 123–129.

Spina, F., Junghanns, C., Donelli, I., Nair, R., Demarche, P., Romagnolo, A., Freddi, G., Agathos, S.N. and Varese, G.C. (2016) Stimulation of laccases from

*Trametes pubescens* : Use in dye decolorization and cotton bleaching.

*Preparative Biochemistry and Biotechnology*. 46 (7), 639–647.

Srinivas, K. and King, J. (2011) Binary Diffusion Coefficients of Biomass-Based Carbochemicals In Subcritical Water Using Chromatographic Peak Broadening Technique. *AIChE Annual Meeting*,

Stejskal, J. and Gilbert, R.G. (2006) Polyaniline: Preparation of a conductive polymer. (IUPAC Technical Report). *Pure and Applied Chemistry*. 74 (5), p.857–867.

Stoilova, I., Krastanov, A. and Stanchev, V. (2010) Properties of crude laccase from *Trametes versicolor* produced by solid-substrate fermentation. *Advances in Bioscience and Biotechnology*. 01 (03), 208–215.

Strathdee, F. and Free, A. (2013) Denaturing Gradient Gel Electrophoresis (DGGE). *Methods in molecular biology (Clifton, N.J.)*. [Online]. pp. 145–157.

Strycharz-Glaven, S.M., Glaven, R.H., Wang, Z., Zhou, J., Vora, G.J. and Tender, L.M. (2013) Electrochemical investigation of a microbial solar cell reveals a nonphotosynthetic biocathode catalyst. *Applied and environmental microbiology*. 79 (13), 3933–42.

Sun, H., Yang, H., Huang, W. and Zhang, S. (2015) Immobilization of laccase in a sponge-like hydrogel for enhanced durability in enzymatic degradation of dye pollutants. *Journal of Colloid and Interface Science*. 450, 353–360.

Sun, J., Li, W., Li, Y., Hu, Y. and Zhang, Y. (2013) Redox mediator enhanced simultaneous decolorization of azo dye and bioelectricity generation in air-cathode microbial fuel cell. *Bioresource Technology*. 142, 407–414.

Sun, L., Toyonaga, M., Ohashi, A., Tourlousse, D.M., Matsuura, N., Meng, X.-Y., Tamaki, H., Hanada, S., Cruz, R., Yamaguchi, T. and Sekiguchi, Y. (2016) *Lentimicrobium saccharophilum* gen. nov., sp. nov., a strictly anaerobic bacterium representing a new family in the phylum Bacteroidetes, and proposal of *Lentimicrobiaceae* fam. nov. *International Journal of Systematic and Evolutionary Microbiology*. 66 (7), 2635–2642.

Szczupak, A., Kol-Kalmanz, D. and Alfonta, L. (2012) A hybrid biocathode: surface

- display of O<sub>2</sub>-reducing enzymes for microbial fuel cell applications. *Chemical Communications*. 48 (1), 49–51.
- Taheran, M., Naghdi, M., Brar, S.K., Knystautas, E.J., Verma, M. and Surampalli, R.Y. (2017) Covalent Immobilization of Laccase onto Nanofibrous Membrane for Degradation of Pharmaceutical Residues in Water. *ACS Sustainable Chemistry & Engineering*. 5 (11), 10430–10438.
- Tauber, M.M., Gübitz, G.M. and Rehorek, A. (2008) Degradation of azo dyes by oxidative processes – Laccase and ultrasound treatment. *Bioresource Technology*. 99 (10), 4213–4220.
- Tauber, M.M., Guebitz, G.M. and Rehorek, A. (2005) Degradation of Azo Dyes by Laccase and Ultrasound Treatment Degradation of Azo Dyes by Laccase and Ultrasound Treatment. *Society*. 71 (5), 2600–2607.
- Teerapatsakul, C., Bucke, C., Parra, R., Keshavarz, T. and Chitradon, L. (2007) Dye decolorisation by laccase entrapped in copper alginate. *World Journal of Microbiology and Biotechnology*. 24 (8), 1367–1374.
- Teerapatsakul, C., Parra, R., Keshavarz, T. and Chitradon, L. (2017) Repeated batch for dye degradation in an airlift bioreactor by laccase entrapped in copper alginate. *International Biodeterioration & Biodegradation*. 120, 52–57.
- Telke, A.A., Kadam, A.A., Jagtap, S.S., Jadhav, J.P. and Govindwar, S.P. (2010) Biochemical characterization and potential for textile dye degradation of blue laccase from *Aspergillus ochraceus* NCIM-1146. *Biotechnology and Bioprocess Engineering*. 15 (4), 696–703.
- Tilli, S., Ciullini, I., Scozzafava, A. and Briganti, F. (2011) Differential decolorization of textile dyes in mixtures and the joint effect of laccase and cellobiose dehydrogenase activities present in extracellular extracts from *Funalia trogii*. *Enzyme and Microbial Technology*. 49 (5), 465–471.
- Tsukuda, M., Kitahara, K. and Miyazaki, K. (2017) Comparative RNA function analysis reveals high functional similarity between distantly related bacterial 16 S rRNAs. *Scientific Reports*. 7 (1), 9993.
- Ucar, D., Zhang, Y. and Angelidaki, I. (2017) An Overview of Electron Acceptors in

- Microbial Fuel Cells. *Frontiers in microbiology*. 8, 643.
- Upadhyay, P., Shrivastava, R. and Agrawal, P.K. (2016) Bioprospecting and biotechnological applications of fungal laccase. *3 Biotech*. 6 (1), 15.
- Urano, H. and Fukuzaki, S. (2005) The Mode of Action of Sodium Hypochlorite in the Cleaning Process. *Biocontrol Science*. 10 (2), 21–29.
- Urano, H. and Fukuzaki, S. (2011) The Mode of Action of Sodium Hypochlorite in the Decolorization of Azo Dye Orange II in Aqueous Solution. *Biocontrol Science*. 16 (3), 123–126.
- Ushiba, Y., Takahara, Y. and Ohta, H. (2003) *Sphingobium amiense* sp . nov ., a novel nonylphenol-degrading bacterium isolated from a river sediment. *International Journal of Systematic and Evolutionary Microbiology*. 53, 2045–2048.
- Velasquez-Orta, S.B., Curtis, T.P. and Logan, B.E. (2009) Energy from algae using microbial fuel cells. *Biotechnology and Bioengineering*. 103 (6), 1068–1076.
- Verrax, J., Beck, R., Dejeans, N., Glorieux, C., Sid, B., Pedrosa, R.C., Benites, J., Vásquez, D., Valderrama, J.A. and Calderon, P.B. (2011) Redox-active quinones and ascorbate: an innovative cancer therapy that exploits the vulnerability of cancer cells to oxidative stress. *Anti-cancer agents in medicinal chemistry*. 11 (2), 213–21.
- Volkova, N., Ibrahim, V. and Hatti-Kaul, R. (2012) Laccase catalysed oxidation of syringic acid: Calorimetric determination of kinetic parameters. *Enzyme and Microbial Technology*. 50 (4–5), 233–237.
- Wang, H., Hollywood, K., Jarvis, R.M., Lloyd, J.R. and Goodacre, R. (2010) Phenotypic characterization of *Shewanella oneidensis* MR-1 under aerobic and anaerobic growth conditions by using fourier transform infrared spectroscopy and high-performance liquid chromatography analyses. *Applied and environmental microbiology*. 76 (18), 6266–76.
- Wang, Q., Garrity, G.M., Tiedje, J.M. and Cole, J.R. (2007) Naive Bayesian classifier for rapid assignment of rRNA sequences into the new bacterial taxonomy. *Applied and environmental microbiology*. 73 (16), 5261–7.

- Wang, X., Feng, Y., Liu, J., Lee, H., Li, C., Li, N. and Ren, N. (2010) Sequestration of CO<sub>2</sub> discharged from anode by algal cathode in microbial carbon capture cells (MCCs). *Biosensors and Bioelectronics*. 25 (12), 2639–2643.
- Wang, Z., Xue, M., Huang, K. and Liu, Z. (2011) Textile dyeing wastewater treatment. *Treating Textile Effluent*, [http://www.intechopen.com/source/pdfs/22395/intech-textile\\_dyeing\\_wastewater\\_treatment.pdf](http://www.intechopen.com/source/pdfs/22395/intech-textile_dyeing_wastewater_treatment.pdf). 91–116.
- Wang, Z., Zheng, Y., Xiao, Y., Wu, S., Wu, Y., Yang, Z. and Zhao, F. (2013) Analysis of oxygen reduction and microbial community of air-diffusion biocathode in microbial fuel cells. *Bioresource Technology*. 14474–79.
- Waring, D.R. and Hallas, G. (Geoffrey) (1990) *The Chemistry and application of dyes*. Plenum Press, Springer, US.
- Wolin, E.A., Wolin, M.J. and Wolfe, R.S. (1963) Formation of Methane by Bacterial Extracts. *The Journal of biological chemistry*. 238, 2882–6.
- Wong, S.S. and Wong, L. (1992) Chemical Crosslinking and the Stabilization of Proteins and Enzymes - Review. *Enzyme Microb Technol*. 14 (11), 866–874.
- Wu, C., Liu, X.-W., Li, W.-W., Sheng, G.-P., Zang, G.-L., Cheng, Y.-Y., Shen, N., Yang, Y.-P. and Yu, H.-Q. (2012) A white-rot fungus is used as a biocathode to improve electricity production of a microbial fuel cell. *Applied Energy*. 98, 594–596.
- Wu, J., Eiteman, M.A. and Law, S.E. (1998) Evaluation of Membrane Filtration and Ozonation Processes for Treatment of Reactive-Dye Wastewater. *Journal of Environmental Engineering*. 124 (3), 272–277.
- Wu, T., Wang, X.S., Cohen, B. and Ge, H. (2010) Molecular Modeling of Normal and Sick Hemoglobins. *International Journal for Multiscale Computational Engineering*. 8 (2), 237–244.
- Wu, Y., Teng, Y., Li, Z., Liao, X. and Luo, Y. (2008) Potential role of polycyclic aromatic hydrocarbons (PAHs) oxidation by fungal laccase in the remediation of an aged contaminated soil. *Soil Biology and Biochemistry*. 40 (3), 789–796.

- Xia, X., Sun, Y., Liang, P. and Huang, X. (2012) Long-term effect of set potential on biocathodes in microbial fuel cells: Electrochemical and phylogenetic characterization. *Bioresource Technology*. 120, 26–33.
- Xing, D., Zuo, Y., Cheng, S., Regan, J.M. and Logan, B.E. (2008) Electricity Generation by *Rhodopseudomonas palustris* DX-1. *Environmental Science & Technology*. 42 (11), 4146–4151.
- Xu, F. (1997) Effects of redox potential and hydroxide inhibition on the pH activity profile of fungal laccases. *Journal of Biological Chemistry*. 272 (2), 924–928.
- Xu, F. (1996) Oxidation of phenols, anilines, and benzenethiols by fungal laccases: Correlation between activity and redox potentials as well as halide inhibition. *Biochemistry*. 35 (23), 7608–7614.
- Yan, K., Wang, H., Zhang, X. and Yu, H. (2009) Bioprocess of triphenylmethane dyes decolorization by *Pleurotus ostreatus* BP under solid-state cultivation. *Journal of Microbiology and Biotechnology*. 19 (11), 1421–1430.
- Yang, B., Wang, Y. and Qian, P.Y. (2016) Sensitivity and correlation of hypervariable regions in 16S rRNA genes in phylogenetic analysis. *BMC Bioinformatics*. 17 (1), 1–8.
- Yang, H.-Y., He, C.-S., Li, L., Zhang, J., Shen, J.-Y., Mu, Y. and Yu, H.-Q. (2016) Process and kinetics of azo dye decolourization in bioelectrochemical systems: effect of several key factors. *Scientific Reports*. 6 (1), 27243.
- Yang, S.-O., Sodaneath, H., Lee, J.-I., Jung, H., Choi, J.-H., Ryu, H.W. and Cho, K.-S. (2017) Decolorization of acid, disperse and reactive dyes by *Trametes versicolor* CBR43. *Journal of Environmental Science and Health, Part A*. 52 (9), 862–872.
- Yiqi Yang; Wyatt II, David Travis; Bahorsky, M. (1998) Decolorization of Dyes Using UV/H<sub>2</sub>O<sub>2</sub> Photochemical Oxidation. *Textile Chemist & Colorist*. 30 (4), 27–35.
- You, S., Zhao, Q., Zhang, J., Jiang, J. and Zhao, S. (2006) A microbial fuel cell using permanganate as the cathodic electron acceptor. *Journal of Power Sources*. 1621409–1415.

- Young, C.-C., Kampfer, P., Chen, W.-M., Yen, W.-S., Arun, A.B., Lai, W.-A., Shen, F.-T., Rekha, P.D., Lin, K.-Y. and Chou, J.-H. (2007) *Luteimonas composti* sp. nov., a moderately thermophilic bacterium isolated from food waste. *International Journal of Systematic and Evolutionary Microbiology*. 57 (4), 741–744.
- Yuan, H., Hou, Y., Abu-Reesh, I.M., Chen, J. and He, Z. (2016) Oxygen reduction reaction catalysts used in microbial fuel cells for energy-efficient wastewater treatment: a review. *Mater. Horiz.* 3 (5), 382–401.
- Zaybak, Z., Pisciotta, J.M., Tokash, J.C. and Logan, B.E. (2013) Enhanced start-up of anaerobic facultatively autotrophic biocathodes in bioelectrochemical systems. *Journal of Biotechnology*. 168 (4), 478–485.
- Van der Zee, F.P., Lettinga, G. and Field, J.A. (2000) The role of (auto)catalysis in the mechanism of an anaerobic azo reduction. *Water Science and Technology*. 42 (5–6), 301–308.
- Zeng, S., Qin, X. and Xia, L. (2017) Degradation of the herbicide isoproturon by laccase-mediator systems. *Biochemical Engineering Journal*. 119, 92–100.
- Zeng, X., Cai, Y., Liao, X., Zeng, X., Li, W. and Zhang, D. (2011) Decolorization of synthetic dyes by crude laccase from a newly isolated *Trametes trogii* strain cultivated on solid agro-industrial residue. *Journal of Hazardous Materials*. 187 (1–3), 517–525.
- Zhang, F., Knapp, J.S. and Tapley, K.N. (1999) Development of bioreactor systems for decolorization of Orange II using white rot fungus. *Enzyme and Microbial Technology*. 24 (1–2), 48–53.
- Zhang, G., Zhao, Q., Jiao, Y., Wang, K., Lee, D.-J. and Ren, N. (2012) Biocathode microbial fuel cell for efficient electricity recovery from dairy manure. *Biosensors and Bioelectronics*. 31 (1), 537–543.
- Zhang, G., Zhao, Q., Jiao, Y., Zhang, J., Jiang, J., Ren, N. and Kim, B.H. (2011) Improved performance of microbial fuel cell using combination biocathode of graphite fiber brush and graphite granules. *Journal of Power Sources*. 196 (15), 6036–6041.

- Zhang, R.-G., Tan, X., Zhao, X.-M., Deng, J. and Lv, J. (2014) *Moheibacter sediminis* gen. nov., sp. nov., a member of the family Flavobacteriaceae isolated from sediment, and emended descriptions of *Empedobacter brevis*, *Wautersiella falsenii* and *Weeksella virosa*. *International Journal of Systematic and Evolutionary Microbiology*. 64 (5), 1481–1487.
- Zhang, S., Wu, Z., Chen, G., Wang, Z., Zhang, S., Wu, Z., Chen, G. and Wang, Z. (2018) An Improved Method to Encapsulate Laccase from *Trametes versicolor* with Enhanced Stability and Catalytic Activity. *Catalysts*. 8 (7), 286.
- Zhang, X., Hua, M., Lv, L. and Pan, B. (2015) Ionic polymer-coated laccase with high activity and enhanced stability: application in the decolourisation of water containing AO7. *Scientific reports*. 58253.
- Zhao, J., Zhang, C., Sun, C., Li, W., Zhang, S., Li, S. and Zhang, D. (2018) Electron transfer mechanism of biocathode in a bioelectrochemical system coupled with chemical absorption for NO removal. *Bioresource Technology*. 254, 16–22.
- Zhou, M., He, H., Jin, T. and Wang, H. (2012) Power generation enhancement in novel microbial carbon capture cells with immobilized *Chlorella vulgaris*. *Journal of Power Sources*. 214, 216–219.
- Zille, A. (2006) 'Redox biodegradation of azo dyes', in *4th International Conference on Textile Biotechnology*. [Online]. 2006 Seoul, Korea.
- Zille, A., Górnacka, B., Rehorek, A. and Cavaco-Paulo, A. (2005) Degradation of azo dyes by *Trametes villosa* laccase over long periods of oxidative conditions. *Applied and environmental microbiology*. 71 (11), 6711–6718.
- Zou, Y., Pisciotta, J., Billmyre, R.B. and Baskakov, I. V. (2009) Photosynthetic microbial fuel cells with positive light response. *Biotechnology and Bioengineering*. 104 (5), 939–946.

## Webpages

- [www.sophied.net](http://www.sophied.net)
- <https://civildigital.com/pollution-control-in-dye-industry/>
- [www.wfduk.org](http://www.wfduk.org)
- <https://emea.illumina.com>



Contents lists available at ScienceDirect

Enzyme and Microbial Technology

journal homepage: [www.elsevier.com/locate/emt](http://www.elsevier.com/locate/emt)



## Decolourisation of Acid orange 7 in a microbial fuel cell with a laccase-based biocathode: Influence of mitigating pH changes in the cathode chamber



Priyadharshini Mani<sup>a,\*</sup>, Taj Keshavarz<sup>a</sup>, T.S Chandra<sup>b</sup>, Godfrey Kyazze<sup>a</sup>

<sup>a</sup> Faculty of Science and Technology, University of Westminster, London W1W 6UW, United Kingdom

<sup>b</sup> Department of Biotechnology, Indian Institute of Technology-Madras, Chennai-36, India

### ARTICLE INFO

#### Article history:

Received 11 July 2016

Received in revised form 16 October 2016

Accepted 17 October 2016

Available online 18 October 2016

#### Keywords:

Microbial fuel cell

Azo dye decolourisation

Laccase

Biocathode

pH

Salinity

Acid orange 7

### ABSTRACT

Biocathodes may be a suitable replacement of platinum in microbial fuel cells (MFCs) if the cost of MFCs is to be reduced. However, the use of enzymes as bio-cathodes is fraught with loss of activity as time progresses. A possible cause of this loss in activity might be pH increase in the cathode as pH gradients in MFCs are well known. This pH increase is however, accompanied by simultaneous increase in salinity; therefore salinity may be a confounding variable. This study investigated various ways of mitigating pH changes in the cathode of MFCs and their effect on laccase activity and decolourisation of a model azo dye Acid orange 7 in the anode chamber. Experiments were run with catholyte pH automatically controlled via feedback control or by using acetate buffers (pH 4.5) of various strength (100 mM and 200 mM), with CMI7000 as the cation exchange membrane. A comparison was also made between use of CMI7000 and Nafion 117 as the transport properties of cations for both membranes (hence their potential effects on pH changes in the cathode) are different. Results show that using Nafion 117 membrane limits salinity and pH changes in the cathode (100 mM acetate buffer as catholyte) leading to prolonged laccase activity and faster AO7 decolourisation compared to using CMI7000 as a membrane; similarly automatic pH control in the cathode chamber was found to be better than using 200 mM acetate buffer. It is suggested that while pH control in the cathode chamber is important, it does not guarantee sustained laccase activity; as salinity increases affect the activity and it could be mitigated using a cation selective membrane.

© 2016 Elsevier Inc. All rights reserved.

### 1. Introduction

Microbial fuel cells (MFC) are a promising technology in the treatment of wastewater and simultaneous electricity generation. However, there are operational and technological challenges that prevent the use of MFCs for practical applications. The major hurdles are coulombic losses, high internal resistances, poor reaction kinetics of the oxygen reduction reaction (ORR) at the cathode and development of pH gradients across the membrane all of which affect the performance of the system [1].

The efficiency of the oxygen reduction reaction (ORR) at the cathode is affected by high overpotentials at the electrode and oxygen mass transfer limitation. Although platinum is currently the most effective and commonly used catalyst, its high cost and

unsustainability hinders the scaling up of MFCs. Transition metal based catalysts such Mn, Co, V and their oxide forms have been used as cathode catalysts in MFCs as a replacement for platinum [2–4]. These catalysts have produced power comparable to Pt but they are also unsustainable and are not stable. The possible leaching of the metals into the environment and their toxic effects is a concern [5].

To improve the cathode reaction and reduce the cost, biocathodes such as microorganisms and enzymes have been investigated for their catalytic activity. Oxidoreductase enzymes such as manganese peroxidase (MnP), bilirubin oxidase and laccase have been utilised as catalysts at the cathode of MFCs [6–8]. Enzymes are sustainable and their production is more environmentally friendly compared to metal-based catalysts. Enzymes (e.g. laccase) have an advantage over microorganisms as a biocathode in the sense that they do not need a carbon source (and other nutrients) to maintain them. The use of a carbon source would not only add to the operational costs but also add COD to a system whose objective is partly to remove COD from wastewater.

\* Corresponding author at: Faculty of Science and Technology, University of Westminster, London W1W 6UW, United Kingdom.

E-mail address: [Priyadharshini.Mani@my.westminster.ac.uk](mailto:Priyadharshini.Mani@my.westminster.ac.uk) (P. Mani).

Article

# The Role of Natural Laccase Redox Mediators in Simultaneous Dye Decolorization and Power Production in Microbial Fuel Cells

Priyadharshini Mani <sup>1,\*</sup>, Vallam Thodi Fidal Kumar <sup>2</sup>, Taj Keshavarz <sup>1</sup>, T Sainathan Chandra <sup>2</sup> and Godfrey Kyazze <sup>1,\*</sup>

<sup>1</sup> Faculty of Science and Technology, University of Westminster, 115 New Cavendish Street, London W1W 6UW, UK; T.Keshavarz@westminster.ac.uk

<sup>2</sup> Department of Biotechnology, Indian Institute of Technology (Madras), Chennai 600036, India; vtfkbt@gmail.com (V.T.F.K.); chandrasainathan@gmail.com (T.S.C.)

\* Correspondence: Priyadharshini.Mani@my.westminster.ac.uk (P.M.); G.Kyazze@westminster.ac.uk (G.K.)

Received: 1 November 2018; Accepted: 8 December 2018; Published: 10 December 2018

**Abstract:** Redox mediators could be used to improve the efficiency of microbial fuel cells (MFCs) by enhancing electron transfer rates and decreasing charge transfer resistance at electrodes. However, many artificial redox mediators are expensive and/or toxic. In this study, laccase enzyme was employed as a biocathode of MFCs in the presence of two natural redox mediators (syringaldehyde (Syr) and acetosyringone (As)), and for comparison, a commonly-used artificial mediator 2,2'-azinobis(3-ethylbenzthiazoline-6-sulfonic acid) (ABTS) was used to investigate their influence on azo dye decolorization and power production. The redox properties of the mediator-laccase systems were studied by cyclic voltammetry. The presence of ABTS and As increased power density from  $54.7 \pm 3.5$  mW m<sup>-2</sup> (control) to  $77.2 \pm 4.2$  mW m<sup>-2</sup> and  $62.5 \pm 3.7$  mW m<sup>-2</sup> respectively. The power decreased to  $23.2 \pm 2.1$  mW m<sup>-2</sup> for laccase with Syr. The cathodic decolorization of Acid orange 7 (AO7) by laccase indicated a 12–16% increase in decolorization efficiency with addition of mediators; and the Laccase-Acetosyringone system was the fastest, with 94% of original dye (100 mgL<sup>-1</sup>) decolorized within 24 h. Electrochemical analysis to determine the redox properties of the mediators revealed that syringaldehyde did not produce any redox peaks, inferring that it was oxidized by laccase to other products, making it unavailable as a mediator, while acetosyringone and ABTS revealed two redox couples demonstrating the redox mediator properties of these compounds. Thus, acetosyringone served as an efficient natural redox mediator for laccase, aiding in increasing the rate of dye decolorization and power production in MFCs. Taken together, the results suggest that natural laccase redox mediators could have the potential to improve dye decolorization and power density in microbial fuel cells.

**Keywords:** acetosyringone; dye decolorization; laccase; natural redox mediators; power density; syringaldehyde

## 1. Introduction

Microbial fuel cells (MFCs) could have potential in treating dyeing effluents with simultaneous power production. At the cathode of MFCs, platinum and metal oxide catalysts are commonly used for the oxygen reduction reaction (ORR). In recent years oxidoreductase enzymes e.g., laccase, have been explored as cathode catalysts in MFCs as a possible alternative to platinum as a way of reducing the cost of materials needed to construct MFCs [1,2]. Laccase is a multi-copper containing enzyme that is capable of one electron oxidation of other substrates and four electron reduction of O<sub>2</sub>

## Conference Publications

Mani, P., Keshavarz, T., Kyazze, G. and Chandra, S. 2016. Improving the performance of microbial fuel cells using laccase-based biocathodes. Aulenta, F. and Majone, M. (ed.) EU-ISMET 2016: The 3rd European Meeting of the International Society for Microbial Electrochemistry and Technology. Department of Chemistry (NEC) Sapienza, University of Rome, Rome, Italy 26 - 29 Sep 2016 ISMET.

Kyazze, G., Mani, P., Bowman, K., Farahmand, N., Breheny, M. and Keshavarz, T. 2018. Degradation of azo dyes (Acid orange 7) in a microbial fuel cell: comparison between anodic microbial-mediated reduction and cathodic laccase-mediated oxidation. 4th European Meeting of the International Society for Microbial Electrochemistry and Technology. Newcastle University, Newcastle upon Tyne, 12 Sep 2018.

## Appendix 1

**Table A1:** The performance of the immobilized electrodes in the 2<sup>nd</sup> cycle of MFC.

<b>Laccase immobilization methods</b>	<b>Max.Power Density (mW m<sup>-2</sup>)</b>	<b>Dye decolourization Efficiency (%)</b>	<b>Relative Enzyme Activity after 2<sup>nd</sup> cycle (%)</b>
PANI Lac	28	58	61
Nafion Lac	16.2	50	40
Cu-Alg Lac	10	55	38

**Table A2:** The performance of the immobilized electrodes in the 3<sup>rd</sup> cycle of MFC.

<b>Laccase immobilization methods</b>	<b>Max.Power Density (mW m<sup>-2</sup>)</b>	<b>Dye decolourization Efficiency (%)</b>	<b>Relative Enzyme Activity after 3<sup>rd</sup> cycle (%)</b>
PANI Lac	23.6	50	45
Nafion Lac	11	35	30
Cu-Alg Lac	6	32.4	26

## Appendix 2

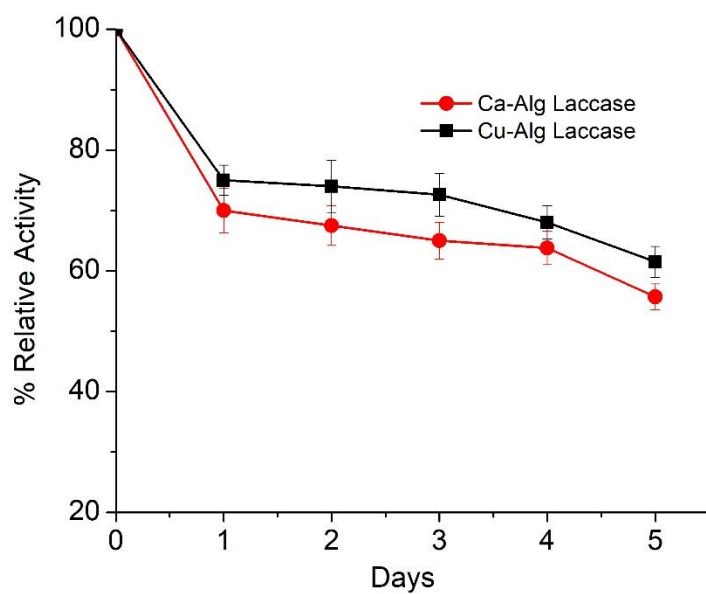


**Figure A1:** The immobilized enzyme activity for Calcium and copper alginate beads over a period of 5 days

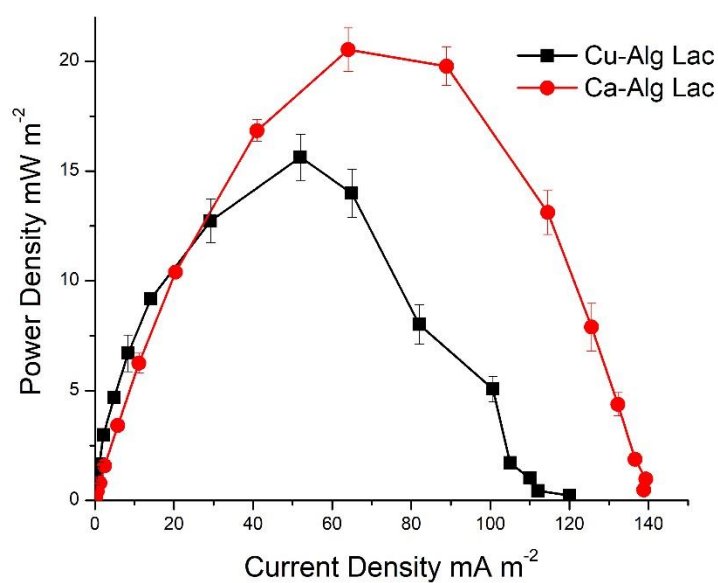


**Figure A2:** The maximum power density comparison for laccase immobilized in calcium and copper alginate beads

## Appendix 3

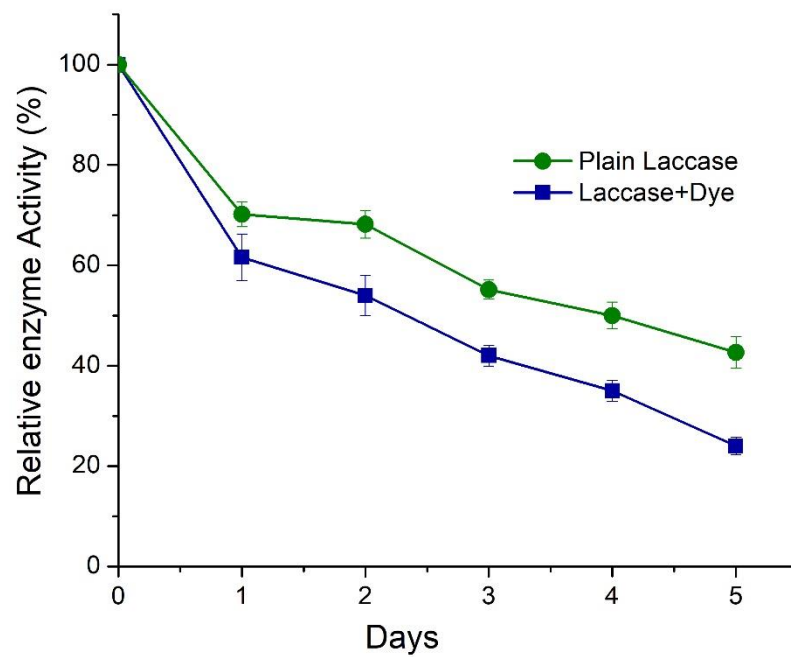


**Figure A3:** The relative enzyme activity of laccase in the absence and presence of the dye over a period of 5 days.

## Appendix 4

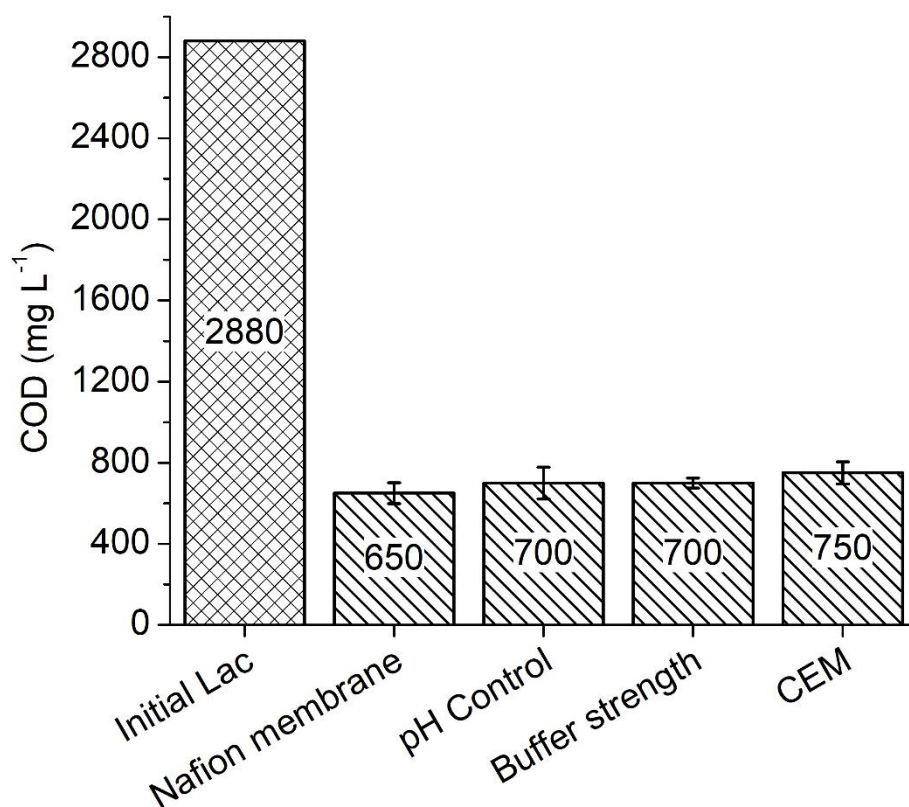


**Figure A4.1:** Initial and final COD Profile of the variables in chapter 3

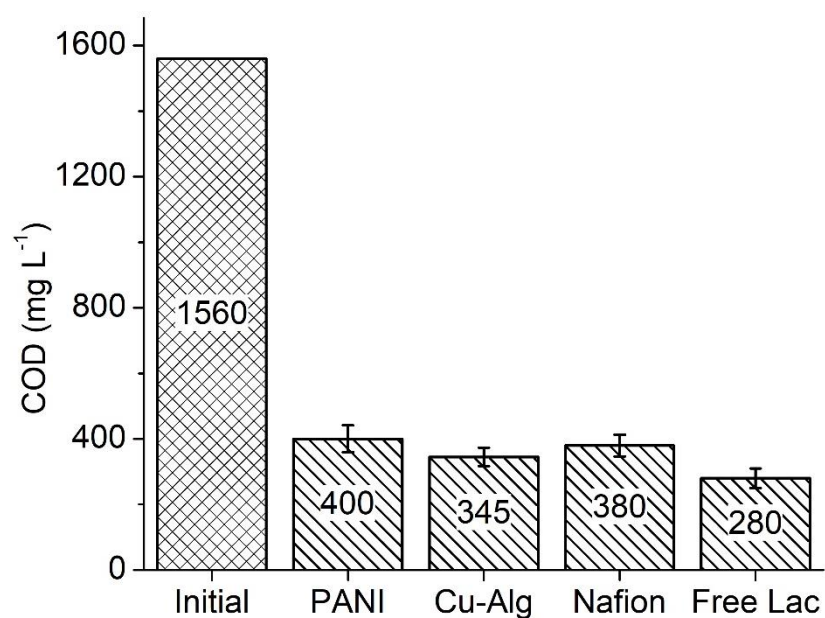


**Figure A4.2:** Initial and final COD of immobilized laccase in chapter 4

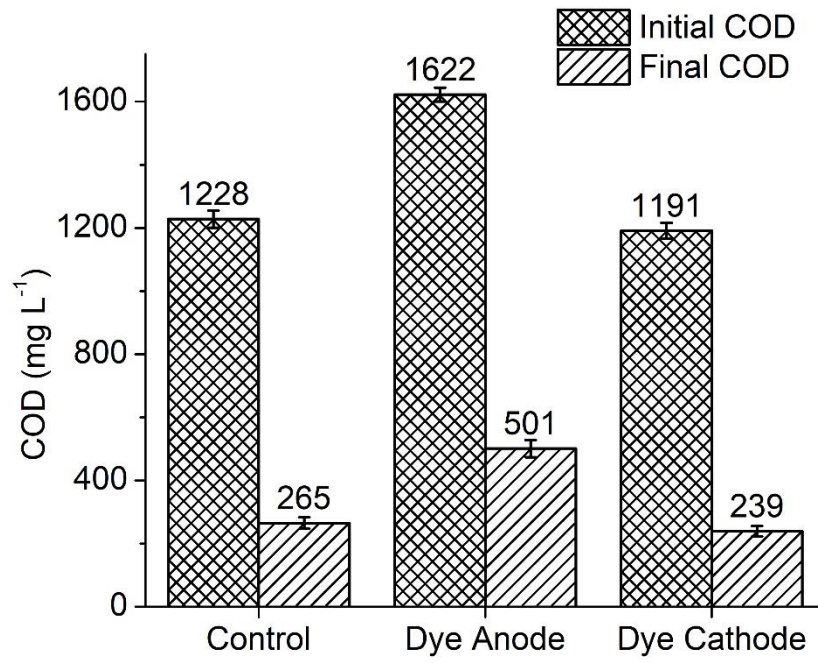


**Figure A4.3:** Initial and Final COD profiles for variables in chapter 5

## Appendix 5

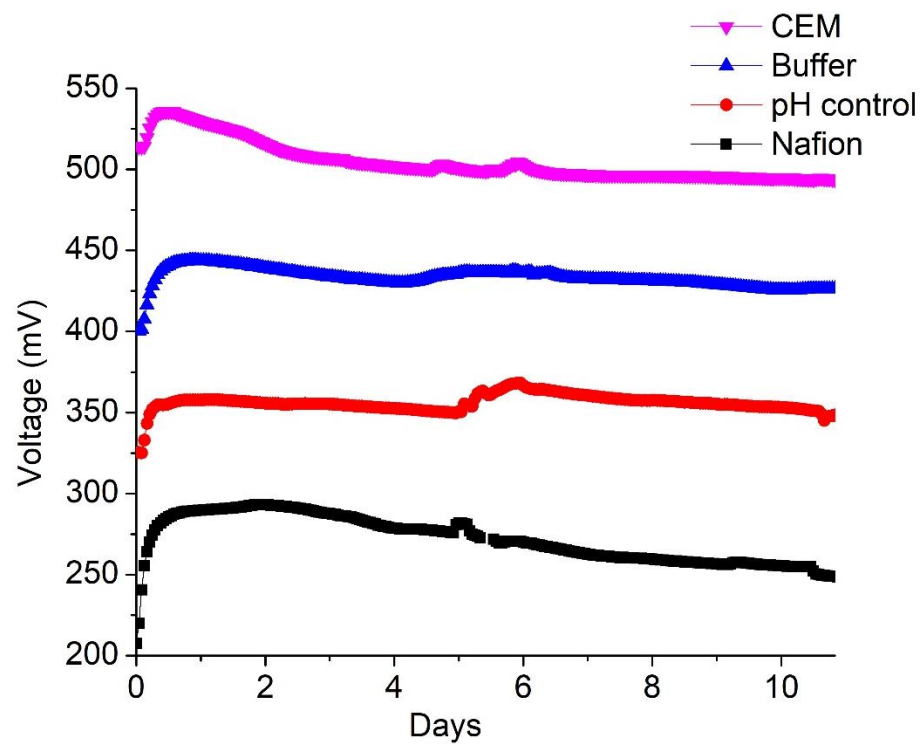


Figure A5.1: Voltage generated over a period of 10 days at a resistance of 2 K $\Omega$  in chapter 3.

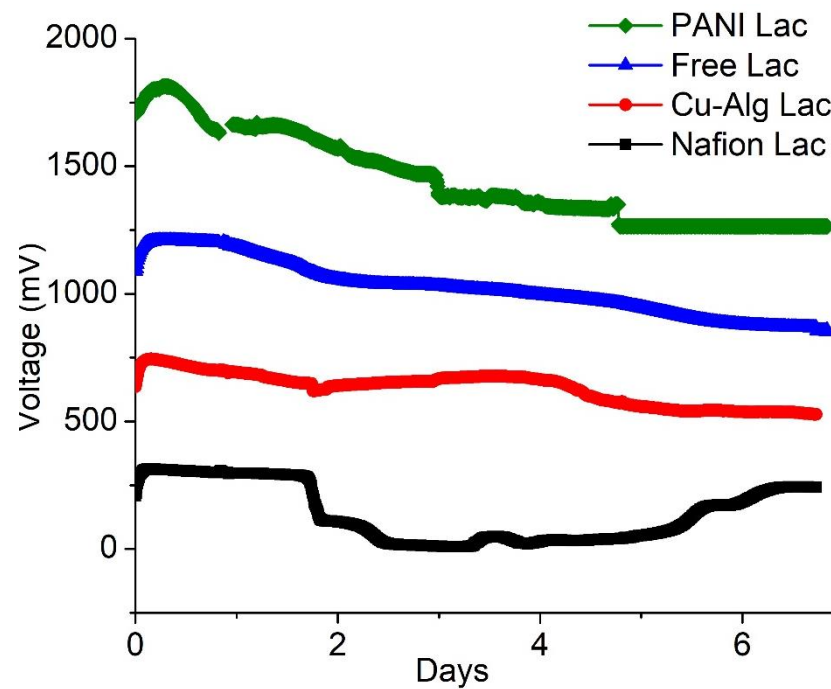


Figure A5.2: Voltage generated over a period of 7 days at a resistance of 2 K $\Omega$  in chapter 4.

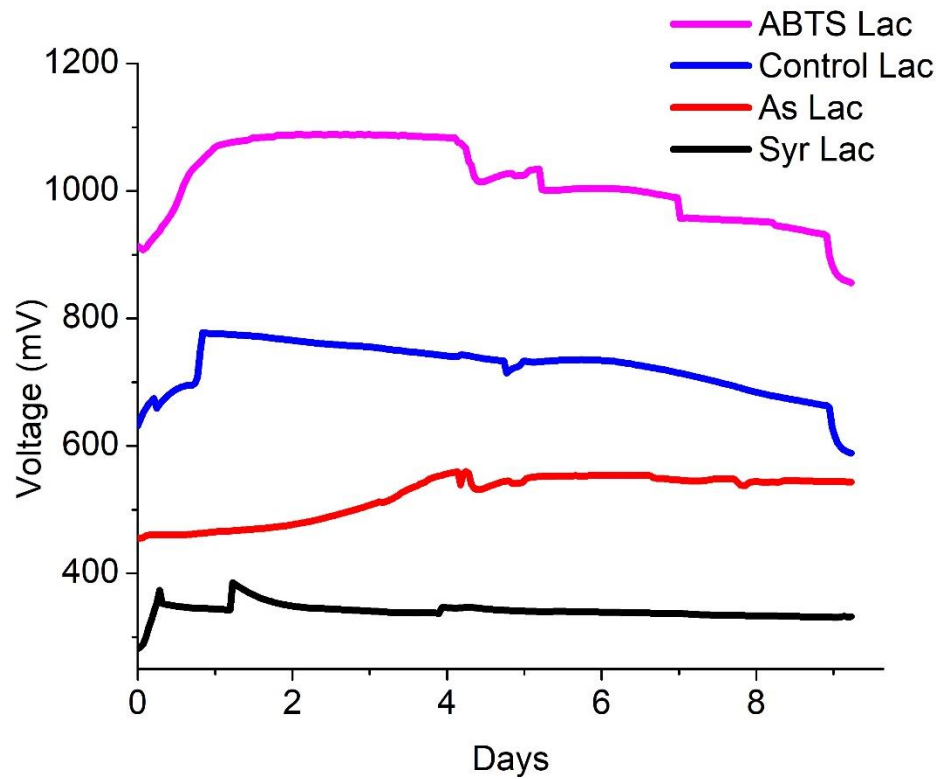


Figure A5.3: Voltage generated over a period of 9 days at a resistance of 2 K $\Omega$  in chapter 6.

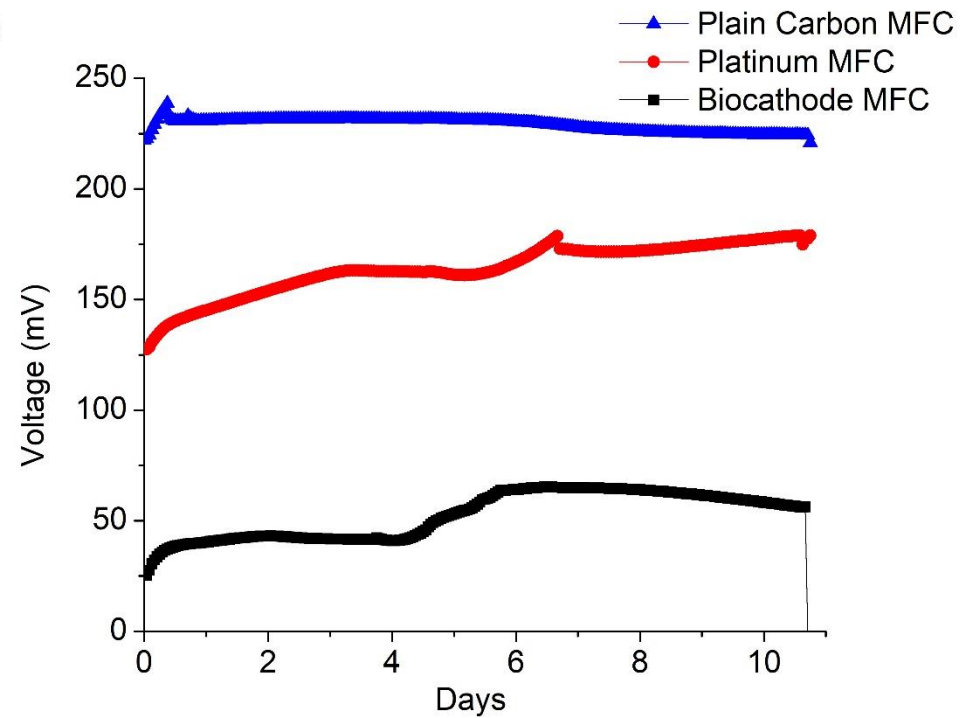
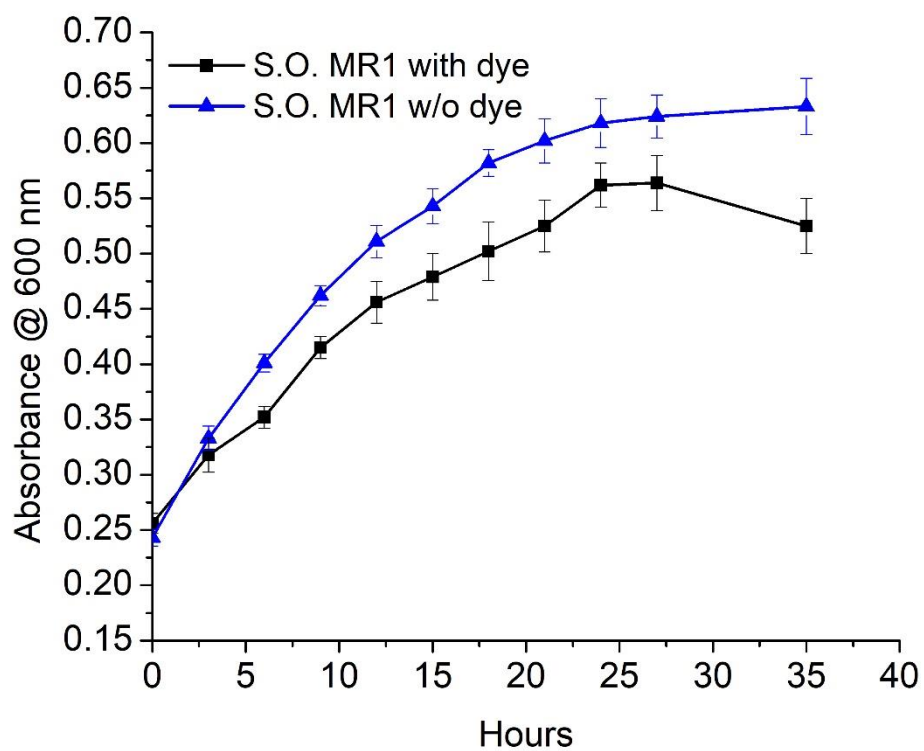


Figure A5.4: Voltage generated over a period of 10 days at a resistance of 200  $\Omega$  in chapter 7.

## Appendix 6



**Figure A6:** Growth curve of *S. oneidensis* in the presence and absence of Acid orange 7 dye

# Appendix 7

## Next Generation Sequencing: Bioinformatics analysis by NovoGene

### 1. Paired-end reads assembly and quality control

#### 1.1 Data split

Paired-end reads was assigned to samples based on their unique barcode and truncated by cutting off the barcode and primer sequence.

#### 1.2 Sequence assembly

Paired-end reads were merged using FLASH (V1.2.7,<http://ccb.jhu.edu/software/FLASH/>) (Magoč and Salzberg, 2011), a very fast and accurate analysis tool, which was designed to merge paired-end reads when at least some of the reads overlap the read generated from the opposite end of the same DNA fragment, and the splicing sequences were called raw tags.

#### 1.3 Data Filtration

Quality filtering on the raw tags were performed under specific filtering conditions to obtain the high-quality clean tags according to the QIIME (V1.7.0, <http://qiime.org/index.html>) quality controlled process (Bokulich et al., 2013; Caporaso et al., 2010).

#### 1.4 Chimera removal

The tags were compared with the reference database (Gold database, [http://drive5.com/uchime/uchime\\_download.html](http://drive5.com/uchime/uchime_download.html)) using UCHIME algorithm (UCHIME Algorithm, [http://www.drive5.com/usearch/manual/uchime\\_algo.html](http://www.drive5.com/usearch/manual/uchime_algo.html)) (Edgar et al., 2011) to detect chimera sequences, and then the chimera sequences were removed (Haas et al., 2011). Then the Effective Tags finally obtained.

### 2. OTU cluster and Species annotation

#### 2.1 OTU Production

Sequences analysis were performed by Uparse software (Uparse v7.0.1001, <http://drive5.com/uparse/>) (Edgar, 2013). Sequences with  $\geq 97\%$  similarity were assigned to the same OTUs. Representative sequence for each OTU was screened for further annotation.

## 2.2 Species annotation

For each representative sequence, the GreenGene Database (<http://greengenes.lbl.gov/cgi-bin/nph-index.cgi>) (DeSantis et al., 2006) was used based on RDP classifier (Version 2.2, <http://sourceforge.net/projects/rdp-classifier/>) [algorithm](#) to annotate taxonomic information (Wang et al., 2007).

## 2.3 Phylogenetic relationship Construction

In order to study phylogenetic relationship of different OTUs, and the difference of the dominant species in different samples (groups), multiple sequence alignment were conducted using the MUSCLE software (Version 3.8.31, <http://www.drive5.com/muscle/>) (Edgar, 2004).

## 2.4 Data Normalization

OTUs abundance information were normalized using a standard of sequence number corresponding to the sample with the least sequences. Subsequent analysis of alpha diversity and beta diversity were all performed basing on this output normalized data.

## 3. Alpha Diversity

Alpha diversity is applied in analyzing complexity of species diversity for a sample through 6 indices, including Observed-species and Shannon diversity. All indices in the samples were calculated with QIIME (Version 1.7.0) and displayed with R software (Version 2.15.3).

## 4. Beta Diversity

Beta diversity analysis was used to evaluate differences of samples in species complexity, Beta diversity on both weighted and unweighted unifracs were calculated by QIIME software (Version 1.7.0).

Principal Coordinate Analysis (PCoA) was performed to get principal coordinates and visualize from complex, multidimensional data. A distance matrix of weighted or unweighted unifracs among samples obtained before was transformed to a new set of orthogonal axes, by which the maximum variation factor is demonstrated by first principal coordinate, and the second maximum one by the second principal coordinate, and so on. PCoA analysis was displayed by WGCNA package, stat packages and ggplot2 package in R software (Version 2.15.3).

# Appendix 8

## DGGE-Sanger Sequencing Results

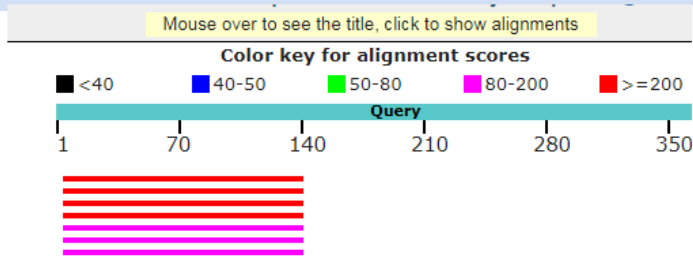
The samples subjected to PCR-DGGE were sequenced using Sanger method. The sequences obtained from the bands were as follows:

### Sequence 1

```
AACTGGGCTCTCCTCCGCTCCGTCATCATCGTCACGGGTGAAGAGCTTTA
CAACCCTAAGGCCTTCCTCA
CTCACGCGGCATGGCTGGATCAGGGTTTCCCCCATTGTCCAATATTCCCC
ACTGCTGCCTCCCGTAGGAG
TATTGCTGCCTCCAAGGAGTAAATTACGGAGGACTAGCGTGGTGGCAT
GTCGCTGGATTGGGGACTGCA
TCCCCGAGACAAGGAGAGCAGCTGCGGAAAAAACAGCCCAGTCCTTGGC
CCGCCCTCTTAATGATTAAT
TCCCGTTTGTAAATCTGTTGCAGTTCCGAAGAAGATTGTGATACTCCTTAG
GAGCTTGTTGCGTTTGATCC
TTGGAGTGGATTGTGGAATGGATTTATAGTGGTGTGC
```

### Blast Results

<b>RID</b>	U29ACNV5016 (Expires on 09-20 00:18 am)	<b>Database Name</b>	rRNA_typestrains/prokaryotic_16S_ribosomal_RNA
<b>Query ID</b>	lcl Query_196029	<b>Description</b>	16S ribosomal RNA (Bacteria and Archaea)
<b>Description</b>	None	<b>Program</b>	BLASTN 2.8.0+ <a href="#">Citation</a>
<b>Molecule type</b>	nucleic acid		
<b>Query Length</b>	387		



Sequences producing significant alignments.

Expect: [All](#) [None](#) Selected: 0

Alignments [Download](#) [GenBank](#) [Graphics](#) [Distance tree of results](#)

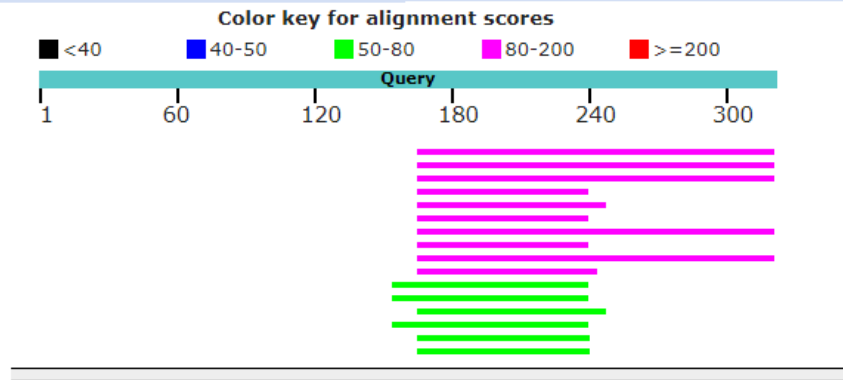
	Max score	Total score	Query cover	E value	Ident	Accession
<a href="#">Magnetospirillum marisnigri strain SP-1 16S ribosomal RNA, partial sequence</a>	202	202	35%	1e-51	93%	<a href="#">NR_149242.1</a>
<a href="#">Bartonella bacilliformis strain KC583 16S ribosomal RNA, partial sequence</a>	202	202	35%	1e-51	93%	<a href="#">NR_074203.1</a>
<a href="#">Phaeospirillum chandramohanii strain JA145 16S ribosomal RNA gene, partial sequence</a>	202	202	35%	1e-51	93%	<a href="#">NR_042661.1</a>

## Sequence 2

AGGAGCTTCTCTGAGTACCGTCAGCCTCGATACTCGACGGGGGGGTTATT  
 CCTGAAAGAGCTCTTTACAA  
 CCCATAAGGGTGTCTTCCTGGACGCGGCCCGGTGGGGTTCAGACTTGCGTG  
 CATGGCCCAAGATTCATTAC  
 GGCTGCCTCCCGTAGGAGTAAGTAAATATTGGGCAATGGACGCAAGTCT  
 GACCCACCGGCCGGGCAGGAG  
 GAAGCCGTATGGGTTGTAAACTGCTTTTATCGGGAATACCCCGGTTCGAGT  
 ATCGGGGCTAAGGTACATGA  
 AGAATAAACATCGCTAACTCCGTGCCGCACCCGGTAATAG

## Blast Results

<b>RID</b>	<a href="#">U29VSKJG016</a> (Expires on 09-20 00:27 am)	<b>Database Name</b>	rRNA_typetrains/prokaryotic_16S_ribosomal_RNA
<b>Query ID</b>	Id Query_51791	<b>Description</b>	16S ribosomal RNA (Bacteria and Archaea)
<b>Description</b>	None	<b>Program</b>	BLASTN 2.8.0+ <a href="#">▶ Citation</a>
<b>Molecule type</b>	nucleic acid		
<b>Query Length</b>	320		



	Max score	Total score	Query cover	E value	Ident	Accession
<a href="#">Adhaeribacter aquaticus strain MBRG1.5 16S ribosomal RNA, partial sequence</a>	104	104	48%	3e-22	80%	<a href="#">NR_042235.1</a>
<a href="#">Adhaeribacter terrae strain HY02 16S ribosomal RNA, partial sequence</a>	99.0	99.0	48%	1e-20	79%	<a href="#">NR_157726.1</a>
<a href="#">Spirosoma pulveris strain JSH5-14 16S ribosomal RNA, partial sequence</a>	99.0	99.0	48%	1e-20	79%	<a href="#">NR_146704.1</a>

